General Disclaimer

One or more of the Following Statements may affect this Document

- This document has been reproduced from the best copy furnished by the organizational source. It is being released in the interest of making available as much information as possible.

- This document may contain data, which exceeds the sheet parameters. It was furnished in this condition by the organizational source and is the best copy available.

- This document may contain tone-on-tone or color graphs, charts and/or pictures, which have been reproduced in black and white.

- This document is paginated as submitted by the original source.

- Portions of this document are not fully legible due to the historical nature of some of the material. However, it is the best reproduction available from the original submission.

(NASA-CR-169627) RF MODEL OF THE DISTRIBUTION SYSTEM AS A COMMUNICATION CHANNEL, PHASE 2. VOLUME 2: TASK REPORTS Final Report (General Electric Co.) 313 p HC A14/MF A01 CSCL 17B G3/32

N83-14320

Unclas 02186

RF MODEL OF THE DISTRIBUTION SYSTEM AS A COMMUNICATION CHANNEL

PHASE II

VOLUME II — TASK REPORTS

FINAL REPORT
Contract No. 955647

July 28, 1982

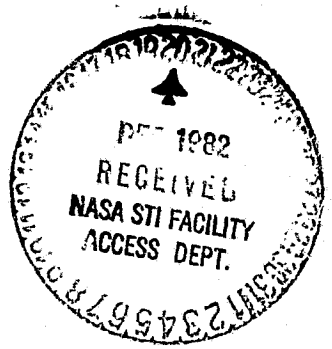

R.C. Rustay
J.T. Gajjar
R.W. Rankin
R.C. Wentz
R. Wooding

General Electric Company
Corporate Research and Development
Schenectady, New York 12345

Prepared for

Jet Propulsion Laboratory
California Institute of Technology
4800 Oak Grove Drive
Pasadena, California 91103

SRD-82-055-2

RF MODEL OF THE DISTRIBUTION SYSTEM AS A COMMUNICATION CHANNEL

PHASE II

VOLUME II — TASK REPORTS

FINAL REPORT
Contract No. 955647

July 28, 1982

R.C. Rustay
J.T. Gajjar
R.W. Rankin
R.C. Wentz
R. Wooding

General Electric Company
Corporate Research and Development
Schenectady, New York 12345

Prepared for

Jet Propulsion Laboratory
California Institute of Technology
4800 Oak Grove Drive
Pasadena, California 91103

This work was performed for the Jet Propulsion Laboratory, California Institute of Technology sponsored by the U.S. Department of Energy, through an agreement with the National Aeronautics and Space Administration.

SRD-82-055-2

ABSTRACT

This four-volume final report is concerned with Phase II of the DOE/JPL project "RF Model of the Distribution System As a Communication Channel." An earlier Phase I effort was concerned with the design, implementation, and verification of a computerized model for predicting the steady-state sinusoidal response of radial (tree) configured distribution feeders. That work demonstrated the feasibility and validity based on verification measurements made on a limited size portion of an actual live feeder. The Phase II effort is concerned with 1) extending the verification based on a greater variety of situations and network size, 2) extending the model capabilities for reverse direction propagation, 3) investigating parameter sensitivities, 4) improving transformer models, and 5) investigating procedures/fixes for ameliorating propagation "trouble spots."

PREFACE

This volume contains more detailed (than Volume 1) accounts of the major tasks comprising this PHASE II effort. The reports comprising Task (1) and some of Task (2)(B) include verbatum copies of individual internal reports (by R. Wooding).

TABLE OF CONTENTS

TASK	TITLE	PAGE
(1)(A)	Densely Loaded Feeder Sections	1-3
(1)(B)	Full Size Distribution Feeder	1-14
(1)(C)	Overhead-Underground Transitions	1-36
(1)(D)	Meter Terminals on Secondary	1-83
(1)(E)	Extended Frequency Range	1-85
	Summary of Verification Activities	1-87
(2)(-)	Continue "Perturbation Analysis"	2-i
(2)(A)	Perturbation Calculation of Inbound Propagation	2-9
(2)(B)	Inbound Path Propagation Measurements	2-10
(3)(A)	Parameter Sensitivity-Significance of Parameters	3-1
(3)(B)	Parameter Sensitivity-"Set-up" Time Reduction	3-52
(4)	Transformer Modelling	4-1
(5)	Line Compensation and Termination Techniques	5-1

TASK #1

VERIFICATION OF MODEL

TASK 1

TABLE OF CONTENTS

		Page
Foreward		
Task (1)(A)	Densely Loaded Feeder Sections	1-3
Task (1)(B)	Full Size Distribution Feeder	1-14
Task (1)(C)	Overhead-Underground Transitions	1-36
Task (1)(D)	Meter Terminals on Secondary	1-83
Task (1)(E)	Extended Frequency Range	1-85

FOREWORD

The detailed reports to follow for Subtasks (1)(A), (1)(B), and (1)(C) are copies of informal internal memos which were written at the completion of each task. Because of several contingencies which developed, these tasks were not written in chronological order of their numbering. The two principal contingencies requiring refinement of the model were:

a) Discovery that original cable parameters were inaccurate (requiring development of a cable parameter program).

b) Discovery of errors in line length specification using NMPC documentation.

The first caused considerable delay and was the motivation for the tests, reported in Task (1)(C), on an electrically isolated 2-mile underground getaway cable. Similarly, discovering that line lengths as reported in utility documentation is not always accurate, especially for UG cables having much slower speeds of propagation, caused considerable delay. In fact, these two items introduced considerable confounding in early attempts to "unravel" the cause of observed discrepancies between predictions and measurements.

For reasons mentioned in the discussions of subtasks (1)(D) and (1)(E), planned work on these tasks was not accomplished. The discussions presented are verbatum from Volume 1.

Finally, it is noted that during the process of making verification computations many software modifications were made to the DIFNAP system. Some of the most significant were:

a) Adding a single phase ratio transformer capability (software & file) required for subtask (1)(A).

b) Improving the interactive communication logic

c) Significant improvement to internal logic (for example, cumulative voltage transfer matrices)

d) Simplification of distribution transformer logic and files for IDPL = 3.

e) Significant reduction in record size for the "NT_ _ _ _ _ _" random binary file

f) Similar reduction in the "DPU_ _ _ _ _" record size.

g) Including knowledge of actual frequency (in addition to code), passed down automatically through the "DPU _ _ _ _ _" file. This enables use of lumped parameter transformer models.

h) Incorporating software for generating ZETA plotting.

i) Incorporating a procedure for quickly introducing detailed outputing.

MODEL VERIFICATION -
DENSELY LOADED FEEDER SECTIONS

INTRODUCTION

Distribution line carrier voltage propagation measurements were performed on a densely loaded overhead wire distribution circuit. The feeder section of interest is part of the 34556 feeder which originates from Niagara Mohawk Power Company's Grooms Rd. Substation in Clifton Park, N.Y. The nominal operating voltage of this feeder is 13.2 kv line to line. Figure 1 shows the general location of the densely loaded section in relation to the total feeder. Figure 2 is part of an operating map provided by the utility showing the densely loaded section in more detail. This feeder section was selected for study because of the relatively large number of distribution transformers per unit length of circuit.

BACKGROUND

A carrier voltage was placed on the feeder phase conductors at a capacitor bank location, shown at Point 1, Figure 2. Transmission was accomplished by connecting the transmitter as shown in Figure 3, thereby using the power factor correction capacitors to couple the carrier signals onto the phase conductors. The inductor was placed in the capacitor bank ground lead in order to prevent the bank from providing a large current sink to the carrier signals. The transmitter voltage was monitored at this point as shown in Figure 3. Transmission from the capacitor bank location was done as a matter of convenience. Except under unusual conditions, the inductor carrier voltage can be assumed to be very close to the voltage which appeared on the phase conductors. Transmission from the substation would have involved mounting separate capacitors and traps for each phase to determine the individual phase voltages impressed on the feeder section of interest.

ORIGINAL PAGE IS
OF POOR QUALITY

DENSELY LOADED FEEDER SECTION

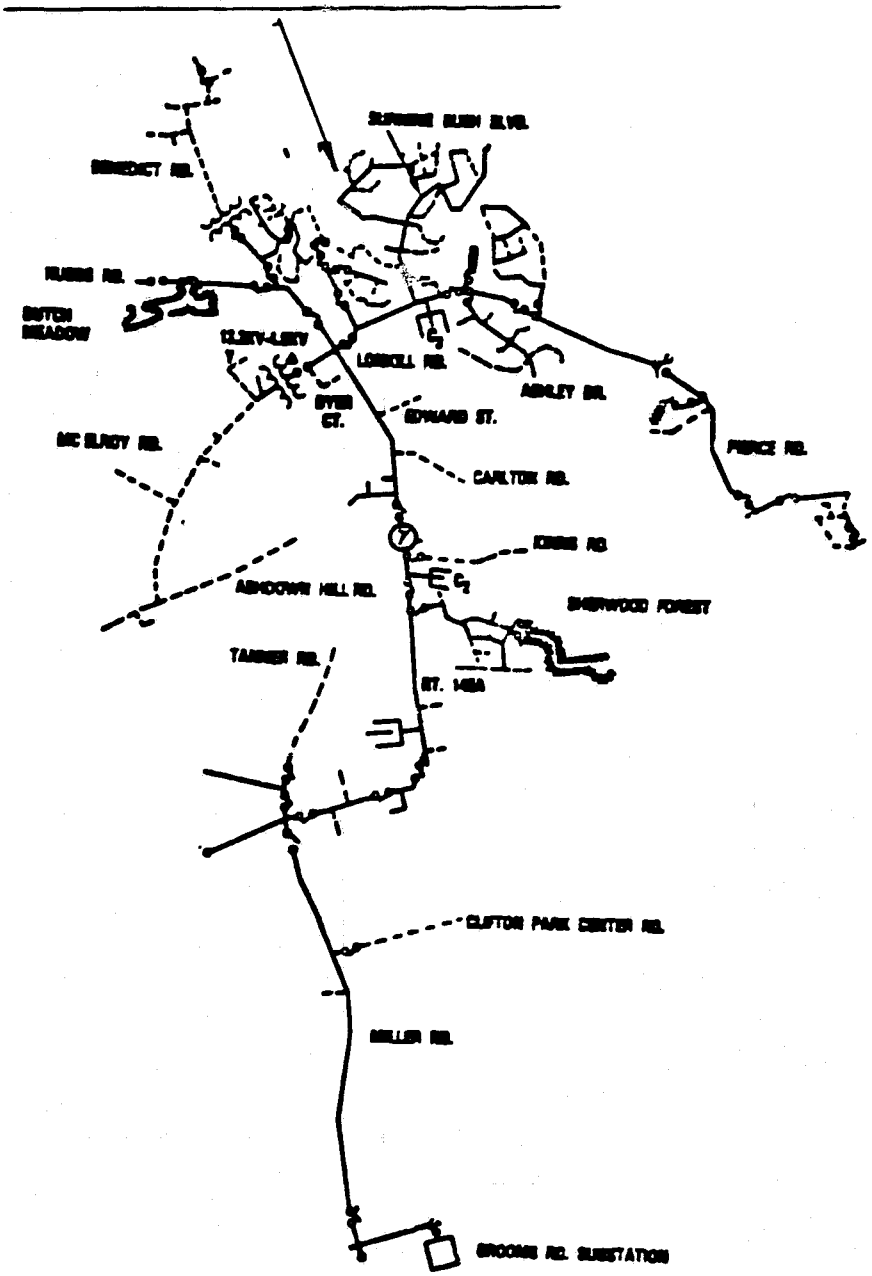

N.M.P.C.
GROOMS ROAD
34556 FEEDER

FIGURE 1

DENSELY LOADED FEEDER SECTION

**ORIGINAL PAGE IS
OF POOR QUALITY**

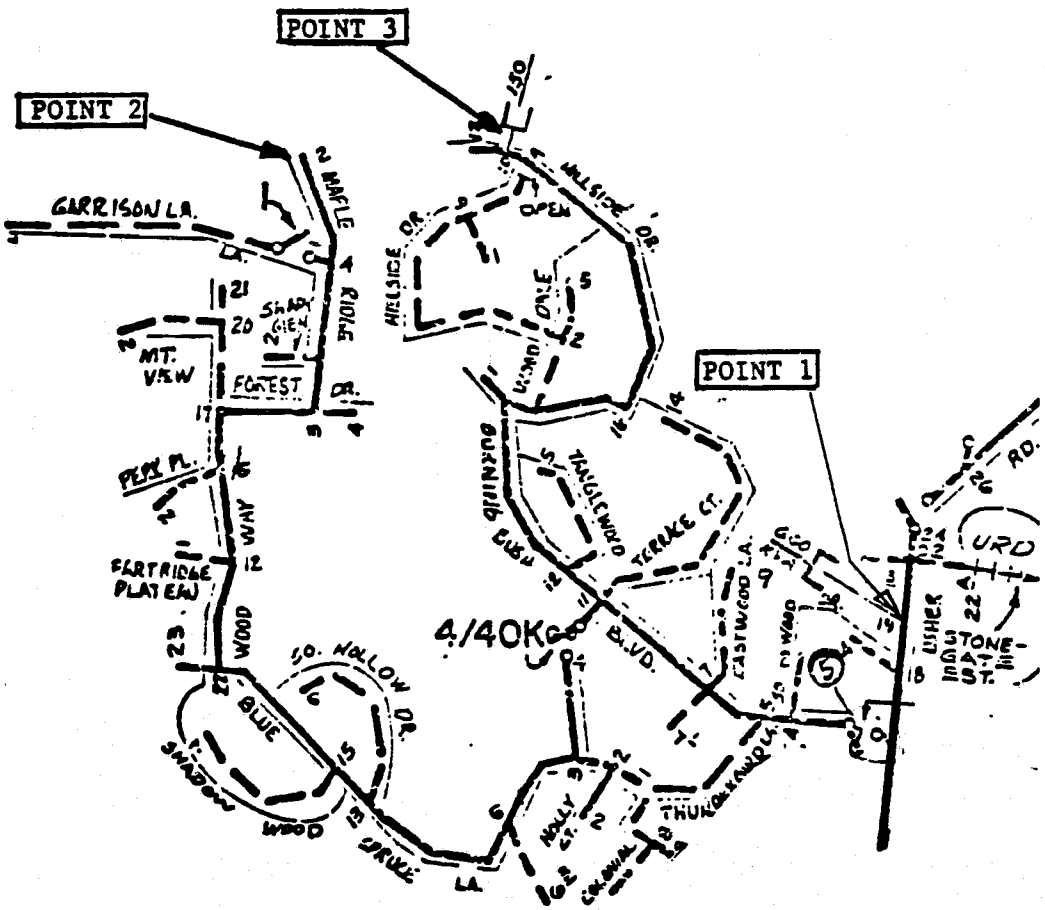

FIGURE 2

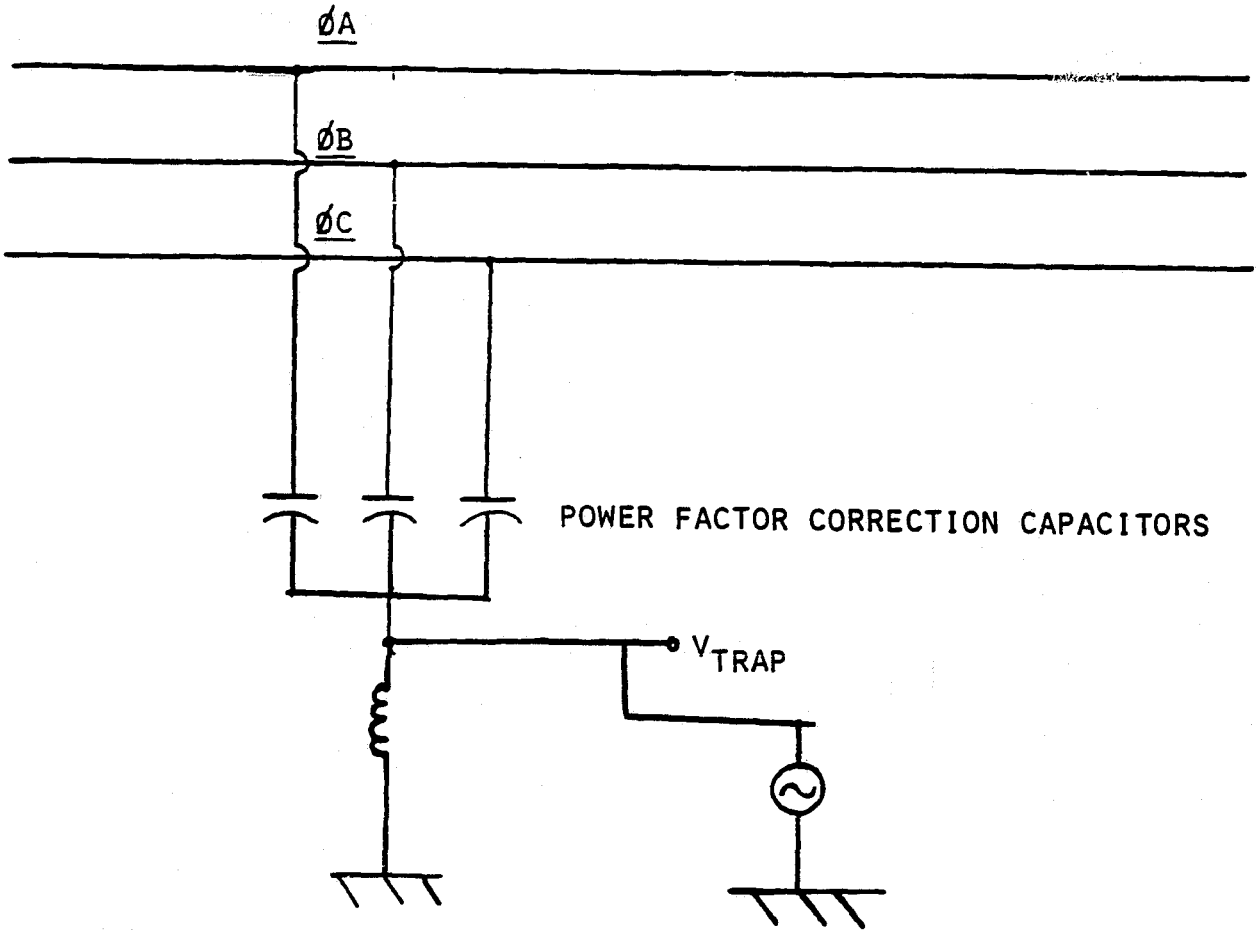

FIGURE 3

A coupling network with appropriate carrier frequency measurement equipment was connected near the end of the densely loaded section. This measurement apparatus, shown in Figure 4, was located at Point 2, Figure 2.

A power factor correction capacitor bank was located at another terminal point of the densely loaded section. This bank was located at Point 3, Figure 2. An inductor was placed in the ground lead of this bank also for the reason mentioned above. The carrier frequency voltage across this inductor was recorded during the measurements.

The end result of the field measurements were voltage transfer ratios. Individual phase voltages at the transmission point were calculated by use of the measured transmit voltage at Point 1. Assuming the admittance of the power factor correction capacitors was much larger than the admittance seen looking out onto the feeder network at the capacitor bank location, the phase voltages at the capacitor bank are nearly equal to the inductor voltage at the transmission point shown in Figure 3. Knowledge of these phase voltages at the transmission point provides a means to calculate individual voltage transfer ratios for each phase between Point 1 and Point 2 on Figure 2. Also, since the inductor voltage (a vector sum representative of the phase voltages at that point) was measured at the capacitor bank at Point 3, voltage transfer ratios between Point 1 and Point 3 were calculated from the measurements.

COUPLING AND MEASUREMENT NETWORK

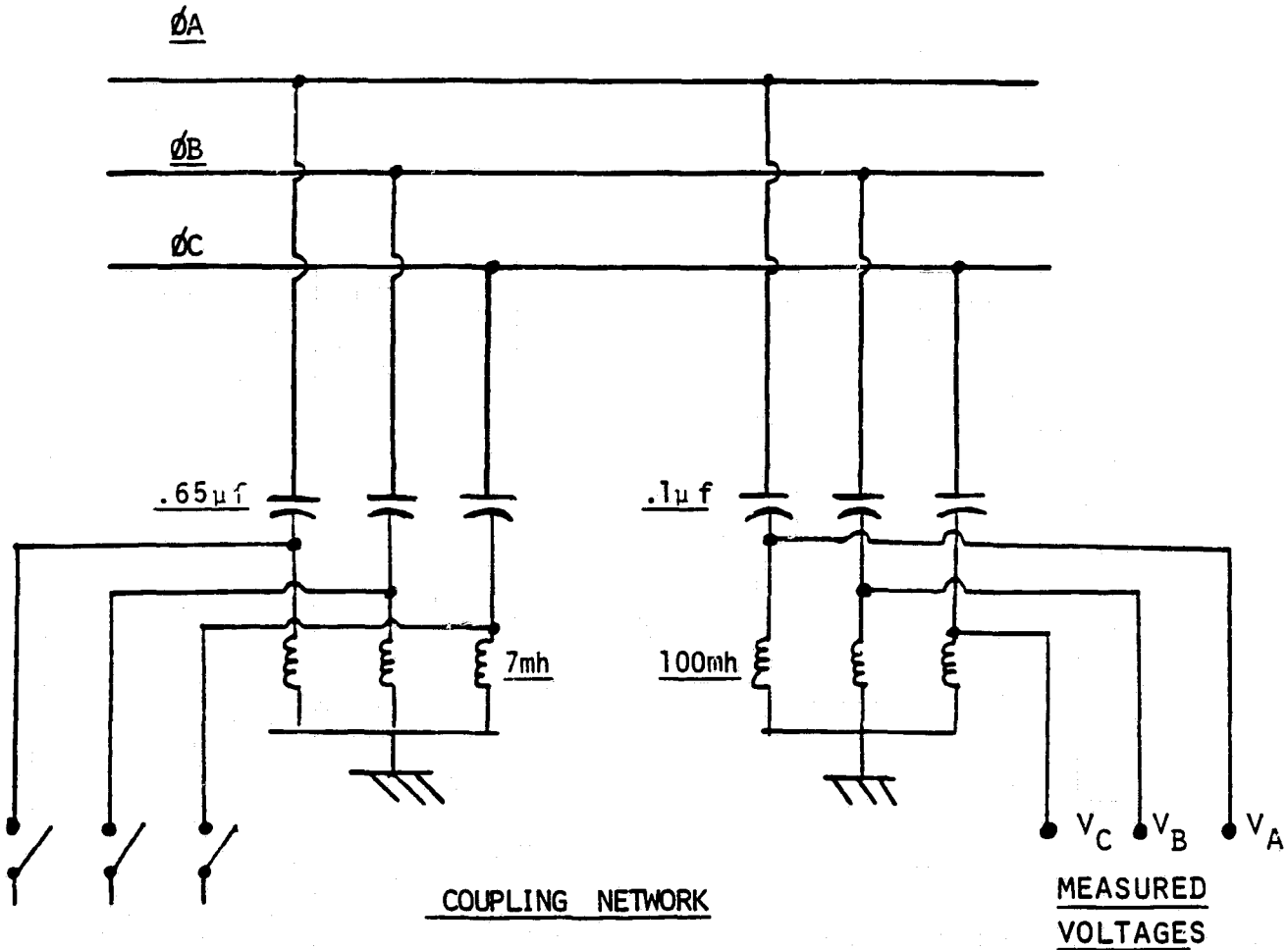

FIGURE 4

Figures 5, 6, and 7 show the comparisons of the measured and computed voltage transfer ratios between Points 1 and 2 for Phases A, B, and C, respectively. Figure 8 shows a comparison of measured and computed voltage transfer ratios between Point 1 and Point 3, the voltages being compared in Figure 8 are the inductor voltages at the capacitor bank locations. (Point 1 and Point 3, Figure 2).

CONCLUSION

The model simulations show agreement of sufficient accuracy with the measured data for communication system engineering purposes. The model results are influenced somewhat by the loading level of the distribution transformers. These simulations assumed a 20% load factor on the distribution transformers. This loading level was assumed after conferring with utility personnel, taking into consideration weather conditions and the time of day at which the measurements were made, with regard to system electrical loading. The power factor of the load on the distribution transformer secondaries was assumed to be .8 lagging. It should also be kept in mind the model assumed a time invariant network with respect to loading, while during the field test there probably was some variation in the feeder loading.

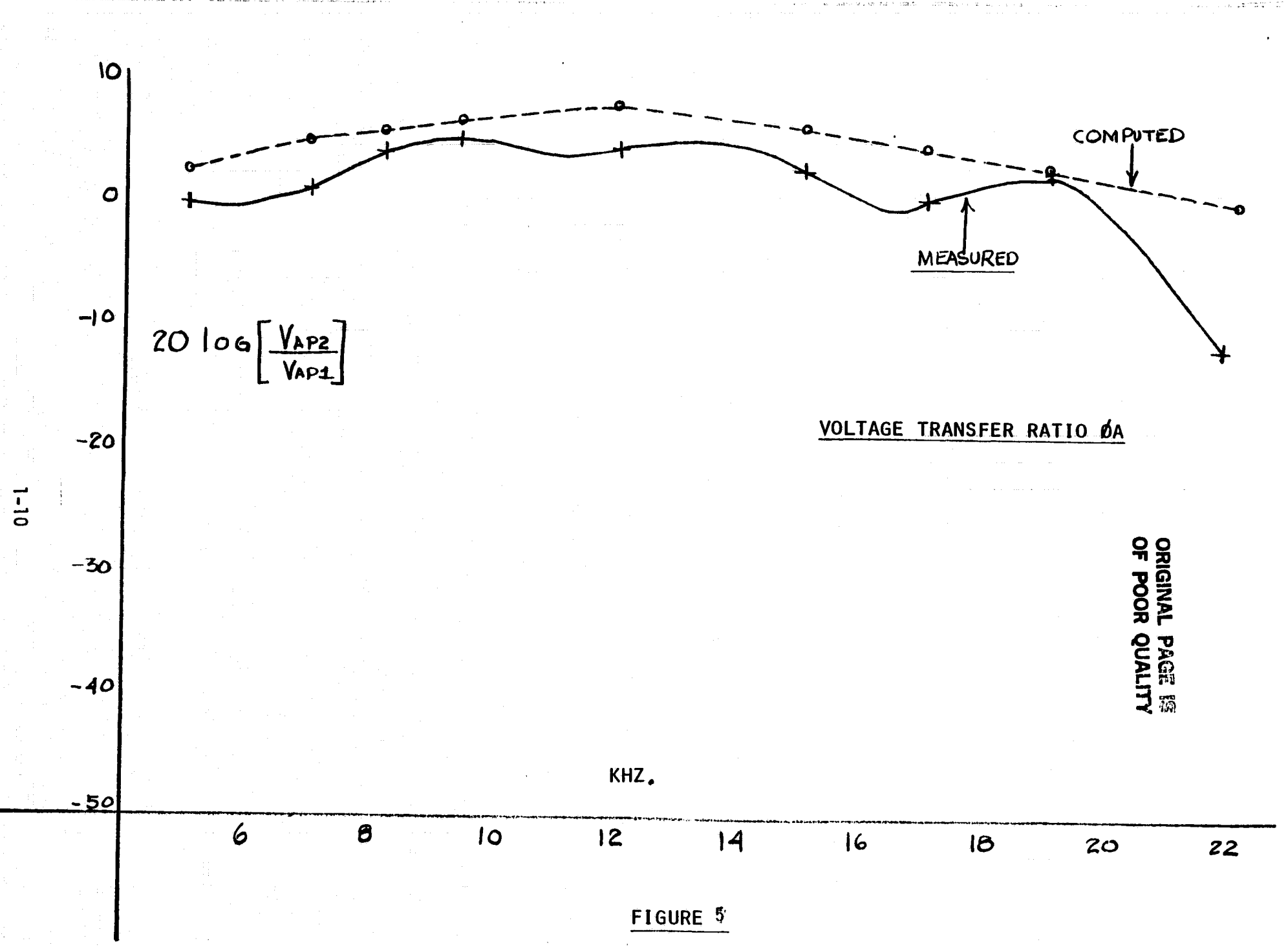

FIGURE 5

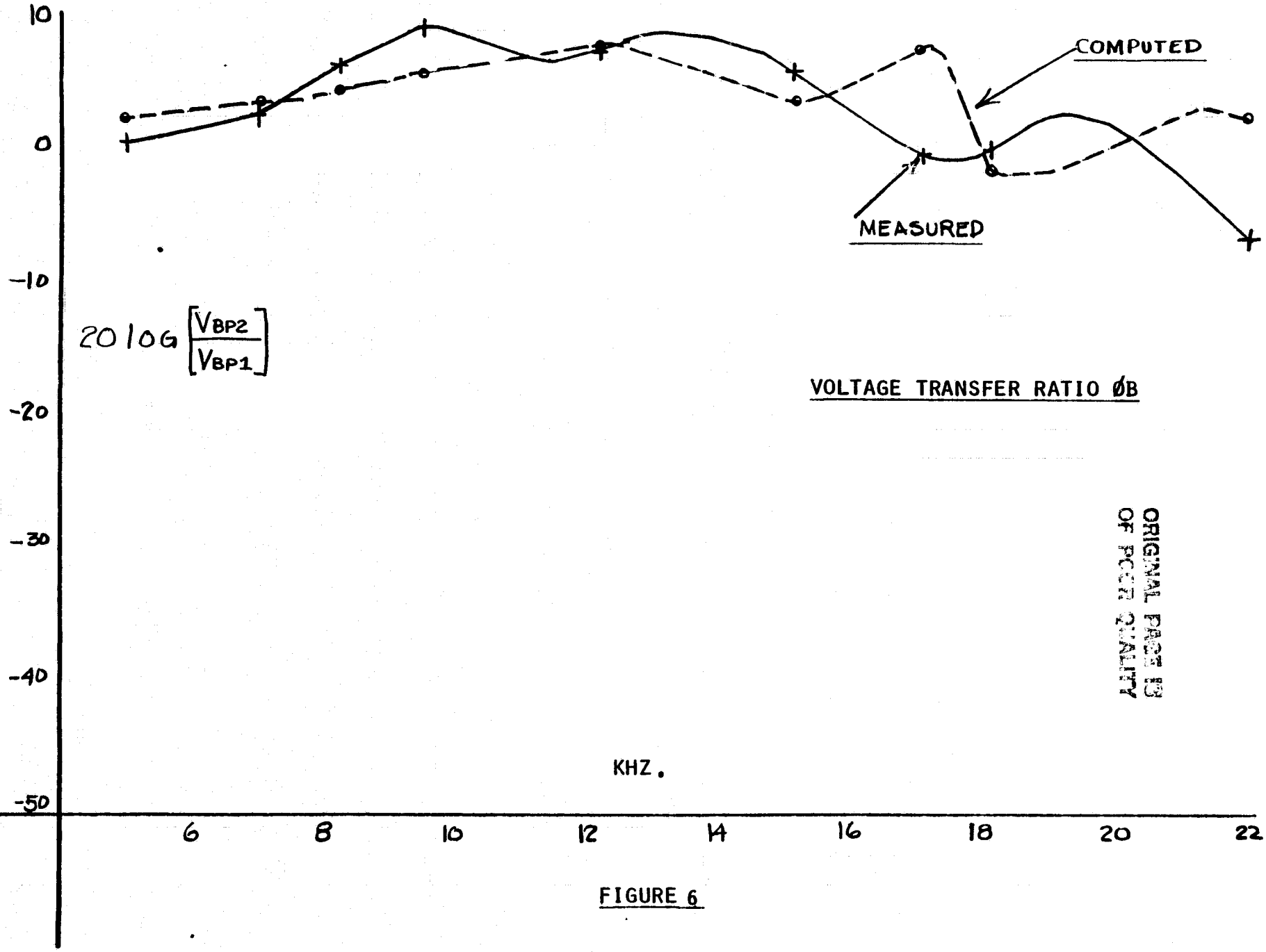

FIGURE 6

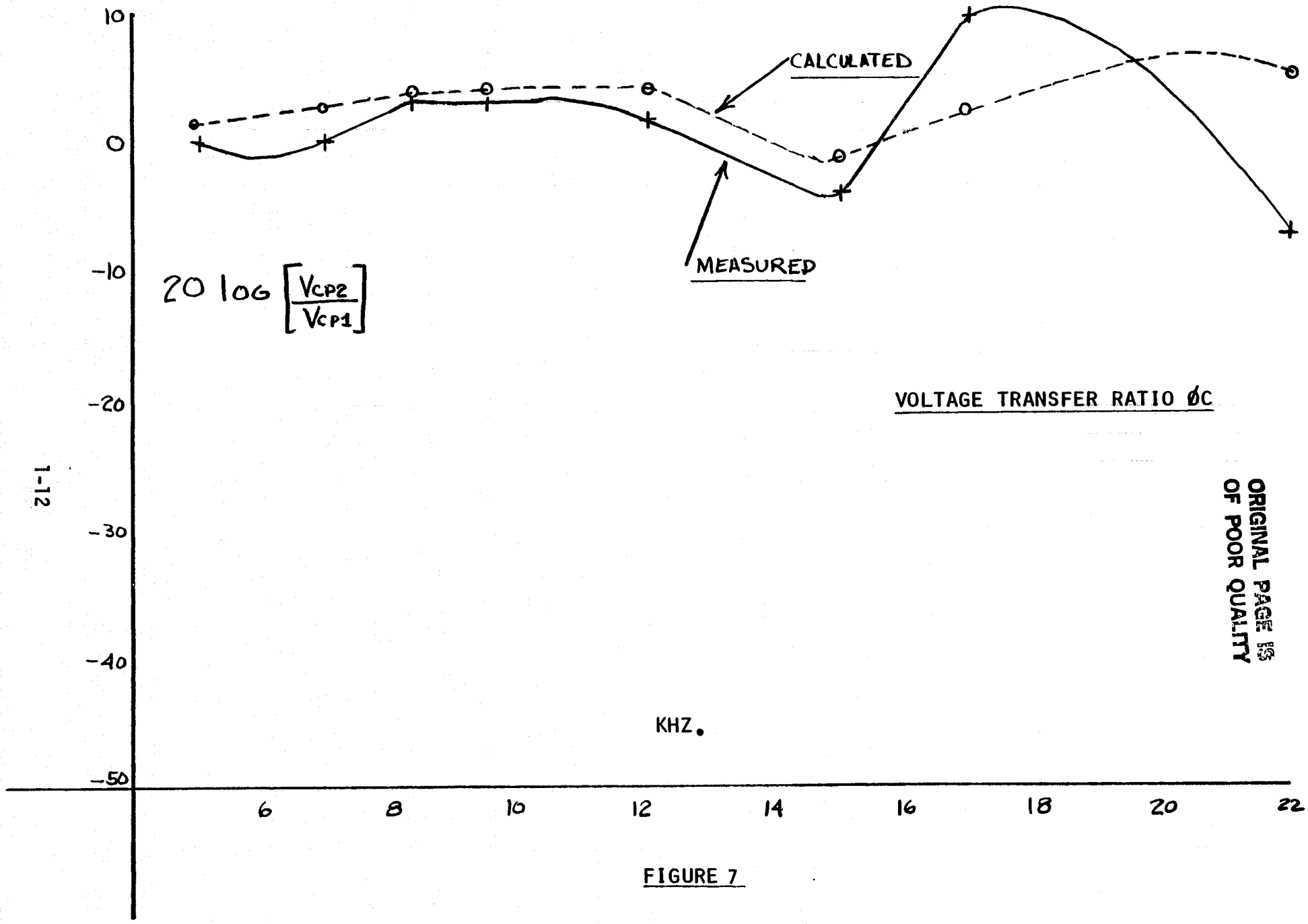

FIGURE 7

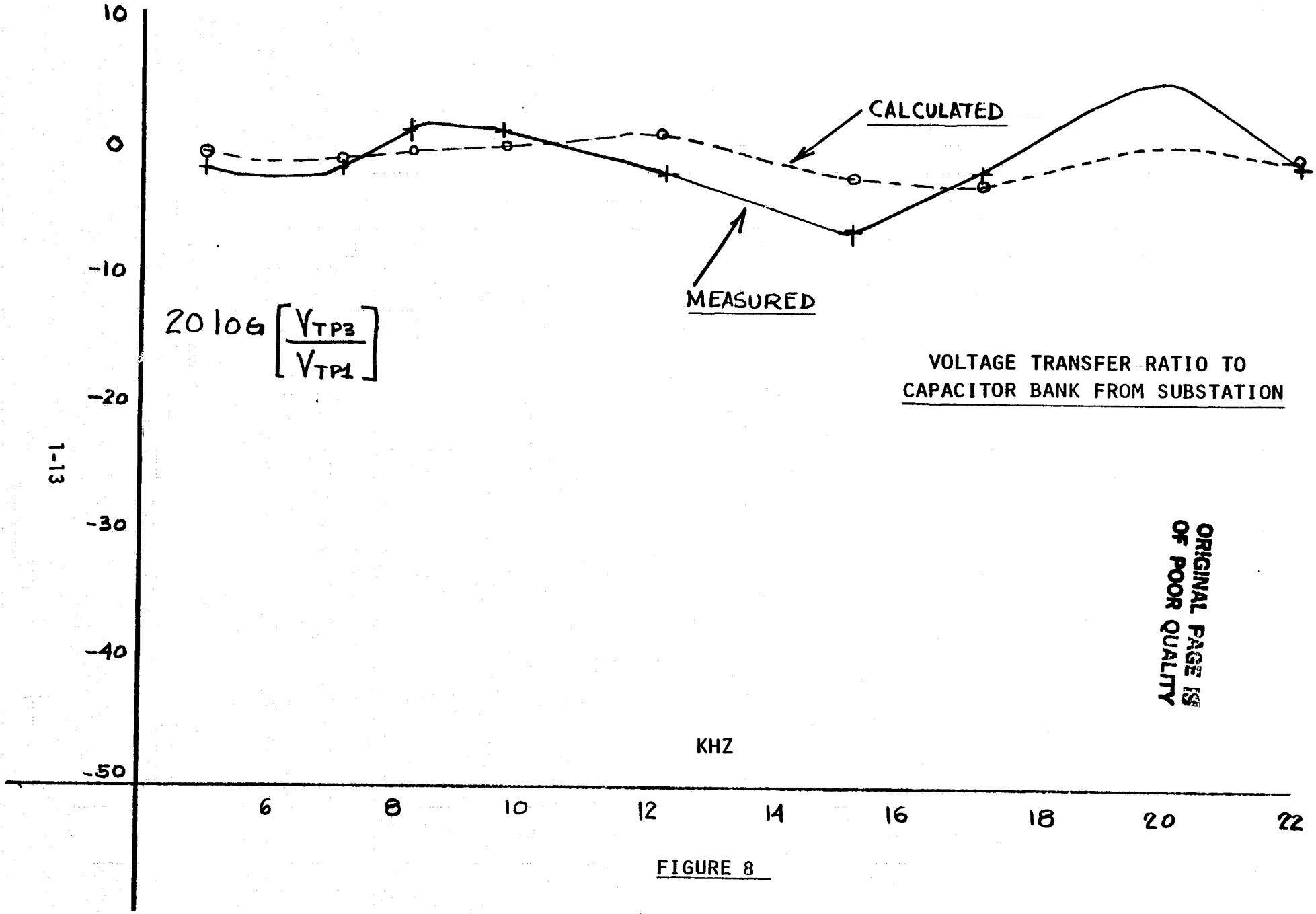

FIGURE 8

TASK (1)(B)

DIFNAP MODEL VERIFICATION
FULL SIZE DISTRIBUTION FEEDER

Introduction

Distribution line carrier voltage propagation measurements were performed on feeder 34556 of the Niagara Mohawk Grooms Road Substation in Clifton Park, N.Y. The feeder operating voltage is 13.2 kv line to line with single phase sections where the operating voltage is reduced to 4.8 kv line to line. These sections are shown in Figure 1. Simulations of these measurements were performed using the DIFNAP system programs in order to verify their utility in predicting distribution line carrier propagation as an aid to communication system engineering.

Background

Feeder 34556 is a radial distribution circuit. The total length of the main trunk circuit is about 10 miles. The following common distribution system features are found on 34556.

1) Power factor correction capacitors
2) Direct buried underground cables
3) Ratio bank transformer's (13.2 kv - 4.8 kv)
4) Long single phase branches
5) "Densely" loaded residential areas
6) 3Ø commercial & light industrial loads
7) Several different overhead conductor geometries and conductor sizes.

The points labeled 1,2,3 & 4 on Figure 1 denote the location of 3Ø capacitor banks. An inductor was placed in the ground lead of the capacitor bank's as shown in Figure 2. This was done in order to prevent the capacitors from providing a large current sink to the carrier signals. During the measurements, the carrier voltage across the inductor was monitored and recorded to give an indication of the vector sum of the phase voltages. Sufficient precautions were taken to prevent 60 Hz. voltages from affecting the carrier voltage measurements.

Individual phase voltages were monitored at point (2), Figure 1. At this point, access was gained to the individual overhead phase conductors. Within a few hundred feet of this pole is a cable riser providing service for the Country Knolls West residential area which is served by direct buried underground cable. Extensive measurements and DIFNAP simulations on this cable network were reviewed in a previous report. The coupling network employed at Carlton Rd. (point 2, Figure 1) is shown in Figure 3.

During the field measurement, three distinct conditions existed on the feeder which were treated by simulation. These conditions were:

Condition 1. No coupling network connected at Carlton Rd. Inductor voltages were monitored at Points (2) and (3) shown on Figure 1. Transmit voltages were monitored on Phase A at the substation as shown in Figure 4. Phase voltages were assumed equal at the substation for modeling purposes.

Condition 2. Coupling network connected at Carlton Rd., but with tuning inductors disconnected. Individual phase voltages were monitored at Carlton Rd. Inductor and transmit voltages monitored as in Condition 1.

ORIGINAL PAGE IS
OF POOR QUALITY

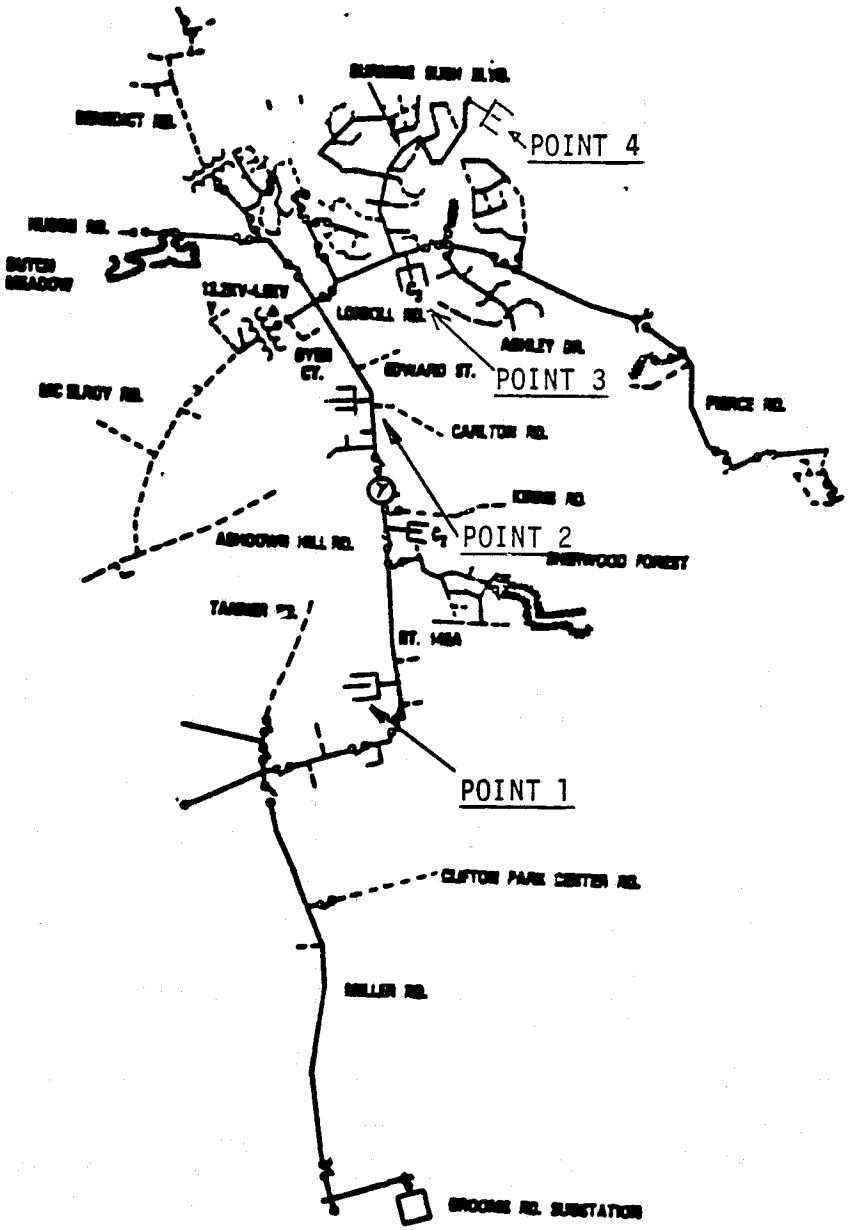

FIGURE 1
GRSS 34556
FEEDER

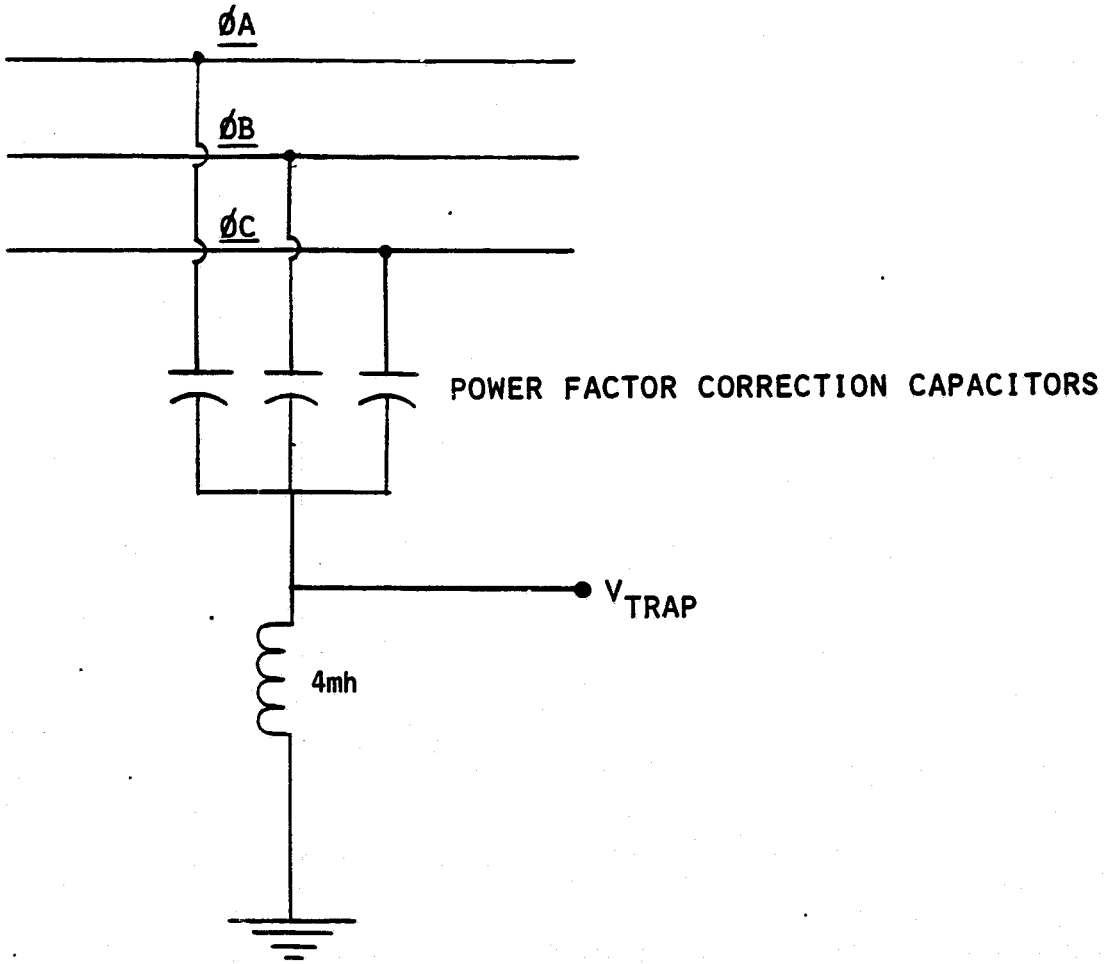

FIGURE 2

POINTS 1,2,3,4 POWER FACTOR CORRECTION CAPACITORS AND NEUTRAL LEAD INDUCTOR

POINT		3økvar
1		300
2		300
3		600
4	1-17	150

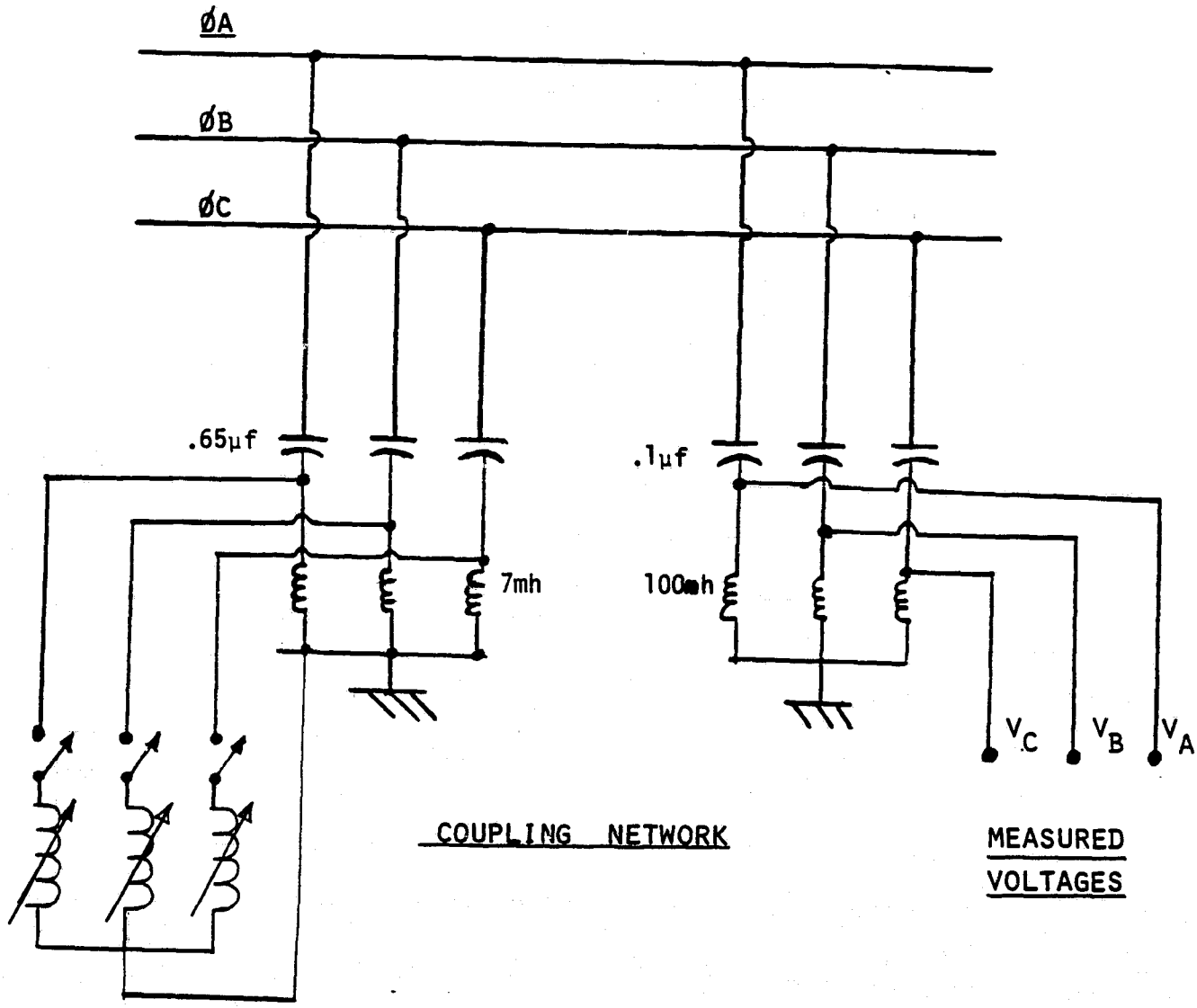

FIGURE 3

POINT 2 SHUNT LOADING NETWORK

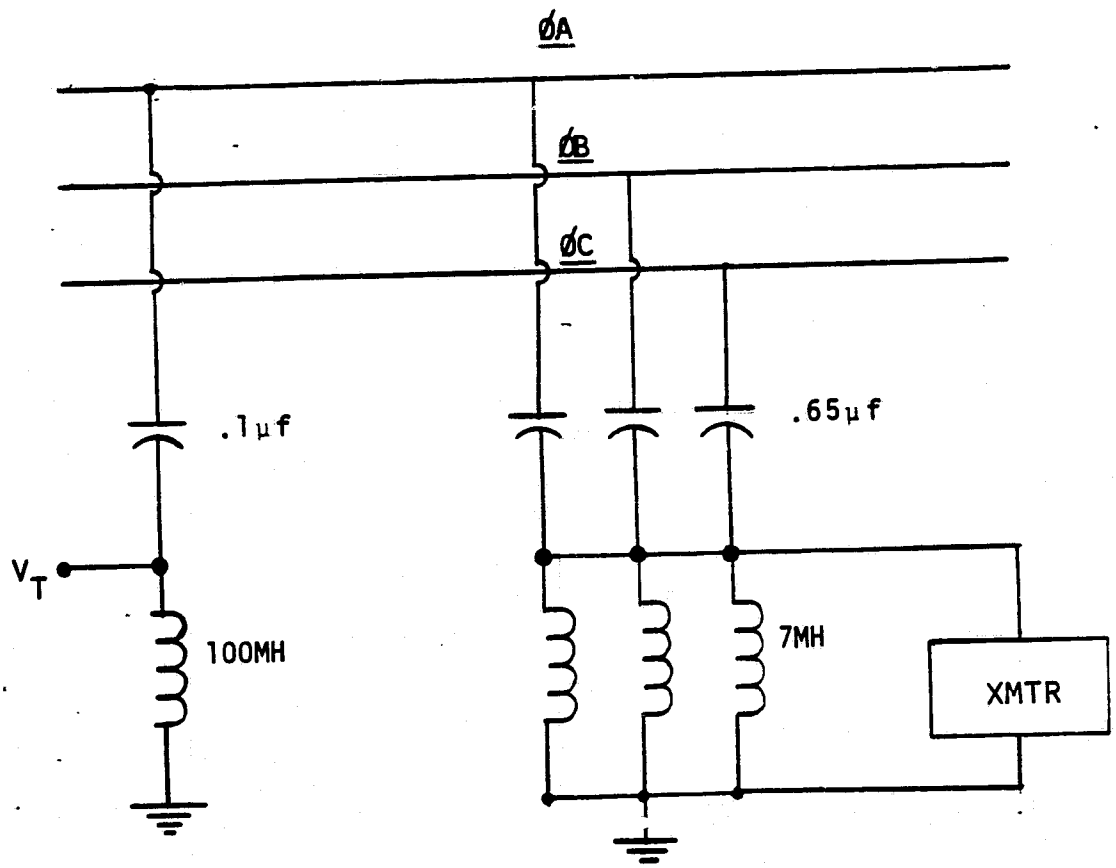

FIGURE 4

EQUIPMENT CONFIGURATION AT G.R.S.S.

Condition 3. Coupling network connected with tuning inductors in place at Carlton Rd. The same quantities mentioned in Condition 2 were again recorded.

Simulations were performed at the following frequencies:

5010 Hz
6990 Hz
8130 Hz
9510 Hz

Corresponding to measurements performed on the feeder. Table 1 provides the diagonal elements of the admittance matrices representing the coupling/tuning network loading under Conditions 2 and 3. The off-diagonal elements of these matrices were assumed to be negligible.

Results

The first situation to be considered will be the Condition 1 outlined above. Under this condition, the network is essentially "normal". Figures 5 and 6 show a comparison of the simulation results and field measurements of the inductor voltages at points 1 and 3, respectively. The inductor voltage was arrived at by making use of the admittance matrix (Y) of the inductor-capacitor network. The current vector $\bar{I}$ is, $\bar{I} = Y \bar{E}_p$, where $\bar{E}_p$ is the phase voltage vector provided by the program. The sum of the currents in the vector $\bar{I}$ was then used to calculate the voltage across the inductor. The voltage transfer ratio to the capacitor bank at Point 1 is much higher and more uniform across the frequency range than that at Point 3.

Under Condition 2, the coupling network was now attached to the phase conductors at Point 2 on Carlton Rd. This coupling network,

TABLE 1

Diagonal Elements of Coupling Network
Admittance Network - Lossless Elements
Assumed for Conditions 2 & 3

Condition 1 - Not applicable

	Condition 2			Condition 3		
Freq.	Y_A	Y_B	Y_C	Y_A	Y_B	Y_C
5010	-.J0058	-.J0058	-J0058	j.0209	-j.0115	j.058
6990	-.J0037	-.J0037	-.J0037	j.0304	-j.0066	-j.108
8130	-.J0030	-.J0030	-.J0030	j.0364	-j.0053	-j.047
9510	-.J0025	-.J0025	-.J0025	j.0443	-j.0044	-j.029

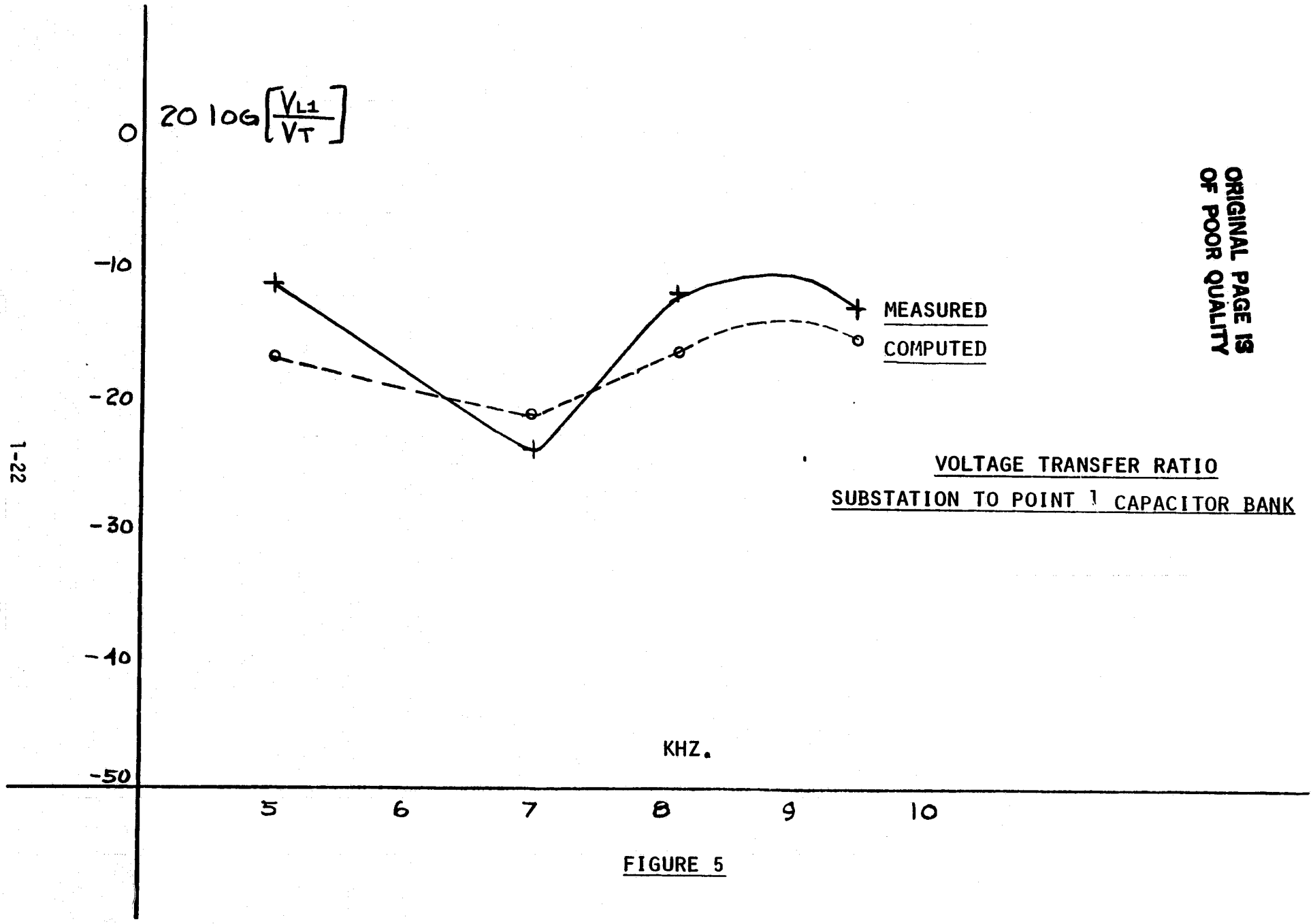

ORIGINAL PAGE IS
OF POOR QUALITY

VOLTAGE TRANSFER RATIO

SUBSTATION TO POINT 1 CAPACITOR BANK

FIGURE 5

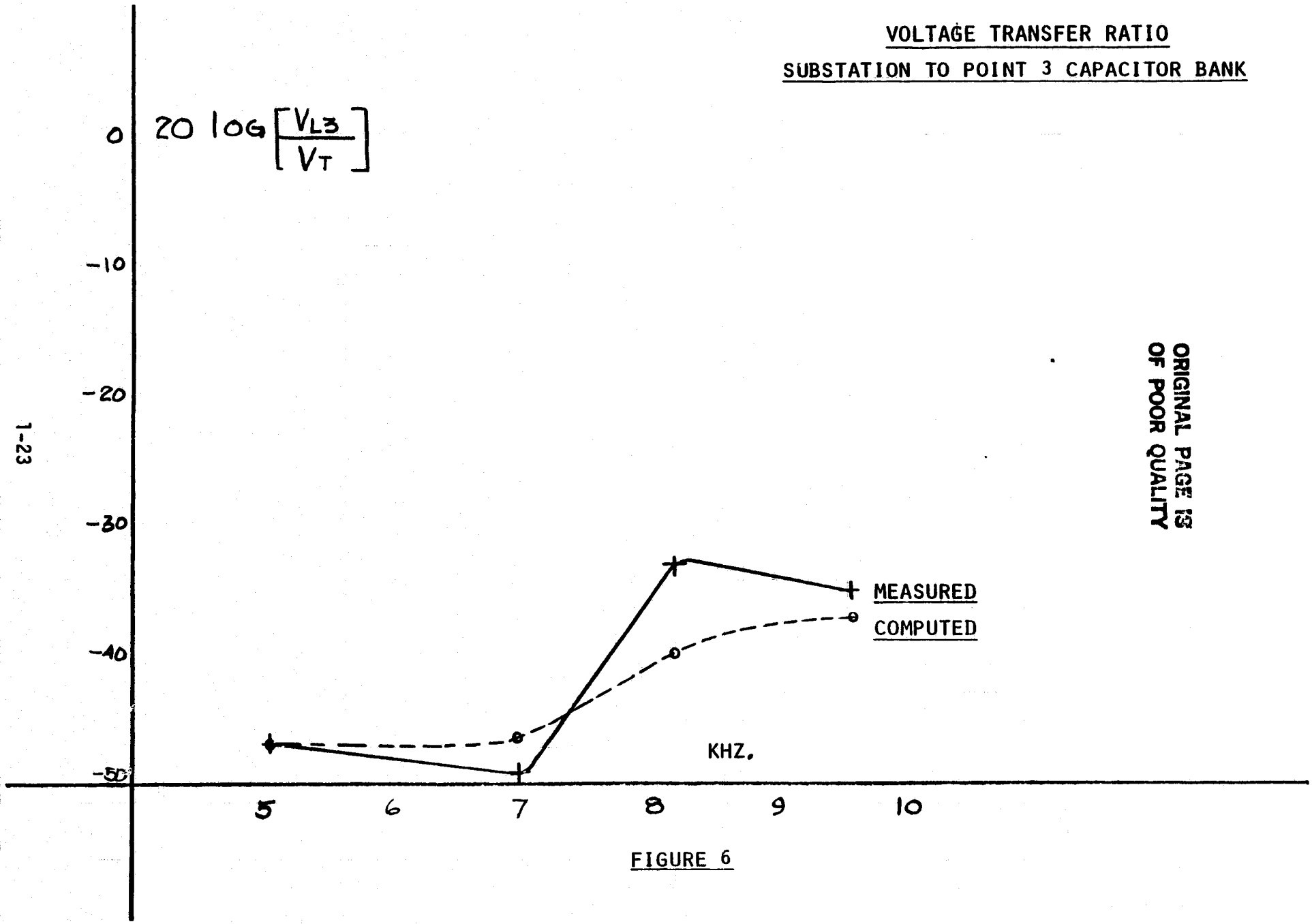

FIGURE 6

diagrammed in Figure 3, represented a significant loading effect on the network. Table 1 shows that without the tuning inductors attached, the coupling network presents an inductive load. Figures 7 & 8 show comparisons of measured & computed results at Points (1) & (3). With the coupling network now attached, it was possible to measure the individual phase voltages. Figures 9, 10 and 11 show comparisons between measured and computed voltages on Phases A, B, and C of Carlton Road under Condition 2.

Under Condition 3, the tuning inductors were attached to the coupling/network. These inductors were then varied independently in order to maximize the voltage transfer from the substation to the capacitor bank at Point 3, Figure 1. Table 1 shows that Phases A and C were loaded capacitively, while Phase B was loaded inductively at Carlton Rd. at 5010 Hz. The tuning elements then remained fixed as frequency was increased. Figures 12 and 13 show the results obtained for the inductor voltages at Points 1 and 3, respectively. Figures 14, 15 and 16 show the phase voltage results under Condition 3 on Phases A, B, and C, respectively.

Conclusions

The simulations performed on the 34556 distribution feeder and subsequent comparisons to measured results were subject to several assumptions. These being:

1) The network configuration was specified accurately by utility personnel and on system maps.
2) Conductor lengths specified on utility map were accurate for engineering purposes.

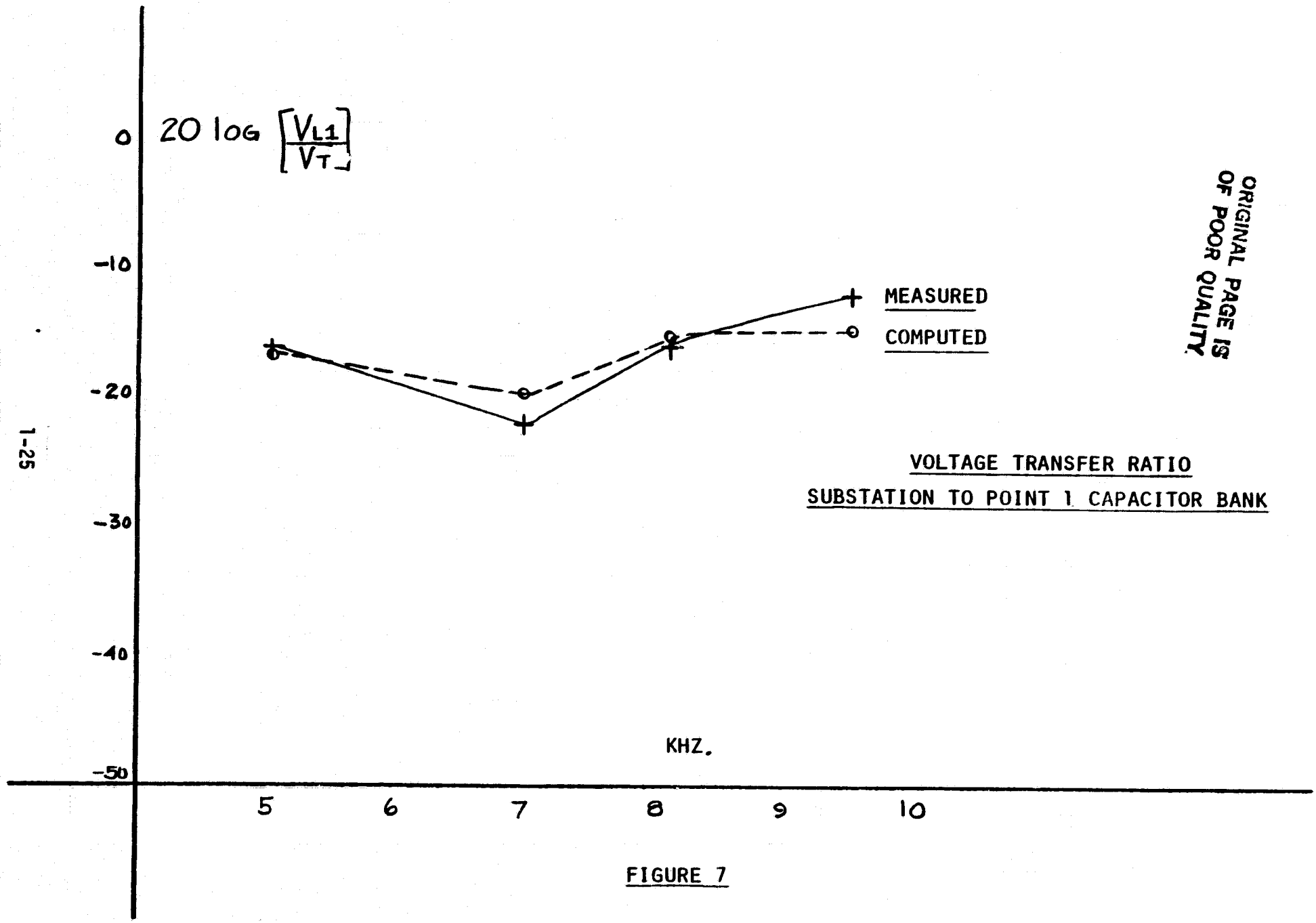

VOLTAGE TRANSFER RATIO

SUBSTATION TO POINT 1 CAPACITOR BANK

FIGURE 7

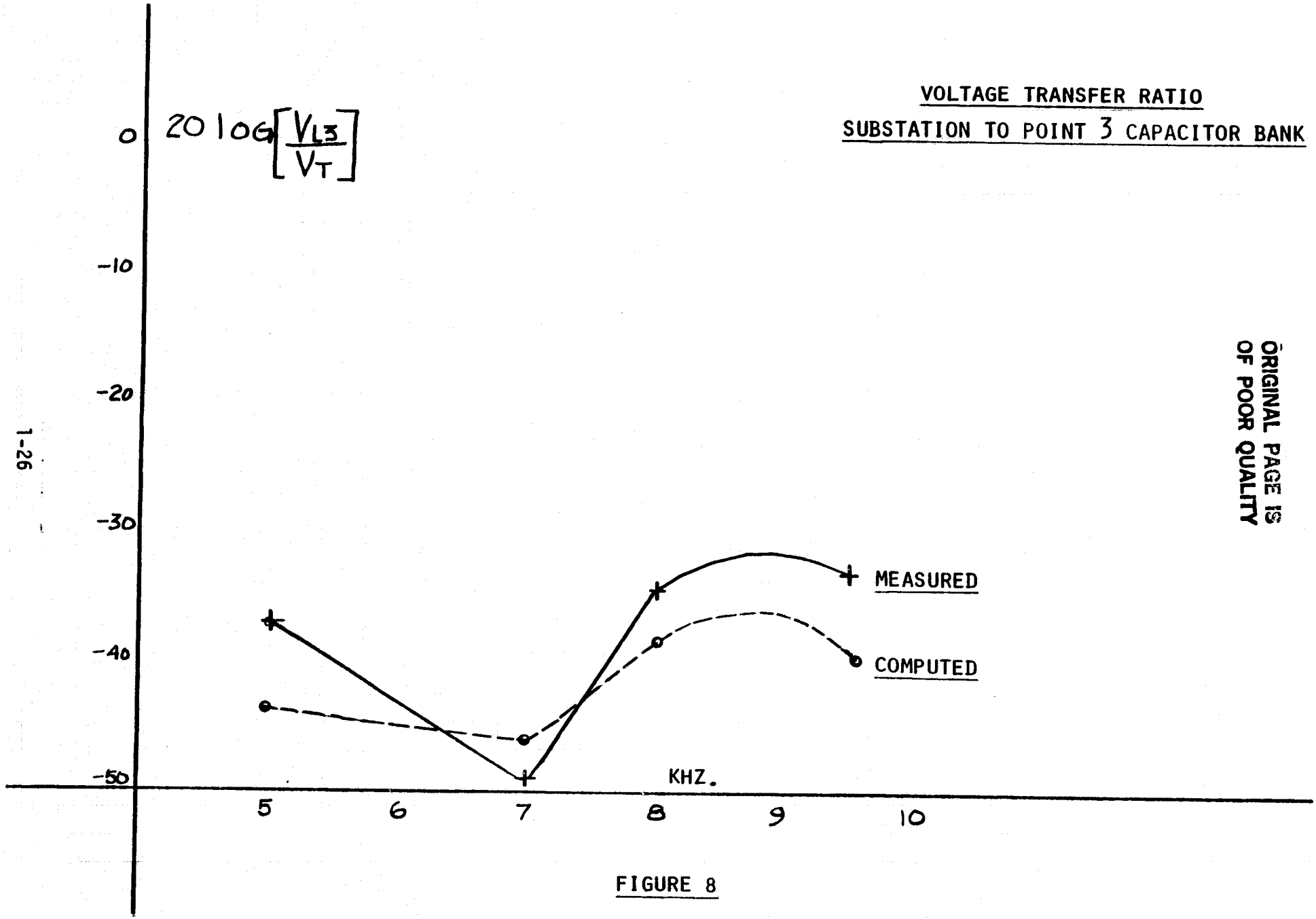

FIGURE 8

ORIGINAL PAGE IS
OF POOR QUALITY

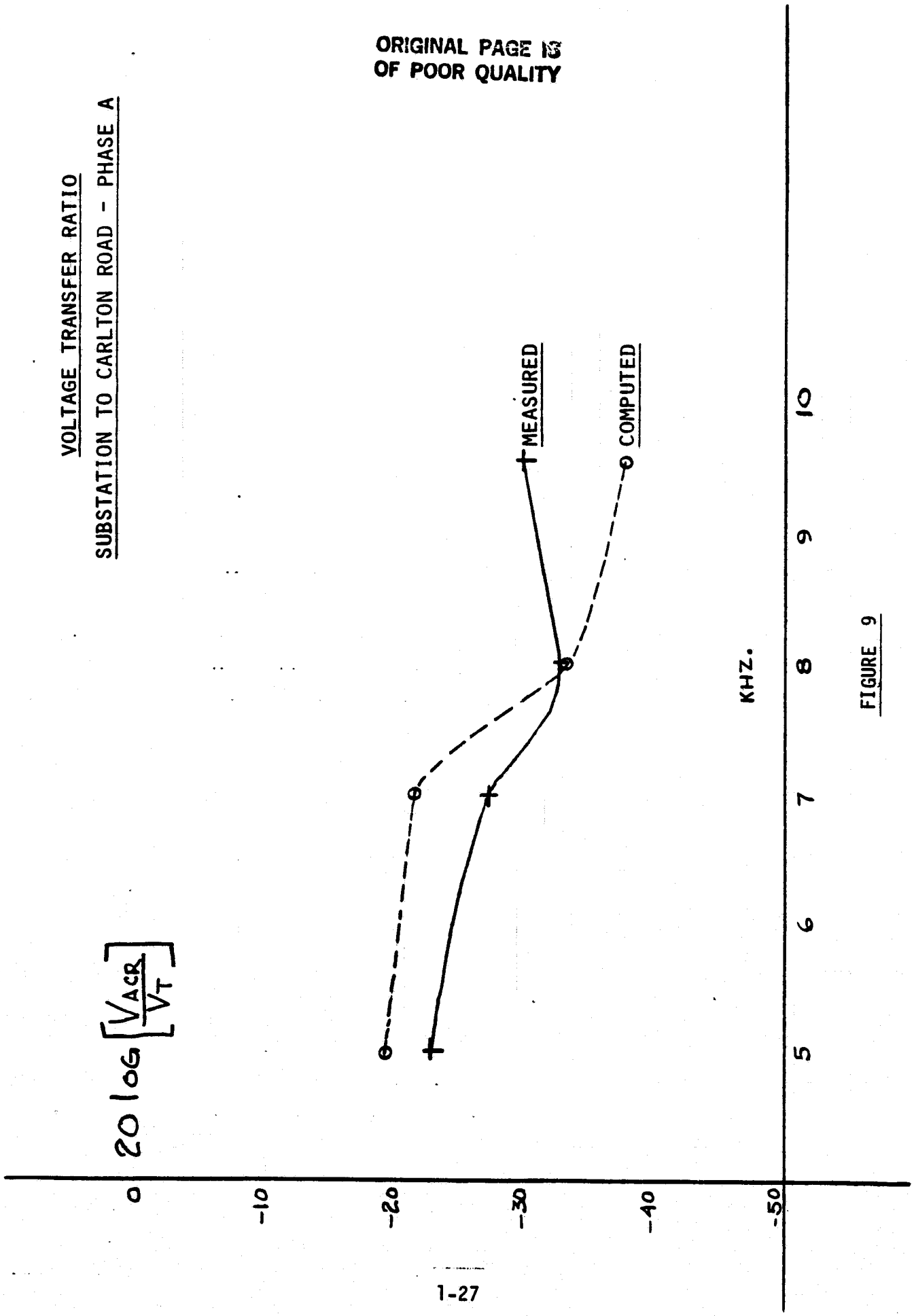

FIGURE 9

ORIGINAL PAGE IS
OF POOR QUALITY

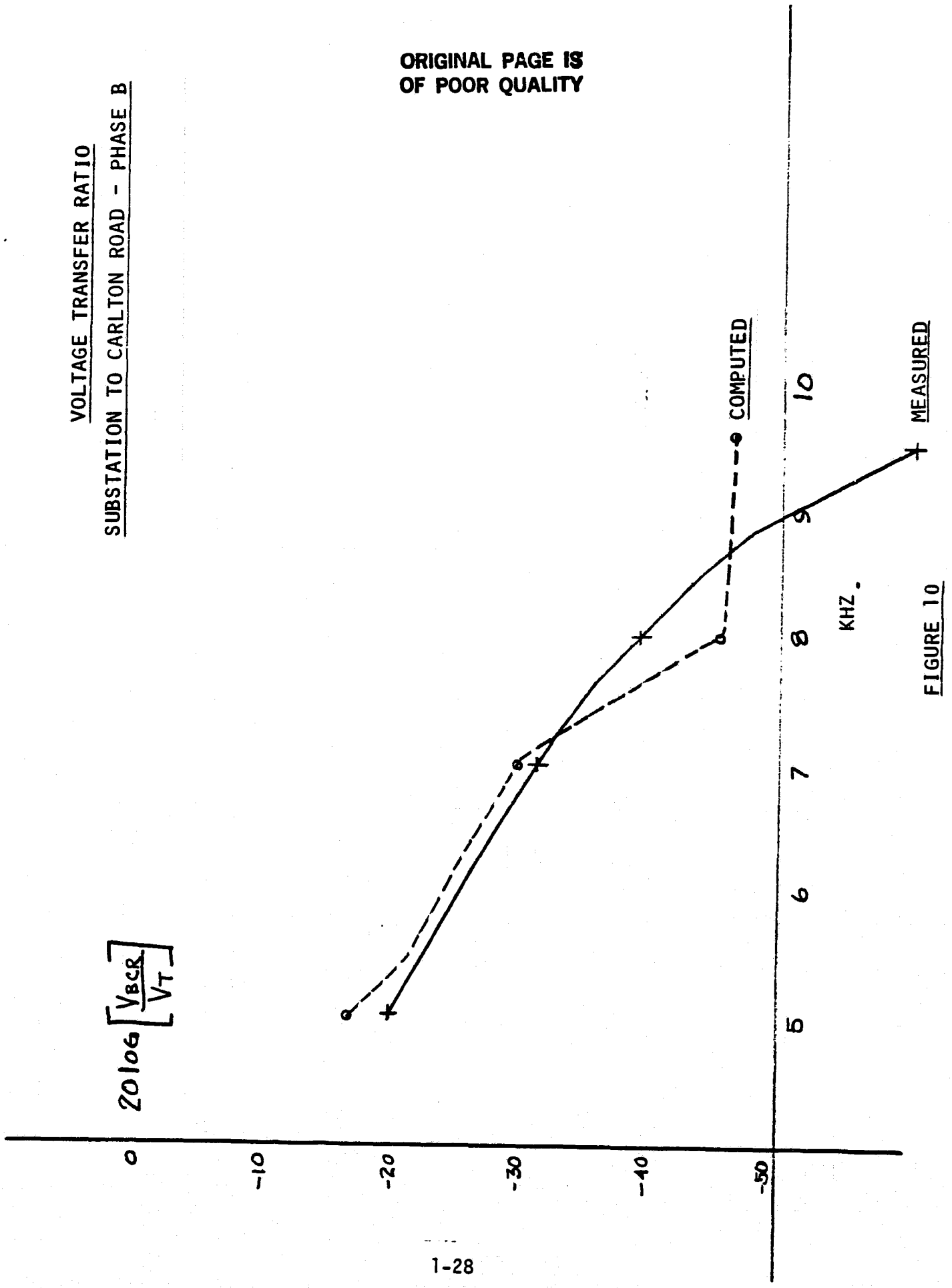

FIGURE 10

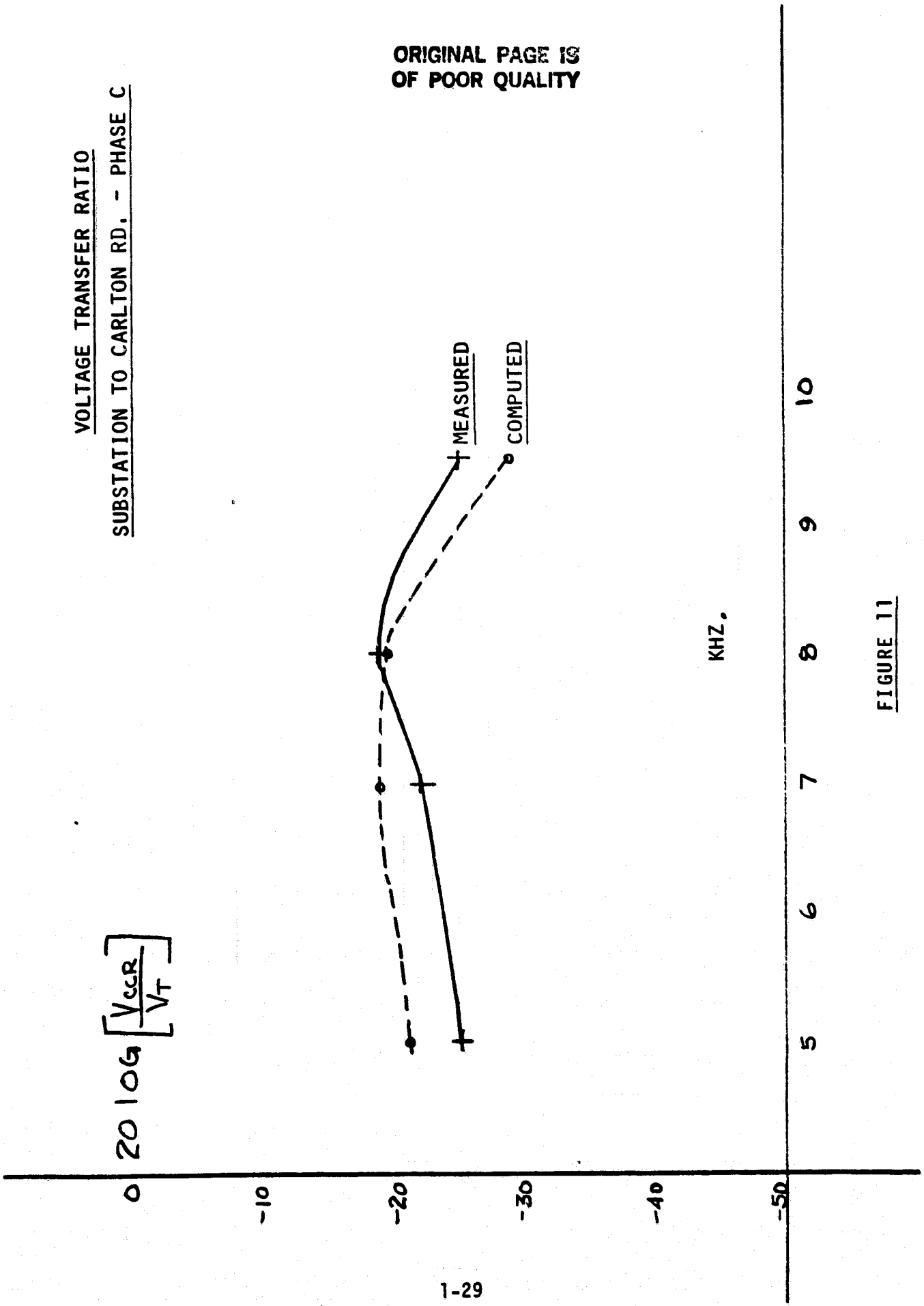

FIGURE 11

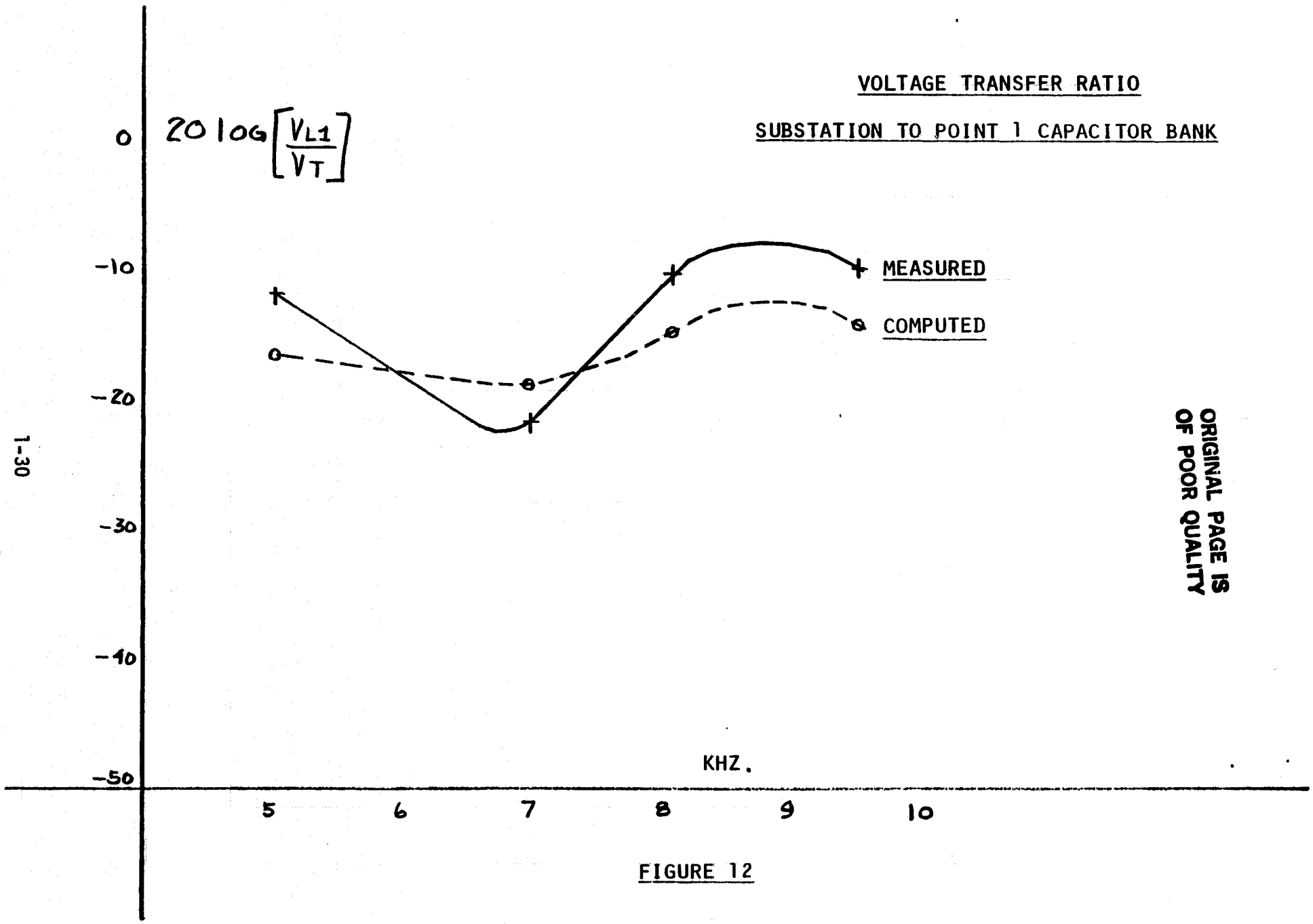

FIGURE 12

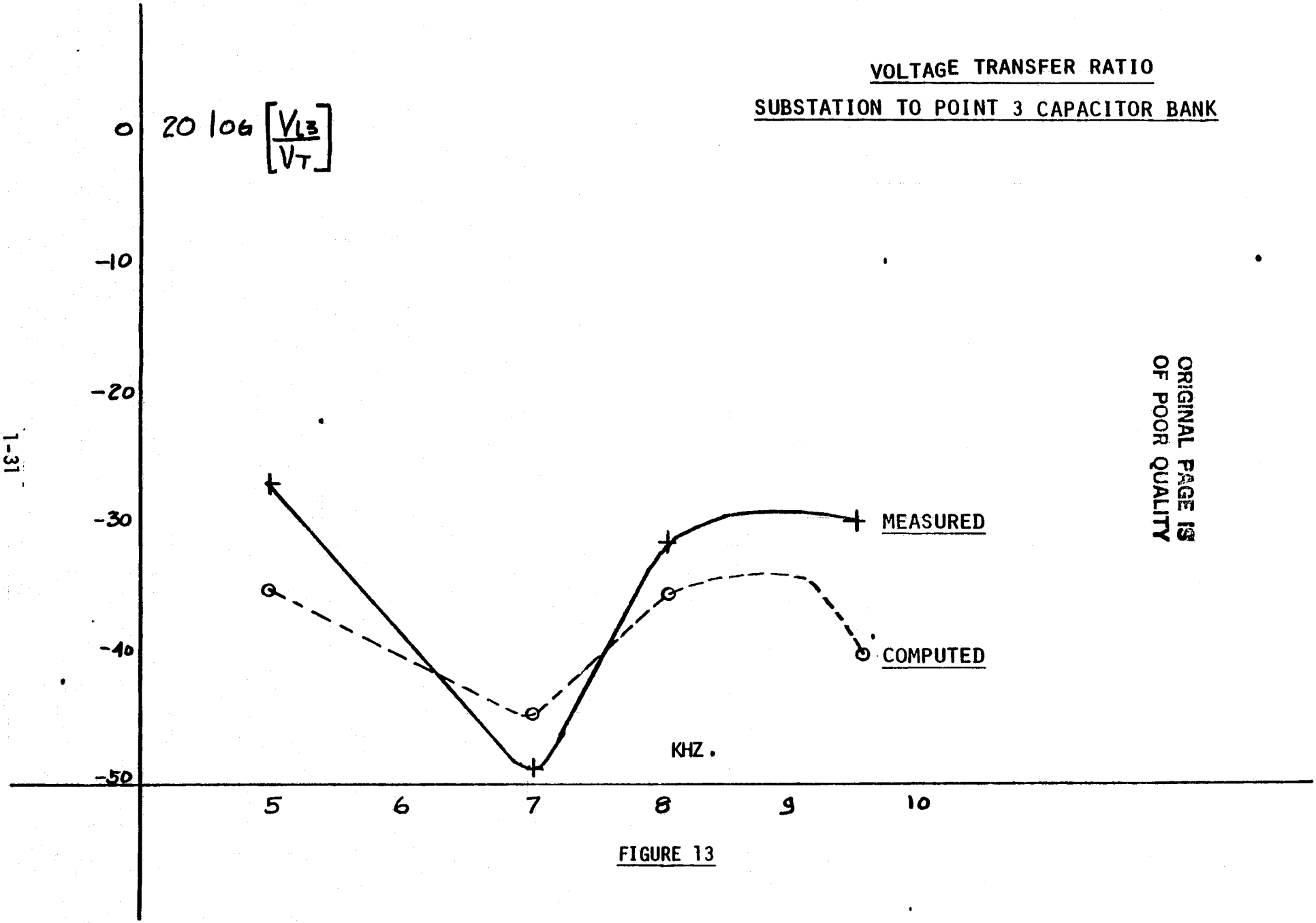

FIGURE 13

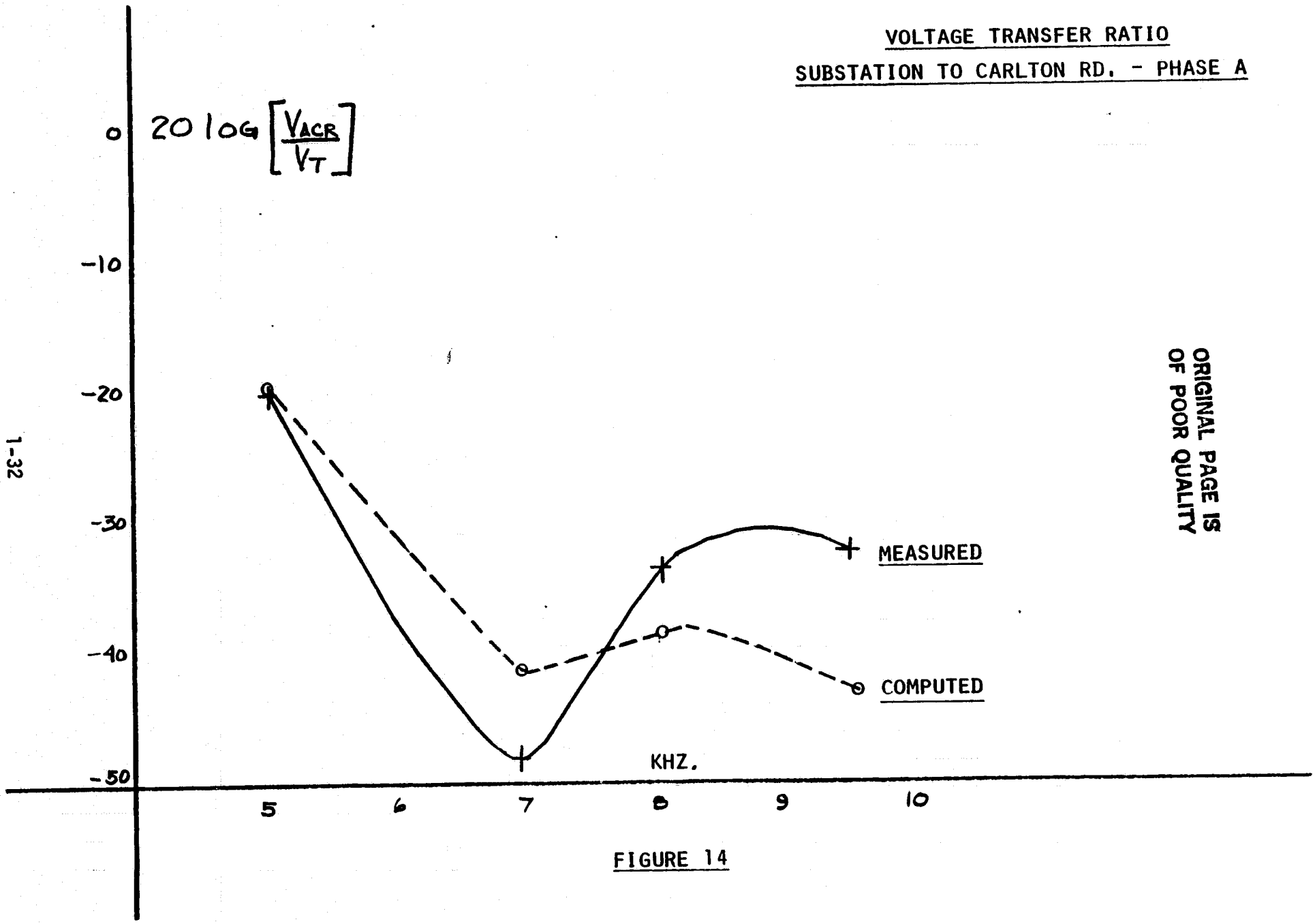
VOLTAGE TRANSFER RATIO
SUBSTATION TO CARLTON RD. - PHASE A
$20 \log \left[\frac{V_{ACR}}{V_T}\right]$
0
-10
-20
-30
-40
-50
5
6
7
8
9
10
KHZ.
MEASURED
COMPUTED
ORIGINAL PAGE IS
OF POOR QUALITY

FIGURE 14

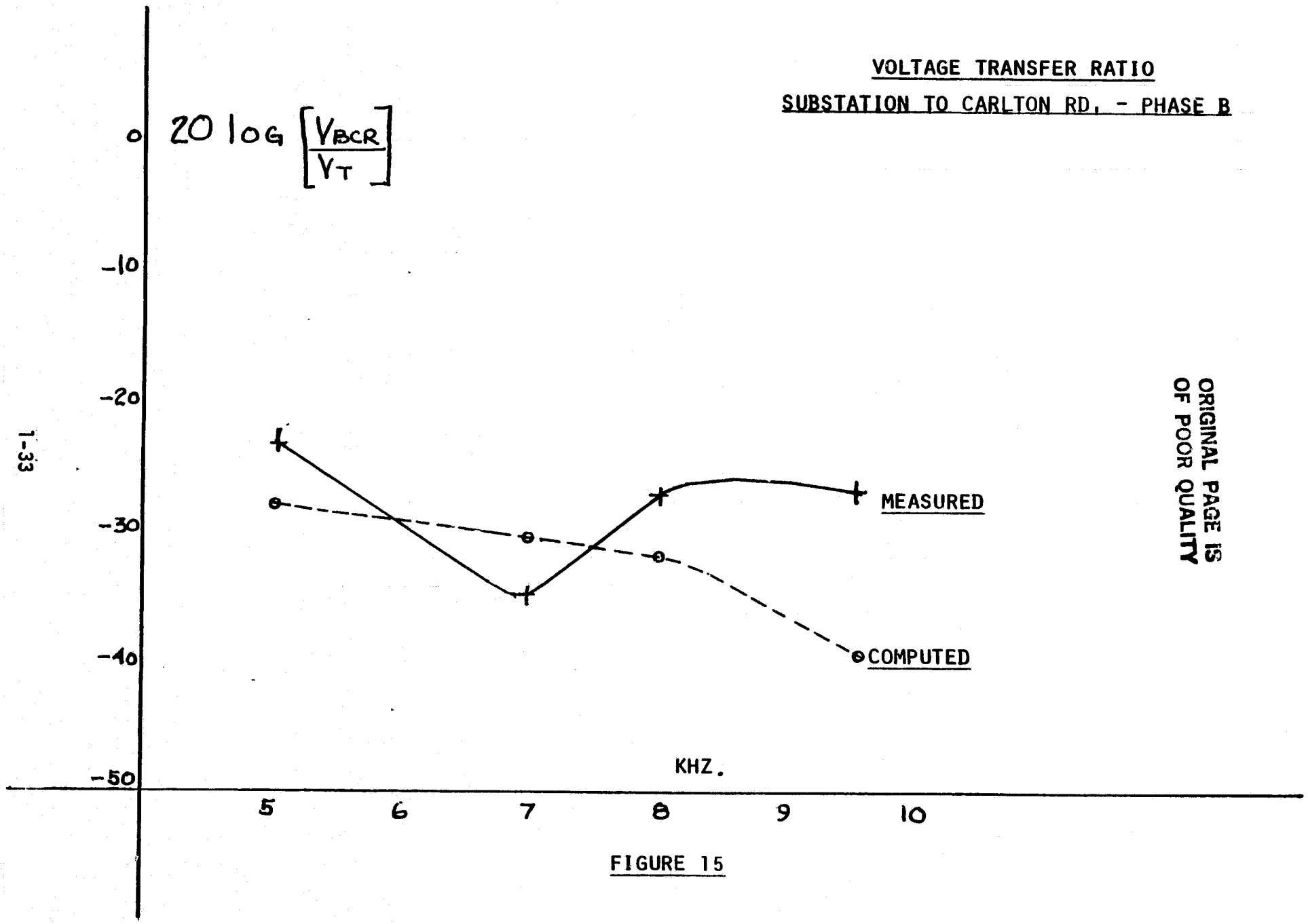

FIGURE 15

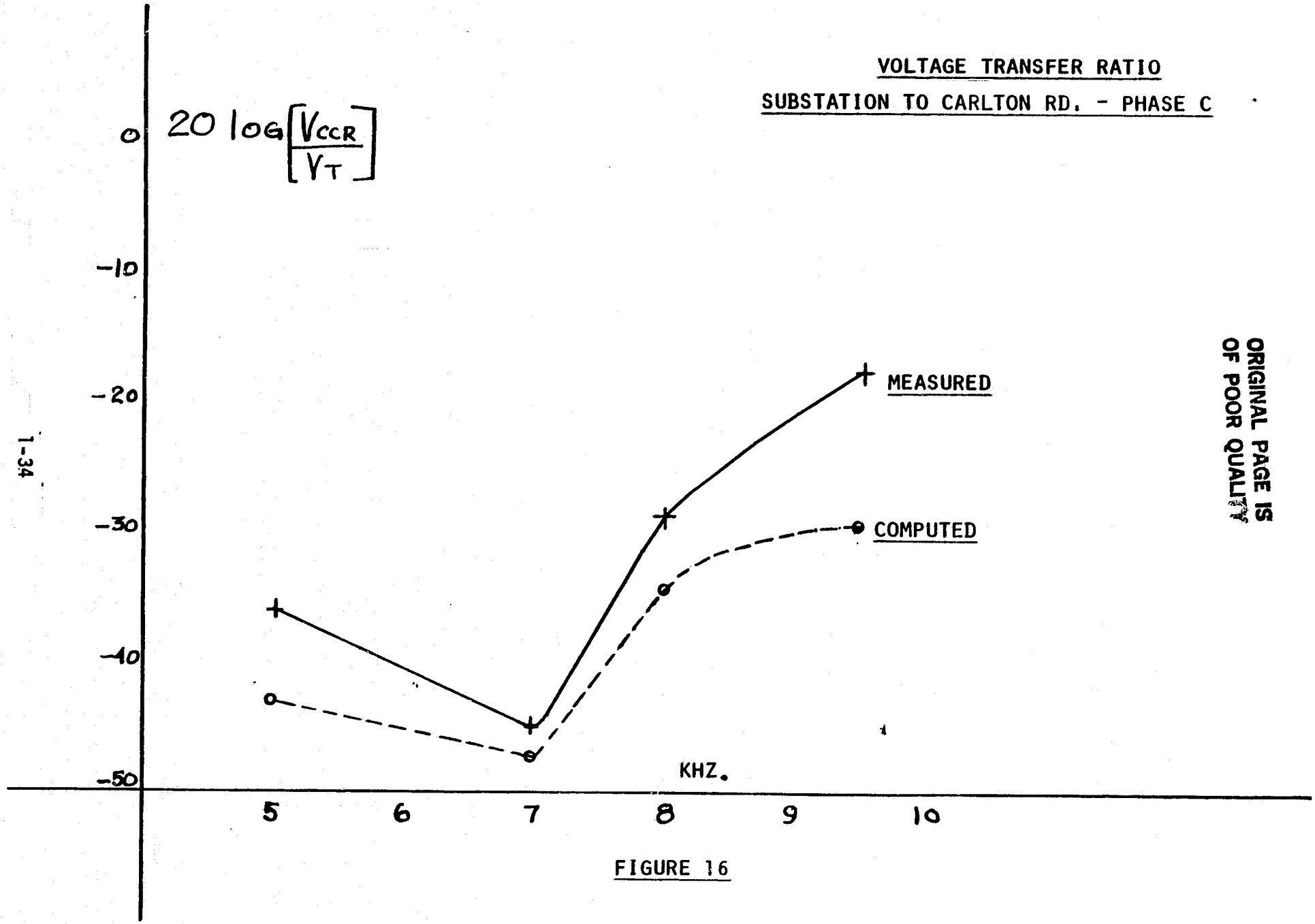

FIGURE 16

3) The assumption that each transformer was loaded to 20% of full kva capacity with a .8 power factor lagging load was a valid representation for distribution transformer loading.

   Under this assumption, the total connected load kva employed in the model was 3200 kva, if the load factor mentioned above was assumed. The measurements were performed during off-peak loading hours for the most part under moderate climatic conditions with respect to heating and cooling loads.

4) The coupling and tuning network components were known with sufficient accuracy for model purposes, and loss components present in these circuit elements were negligible at the frequency of interest.

5) Errors in field voltage measurements and data reduction were minor.

Since the voltage transfer ratio of the feeder is sensitive to the loading level, it would be advisable for engineering purposes to study the feeder response parametrically as a function of loading level in order to bracket system performance limits.

TASK (1)(C)

Underground-Overhead Transition

Introduction

As previously mentioned in the Foreword, two significant contingencies were encountered during the first attempts at verification. Both of these occurred with "subnetworks" involving underground cables. After considerable delay and extra experimentation, these contingencies were found to be caused by:

a) Inaccurate cable parameters

b) Errors in determining actual line lengths from utility documentation.

The first arose in attempting to adapt the Bonneville EMTP program to compute parameters for a cable configuration which was not explicitly available in its repertoire. To overcome this difficulty, a cable parameters program was developed to handle single conductor concentric, non ferrite sheathed cable. Also, it was discovered by making tests on samples, that the dielectric had a much higher dielectric constant than was originally assumed. Finally, it was discovered that line lengths given on utility documentation often did not take into account extra lengths for short laterals to vaults and transformers, and that often significant cable length was left in terms of a coiled end (for future splicing).

The contingencies resulted in some laboratory tests on cable samples, development of the computer program, and a special field test on a 2-mile underground cable which was electrically isolated and made available by NMPC for testing.

The results of three separate field tests related to underground and underground-overhead transitions are included herein.

Model Verification G.R.S.S. U-G Getaway

INTRODUCTION

This report describes the procedures undertaken to verify a computer model of measurements taken on an underground trunk line feeder cable. The 3Ø cable system treated in this verification effort serves one of the several distribution feeders in place at the Grooms Road Substation of Niagara Mohawk Power Co.

BACKGROUND

A diagram of this feeder configuration is shown in Fig. 1. The trunk line underground feeder leaves G.R.S.S. (Grooms Road Substation) and continues underground for a distance of 1.98 miles, after which the cable surfaces at a riser pole to feed a hybrid overhead-underground distribution system. The trunkline feeder cable was isolated at each end for the purposes of measurement and verification. When isolated, the trunk line cable therefore constitutes an unbranched 3Ø transmission line with various possible terminations.

The main conductor size of the cable is 750,000 CM and the material is aluminum. The neutral conductor is composed of 21 #14 copper wires wrapped concentrically over the main insulation jacket as shown in Figure 2. The main conductor is covered by a semiconducting jacket and the main insulation jacket is covered by a semiconducting jacket as shown in Figure 2. These jackets are present

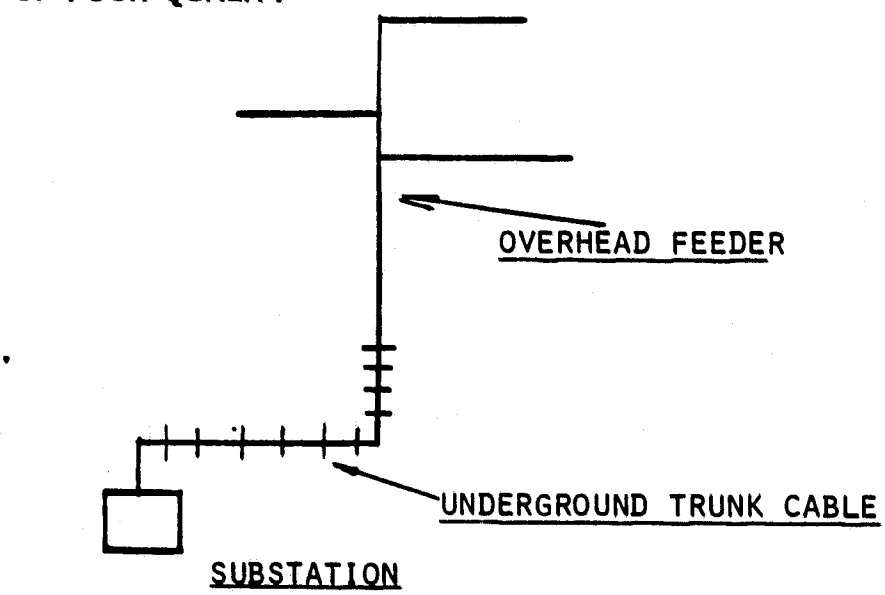

FIGURE 1

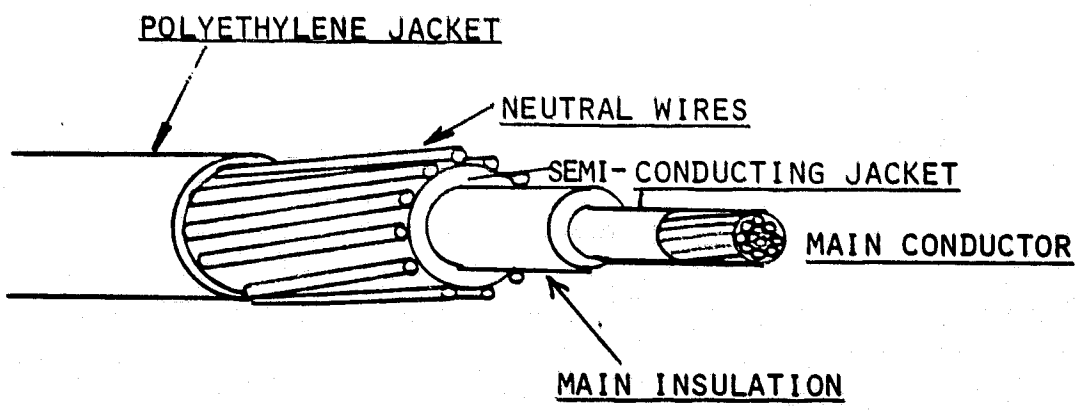

FIGURE 2

for electric field grading purposes. The neutral wires are covered by a polyethylene jacket. The main insulation system is composed of "Kerite", whose relative permittivity is estimated to be about 3.0

These conductors are buried to constitute a 3Ø circuit in equilateral fashion as shown in Figure 3. The burial depth is a minimum of 42 inches. A solid soft drawn #2 copper wire is buried along with the cables to serve as a safety ground. The cable neutral wires are bonded to the copper wires at any splice point, which are a maximum of 1000' apart.

In constructing the computer model of this cable, several factors which affected the model results were not known with a high degree of certainty. Among these factors were:

1) Earth resistivity
2) Main conductor and neutral wire temperature
3) Physical spacing of conductors
4) Exact dielectric constant of insulation system
5) Actual cable length

Efforts were made to employ the cable parameters portion of the E.M.T. program of the Bonneville Power Administration in order to obtain the necessary transmission line parameter data base files. The particular configuration of neutral wires found in these concentric neutral cables was not directly amenable for calculation by use of the EMTP.

A cable parameter program was developed to handle modeling of this type of cable construction.

PHASE CABLES

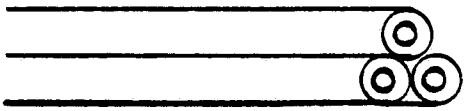

FIGURE 3

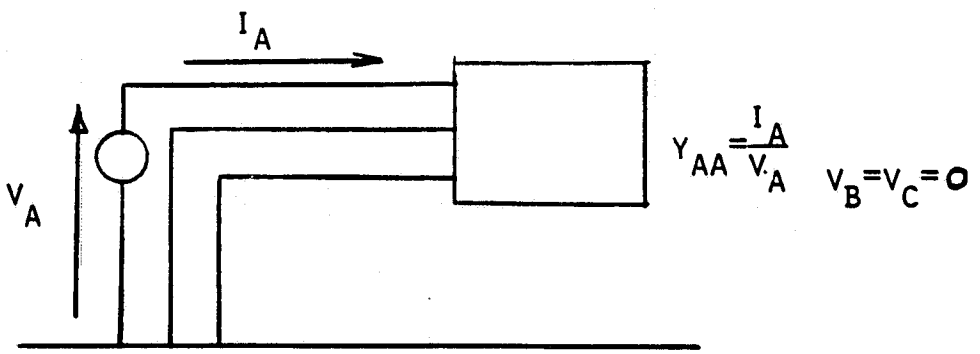

FIGURE 4

To verify the underground cable model, calculations were made for the 3Ø driving point admittance matrix corresponding to that measured at GRSS with the various terminations applied to the end of the isolated underground "getaway" trunk cable shown in Figure 1. The cable parameters and the driving point admittance matrix were calculated for the following frequencies:

6440 Hz
8130 Hz
9510 Hz
12010 Hz
17010 Hz
20010 Hz
21980 Hz

The simulations made at these frequencies were compared with results from the measurements at similar frequencies. According to the network maps provided by N.M.P., the cable length was taken to be 3189M. In general, the measurement of the main diagonal elements of the admittance matrix for a general 3 terminal network was undertaken as shown in

Figure 4, where $Y_{in} = \frac{I_{in}}{V_{in}}$

The cable network model was first configured to simulate the situation where the terminal end of the cable was open-circuited. The results of this computation as a function of frequency are shown in Figure 5 along with the results of the field measurements. Note that the computed admittance magnitude null occurs below that of the measured null. A 5 percent error was assumed in the estimation of the length of the network (5% too long), and the admittance values recomputed with the result shown in Figure 6. In Figure 6, it can be seen that this length modification brings the computed and measured results into good agreement. Due to the uncertainty in the precise length of the cable, and the other important factors mentioned earlier, this recomputation, for purposes of the model verification, is not unreasonable.

Measurements were made to determine the value of the main diagonal of the admittance matrix as a function of frequency with a resistive termination network placed at the end of the cables as shown in Figure 8. The computed and measured response for this situation is shown in Figure 7. By comparison with Figure 5, it can be seen that this termination eliminated some standing wave effects seen in the unterminated case.

Computations performed by the FEEDPUS3 program show the characteristic impedance of the cable under study to be about 15.5Ω. A 15Ω termination was selected.

In the general case, the measurement of the off-diagonal term of the admittance matrix is shown in Figure 9.

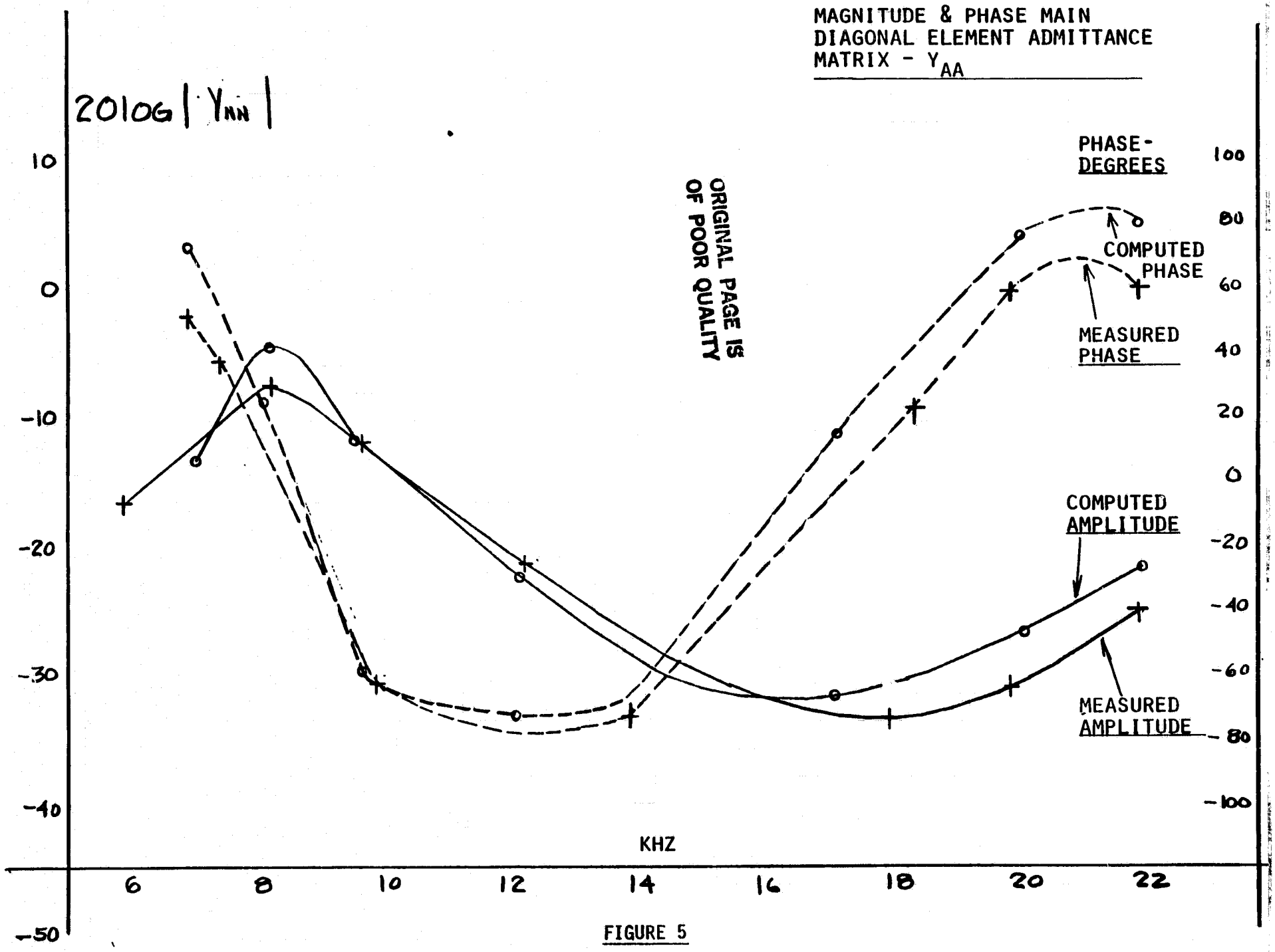
MAGNITUDE & PHASE MAIN
DIAGONAL ELEMENT ADMITTANCE
MATRIX - Y_{AA}
$20\log|Y_{NN}|$
PHASE-
DEGREES
COMPUTED
PHASE
MEASURED
PHASE
COMPUTED
AMPLITUDE
MEASURED
AMPLITUDE
ORIGINAL PAGE IS
OF POOR QUALITY
KHZ
10
0
-10
-20
-30
-40
-50
100
80
60
40
20
0
-20
-40
-60
-80
-100
6
8
10
12
14
16
18
20
22

FIGURE 5

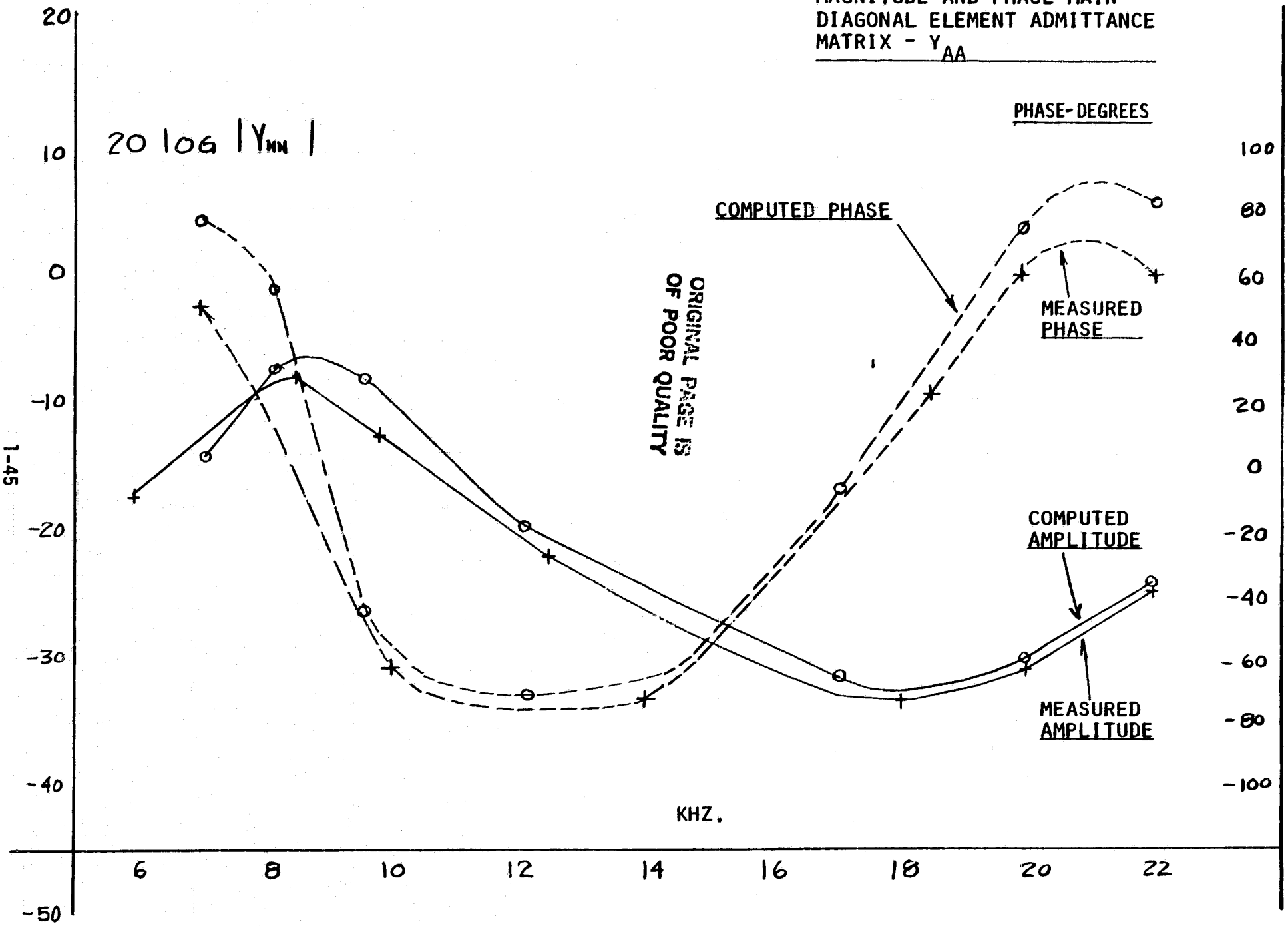
MAGNITUDE AND PHASE-MAIN DIAGONAL ELEMENT ADMITTANCE MATRIX - Y_{AA}
20 log $|Y_{NN}|$
PHASE-DEGREES
COMPUTED PHASE
MEASURED PHASE
COMPUTED AMPLITUDE
MEASURED AMPLITUDE
ORIGINAL PAGE IS OF POOR QUALITY
KHZ.
20
10
0
-10
-20
-30
-40
-50
100
80
60
40
20
0
-20
-40
-60
-80
-100
6
8
10
12
14
16
18
20
22

FIGURE 6

MAGNITUDE & PHASE MAIN DIAGONAL ELEMENT - ADMITTANCE MATRIX Y_{AA}

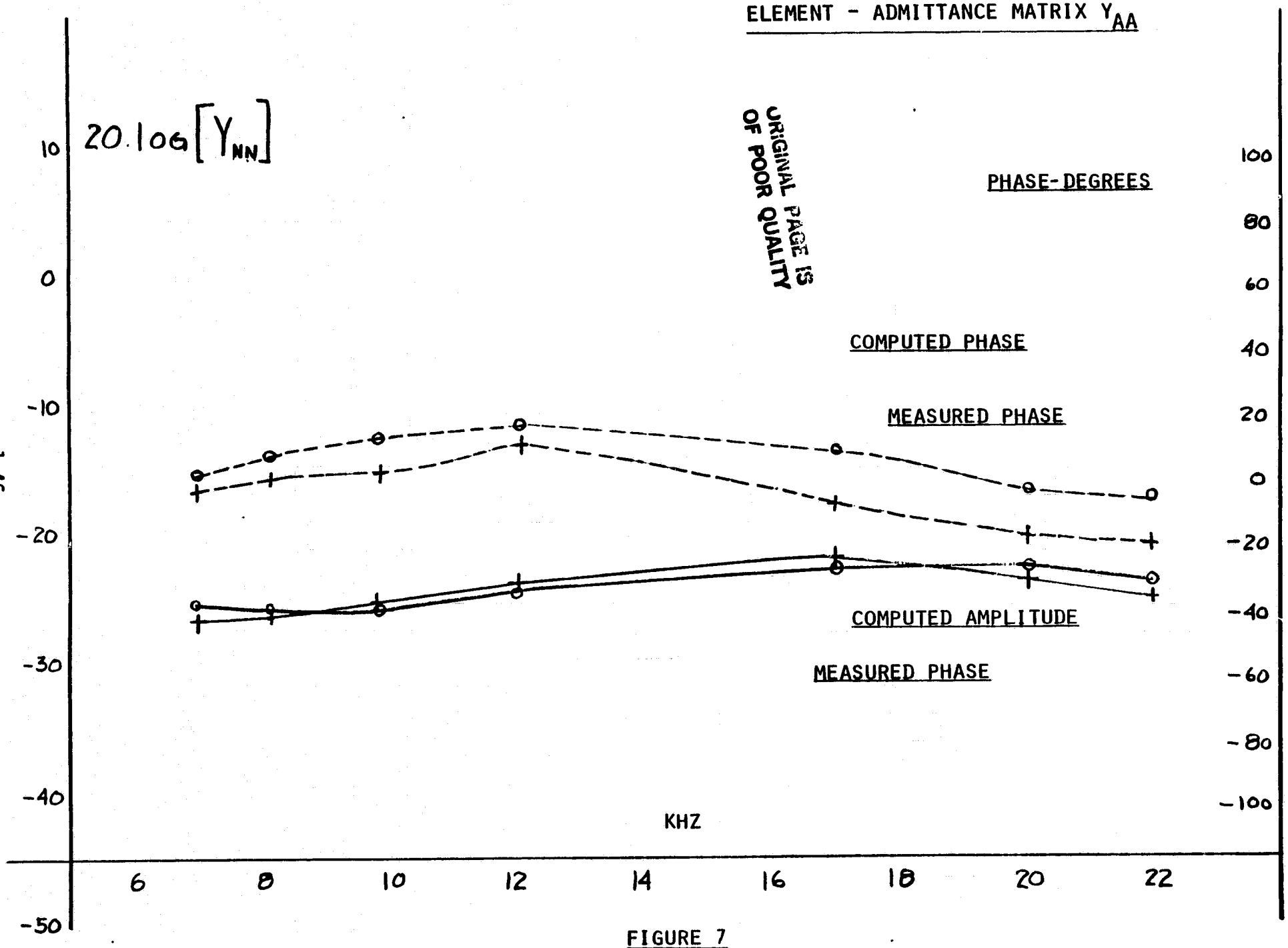

FIGURE 7

The computations performed by the NTWKERH1 program show the magnitude of the off-diagonal terms to be on the order of -40 db., smaller than those of the main diagonal. The measurements, in general, show this term to be only about -20 db smaller than the main diagonal term at first glance. Figure 10 shows the measurements of an off-diagonal term for the terminated cable situation. Notice that the phase measure shows a continuous accumulation of the phase difference between the referenced voltage and the measured phase current. It should also be noted that the two 360° phase rolls occur, on the average, at about 17.2 kHz intervals. Calculations from FEEDPUS3 program show the velocity of propagation to be about .35 the speed of free space propagation for this cable.

From this data one may calculate the 2-way travel distance

$\frac{1}{17.2\ kHz} = 5.8139\ sec \times 10^{-5}$; $D=VT=.35(3 \times 10^{8})(5.8134 \times 10^{-5} sec) = 6104M$.

Now if the current measured in finding the off-diagonal term is the return current traveling out thru one phase conductor and returning thru the other, as shown in Figure 11, rather than the through ground path, the figure obtained above, when divided by 2, should equal the one way distance of the cable.

So,

$$\frac{6104}{2} = 3052M$$

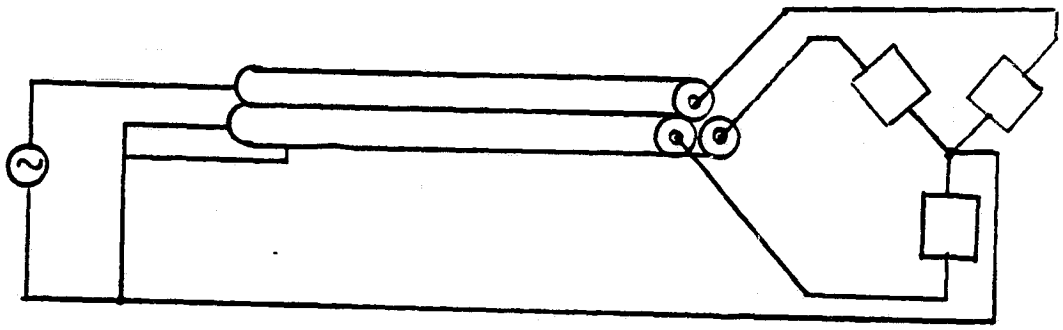

APPROX. 3052 METERS

FIGURE 8

$$Y_{AB} = \frac{I_B}{V_A} \quad V_B = V_C = 0$$

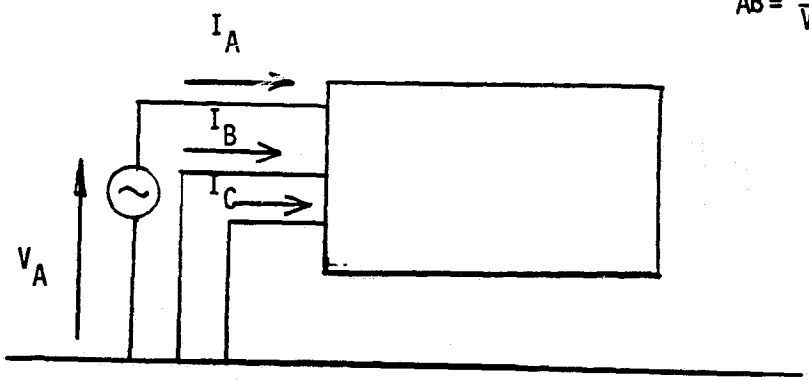

FIGURE 9

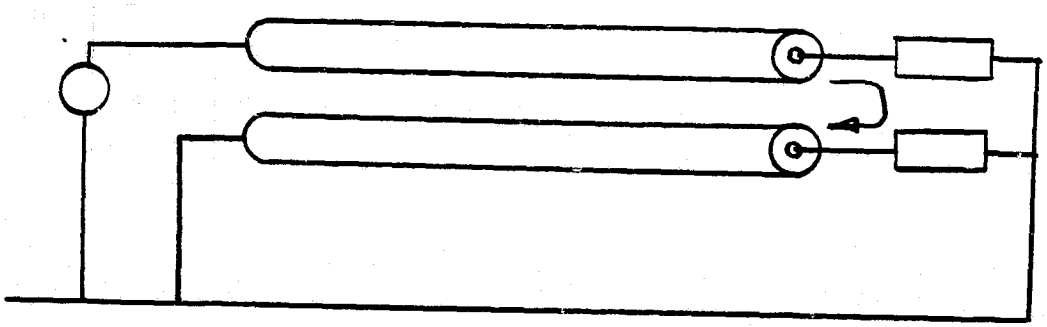

FIGURE 11

MAGNITUDE & PHASE OFF DIAGONAL ELEMENT - ADMITTANCE MATRIX I_B/V_A

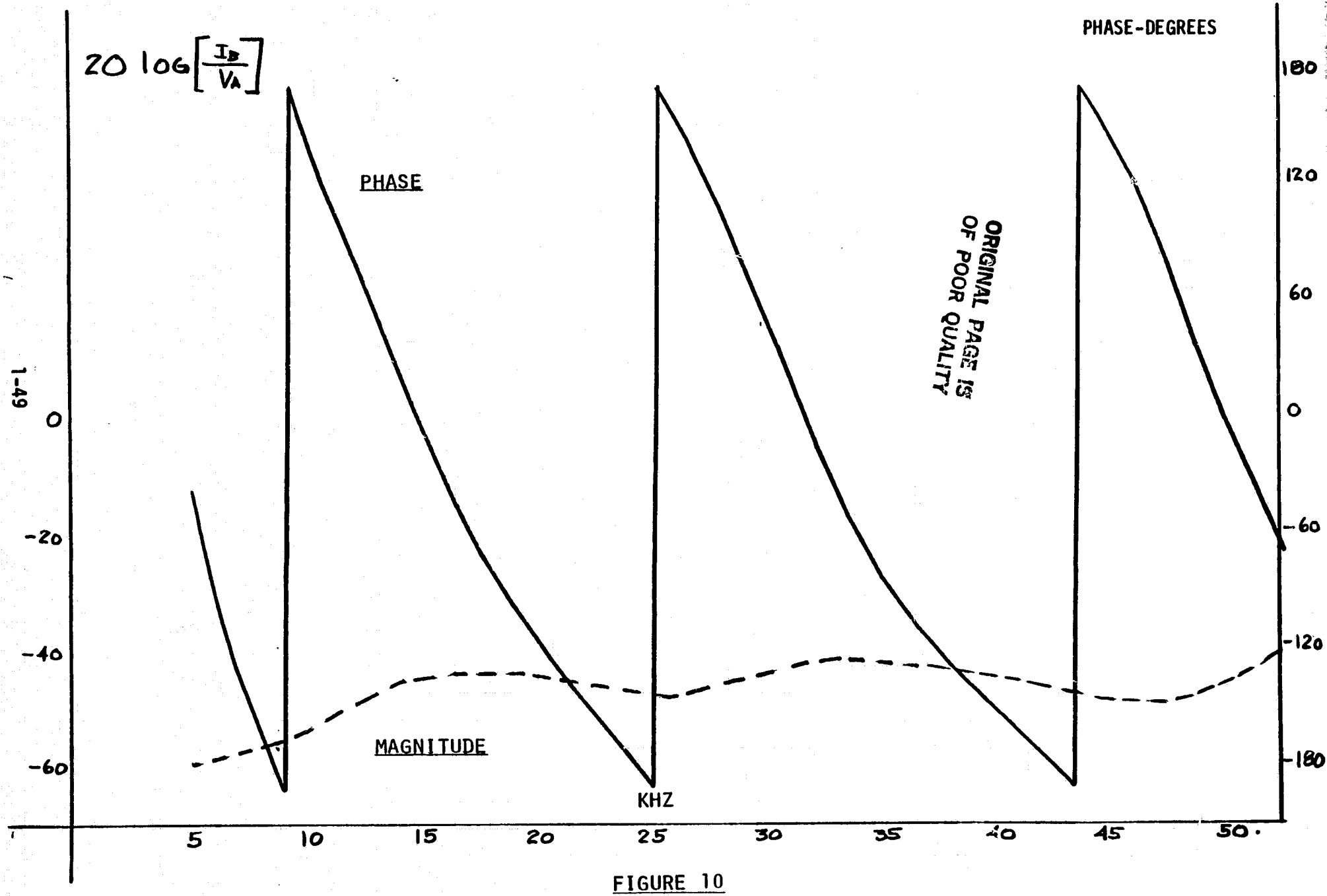

FIGURE 10

When compared to the assumed 3011M. cable length used in the main diagonal measurements, this compares quite favorably. Therefore, if this return current is present, the difference between calculated and measured off-diagonal terms is not surprising. In order to investigate the general possibility of simulating the transport delay situation described above, a delta load was provided as a termination using the computer model. The results obtained from frequency response calculations using the model showed that this general response pattern could be simulated. No attempt was made to simulate the response exactly due to lack of information regarding the exact coupling mechanism. Also, since the computed value of the off-diagonal terms are small relative to the main diagonal terms, the transport mechanism noted above, whatever that may be, could easily mask the off-diagonal measurement. This inability to measure and verify the computation of the off-diagonal term of the admittance matrix is not serious since the degree of coupling between the cables is so low initially that the off-diagonal terms will probably make little difference in general network calculations.

Measurements of the off-diagonal term were taken also for the situation where the cable was open-circuited at the endpoint. The results of these measurements are shown in Fig. 12. By examination of the phase angle plot of the off-diagonal term, it can be seen that the transport mechanism has not completely masked out the mutual coupling between the phase cables.

SUMMARY

In summary, the difficulty in verification of the off-diagonal terms of the cable admittance matrix is not seen to be a detriment to

MAGNITUDE & PHASE - OFF DIAGONAL ELEMENT ADMITTANCE MATRIX $I_B / V_A \; Y_{AB}$

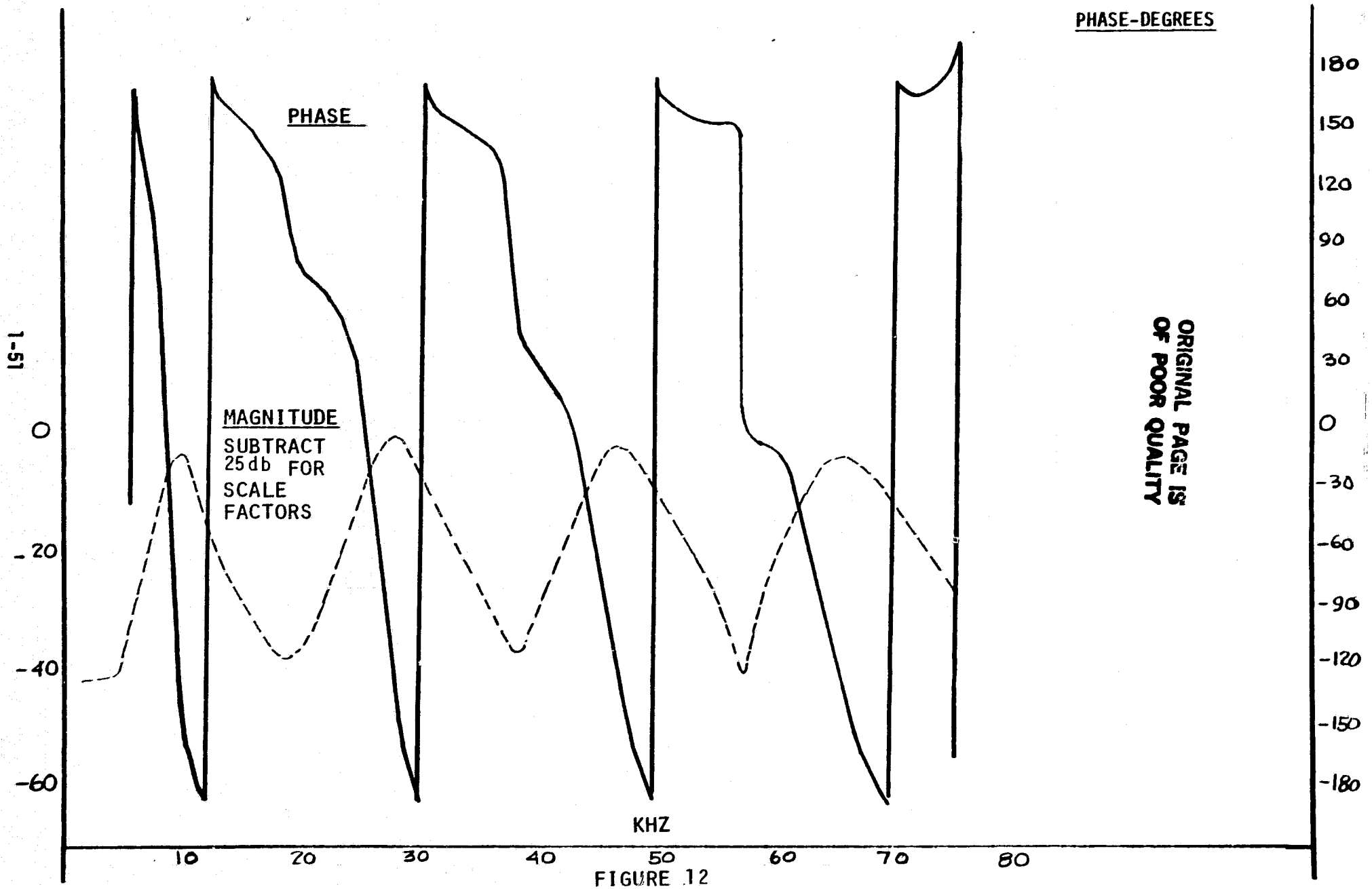

ORIGINAL PAGE IS OF POOR QUALITY

FIGURE 12

the overall modeling effort since the off-diagonal terms are relatively small with respect to the main diagonal of the admittance matrix. Also, it would not seem to be likely that this transport mechanism would exhibit itself under actual network condition, since any large loads (P.F.C. Capacitors, etc.) which provide coupling between phase conductors, would tend to dominate the off-diagonal component of the admittance matrix due to intercable coupling.

MODEL VERIFICATION OF MEASUREMENTS PERFORMED ON COUNTRY KNOLLS SOUTH U.G. NETWORK

INTRODUCTION

This report describes procedures undertaken to verify field measurements made to determine the driving point admittance of an underground tree network at several discrete frequencies using the DIFNAP computer program system.

BACKGROUND

Field measurements were performed in order to measure the elements of the admittance matrix, at various frequencies, of an entire underground tree type distribution network.

In general, the network consists of a large trunk cable with a number of single phase branches implemented with smaller conductor cable. The main trunk cable is about 1600 meters long and is composed of 500 KCMIL concentric neutral cable. The single phase branch circuits are composed of #2 A.W.G. concentric neutral cable.

In order to measure the elements of the main diagonal of the admittance matrix, the general configuration shown in Figure 1 was employed. A voltage was placed on one of the phases while the other two phases should be at reference potential. The phasor ratio of the voltage and current on the excited phase yields the value of the main diagonal element. In practice, the voltages on the non excited

phases were not able to be lowered sufficiently close to reference potential. This difficulty arose due to the fact that the distribution feeder circuits were measured while energized, eliminating the use of direct grounding. During the initial field measurements, a series L-C tuned circuit was employed to provide a low impedance path to ground on the unexcited phases for the carrier signal. This technique provided a maximum 20 db differential between the voltage on the excited phase and that of the "grounded" phases, with the norm being closer to 15 db differential. In order to provide a more suitable "ground" on the unexcited phases, a voltage cancellation technique was used on the unexcited phases. During follow-up field measurements, this technique forced the voltage differential into the neighborhood of 45 db.

The measurement of the off-diagonal terms was undertaken as shown in Figure 2.

Figure 3 shows the results of the field measurements of the main diagonal element of the admittance matrix for Phase A of the underground network in addition to the values computed by use of the NTWKERH1 computer program. Values are shown for measurement and computations between the frequencies of 5 kHz and 25 kHz.

Field test results obtained using both nulling techniques are employed. The results from the first

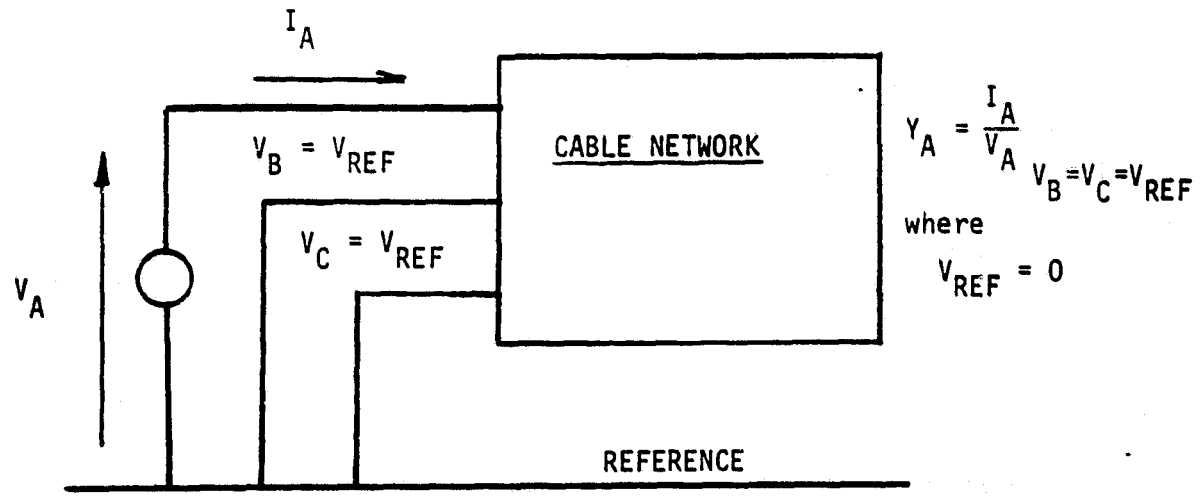

FIGURE 1

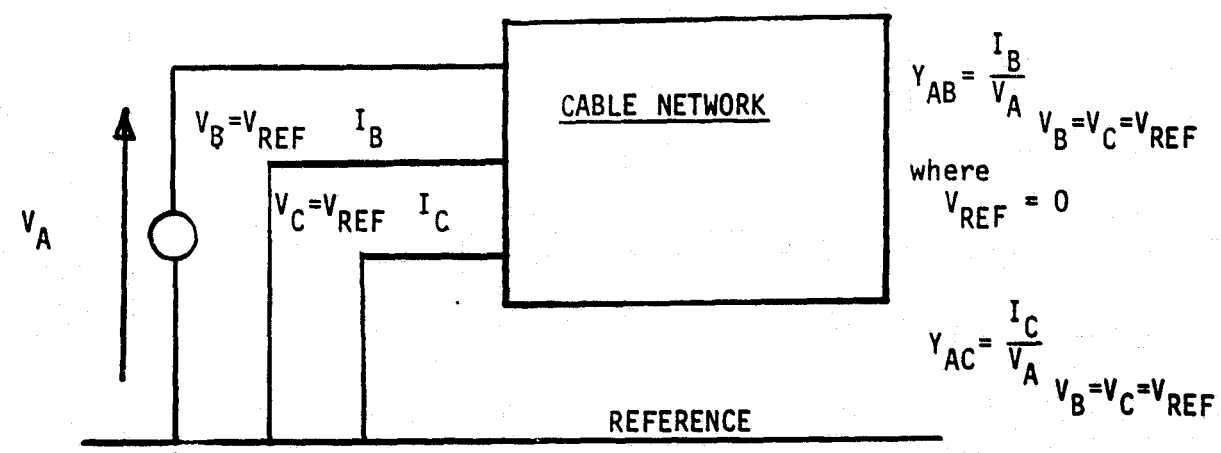

FIGURE 2

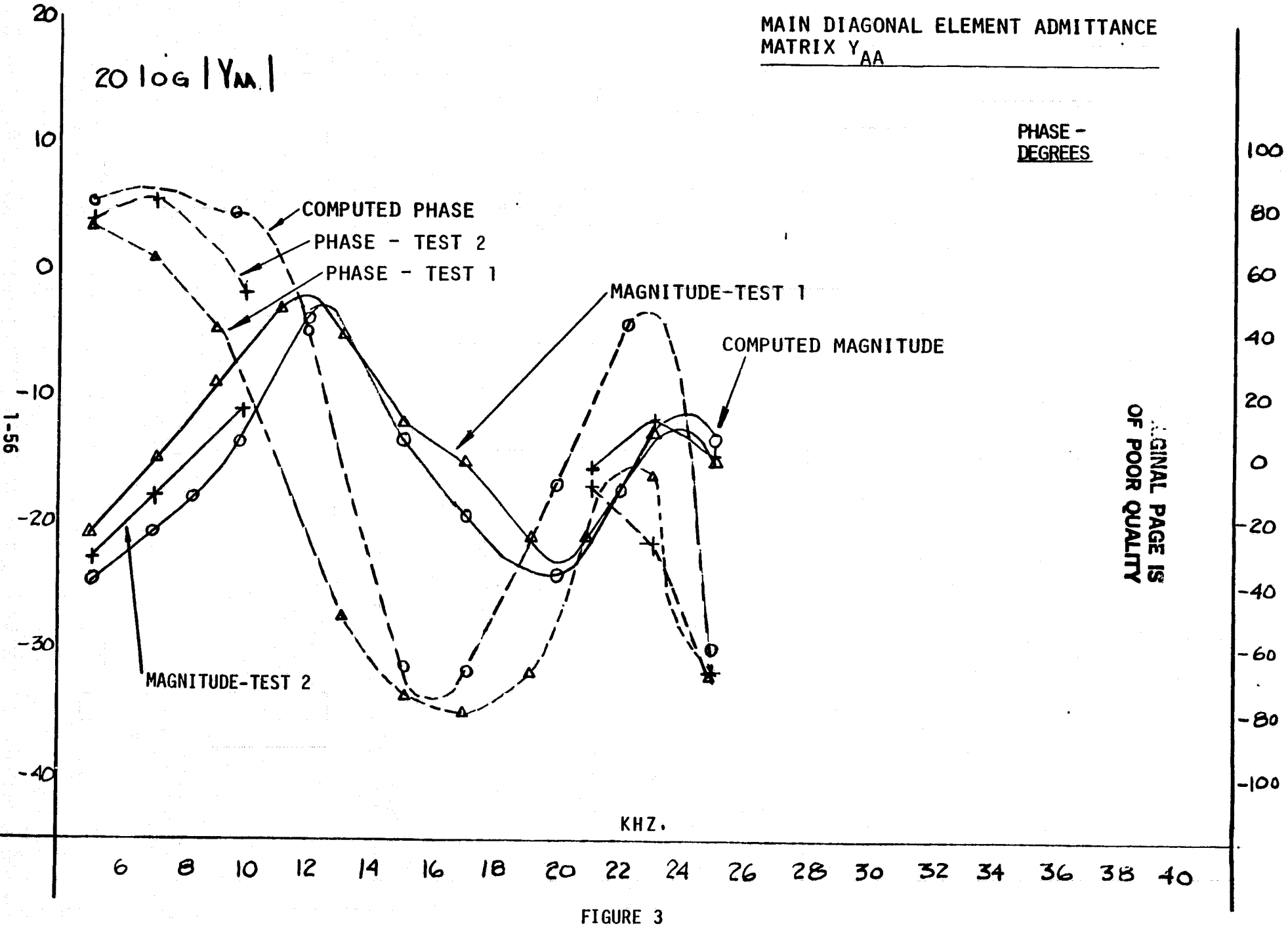

FIGURE 3

set of field measurements are used even though they are less desirable than the results of the second set, since the second series of measurements measured the following frequencies between 5 and 25 kHz:

5010 HZ.
6990 HZ.
9510 HZ.
21010 HZ.
23010 HZ.
25010 HZ.

These frequencies were not sufficient to fully reflect resonance effects in the cable network so results from the first series of tests were included. Frequencies measured in common on both tests show good agreement, taking into account the dynamic nature of the network with respect to relative loading levels.

Figures 4 and 5 show the results of the measurements and computer simulations of the main diagonal elements of the admittance matrix for Phases B & C of the underground cable network.

From inspection of Figures 3, 4, and 5, it can be seen that there is good agreement between the frequencies at which the relative minima and maxima of magnitude and phase occur.

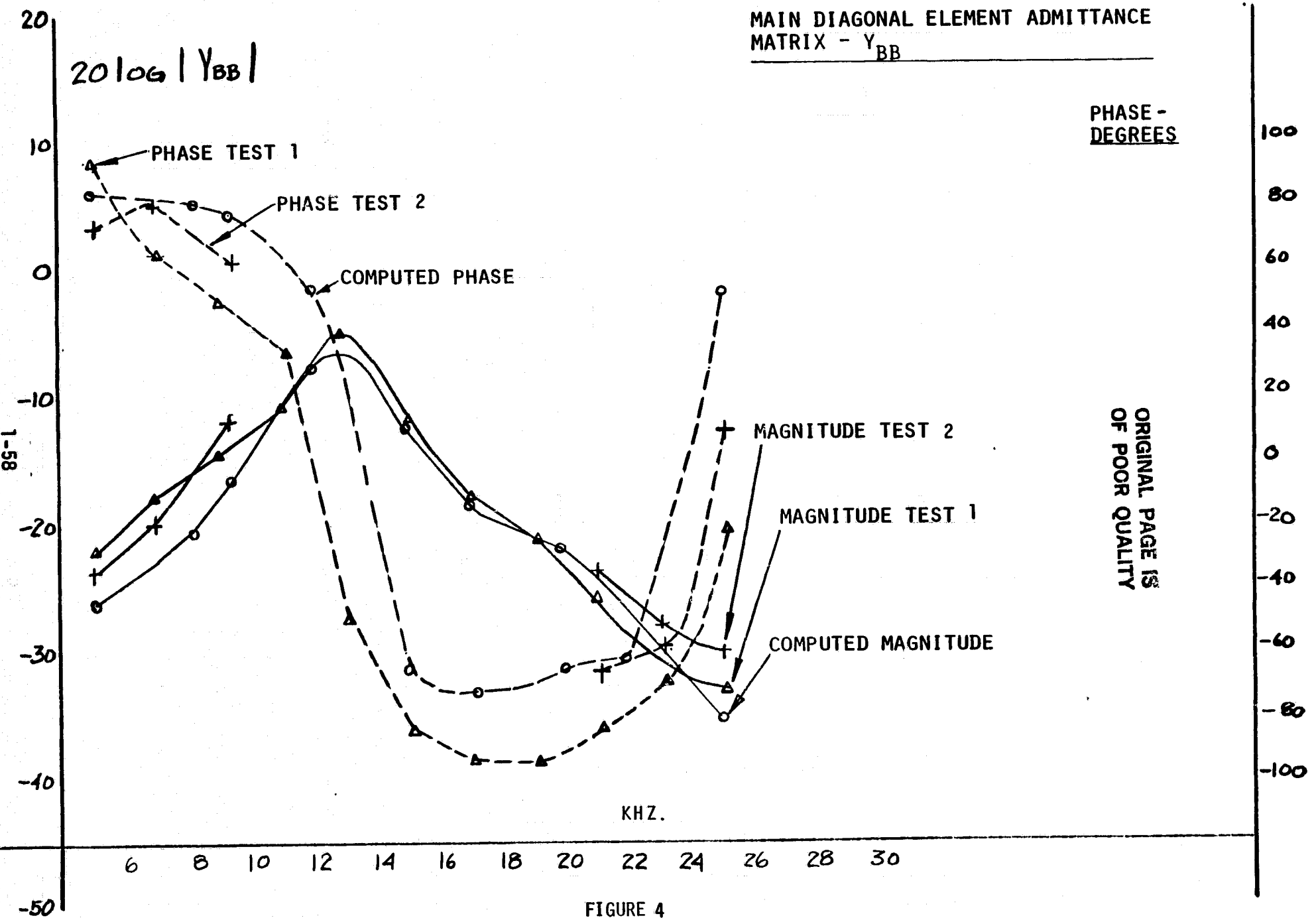

ORIGINAL PAGE IS OF POOR QUALITY

FIGURE 4

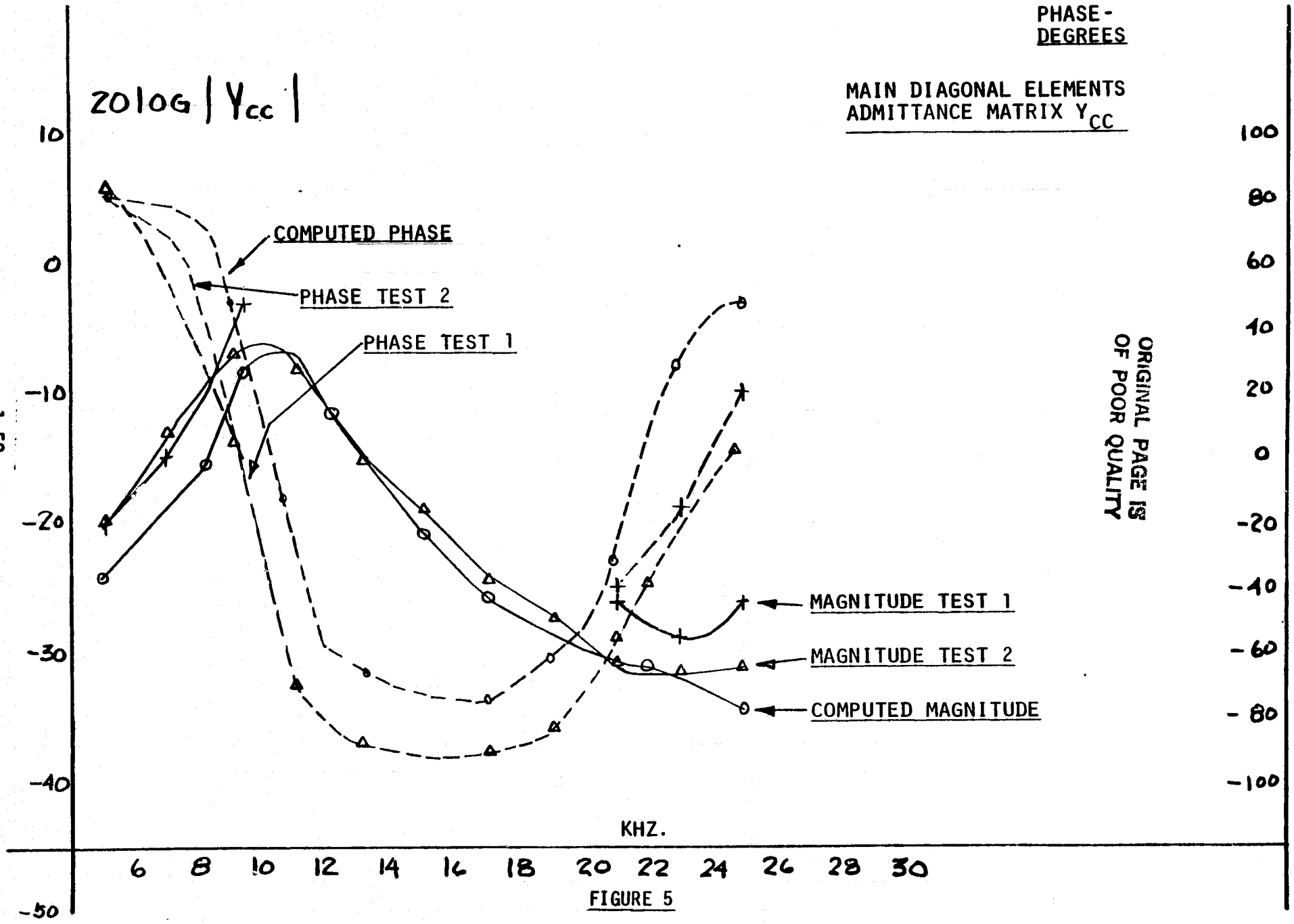

FIGURE 5

A distribution transformer loading level of 40% of full load rating was selected on the basis of the time of day at which the tests were performed and weather conditions.

It can be seen from the results shown in Figures 3, 4, and 5 that the model is quite useful in simulating the response of the U.G. cable network considering the uncertainties noted above and the accuracy needed for communication system design.

Sufficient data was taken to compute the off diagonal terms of the admittance during the field tests. The results of the field test show the magnitude of the off diagonal terms to be about 30 db smaller than those on the main diagonal. Results of the computer model simulation show these off diagonal terms to be on the order of 60 db smaller than those on the main diagonal. These results reflect the high degree of shielding between the phase cables.

MODEL VERIFICATION OF FIELD MEASUREMENT PERFORMED ON CARLTON RD. O.H. - U.G. NETWORK

INTRODUCTION

Sufficient field data was gathered to provide a measure of the complete admittance matrix of the overhead-underground network originating approximately at the junction of Carlton Rd. and the Jonesville-Elnora Rd. in Clifton Park, on the NMPC 34556 feeder.

In approximate terms, the network consists of 650 meters of 3Ø open wire primary feeding a large underground trunk cable of 500 meters length. Several 1Ø feeder cables are branched from this trunk and are about 600 meters in length. The trunk cable consists of 500 KCM concentric neutral cable. The feeder cables are #2 A.W.G. size, with concentric neutrals.

A description of the definition of the elements of the admittance matrix is given in two earlier reports describing verification efforts on underground cable networks.

During the admittance matrix measurements, each phase was excited individually, while the other two phases were theoretically brought to signal reference potential. While transmission occurred on each phase, secondary line to neutral voltage was measured on a distribution transformer on a single phase branch. These secondary DT voltages were used to infer the primary voltage on the cable by adding a turns ratio correction to this voltage (36 db). Using these estimated values of primary

voltage, a measure of the voltage transfer ratio of O.H. - U.G. network could be obtained. The admittance matrix was then calculated using the NTWKERH1 program while the voltage transfer was calculated using the NTWKANH1 program.

Field measurements were also performed to collect data on the above mentioned quantities when a reactive load (composed of the test van coupling network) was placed on the end of the trunk cable. The reactive load on each phase of the trunk cable was varied in order to maximize the voltage transfer outbound between the substation and a capacitor bank location (capacitor bank at point K, Figure 1). The reactive loads were varied as a crude experiment to see if voltage transfer between the substation and point K could be influenced by the reactive load at the end of the trunk cable. Simulations were performed on the network for this condition also.

All D.T.'s on the network were assumed to be loaded to 40% capacity with a unity power factor load. This loading level was selected with due consideration of time of day and weather conditions as influences on electricity usage.

Results

Figures 2, 3, and 4 are comparisons of the measured and computed values of the main diagonal of the admittance matrix when the network was not modified. The frequencies at which measurements were taken were:

5010 Hz
6990 Hz
9510 Hz
21090 Hz
23070 Hz
25510 Hz

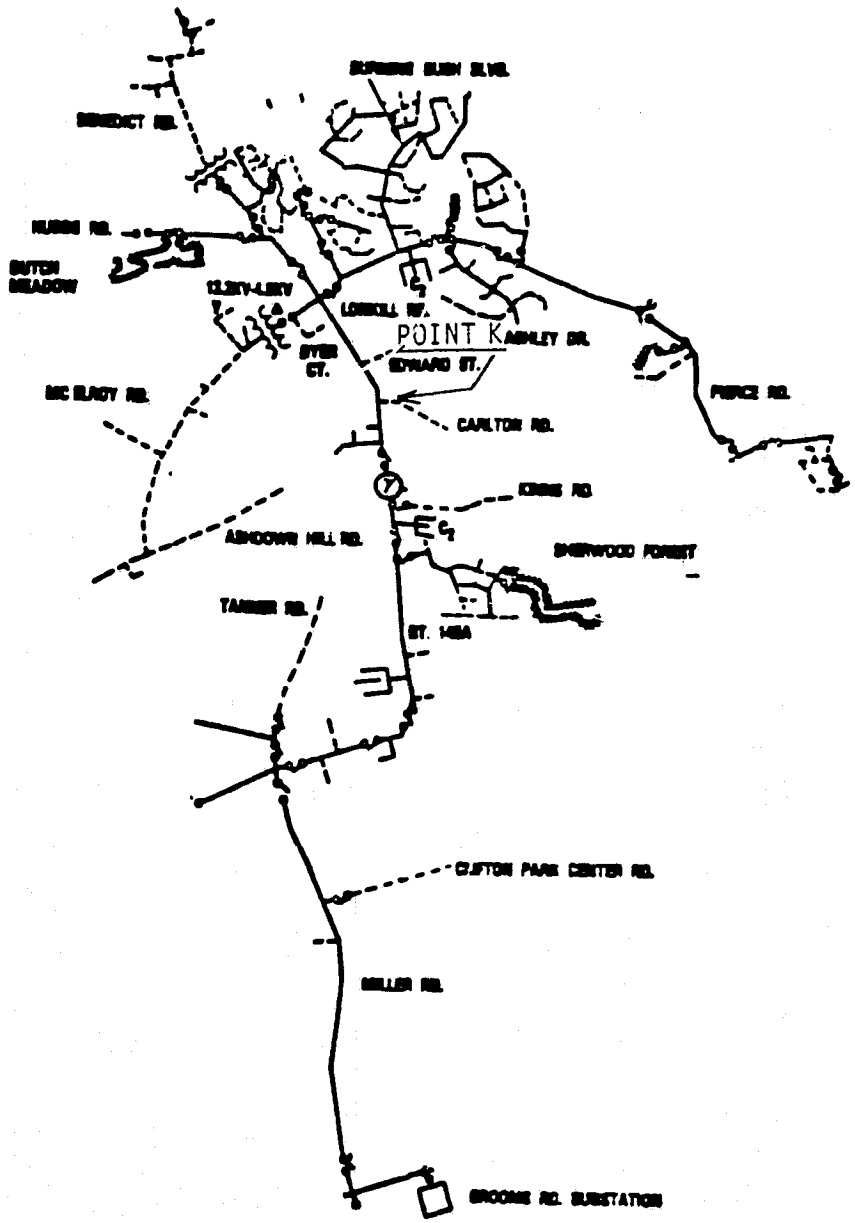

FIGURE 1

N.M.P.C. 34556 FEEDER

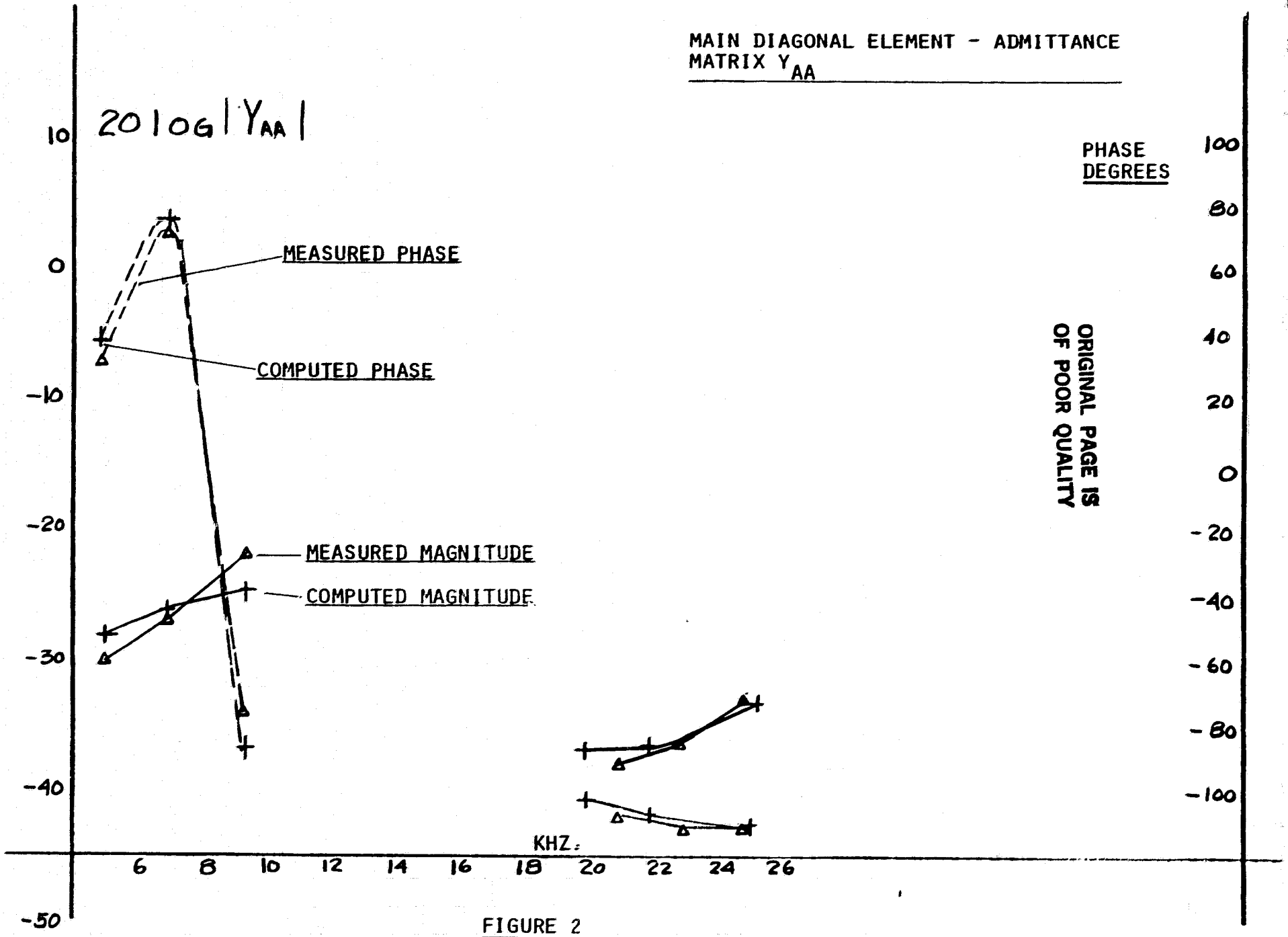
MAIN DIAGONAL ELEMENT - ADMITTANCE MATRIX Y_{AA}
$20\log|Y_{AA}|$
PHASE DEGREES
MEASURED PHASE
COMPUTED PHASE
MEASURED MAGNITUDE
COMPUTED MAGNITUDE
ORIGINAL PAGE IS OF POOR QUALITY
KHZ.
10
0
-10
-20
-30
-40
-50
100
80
60
40
20
0
-20
-40
-60
-80
-100
6
8
10
12
14
16
18
20
22
24
26

FIGURE 2

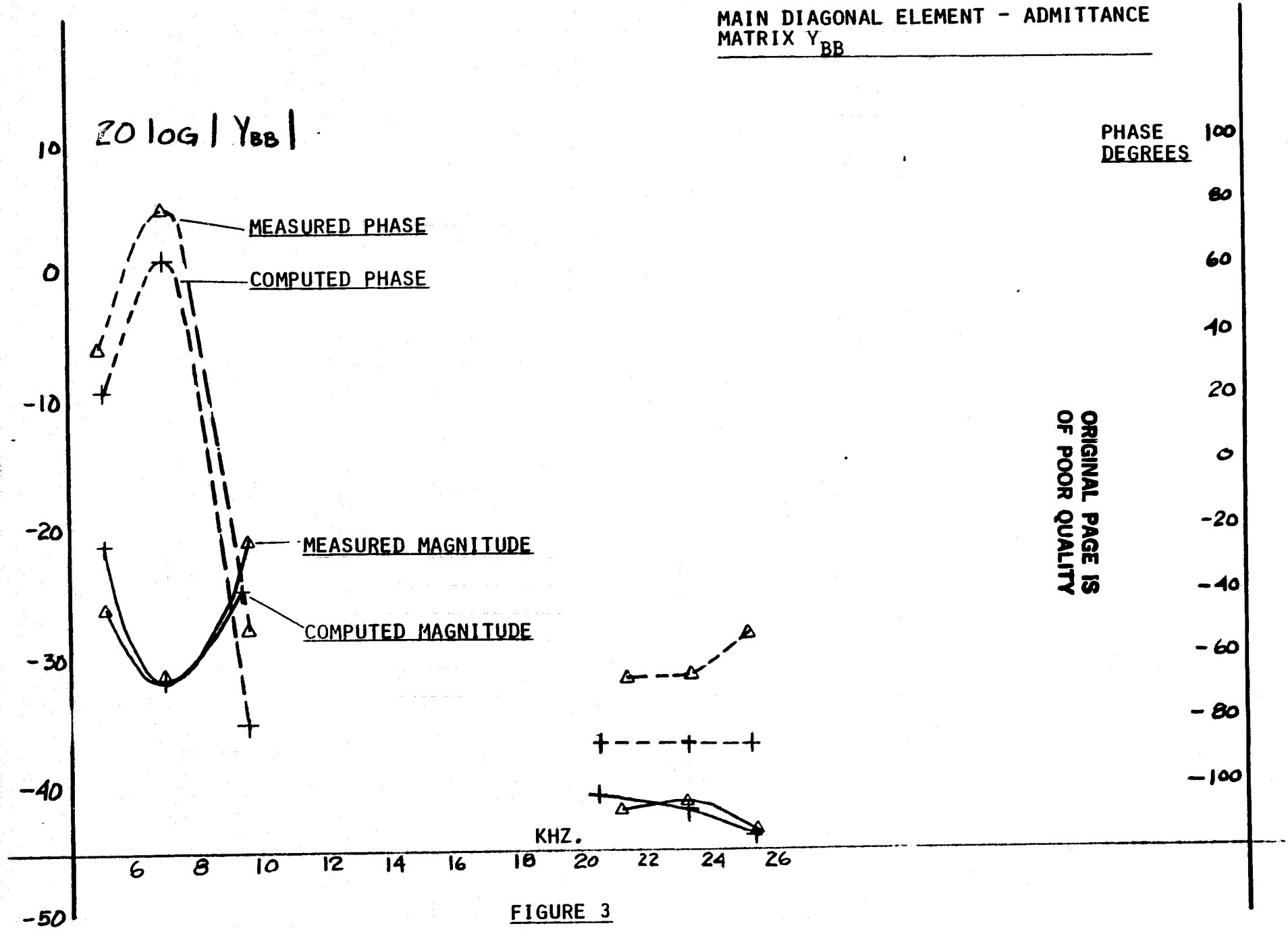
MAIN DIAGONAL ELEMENT - ADMITTANCE MATRIX Y_{BB}
$20 \log |Y_{BB}|$
PHASE DEGREES
MEASURED PHASE
COMPUTED PHASE
MEASURED MAGNITUDE
COMPUTED MAGNITUDE
KHZ.
10
0
-10
-20
-30
-40
-50
100
80
60
40
20
0
-20
-40
-60
-80
-100
6
8
10
12
14
16
18
20
22
24
26
ORIGINAL PAGE IS OF POOR QUALITY

FIGURE 3

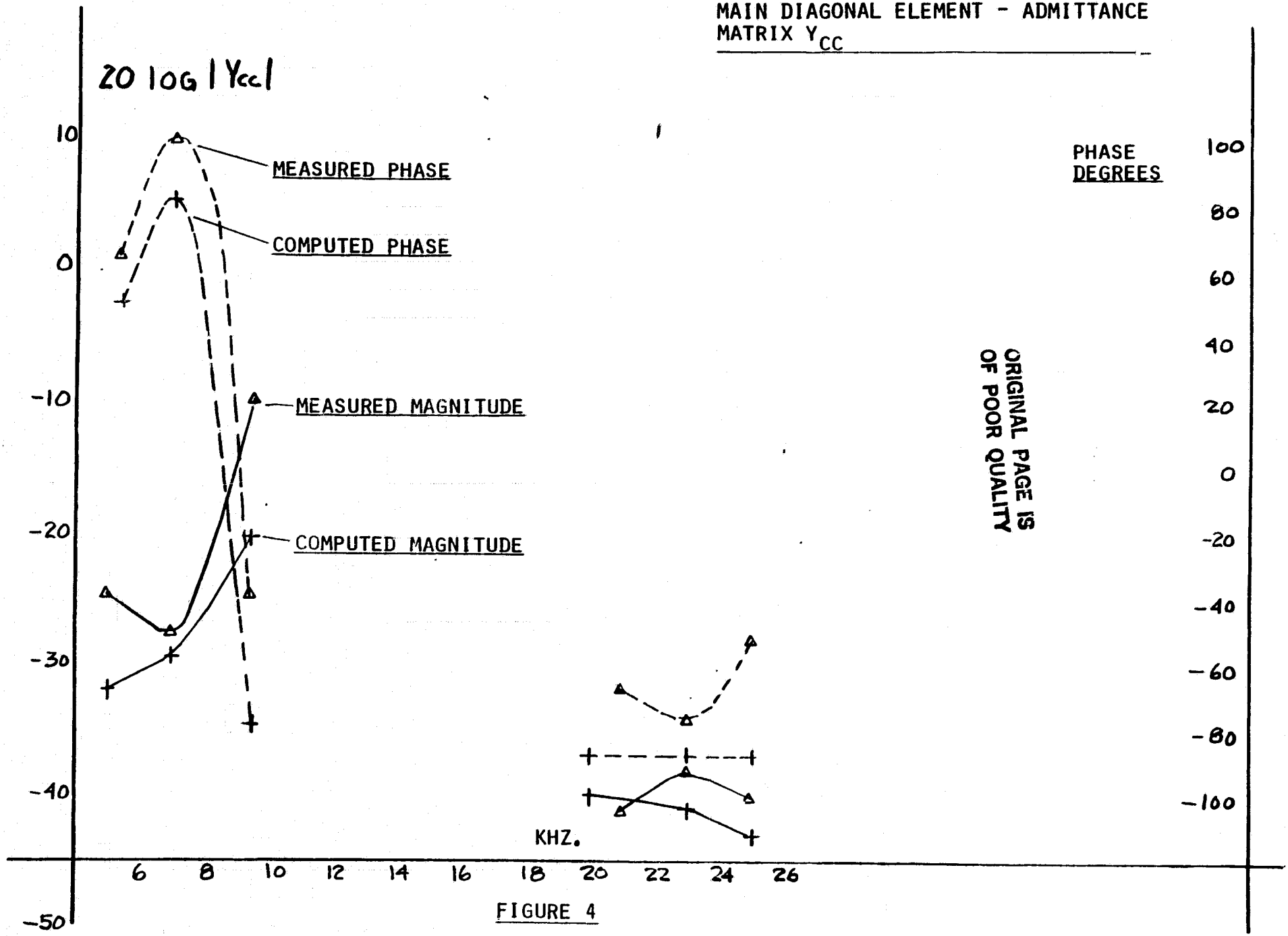

FIGURE 4

Simulations and measurements were performed for the off-diagonal elements as well. In this case, a 3x3 admittance matrix is involved. The Y_{12}, Y_{13}, Y_{23} elements were examined. Figures 5, 6, and 7 show model results and corresponding measurements.

Figures 8 and 9 show results of voltage transfer measurements and modeling. As mentioned above, carrier signal voltages were monitored on the secondary of a distribution transformer. These voltages were measured line to neutral. In order to obtain a rough idea of the voltage on the primary conductor, a correction for the transformer turns ratio was added (36 db) to this secondary voltage. The NTWKANH1 program was then used to perform the voltage transfer simulation. The D.T. was located on a single phase branch being fed by Phase One. Figure 8 compares measured and computed results of the voltage transfer ratio while transmission occurred on Phase 1. Figure 9 shows the same comparison while transmitting on Phase 2. It should be kept in mind that no attempt was made to account for the voltage transfer characteristics of the D.T. at the various frequencies of interest, only a turns ratio correction was used.

Also, as mentioned earlier, a reactive load was placed on the end of the trunk cable. Simulations and measurements were performed for this condition at the following frequencies:

5010 Hz
6990 Hz
9510 Hz

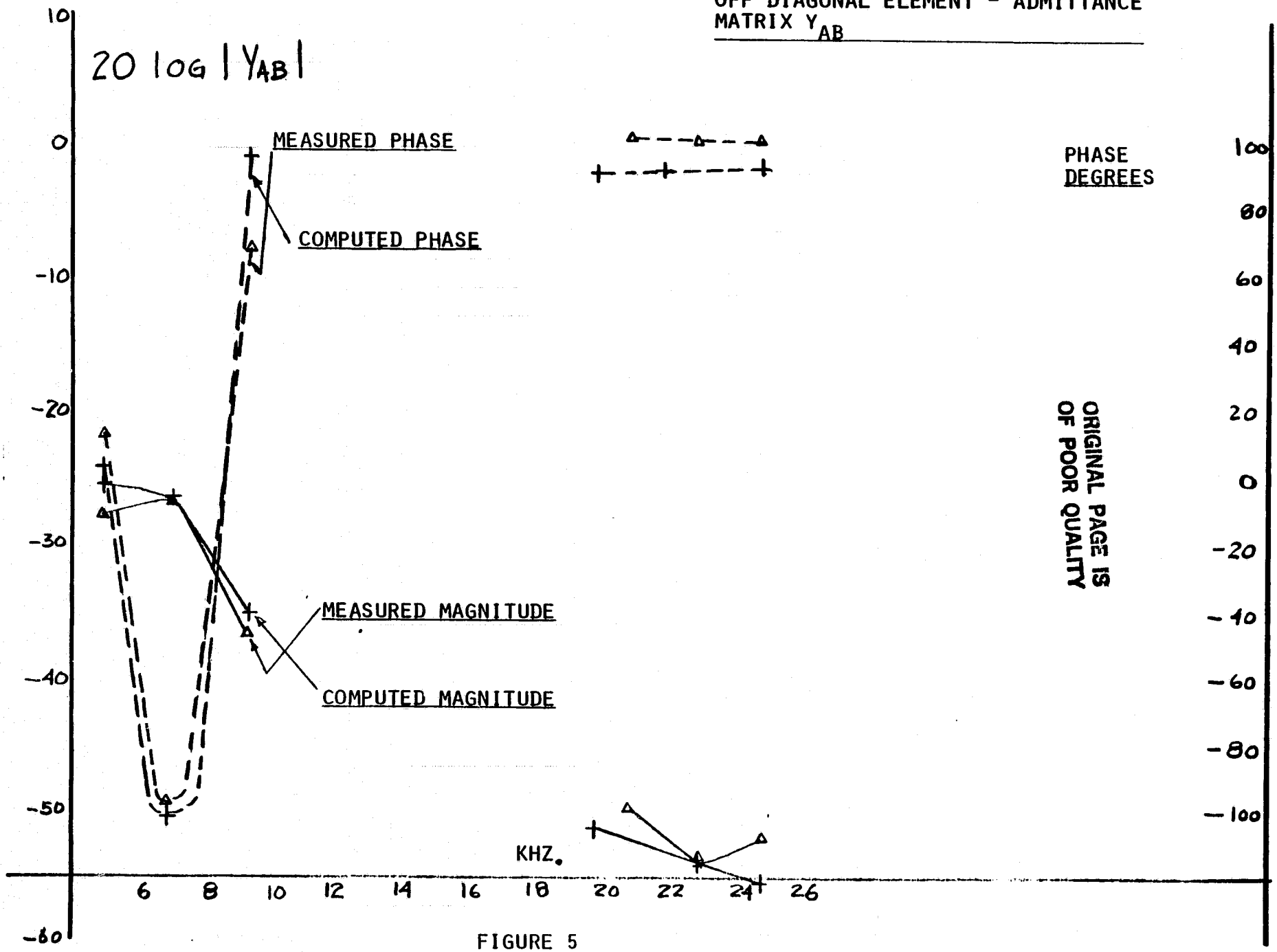
OFF DIAGONAL ELEMENT - ADMITTANCE MATRIX Y_{AB}
20 log | Y_{AB} |
MEASURED PHASE
COMPUTED PHASE
MEASURED MAGNITUDE
COMPUTED MAGNITUDE
PHASE DEGREES
KHZ.
10
0
-10
-20
-30
-40
-50
-60
100
80
60
40
20
0
-20
-40
-60
-80
-100
6
8
10
12
14
16
18
20
22
24
26
ORIGINAL PAGE IS OF POOR QUALITY

FIGURE 5

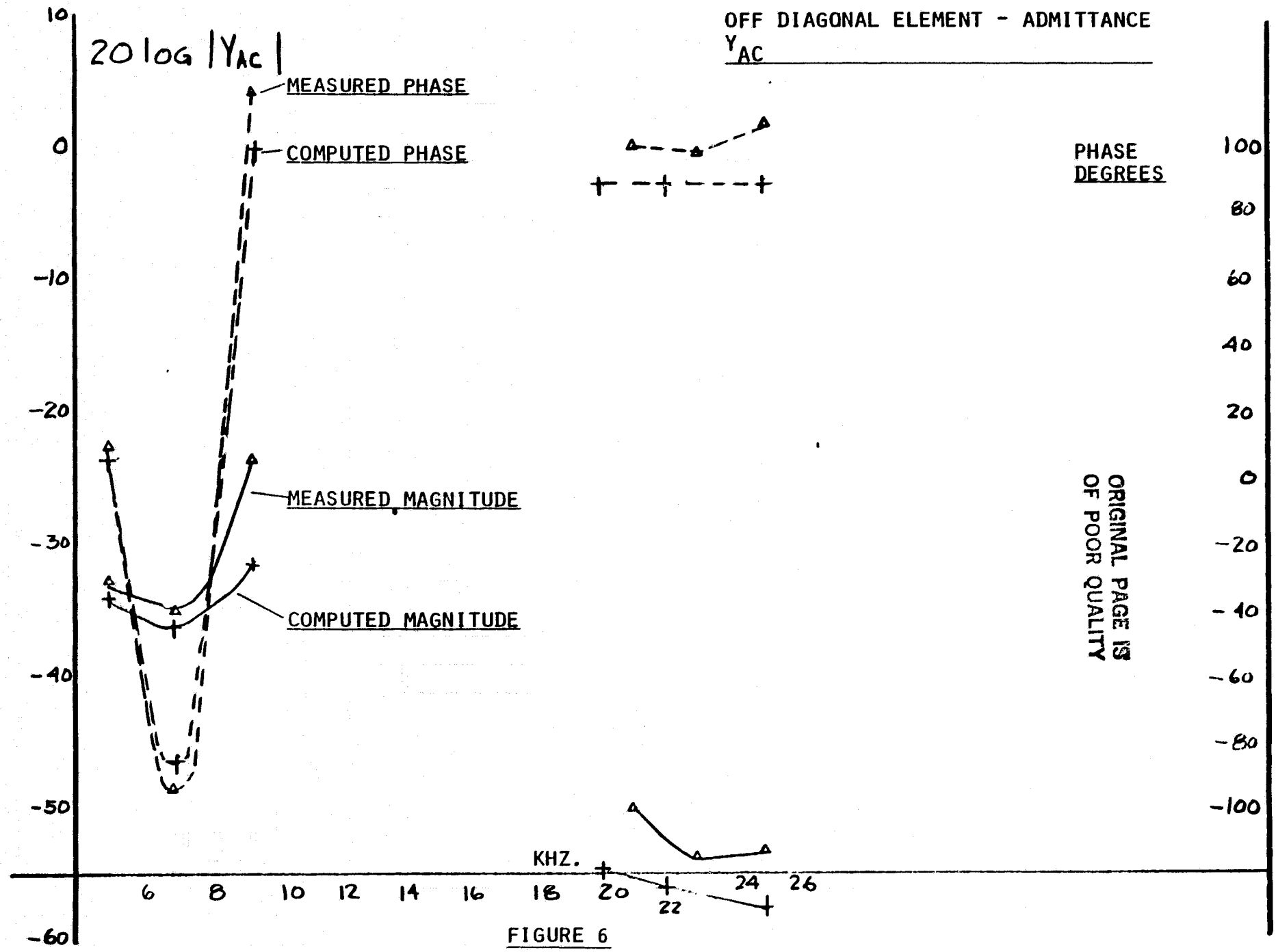

FIGURE 6

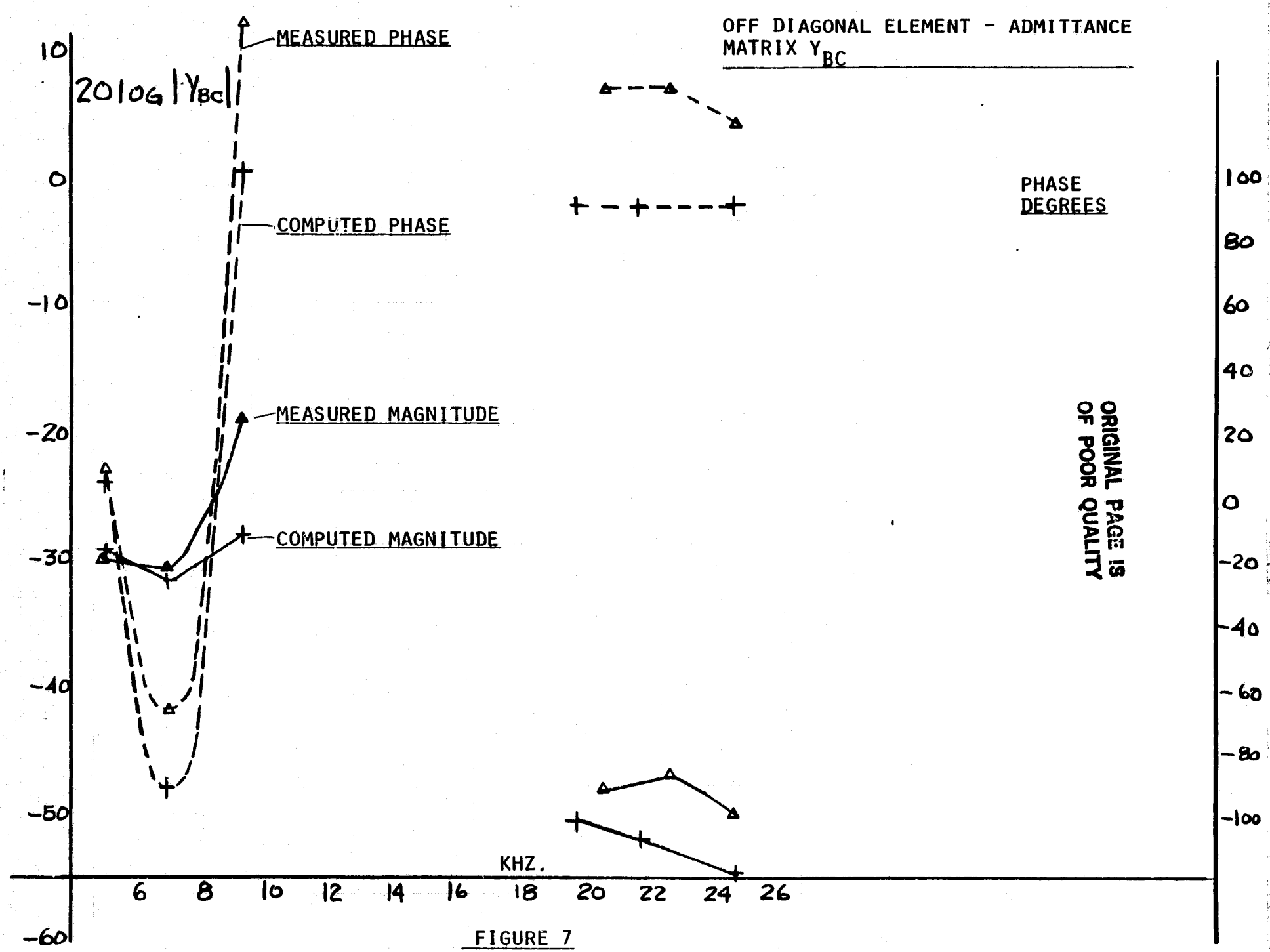

FIGURE 7

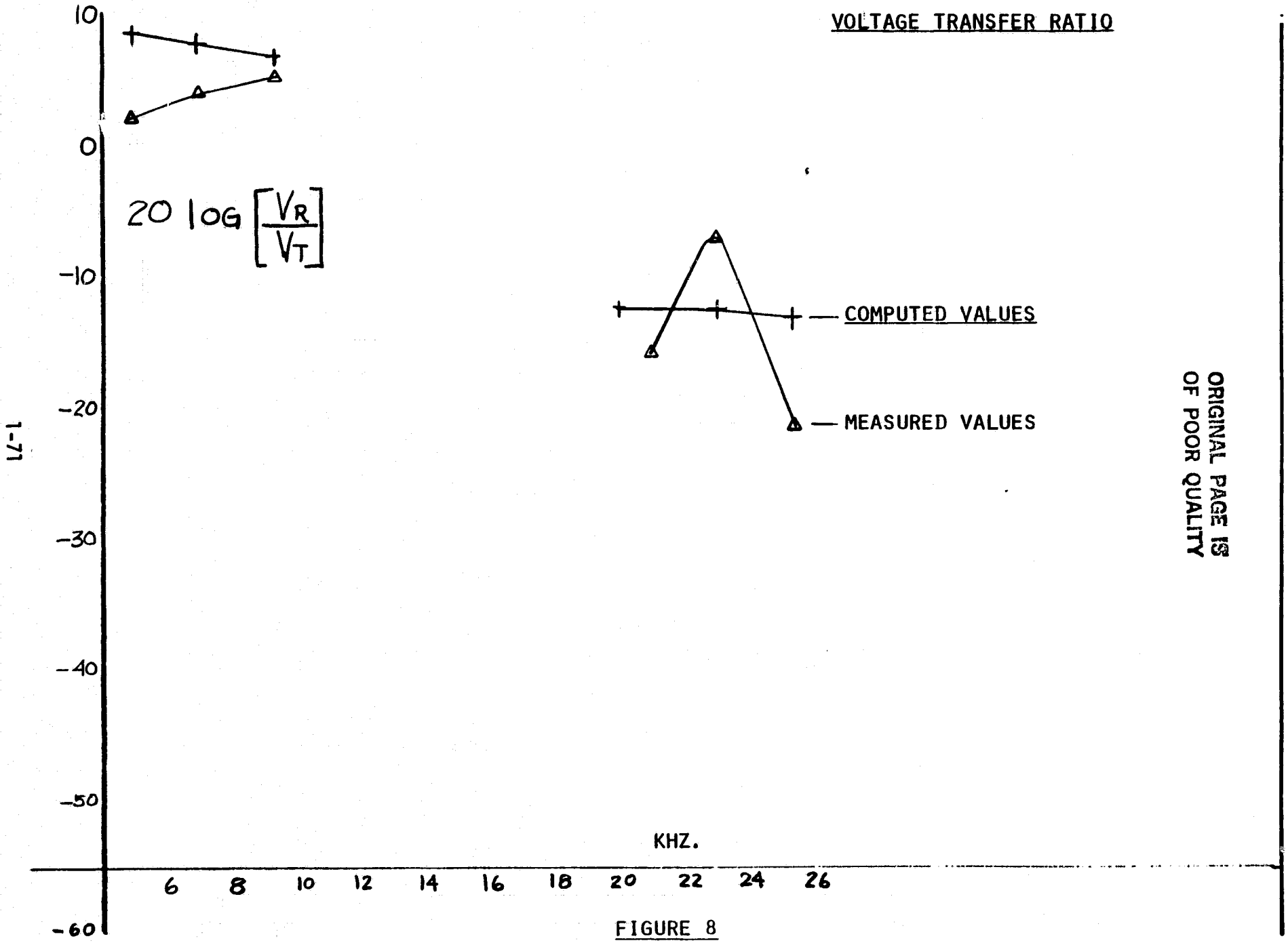

FIGURE 8

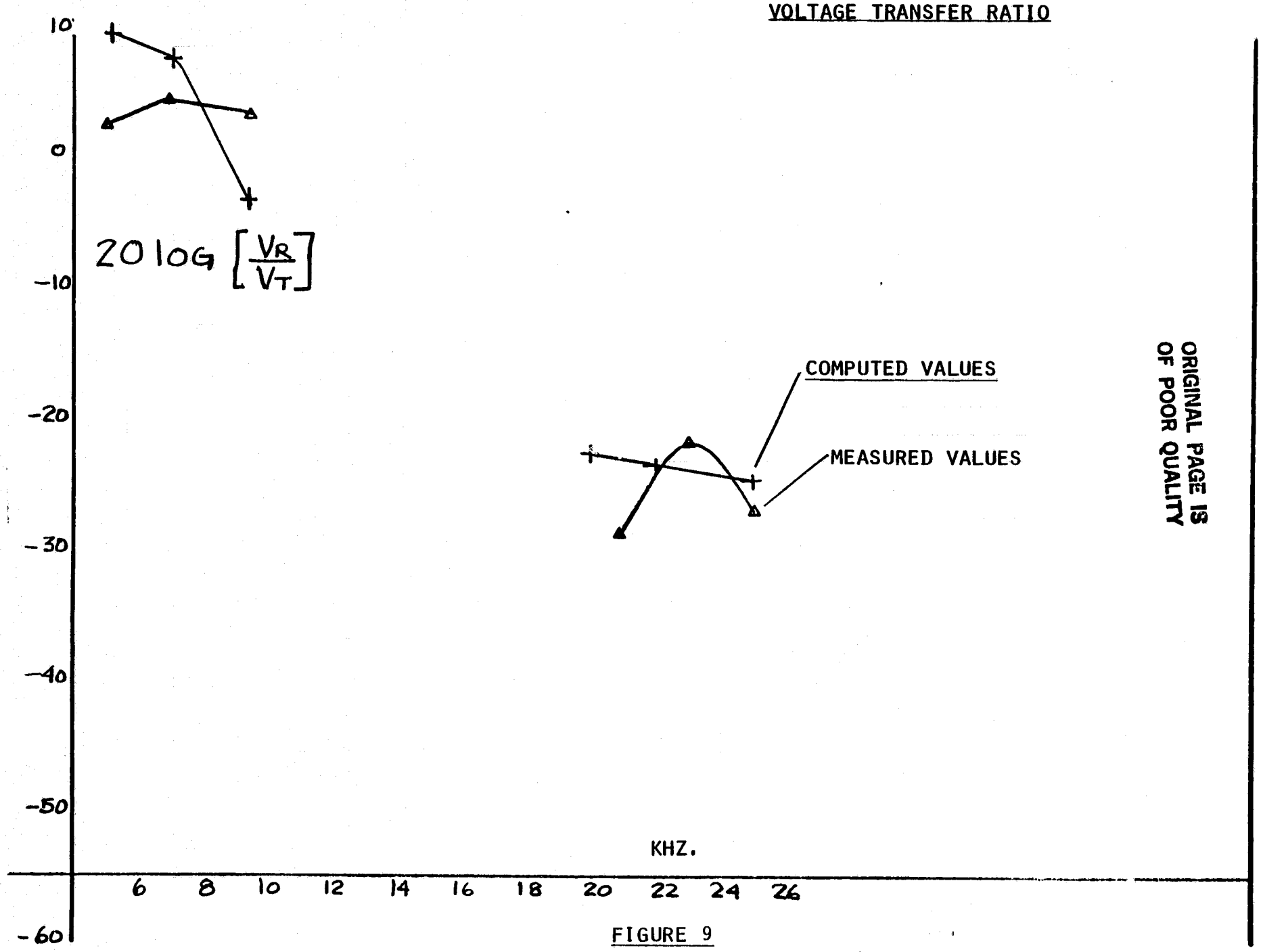

FIGURE 9

Figures 10, 11 and 12 compare the measured and modeled main diagonal elements of the admittance matrix for this modified network condition. The load on each phase was different and was chosen in order to optimize phase voltages further out on the feeder by trial and error methods.

Figures 13, 14 and 15 compare the results of measurement and simulation for the Y_{12}, Y_{13}, and Y_{23} elements, respectively, for this modified network condition.

Again, measurements were taken on the D.T. secondary while the network was in a modified condition. Figure 16 shows the voltage transfer ratio comparison of the computer simulation with the inferred primary voltages from the D.T. while transmitting on Phase A. Figure 17 shows a similar comparison for transmission to Phase B.

Conclusions:

The "Hybrid" overhead-underground network lent itself well to simulation by the NTWKERH1 and NTWKANH1 programs. As opposed to a pure cable network, the relatively short overhead section provided a substantial amount of interphase coupling. (Studies of U.G. cables indicate little mutual coupling). This is illustrated by the fact that reasonable signal levels could be obtained on the Phase B D.T. while transmitting on the other phases during the admittance matrix measurement.

MAIN DIAGONAL ELEMENT ADMITTANCE MATRIX Y_{AA}

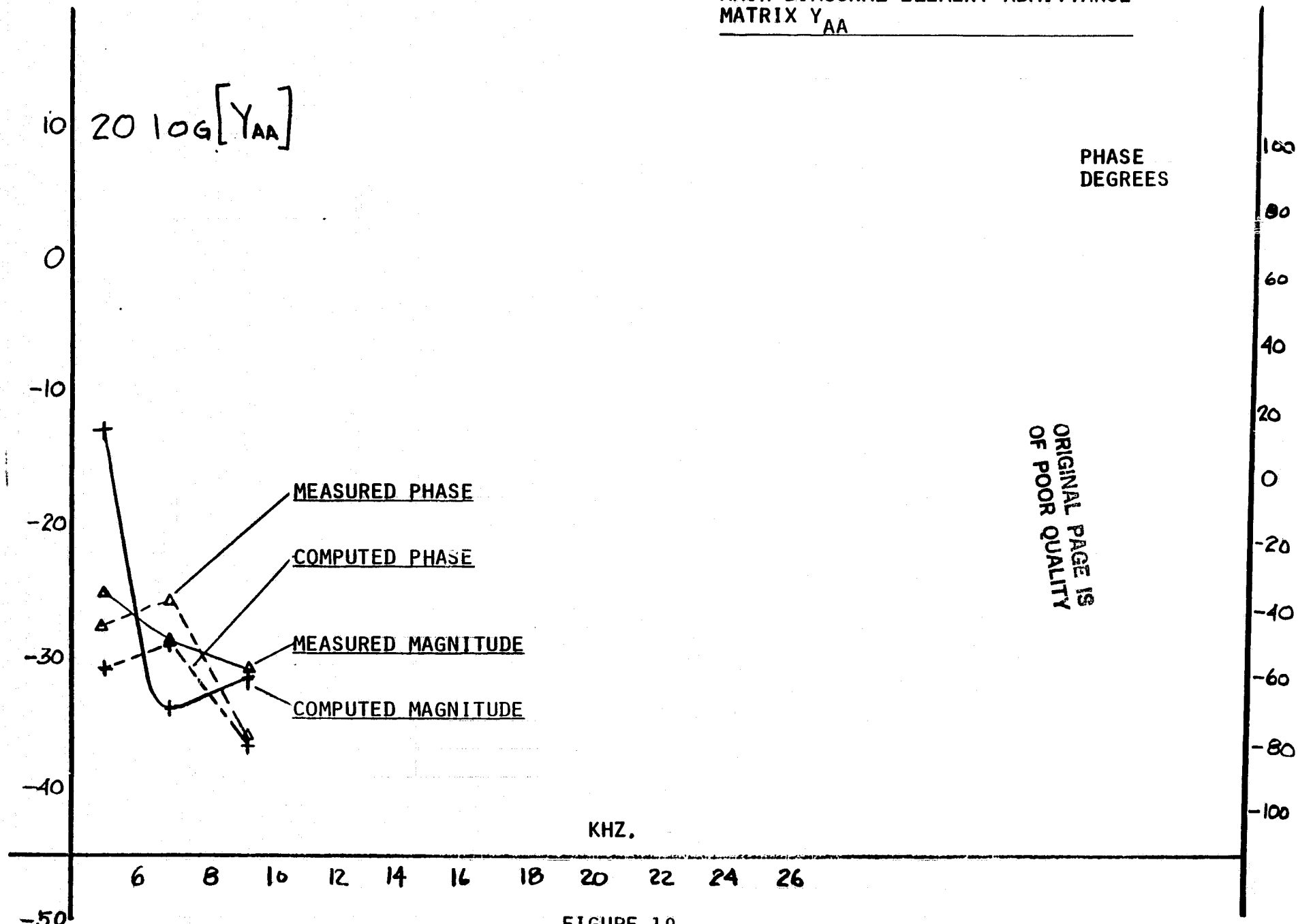

ORIGINAL PAGE IS OF POOR QUALITY

FIGURE 10

MAIN DIAGONAL ELEMENT - ADMITTANCE MATRIX Y_{BB}

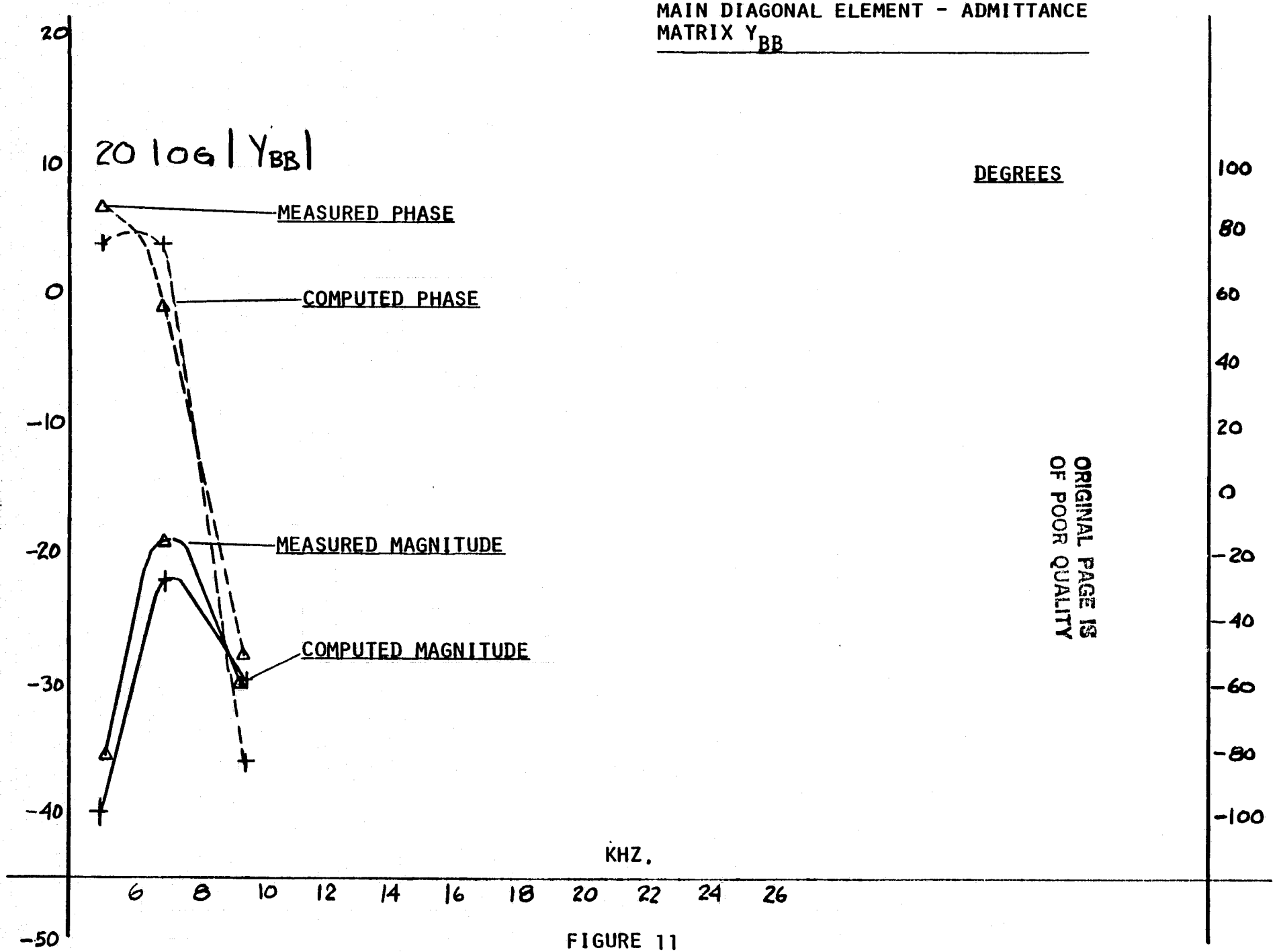

FIGURE 11

MAIN DIAGONAL ELEMENT - ADMITTANCE MATRIX Y_{CC}

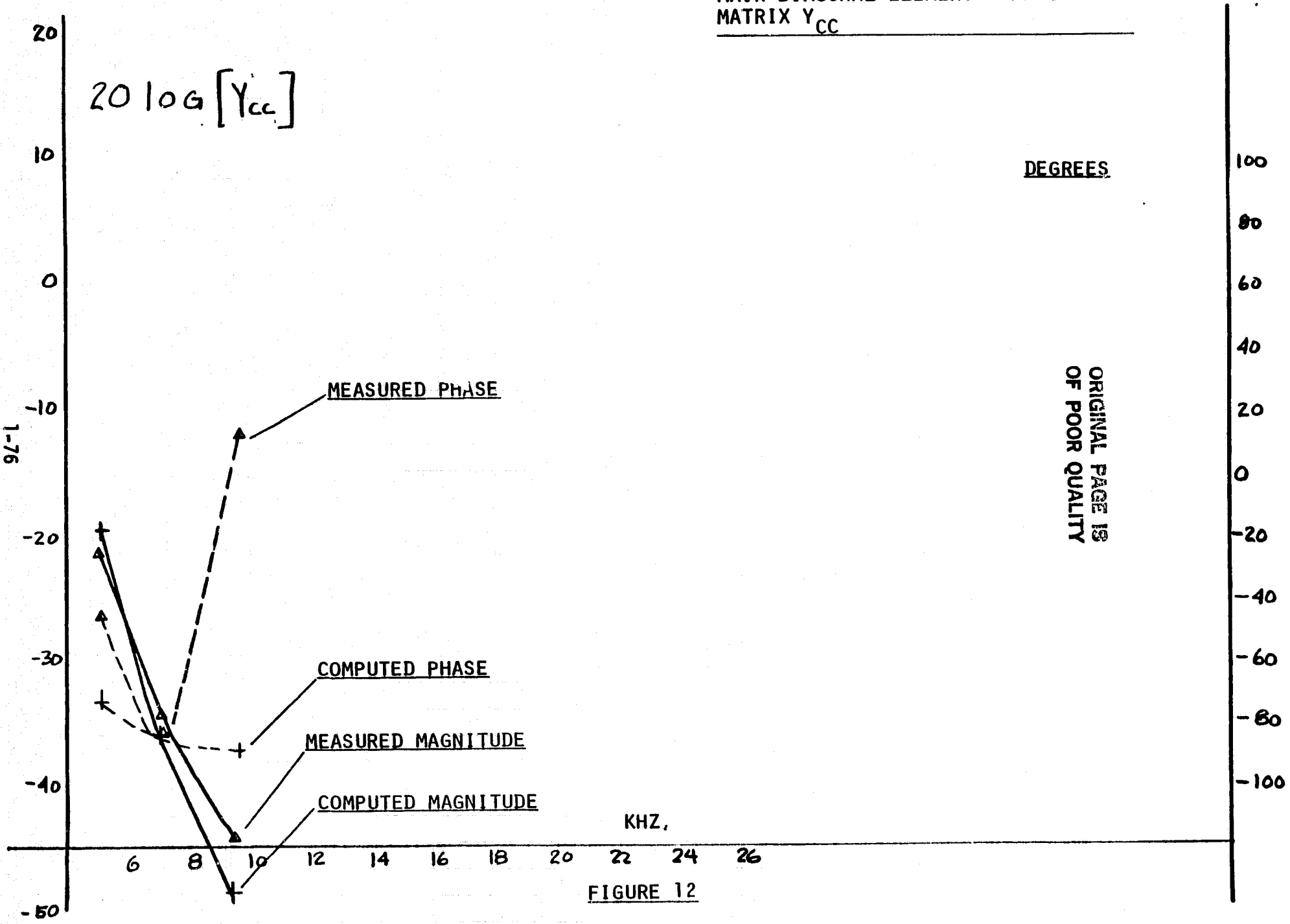

FIGURE 12

OFF DIAGONAL ELEMENT - ADMITTANCE MATRIX Y_{AB}

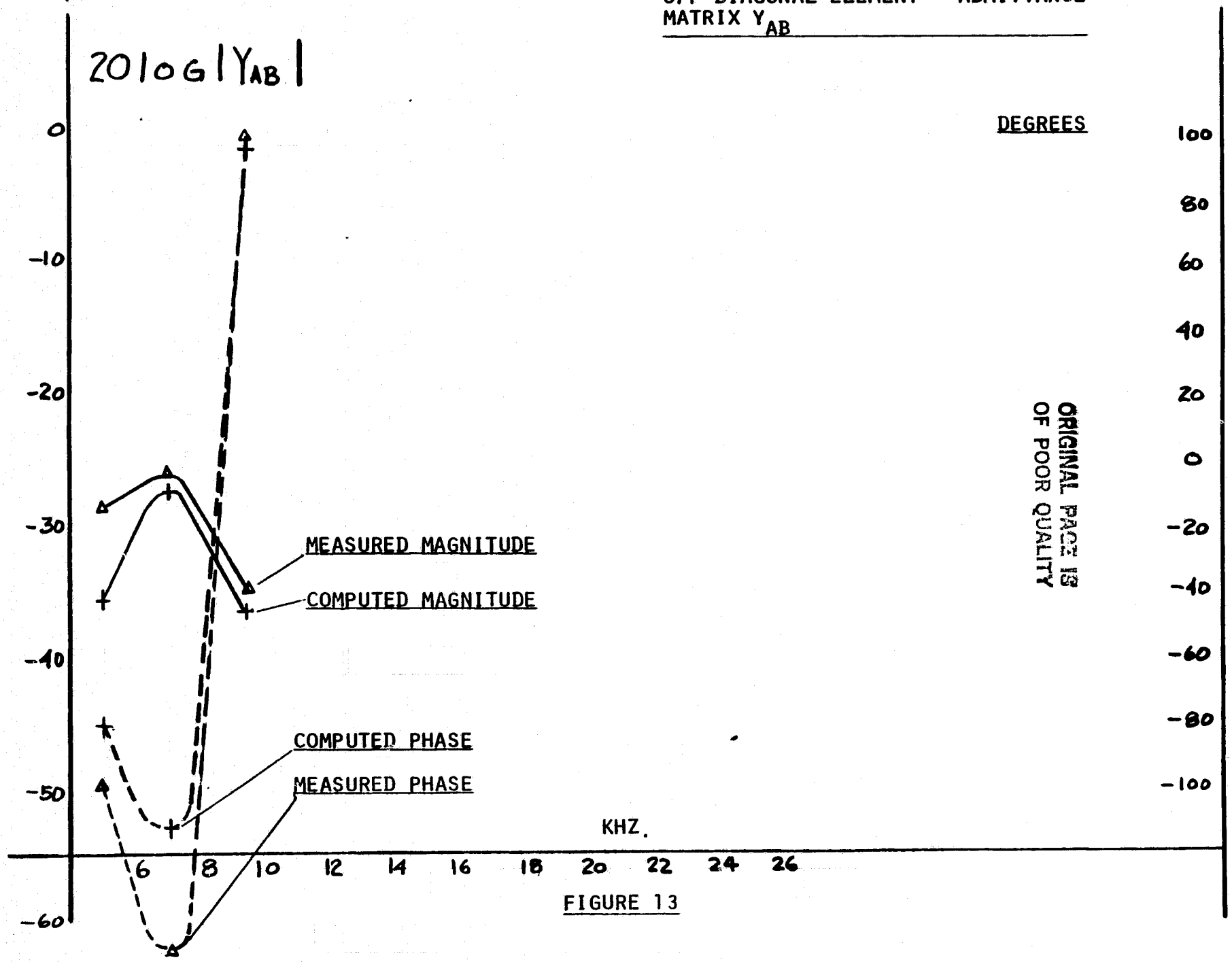

FIGURE 13

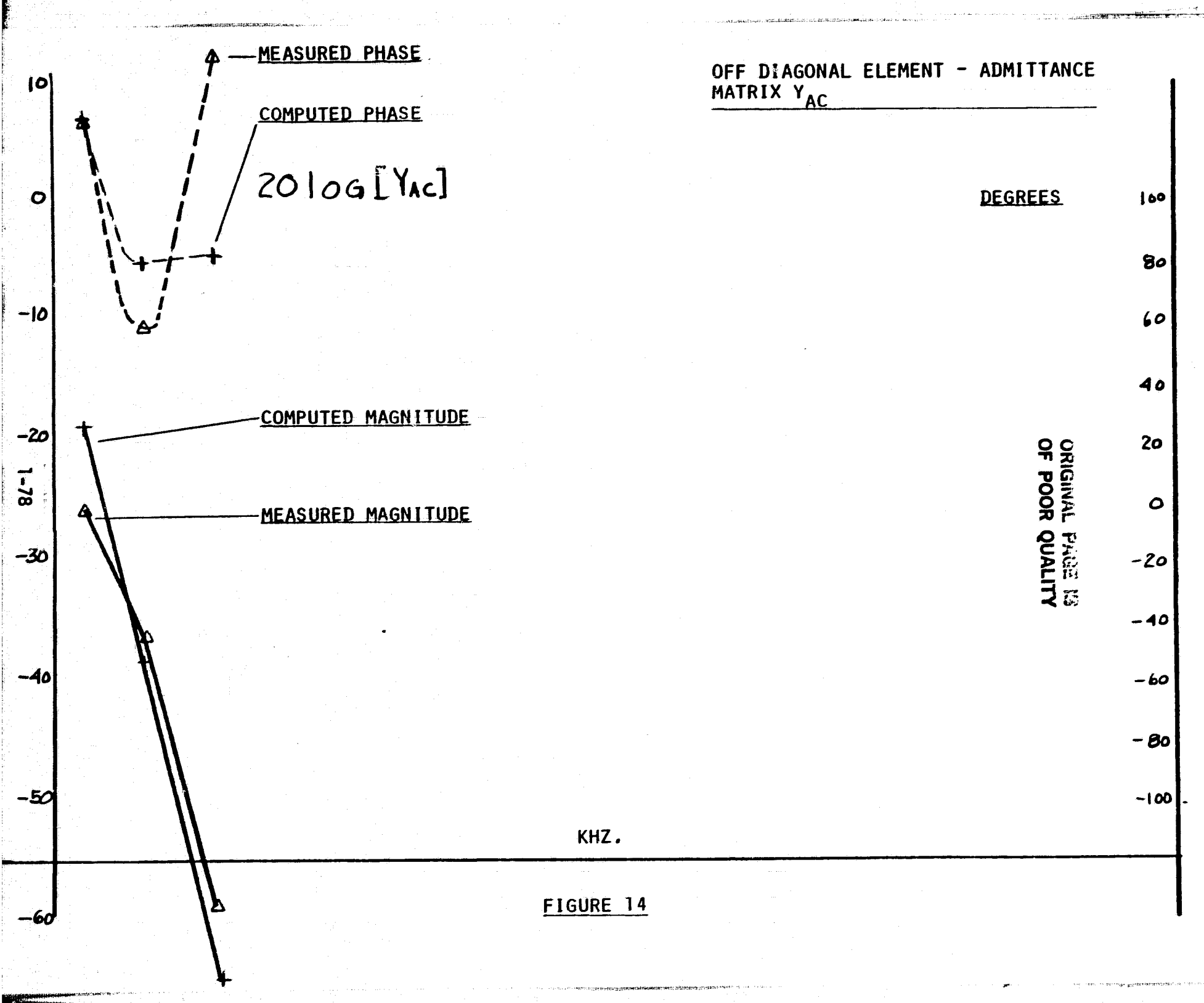

OFF DIAGONAL ELEMENT - ADMITTANCE MATRIX Y_{AC}

FIGURE 14

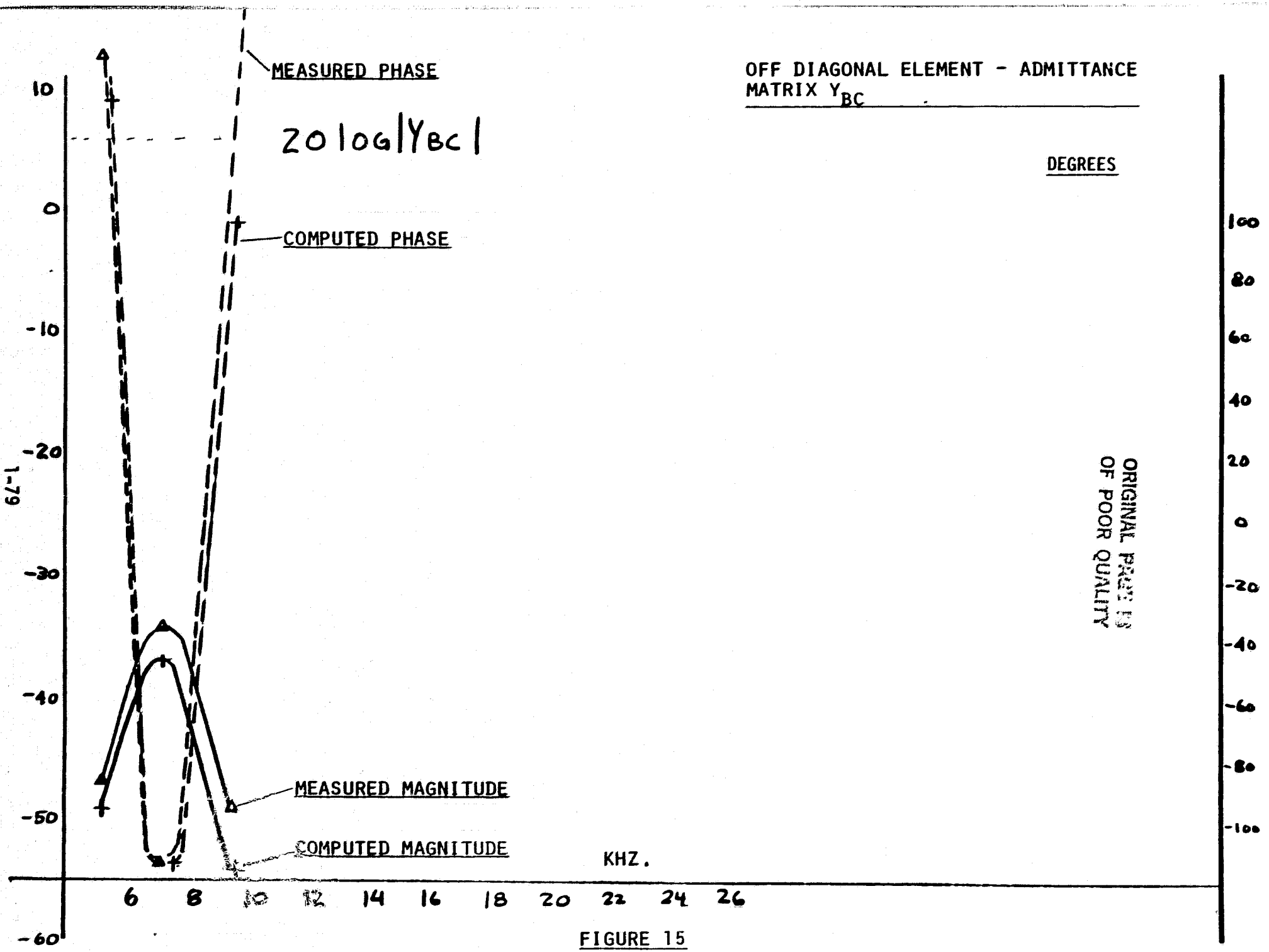

OFF DIAGONAL ELEMENT - ADMITTANCE MATRIX Y_{BC}

FIGURE 15

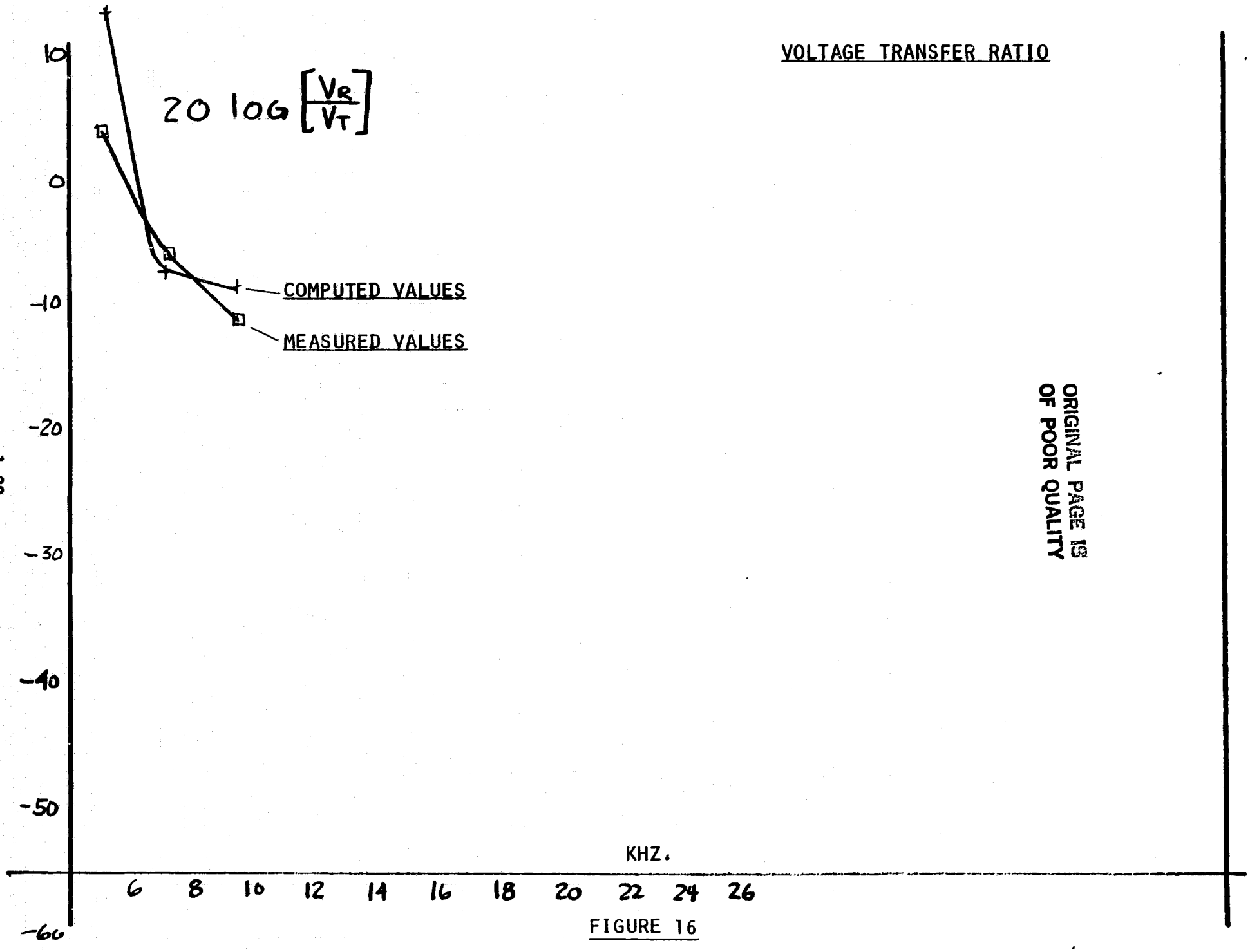

FIGURE 16

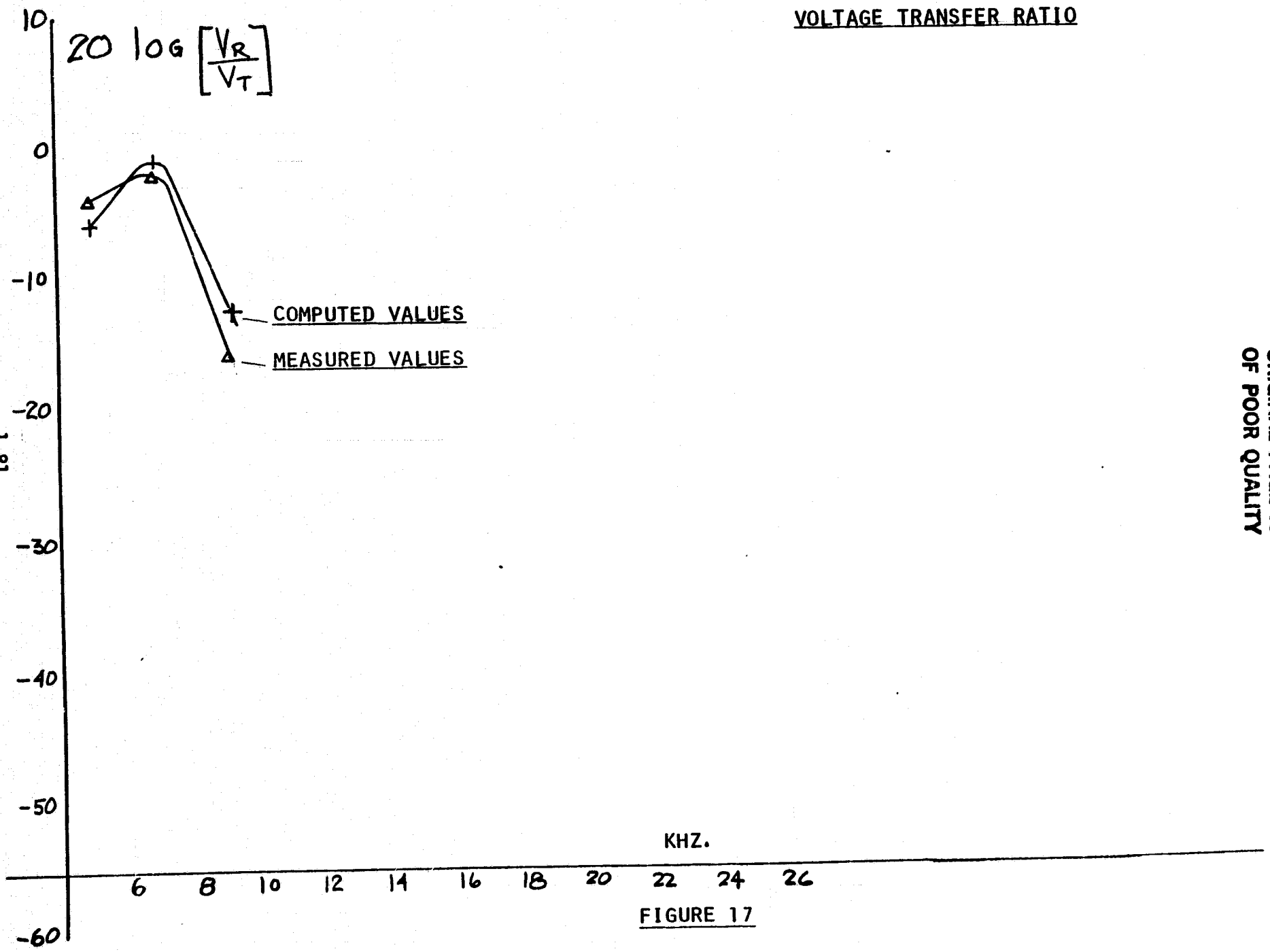

FIGURE 17

The voltage transfer ratio comparison showed good agreement, considering the crude method used to infer the primary voltage at the D.T. during the measurements.

Also, it can be seen that it is quite easy to simulate the effects of the reactive load modification of the network with good accuracy.

Again, it should be noted that various uncertainties are present in the network model such as:

1) Network length uncertainty
2) Conductor temperature
3) System loading (size and location)
4) Earth conductivity

Nevertheless, the results of this simulation would be adequate for communication system engineering.

TASK (1)(D)

Meter Terminals on Secondary*

The purpose of this subtask was to verify the models ability to predict voltages at the "meter terminals" on the secondary service of distribution transformers. Inasmuch as it was not planned as part of this PHASE II effort to have a distribution transformer analytic model implemented, the equivalent prediction is presently performed by a "two-step" process. The first step is to predict propagation on the feeder with distribution transformers (DT) represented by a phasor admittance load connected to the proper phase and representing the DT primary driving point admittance associated with the specified DT and connected secondary load. Then having the predicted feeder phase voltages, an off-line calculation or response curve look up could be used to predict the DT secondary terminal voltage. The voltage propagation down to the meter terminals could also be done off-line using electrically short (primarily a lumped series impedance) secondary circuit representation.

Originally it was hoped to find a DT on NMPC feeder 34556 which had a single customer at the end of a long secondary service. To verify with a "multi drop" secondary would have required simultaneous measurement of each customer load-current and voltage which was not considered feasible. However, no long single customer service was found. Therefore, no uniquely applicable test and verification was conducted.

However, several related activities and characteristics have some positive bearing on this objective. First, as part of TASK 1C, propagations were made from a location on the feeder (removed from the DT

---

*This discussion is verbatum from Volume 1

location) to the secondary terminals of various DT's, and the results were supportive. Secondly, as part of TASK 4 DT modeling extensive response measurements were made that show, for the lower frequency range (say less than 25 kHz) the primary to secondary transfer is primarily the turns ratio effect with a few DB accounting for reactance drop caused by secondary load. Finally, any voltage drops on the secondary circuit would depend on an estimate for the simultaneous loads for each customer. Since the secondary circuits are electrically short, the computation, given the loads, presents no conceptual problem.

It is believed, therefore, that compared to predicting propagation on the feeder, analysis of the DT primary to secondary (terminals) transfer and prediction on the secondary terminals present no conceptual difficulty.

TASK (1)(E)

Extended Frequency Range*

The objective of this subtask was to extend the frequency range of verification to satisfy the objective of PHASE I. Because of technical considerations mentioned in 1) and 2) below, it was deemed higher priority to verify first the models capability at the lower frequencies. Hence, the other tasks associated with verifying the model were given scheduling priority. For the reasons cited below, the work called for by this task was not accomplished.

1) Uncertainties in Specifying Line Lengths

As work progressed to the point of verifying the model at lower frequencies, it was realized that apriori estimates (based on utility records) of line lengths are not always reliable. This aspect required a non trivial effort to understand the reason for lack of verification in some of the trials. Because of wavelength considerations, errors in assigning (to the model) line lengths will become "damaging" with higher frequency. Based on our experience, this limit may be 50-100 kHz.

2) Transformer Response

As the transformer modelling and measurements progressed, it appeared more and more promising that with a simple extension (to the 60 Hz R-L-M two winding transformer model, a lumped parameter model could be used to predict transformer response up to 25-50 kHz and which was not too sensitive to variations in construction, i.e., with the simple extension the similarity of 60 Hz performance could be extended to 25-50 kHz. (Characteristics do vary with KVA). Beyond this frequency range, variations in response at PLC due to differences in manufacturing

---

*This material is verbatum from Volume 1

construction may become important. If this is true, than either a much more detailed inventory of transformer characteristics and identification of installed transformers is required, or additional modeling errors accepted.

3) Resource and Time Limitations

During the process of verifying the model, several contingencies were encountered. One involving line length uncertainties was mentioned above. The most significant contingency involved verification with circuits involving underground cables. Identifying the source of the problem, arranging for appropriate tests (see Volume II, Task (1)(C), writing a new cable parameter program involved considerable effort and delay. Another contingency involved making admittance measurements of the Grooms Road Substation. Special measurement equipment had to be designed and built and special facilities installed by Niagara Mohawk Power.

As a result, resources (and time) were not available to proceed with higher frequencies.

4) Vendor Trends to Lower Frequencies

Supporting the above stated priority is what appeared to be a trend by virtually all parties to gravitate to the lower frequencies for distribution feeder communication.

Summary of Verification Activities

As a result of a considerable experience gained in verifying the model, the following caveats are offered:

1) Line length uncertainties, especially for underground sections, can be significant such that, typically, for frequencies greater than 25-50 kHz, these lengths should be correctly defined. Even at lower frequencies, point estimates of a given frequency should be supplemented by a frequency response in the neighborhood to reveal if in the vicinity of a resonance which could be sensitive to line length errors.

   The above mentioned frequency limit is also applicable if the simple lumped parameter transformer model is to be used.

2) Line loading can have a significant effect (in reality and model) so it is recommended that this effect be investigated parametrically for "worst case situations".

3) Inbound calculations which usually involve representation of a substation (admittance load) will be sensitive to estimation errors in this admittance representation unless the design (trapping, etc.) negates the effect of these errors.

Except for item 1) the above represent reality and as such are not a problem in the modeling. Hence, it is recommended that appropriate parameter variations (in relative and specific loading) be conducted to determine worst case effects. Item 1) suggests that in addition to using utility documentation, appropriate questions be asked of the utility operations to uncover possible practices which would in fact yield line lengths different (usually longer) than documented.

Having these caveats in mind, it is our opinion that the model predicts quite well and should be useful for communication design, and that if a continued need exists for this kind of tool that it would be justified to further enhance its capability and convenience (see section containing recommendations in Volume 1).

TASK 2

EXTENSION, IMPLEMENTATION & VERIFICATION OF PERTURBATION THEORY

TASK 2

TABLE OF CONTENTS

	Page
FOREWARD	2-1
TASK 2(-)	2-2
TASK 2(A)	2-8
TASK 2(B)	2-9

CONTRIBUTORS

TASK 2(-)	J. T. Gajjar
TASK 2(A)	R. Wooding, J. T. Gajjar
TASK 2(B)	R. Wooding, R. W. Rankin, M. J. Lukas G. W. Kinloch, W. C. Hughes

C-2

FOREWORD

The work statement specified three types of activities associated with this task, i.e.,

TASK 2(-) Extension and Implementation of Perturbation Theory

TASK 2(A) Use Perturbation to Calculate Inbound Path Propagation

Task 2(B) Measure Inbound Path Propagation

The work associated with the first activity is reported herein supplemented by the material contained in Appendix 1 and 2 in Volume 3. The work and results associated with Task 2(A) and 2(B) are contained herein.

TASK 2(-) EXTENSION AND IMPLEMENTATION OF PERTURBATION THEORY

The DIFNAP system of programs is a useful tool for the analysis of signal flow over power distribution systems configured in the form of distributed, multi-conductor trees. The analysis procedure used in these programs is a two-step procedure. In the first step, starting with the extremities of the network, input admittances are computed for each branch of the tree. Voltage transfer ratios across each section of the tree are also computed and saved. The process culminates in the computation of the input admittance to the entire network. In the second step, the input voltages are determined using the input admittance to the network computed in the first step, and the source parameters. Voltages at various points of the network can be calculated using the input voltages and the voltage transfer matrice computed and saved in the first step.

By computing and saving the admittance parameters of each section during the first step, currents and signal power at various points in the network can also be computed.

It is often of interest to determine the effects of changes in load values on the voltages in the network. The use of the DIFNAP program would normally entail recomputing the entire network with both steps.

In order to permit more efficient computations of effects of load variation, during the PHASE I model development, a technique called the "perturbation theory" was developed. This technique uses the application of the reciprocity theorem, as extended to multi-conductor systems, to the adjoint of the tree structured multiconductor

distribution feeder network.

As a consequence, voltage variation at any point on the network, resulting from the variation of a single load, can be computed by exercising the second step of the procedure only. It was determined that the inbound computation of network input admittances and re-computation of voltage ratios is not necessary. Although we have chosen to call the process application of perturbation theory, since we are dealing with changes in voltage resulting from a change in a load value, the computation is in no way an approximation. In fact, the procedure is computationally exact, even for large variations in load. It can, for instance, be used for computing the effects of faults, both open and short, on signal propagation in the model. Further details of the mathematical development of the theory and algorithm can be found in the Sponsor Reports[1,2] submitted in conjunction with the Phase I report. A tutorial on this subject, written by R. C. Rustay, has been included as Appendix 1 in Volume 3.

The theory and algorithms were developed during the first phase of the model development. Time and resources did not permit us to incorporate the algorithms into the model during that phase.

During the INTERPHASE period following the completion of PHASE I and before the beginning of PHASE II of the project, we realized the importance of an ability to make inbound signal propagation computations from points on the network to a receiver. It was also deemed essential that the location of the receiver be not necessarily the same as that of the source in the outbound computation.

One possible approach to this problem was to create a different network with each load point of the original network being the source point of the new network. By using both of the steps of the DIFNAP program procedures outlined above, the circuit can be analyzed and the inbound signal at the receiver located at any point on the network could be estimated. For a large number of load points, however, this procedure becomes both cumbersome and computationally uneconomical.

The other approach is to make direct use of the reciprocal properties of bilinear, passive networks. In this approach one uses transpose matrix relationships and computations made in the outbound path to determine the reverse path computations. The application of a source at a load point for the purpose of transmitting information, usually also results in a change in admittance at the load point. Thus, in addition to the application of reciprocity, a technique such as the perturbation procedure outlined above, has to be used to make the computations. This approach, however, suffers from the limitations that we can only make computations for the receiver located at the outbound source of the network.

From the mathematical theory developed, for the perturbation approach during Phase I, we recognized the potential for extending this approach to the solution of the reverse path problem. This extension was undertaken and completed during the INTERPHASE period and the perturbation algorithms together with those for the reverse path were implemented into the computer model. Just prior to the beginning of the Phase II effort, we also developed a program which permits the network reversal from any point on the network and using it we were able to prove out the procedure implemented for perturbation

and reverse path propagation.

The perturbation and reverse path procedures are implemented so that they can be entered after the initial processing of the second step for at least one outbound computation. At the end of each forward processing, the interactive program asks the user if a perturbation on reverse path computation is desired.

When the reverse path/perturbation option is chosen, the user next enters the node number of the node at which the load variation takes place or the reverse path source is applied. After verifying this, the program internally checks to determine if the outbound path to this point has been computed. If not, the program proceeds to make the outbound computation to that point.

The user is then asked to choose between a reverse path or perturbation computation. If the reverse path computation is chosen, the program asks him to define the reverse path source as a Norton's equivalent source. If the perturbation computation is chosen, the user defines the change in load. Following the verification of the source, or load change, the user is asked to define the end of the section where the result is desired. The program then computes and displays the outbound voltages, change in the outbound voltage due to the load perturbation or the reverse path source, and the algebraic sum of the two.

The user can then choose another point at which to evaluate the effect of the network change. If not, he can choose another point at which to insert a reverse path source or load perturbation. If he chooses neither, the program exits from the perturbation mode and asks the user if he would like to compute the outbound network with another source.

The user interaction of the analysis program (step 2) with the reverse path option is demonstrated in the printout shown in Figure 2-1. The perturbation interaction is similar except that no current source input is involved.

Operationally, the perturbation/reverse path section does not alter any of the information computed during the outbound path computation, as it does not involve the output macro in its execution. Thus, in repeated applications of the perturbation procedure, consistent results are obtained after several different applications.

The perturbation/reverse path approach permits computation of the effects of introducing a source and/or a load admittance change at any point in the network. The point at which the result is determined can be in another branch of the network or can be in an outbound direction from the point at which the source/load variation are applied. Thus, point-to-point signal propagation and the solution of partial networks can also be accomplished by this approach.

```
=
ENTER FREQ CODE,NETWORK ID NO.,OUTPUT FILE NO.
5,91,1
IFCODE,NIDEN,IOPTN=            5              91              1
IF OK TYPE CR
=
TYPE CR TO BYPASS PLOTTING LOGIC
=
VOLT LIMIT =  0.10000000E 00 IMPEDANCE LIMIT  0.50000000E 02
IF OK TYPE CR
=
TYPE 1 TO SPECIFY A NEW SOURCE, TYPE 2 TO EVALUATE
A NEW SECTION USING EXISTING EXCITATION  INBEDDED IN FILE
=1
DO YOU WANT A VOLTAGE SOURCE DRIVE?
IF OK TYPE CR
=1
CURRENT SOURCE DRIVE=
 1.0000000E 00  1.0000000E 00  1.0000000E 00
 0.             0.             0.

IF OK TYPE CR
=
THE  SOURCE VECTOR WILL CREATED WITHIN
THE PROGRAM BY CURRENT INJECTION.   IF YOU DESIRE A
ZERO EQUIVALENT NORTONS SOURCE ADMITTANCE TYPE CR
=

ENTER A CONCATENATED INTEGER TO INDICATE OUTPUT OPTIONS AS FOLLOWS
1 - OUTPUT VOLTAGE & INPUT CURRENT
2 - NORTON SOURCE ADMITTANCE AND CURRENT
3 - INPUT ADMITTANCE
4 - TOTAL LOAD ON SECTION
5 - VOLTAGE TRANSFER MATRIX
6 - CURRENT DRIVE FOR UNITY VOLTAGE
7 - OVERALL VOLTAGE TRANSFER
9 - MAGNITUDES OF OUTPUT VOLTAGES AND IMPEDANCE LEVELS, LEVEL WARNINGS AND POWER
THE LAST OPTION WILL AFTER THE FIRST PRINTOUT,
DISABLE ALL OTHER OPTIONS

=1
ENTER SECTION NUMBER OF SECTION AT WHICH OUTPUT IS DESIRED
=20
SECTION CHOSEN IS     20 IS THIS CORRECT?
IF OK TYPE CR
=
                                 OUTPUT VOLTAGE   20
 0.102865E 03  -.801776E 03  0.113242E 03  -.848446E 03  0.954756E 02  -.801381E 03
                                  INPUT CURRENT   20
 0.941277E-01  0.120608E-01  0.295563E-01  -.623604E-01  0.949948E-01  0.104168E-01

DO YOU WANT OUTPUT AT ANOTHER SECTION WITH SAME SOURCE?
IF OK TYPE CR
=1

DO YOU WANT THE EFFECTS OF LOAD PERTURBATION
OR A REVERSE PATH PROPOGATION ?
IF OK TYPE CR
=

ENTER SECTION AT WHICH LOAD CHANGE TAKES PLACE
=20
SECTION CHOSEN IS     20 IS THIS CORRECT?
IF OK TYPE CR
```


Figure 2-1

```
IF OK TYPE CR
=
ENTER NORTON SOURCE CURRENT VECTOR AS
   3 COMPLEX NUMBERS
=1,0,1,0,1,0
 1.0000000E 00  1.0000000E 00  1.0000000E 00
 0.             0.             0.

IF OK TYPE CR
=
ENTER CHANGEIN NORTON ADMITTANCE AS
      9 COMPLEX NUMBERS
=0,,,,,,,,,,,,,,,,,,,,,,
 0.             0.             0.
 0.             0.             0.

 0.             0.             0.
 0.             0.             0.

 0.             0.             0.
 0.             0.             0.

IF OK TYPE CR
=

ENTER SECTION AT WHICH EFFECT OF PERTURBATION IS 'TO BE DETERMINED
=20
SECTION CHOSEN IS .    20 IS THIS CORRECT?
IF OK TYPE CR
=

VOLTAGE BEFORE CHANGE
 1.0286541E 02  1.1324235E 02  9.5475565E 01
-8.0177586E 02 -8.4844647E 02 -8.0138065E 02


CHANGE IN VOLTAGE
 2.2493948E 02  2.3024437E 02  2.0571355E 02
-7.1058760E 00 -1.1465082E 01  5.6799455E 00


VOLTAGE AFTER CHANGE
 3.2780489E 02  3.4348672E 02  3.0118912E 02
-8.0888174E 02 -8.5991155E 02 -7.9570070E 02


DO YOU WANT RESULT AT ANOTHER SECTION?
IF OK TYPE CR
=

ENTER SECTION AT WHICH EFFECT OF PERTURBATION IS 'TO BE DETERMINED
=1
SECTION CHOSEN IS      1 IS THIS CORRECT?
IF OK TYPE CR
=

VOLTAGE BEFORE CHANGE
 2.3511039E 02  2.5845466E 02  2.2428622E 02
-8.1599802E 01 -1.0275978E 02 -7.5628699E 01


CHANGE IN VOLTAGE
 1.0157668E 02  1.1394569E 02  9.5481212E 01
-8.0037127E 02 -8.4355851E 02 -7.9827698E 02
```

Figure 2-1

TASK 2(A) PERTURBATION CALCULATION OF INBOUND PROPAGATION

This task was concerned with using the implemented perturbation technique to predict inbound/reverse propagation. What actually was done was to predict inbound propagation using both perturbation techniques and an alternate procedure involving a "network reversal" operation* followed by a normal outbound prediction from the "new" source to, say, the substation. The purpose of using this alternate procedure was first to give an "exact" numerical check on the perturbation arithmetic implementation and also as a more convenient procedure for the general verification of the model. The result of this model verification is contained in the following Task (2)(B) Section.

Since the arithmetic results using the perturbation and the reversed network procedures gave exactly (except for negligible differences due to numerical round off considerations) the same results in all cases, specific numerical results are not presented here. Also, the same procedures were used on other synthetic networks designed to test various topological considerations (conceptually three different topological classes exist, each of which requires somewhat different perturbation logic. Also within each of these classes, various other situations, such as transitions, were tested). As a result of these tests, it is believed that the implemented perturbation logic is validated.

*A main program "NETREVSI" was implemented during the INTERPHASE interval and which can automatically generate from a given network file a new network file having a specified remote node as a new source.

MODEL VERIFICATION - INBOUND PATH PROPAGATION

INTRODUCTION

Inbound signal propagation measurements were performed on a 13.2 kv distribution feeder. This feeder being the 34556 feeder on Niagara Mohawk's Grooms Road Substation in Clifton Park, N.Y. Inbound transmissions were made at a point about 7.7 miles away from the substation. Inbound signals were measured at an intermediate point and at the substation. Computer models were made of these tests for comparison.

BACKGROUND

Carrier signals were transmitted at a capacitor bank location shown on Figure 1. Inbound signals were monitored at Carlton Rd., and the substation. These points are shown in Figure 1. Signals were transmitted by using the power factor correction capacitors already in place. A diagram of this transmitting arrangement is shown in Figure 2. At Carlton Rd., individual phase voltages were monitored. Figure 3 shows a diagram of this voltage monitoring arrangement.

It was not possible to readily measure individual phase voltages at the substation during the field measurements, although the individual phase currents were available. Therefore, the phase currents were used for model verification purposes at the substation. Figure 4 shows a diagram of the measurement apparatus at the substation.

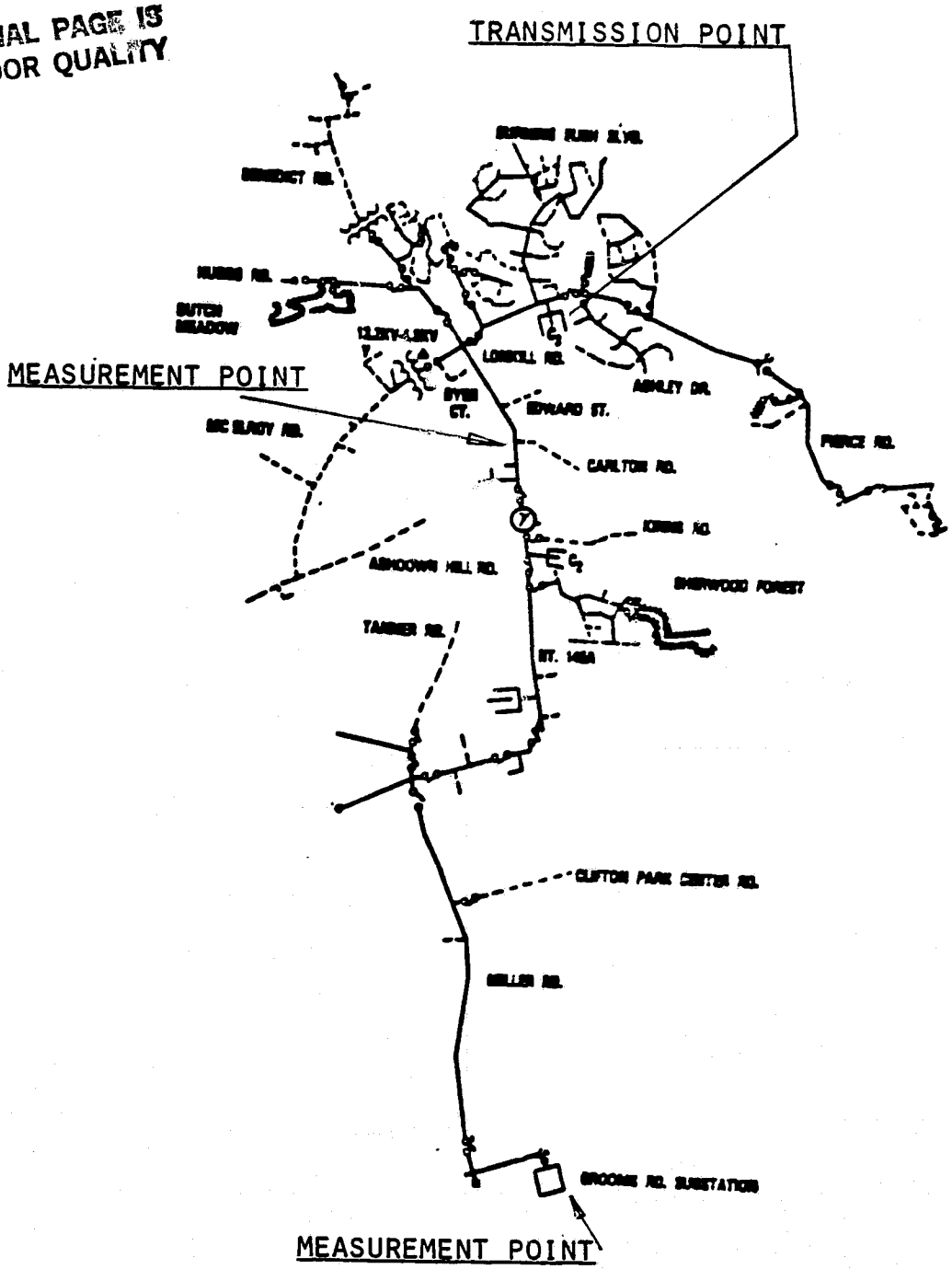

FIGURE 1
34556 FEEDER

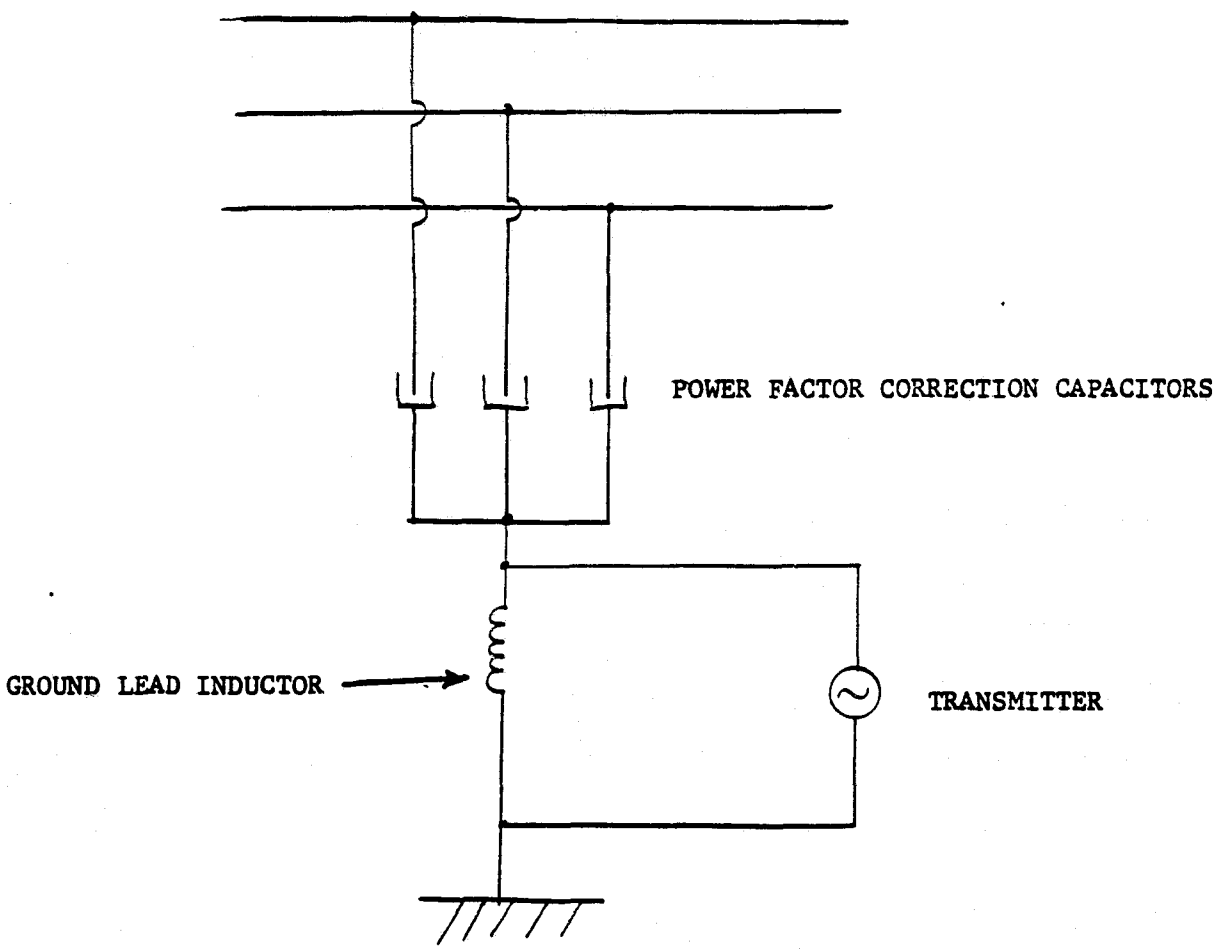

FIGURE 2 TRANSMITTING ARRANGEMENT AT POWER FACTOR CORRECTION CAPACITOR BANK

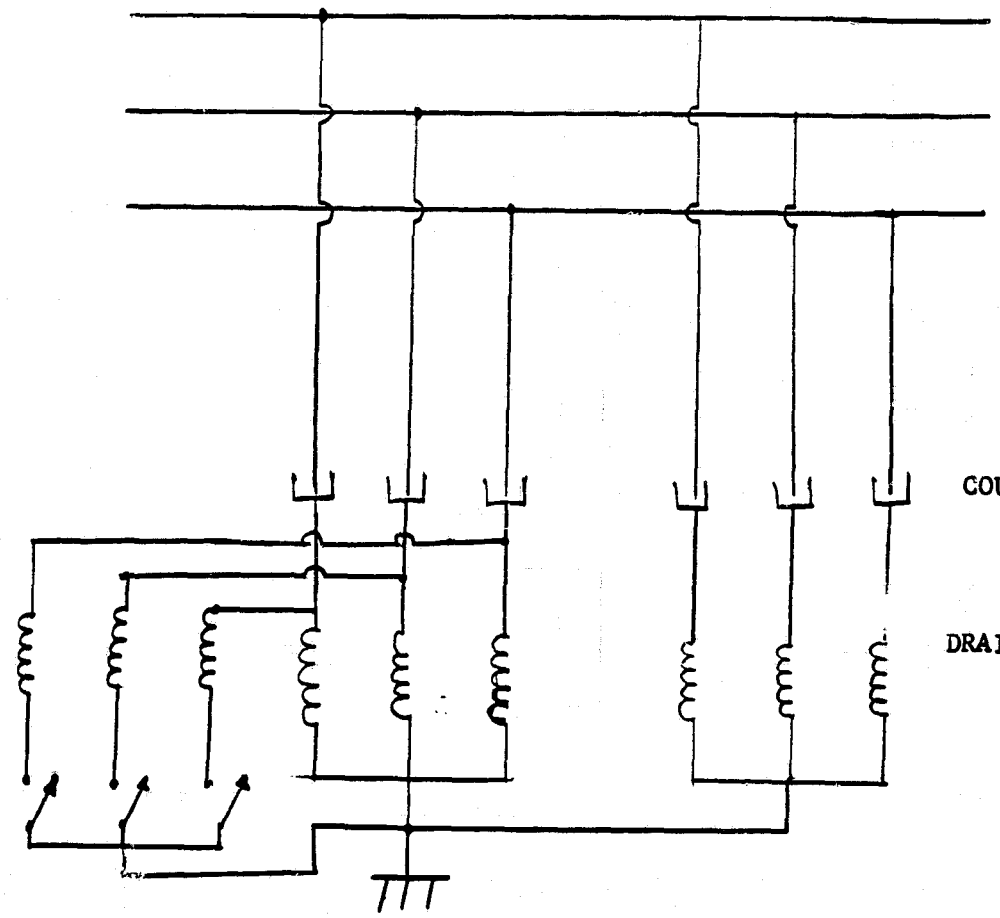

FIGURE 3

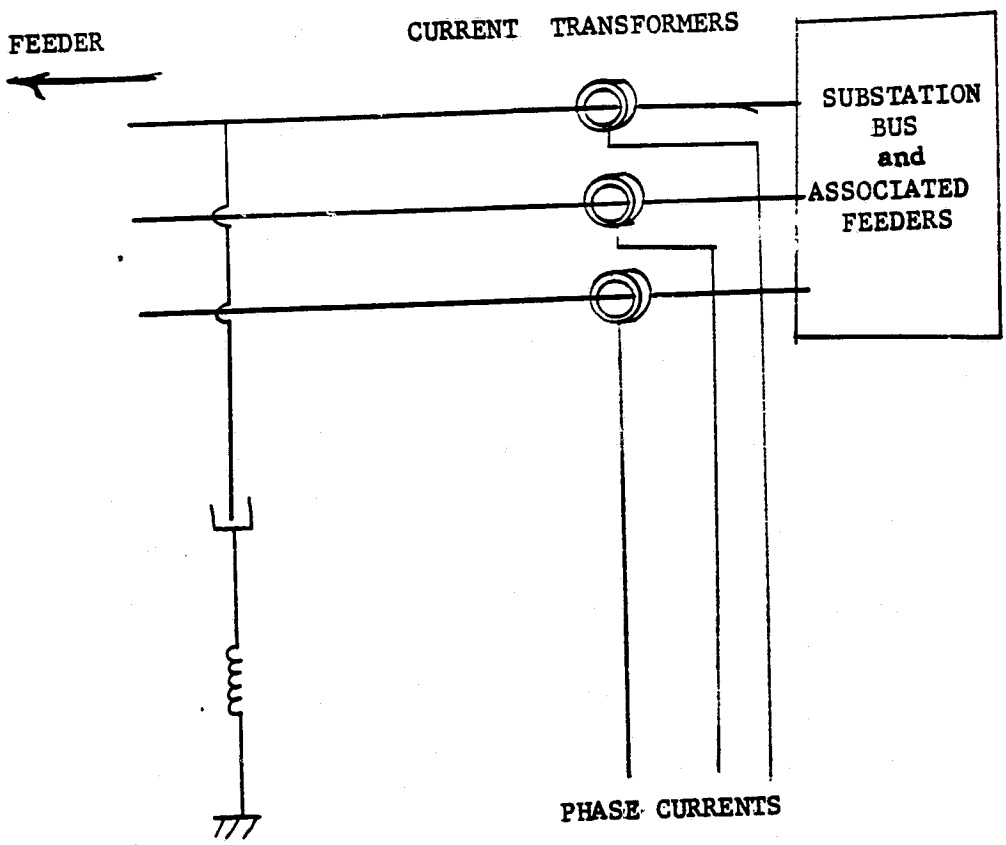

FIGURE 4 CURRENT MEASUREMENTS AT SUBSTATION

RESULTS

Measurement of inbound signal propagation was made under three conditions:

1) No coupling and measurement apparatus at Carlton Rd.
2) Coupling and measurement equipment attached at Carlton Rd. No tuning inductors attached.
3) Coupling and measurement equipment attached at Carlton Rd. Tuning inductors attached.

Therefore, under condition (1), no voltage measurements were obtained at Carlton Rd. Figures 5, 6, and 7 show comparisons of measured and computed values under condition (1). The ratio of the individual phase currents at the substation to the transmitted voltage at the substation is shown. (Transadmittance)

Figures 8, 9, and 10 show the ratio of the individual phase currents at the substation to the transmitted voltage under condition 2. Also, under this condition, the individual phase voltages were monitored at Carlton Rd. The ratio of the individual phase voltages to the transmit voltage at the capacitor bank is shown in Figures 11, 12, and 13, respectively.

Under condition 3, the tuning inductors were attached to the coupling network. Figures 14, 15, and 16 show the ratio of the individual phase currents at the substation to the transmitted voltage at the capacitor bank. Figures 17, 18, and 19 show the measured and computed voltage transfer ratios for the individual phase voltages between the capacitor bank and Carlton Rd.

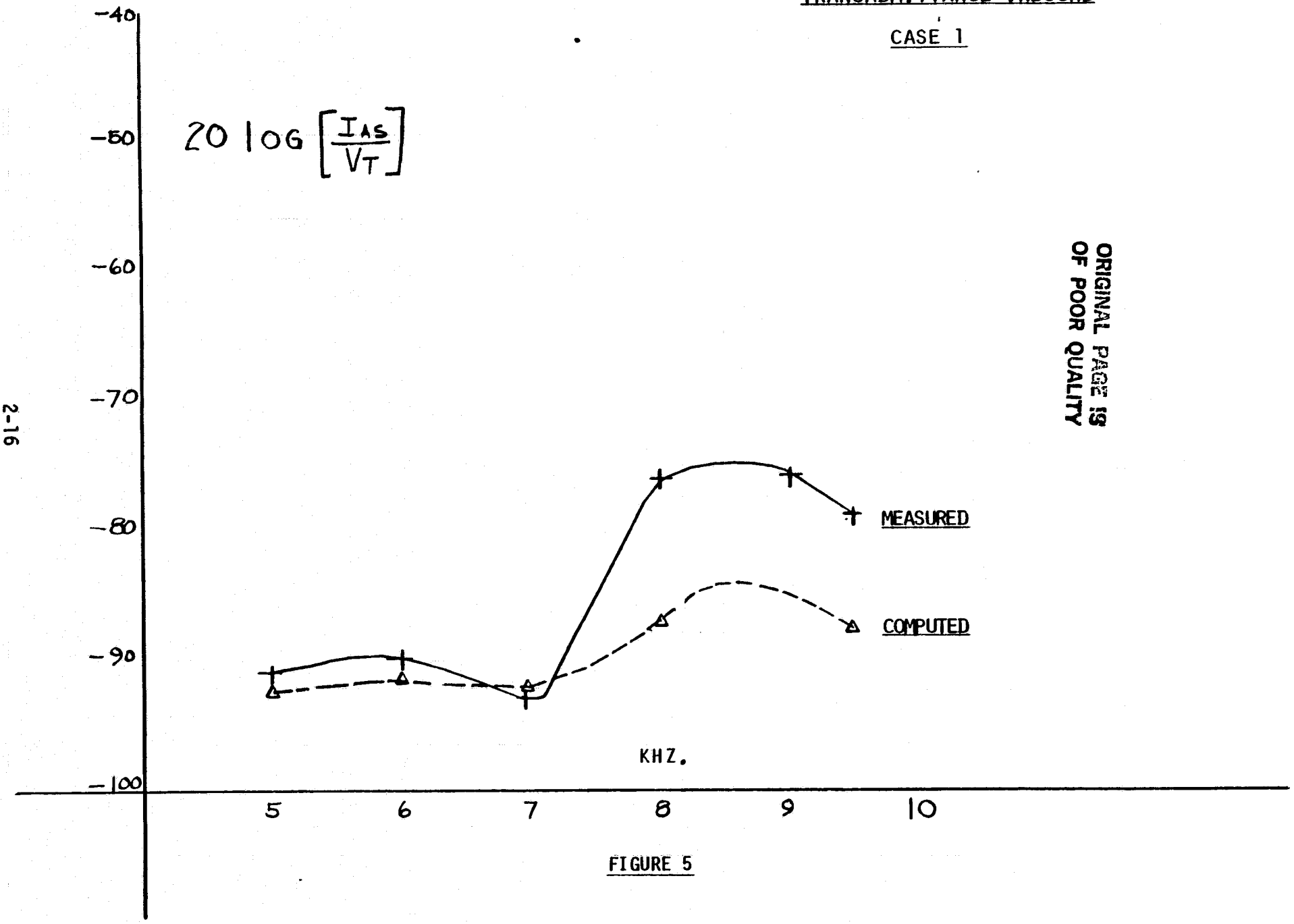

FIGURE 5

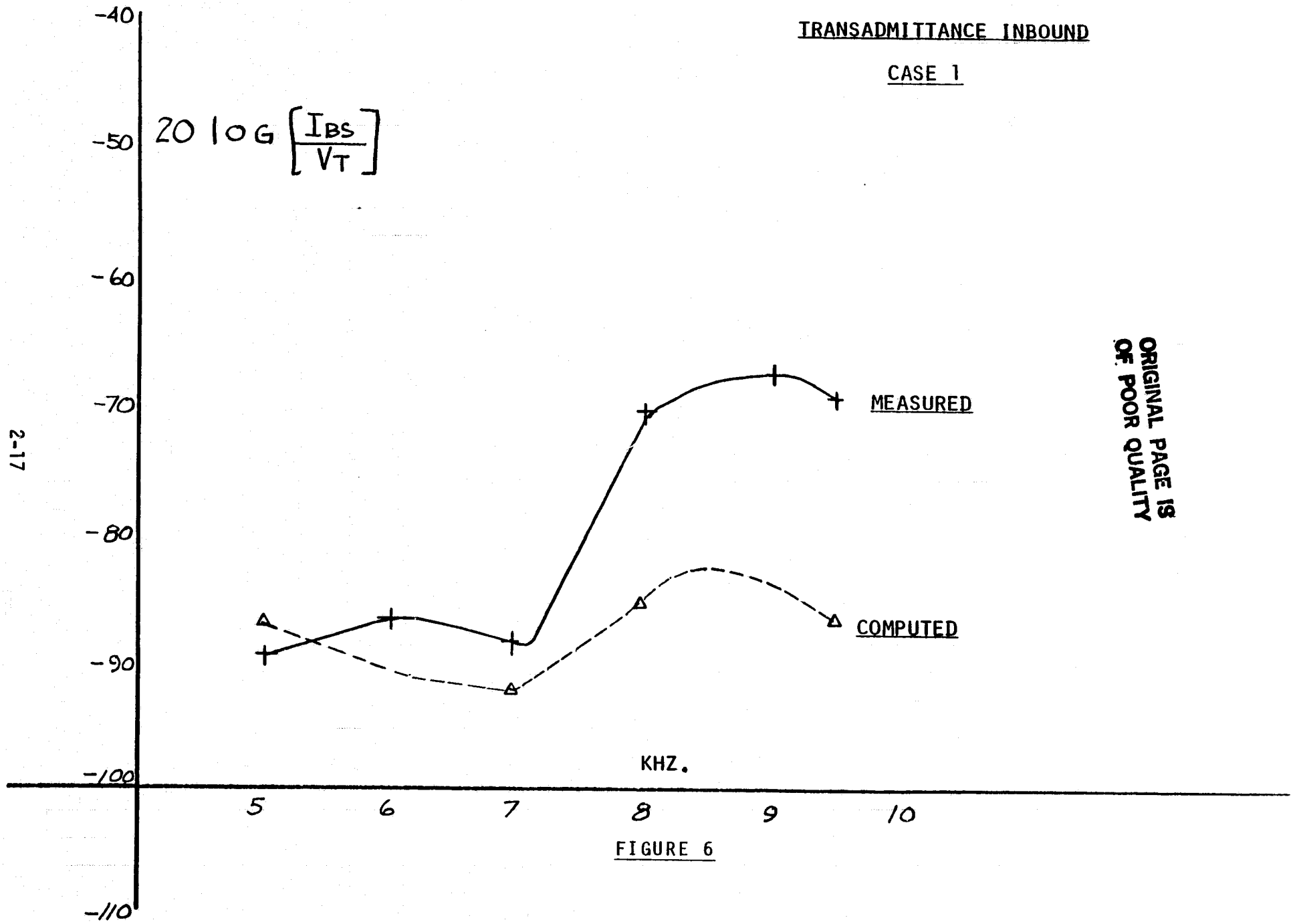

FIGURE 6

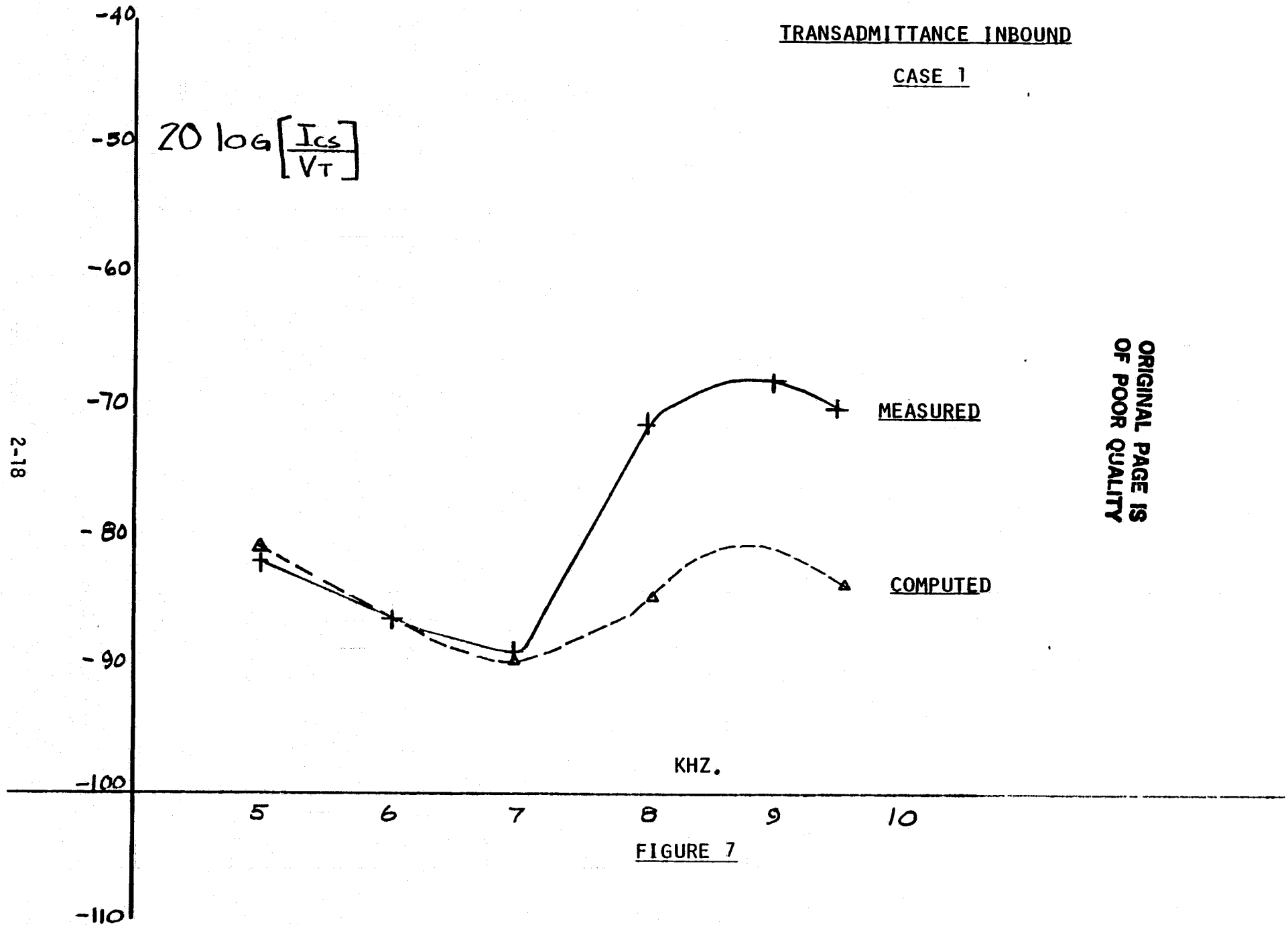

FIGURE 7

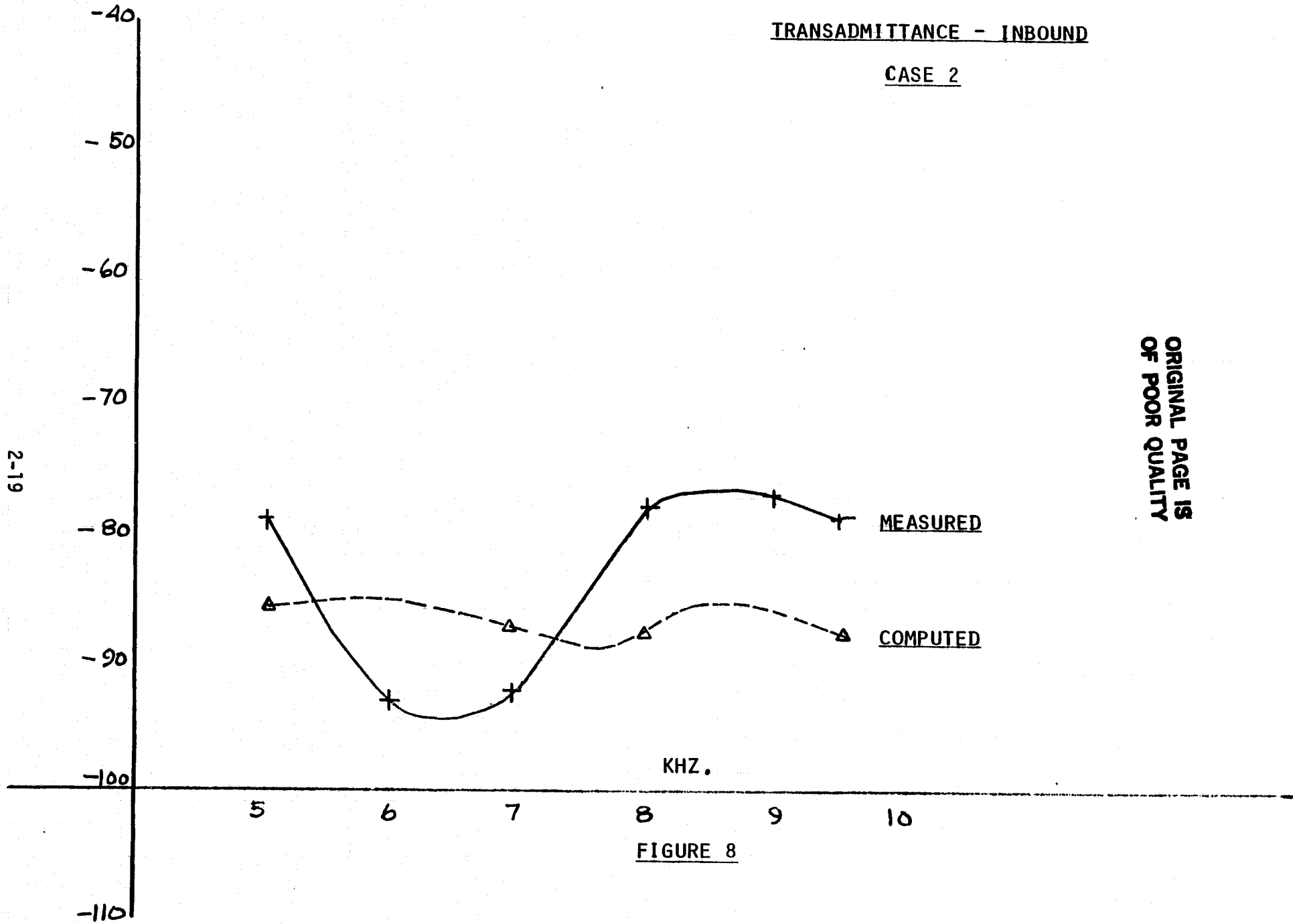

FIGURE 8

ORIGINAL PAGE IS OF POOR QUALITY

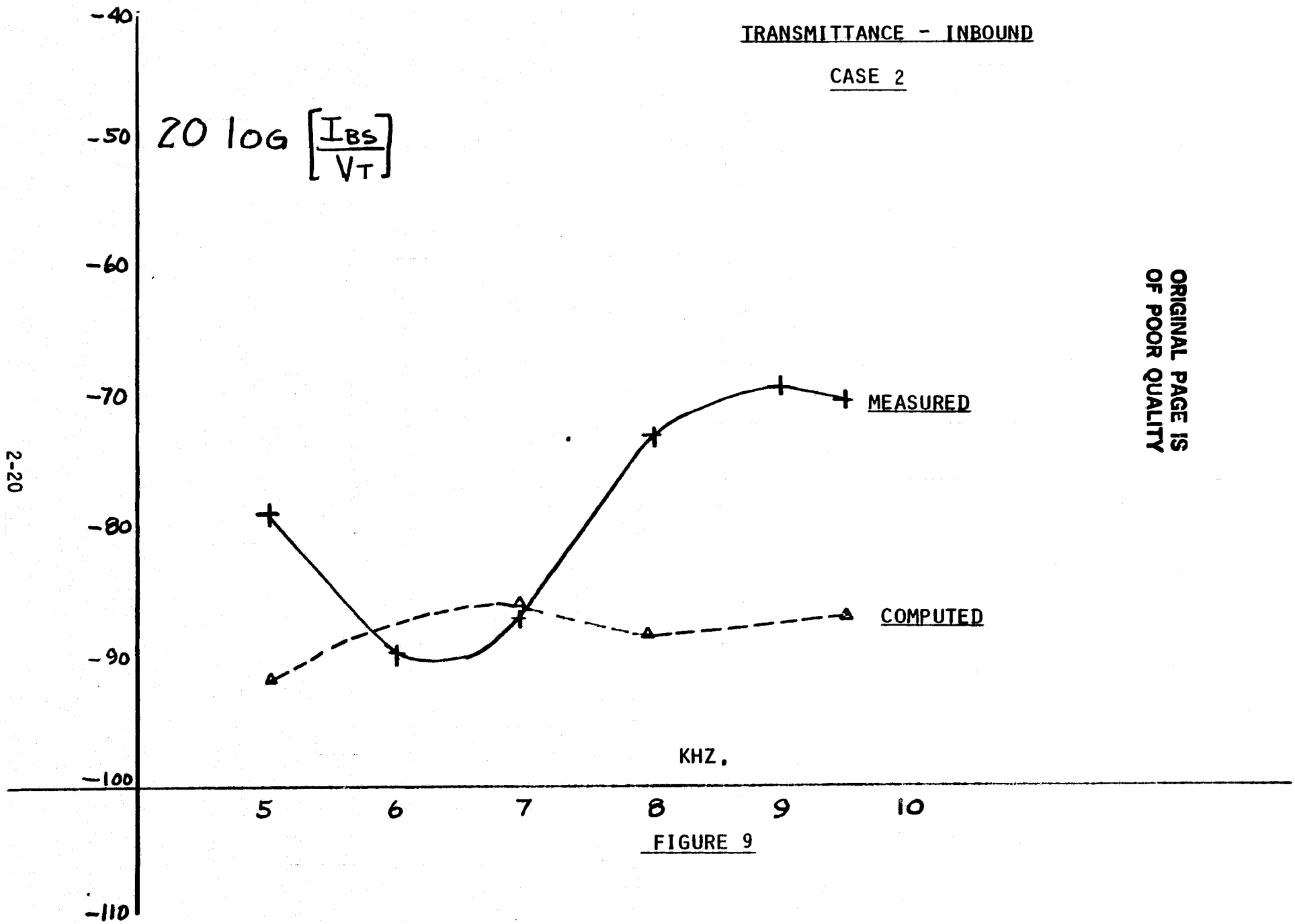

FIGURE 9

TRANSADMITTANCE - INBOUND

CASE 2

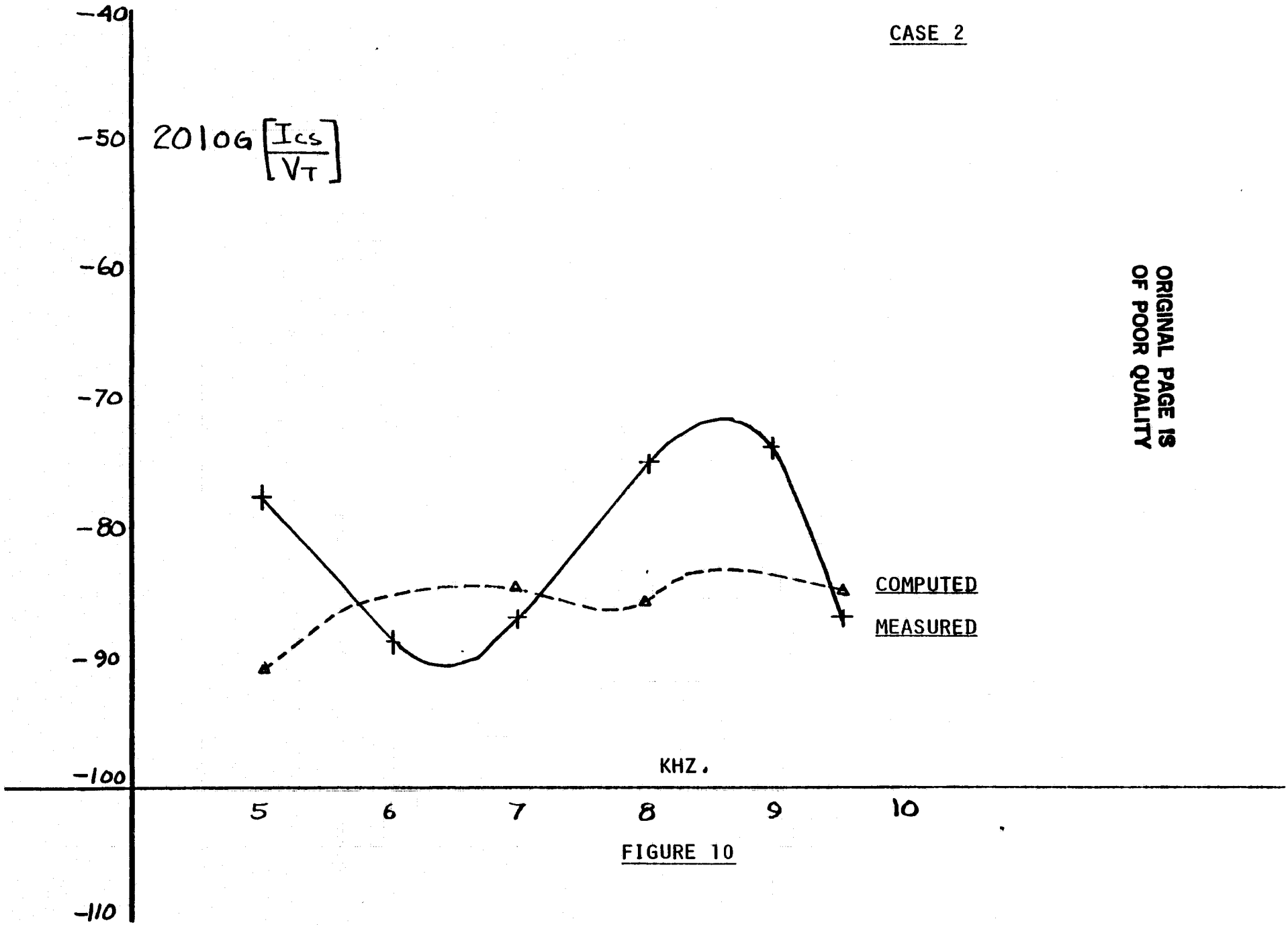

FIGURE 10

VOLTAGE TRANSFER RATIO - INBOUND

CASE 2

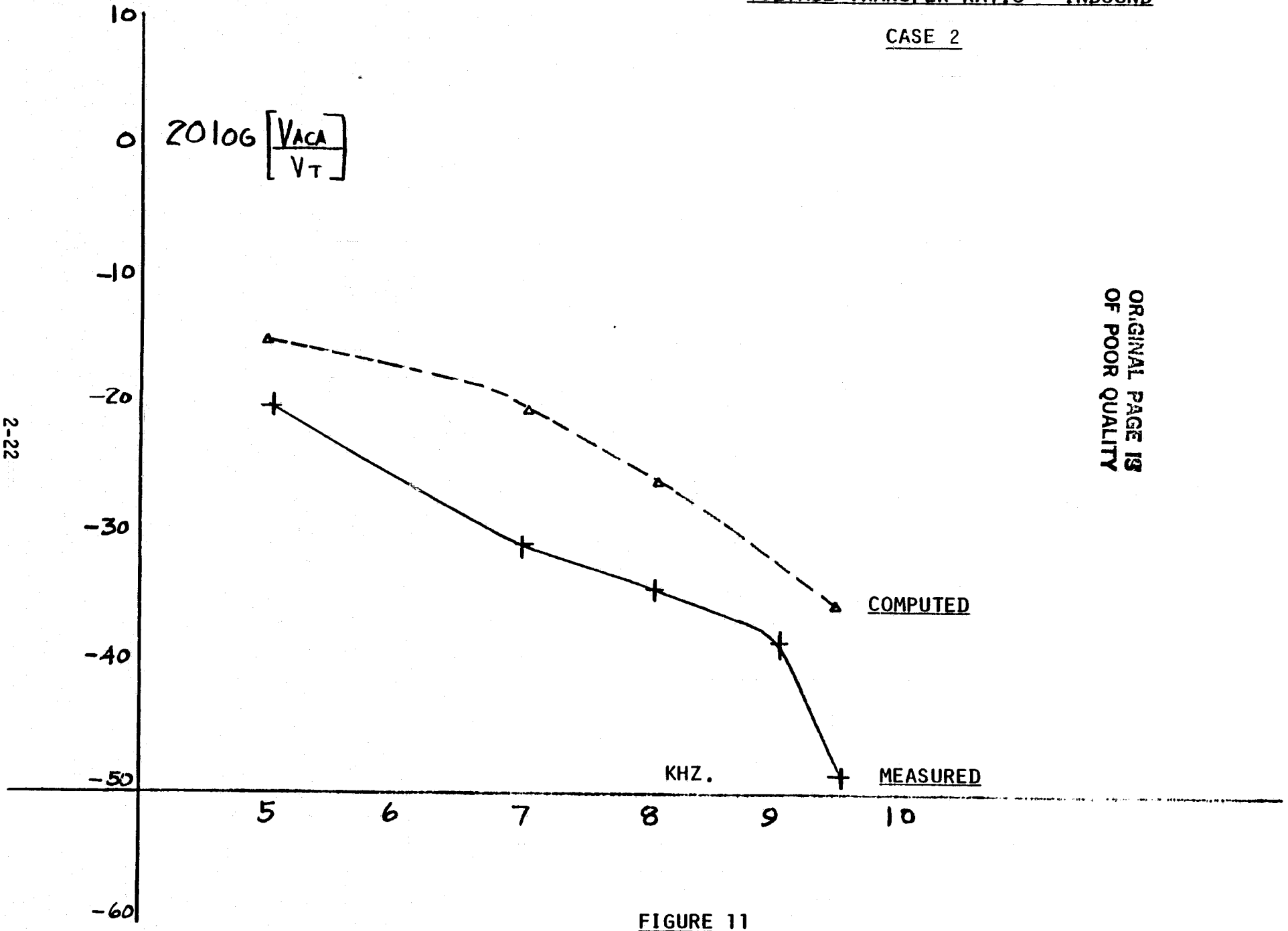

FIGURE 11

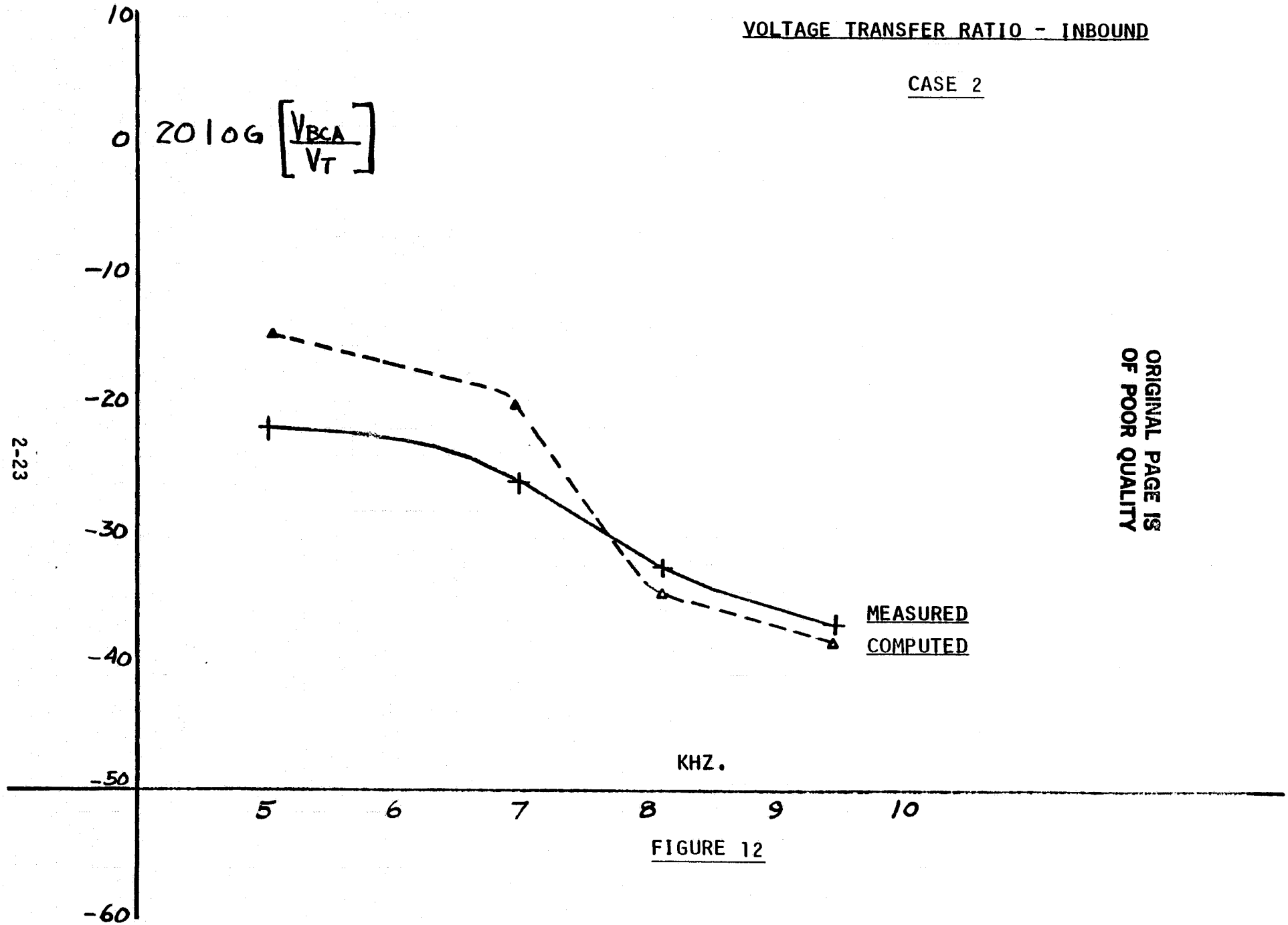

FIGURE 12

VOLTAGE TRANSFER RATIO - INBOUND

CASE 2

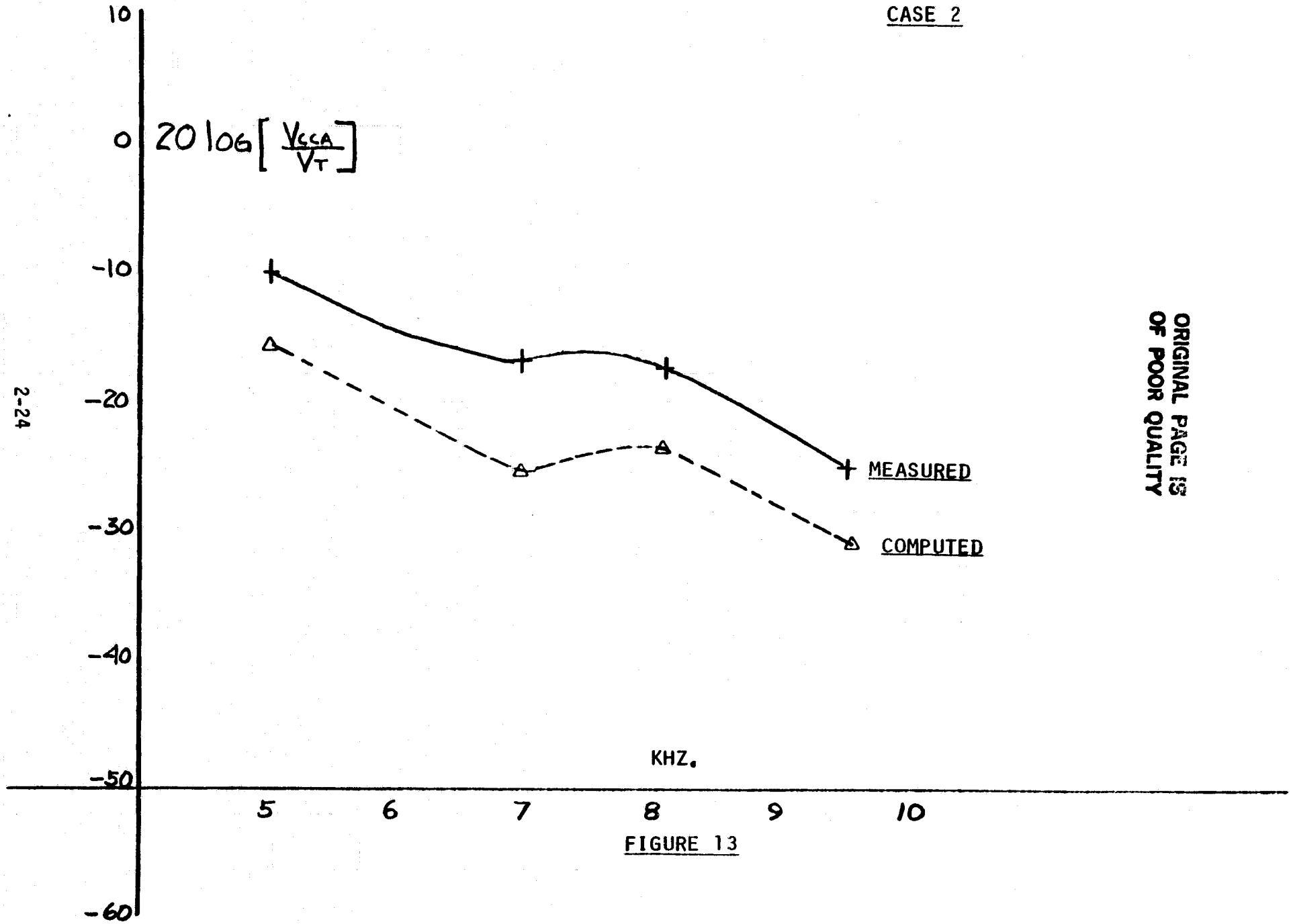

FIGURE 13

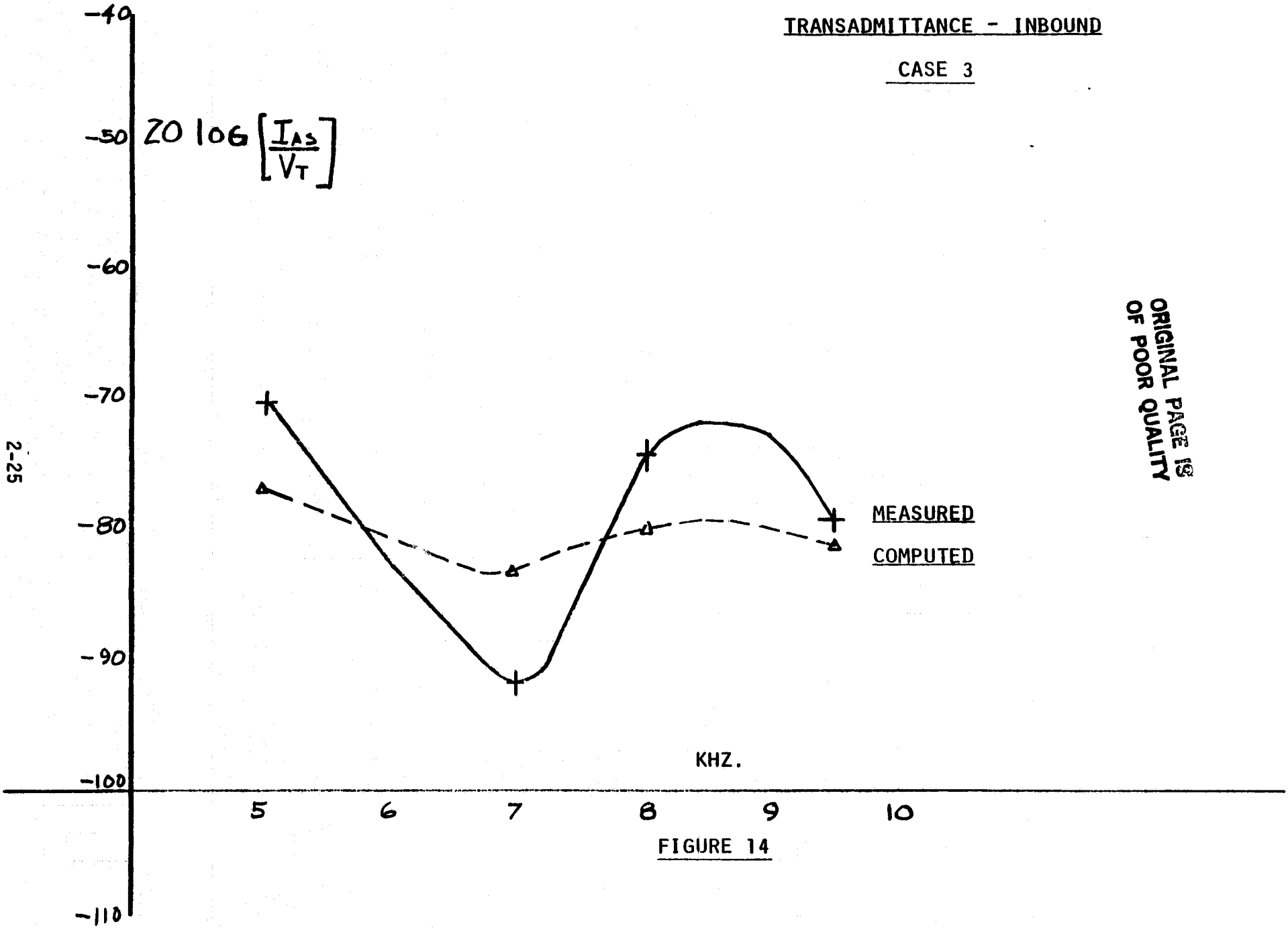

FIGURE 14

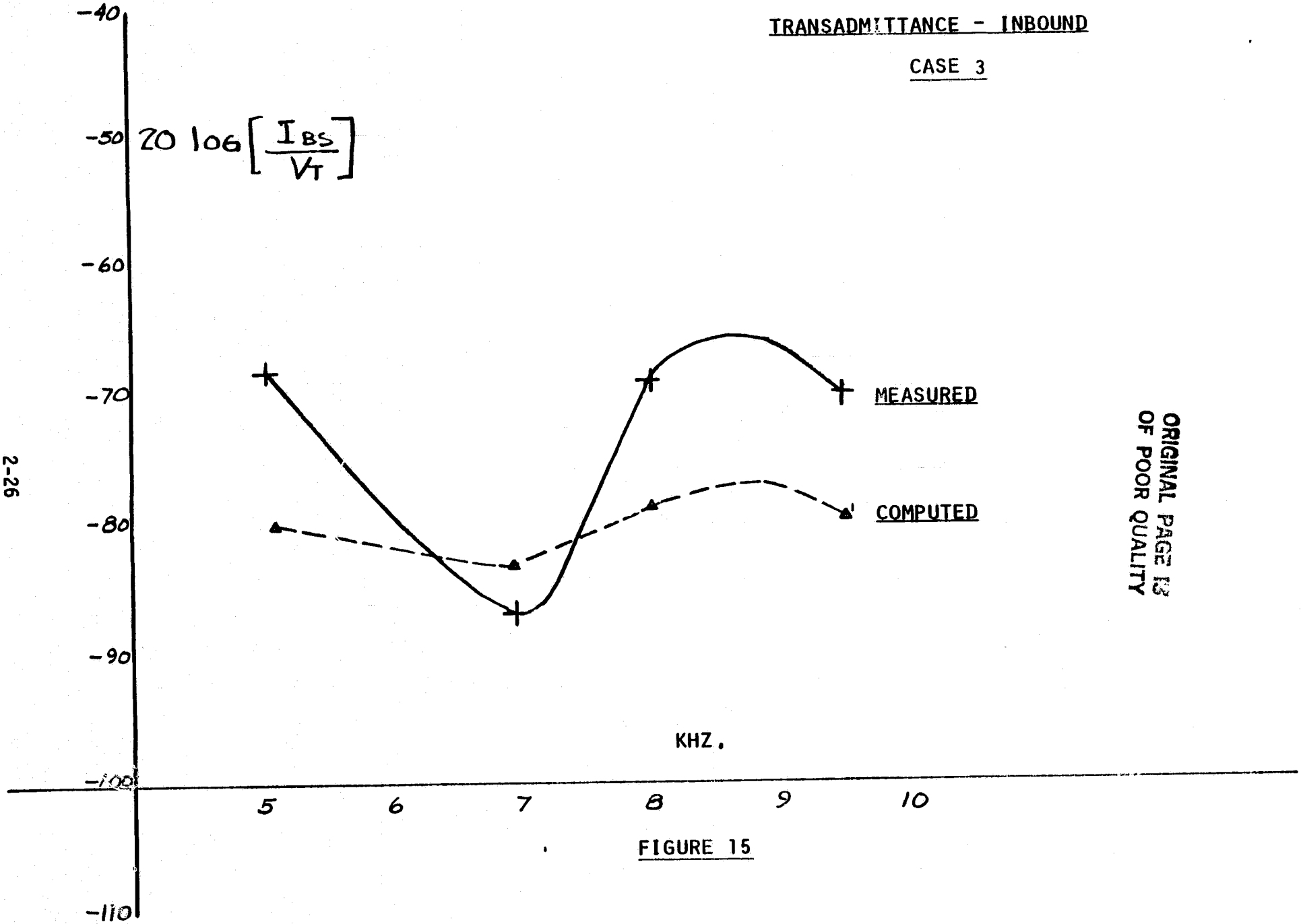

FIGURE 15

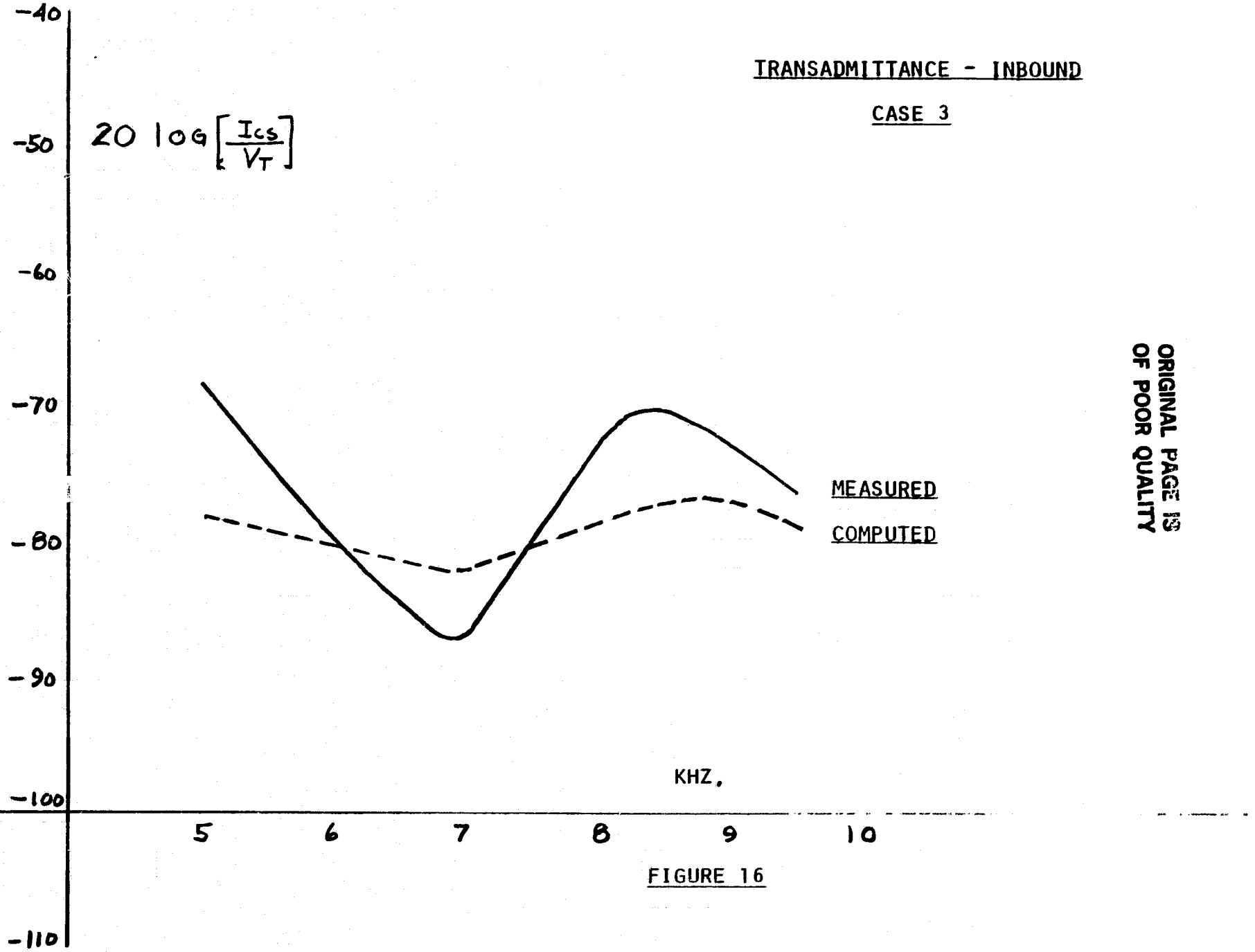

FIGURE 16

VOLTAGE TRANSFER RATIO - INBOUND

CASE 3

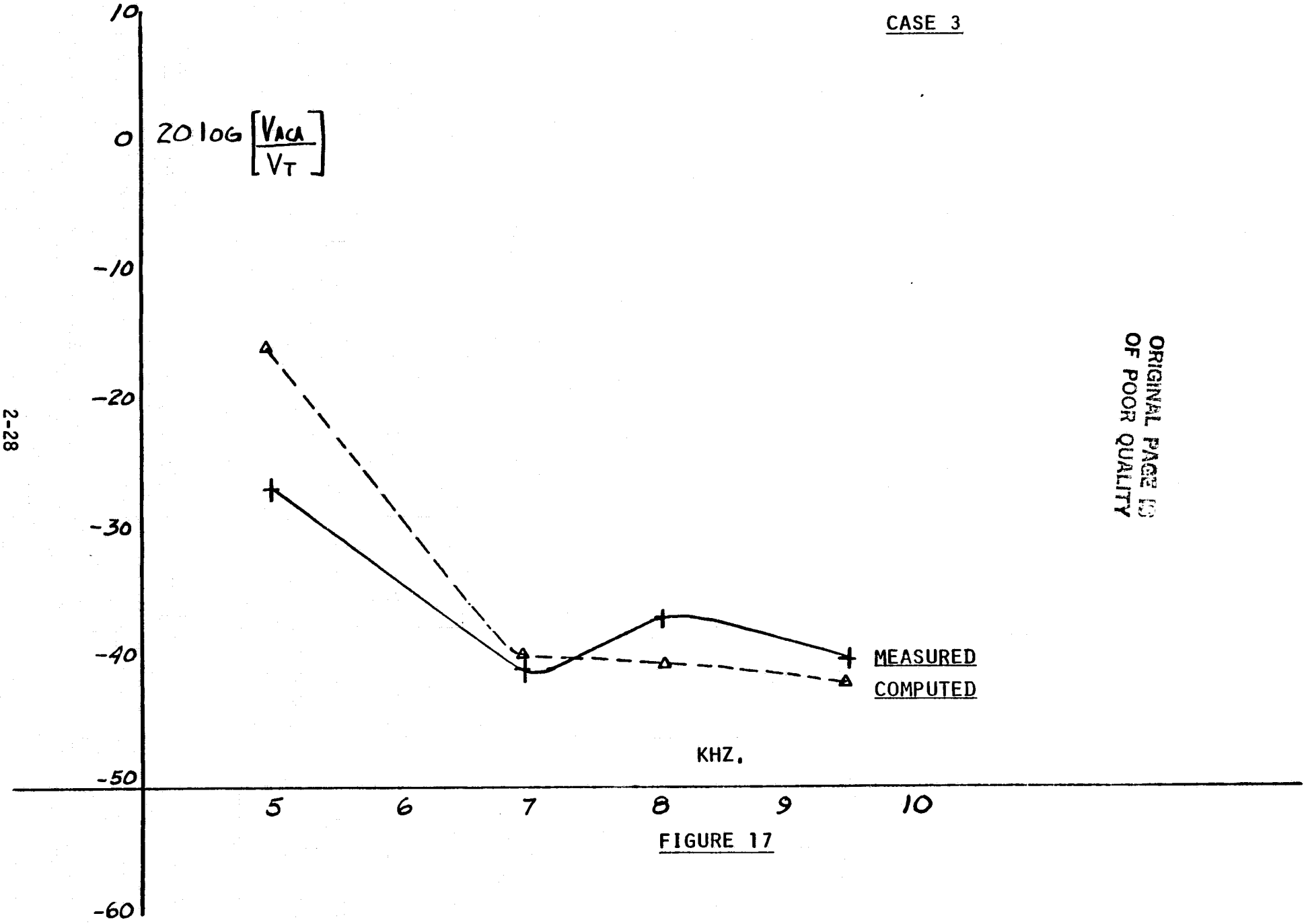

FIGURE 17

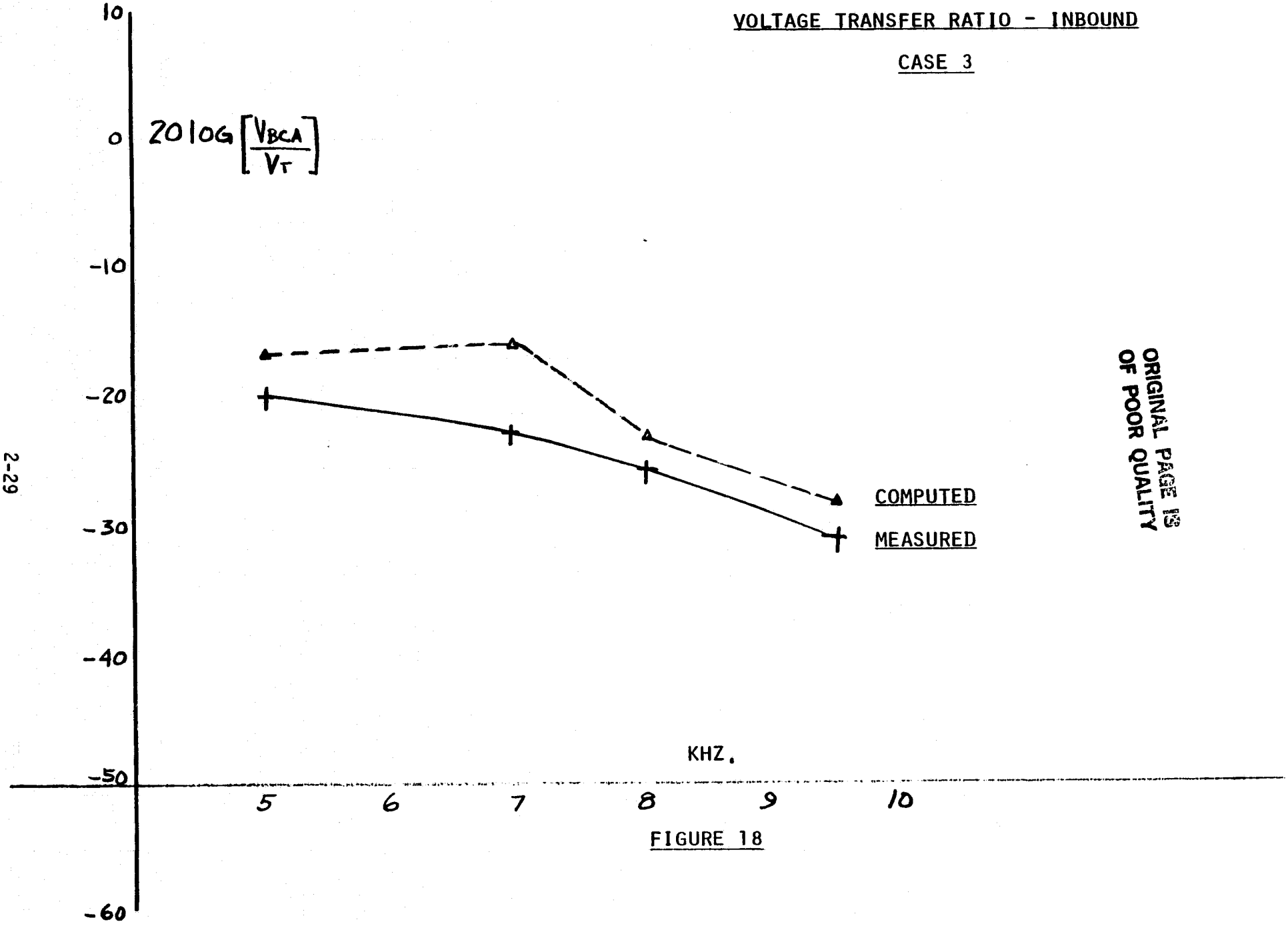

FIGURE 18

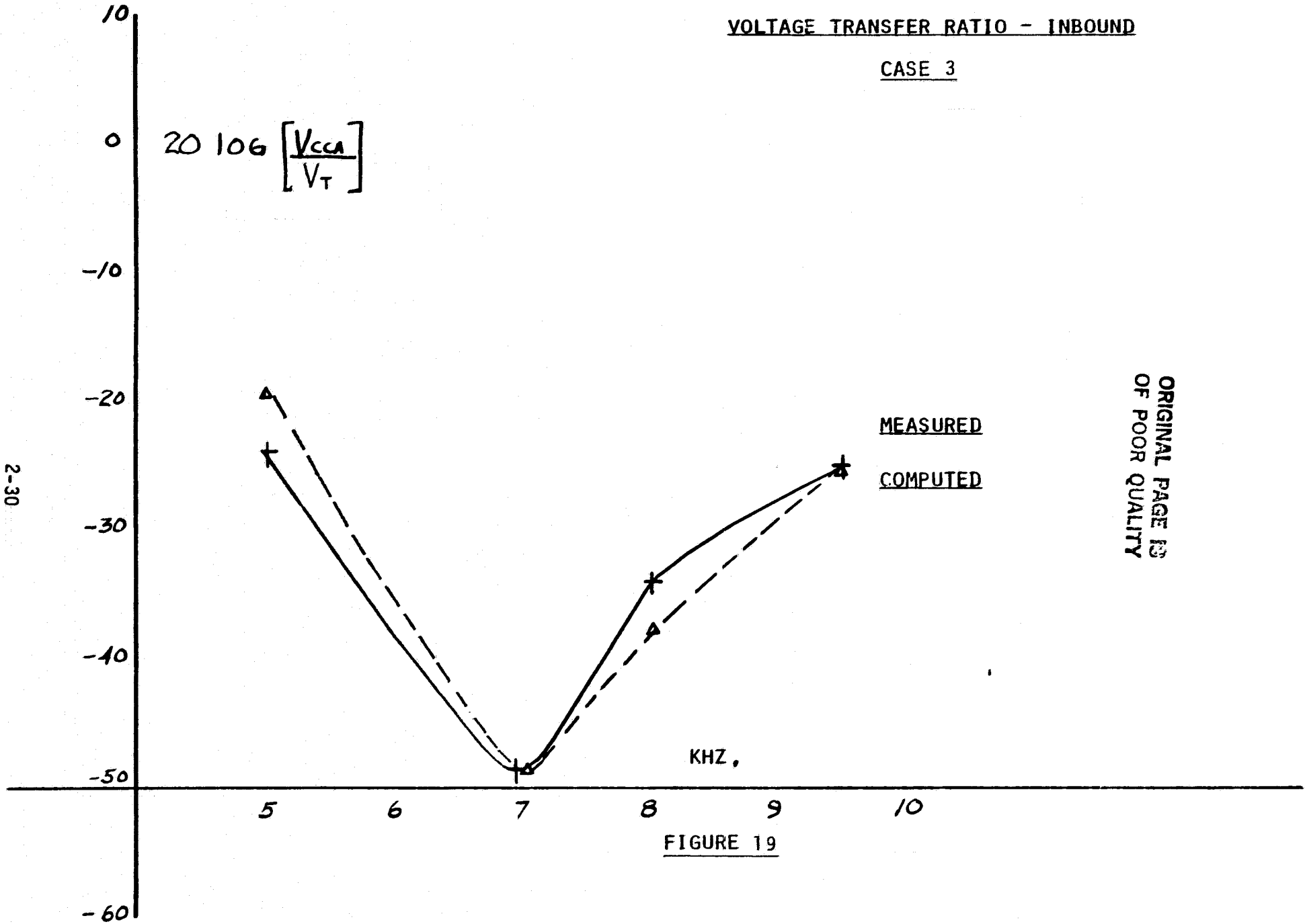

FIGURE 19

CONCLUSIONS

When making calculations of inbound signal propagation, it was necessary to find some representation for the admittance looking back into the substation itself. The substation admittance matrix was obtained by field measurements. These measurements were not performed at the same time the inbound propagation measurements were made. Since the 34556 feeder shares a common substation bus with other distribution feeders, the input admittance of the substation could be quite variable due to changing load levels on the other feeders sharing that bus. Measurement values are directly affected by the substation admittance and have an impact on model verification accuracy.

TASK #3

PARAMETER SENSITIVITY

CONTRIBUTORS

Robert C. Wentz

Robert C. Rustay

TASK 3

TABLE OF CONTENTS

		Page
I.	OVERVIEW	3-1
II.	COMPARISONS	3-2
III.	PARAMETER VARIATIONS	3-12
IV.	RESULTS	3-23
V.	CONCLUSIONS	3-47
VI.	COMMENTS	3-57

I. Overview

The sensitivity of PLC propagation on feeders to parameter variations was investigated using the distribution network computer model. This investigation was concerned with two overall goals. The first goal of this study was simply to determine the relative significance of various parameters on the characteristics of the network as well as on the propagation of a communication signal. The second and more practice-oriented goal of the study was to determine if "set-up" time for computer descriptions of actual distribution networks could be significantly reduced. The underlying concept of this goal was that if certain parameters were found to be insignificant, variations in them could be ignored, thus reducing the complexity of the computer description.

The study was carried out by repetitive analysis of a generic distribution network with each execution of the analysis programs having one or more parameters varied. Comparison routines were added to the software so certain values could be examined with respect to the corresponding values of a reference network. Differences in the compared values were recorded as a percent of the reference value. This representation was selected so that the degree of sensitivity to a given parameter variation could quickly be judged. Other advantages of this representation include the ability to directly compare the sensitivity to variations in parameters that are not related, as well as the ability to compare numerous variations of the same parameter.

The following sections deal with the specifics of the study. Section II is a discussion of the values compared by the study to determine sensitivity - what values were compared, why were these values chosen,

and how were the comparisons made. Section III examines the parameters that were varied in the course of the study, detailing why each variation was made. Section IV contains comments on the more significant results of the study and Section V drawn conclusions from these results. Additional information pertinent to this study is included in Section VI. An Appendix is attached which includes a description of each network that was studied.

No in-depth discussion of theory is attempted in this report. It is assumed that the reader is somewhat familiar with the engineering principles behind the phenomena associated with the operation of a Power Line Carrier (PLC) communication network and that further explanation would prove redundant. Focus is made, instead, on results of the study and conclusions drawn from these results. Naturally, the aspects investigated during the study were influenced to a great extent by their relevance to the overall goals as well as by a host of other factors including time constraints and applicability to the general case. Above all, it must be understood that this is solely a generic demonstration intended to point out basic trends in sensitivity. In no way are the results to be considered typical of all distribution networks.

II. Comparisons

Four properties of the distribution network were selected to form the basis of comparison for all parameter sensitivity variations. Two of these four, the characteristic admittance (Y_0) and the eigenvalues, can be thought of as "internal" to the feeder (i.e., involving changes in the E and H fields in and around the wires) and thus, independent of variations in parameters "external" to the feeder such as transformer loading. The

other two properties, driving point admittance and voltage transfer, incorporate "internal" as well as "external" parameter variations. During evaluation of variations in the so-called "external" parameters, it was not necessary to make comparisons of the characteristic admittance or of the eigenvalues. The other two properties were, however, compared for each and every parameter variation made during the study.

Each of the four network properties is dealt with separately below. The discussions present reasoning for selecting that property, as well as a brief description of how the actual comparisons took place. Because a direct comparison is relatively straightforward, this report omits lengthy details of the comparison routines.

1. Characteristic Admittance - This complex square matrix is dependent only on the line configuration and was chosen for comparison for several reasons. First, it strongly influences the admittance levels associated with an actual line and its external loading. Secondly, via its off-diagonal terms, it gives an indication of the degree of cross coupling between phases. Finally, being dependent only on the line configuration, it, along with the complex vector of eigenvalues which are dependent only on the line configuration and can therefore be computed independently of any network, affords some basis of judging the relative significance of different line types.

   The element by element comparison took place in the following manner. A square complex matrix was initialized with the calculated elements of the characteristic admittance of the reference line configuration. The elements along the matrix diagonal are usually dominated by the complex characteristic admittances between each phase and the neutral, but also contain some cross coupling

admittances. The off-diagonal elements indicate only the cross coupling effects between the individual phases. This matrix was saved for subsequent comparison. Analysis of networks containing parameter variations produced characteristic admittance matrices which could be directly compared, element by element, to the saved reference matrix. Because all matrix elements were expressed in rectangular form (i.e., a + jb), the difference matrix,

$$Y_o \text{ difference} = Y_o \text{ reference} - Y_o \text{ varied}$$

was obtained by direct complex matrix subtraction. Each complex element of the difference matrix was divided by the magnitude of the corresponding element of the reference matrix and then multiplied by 100% to express all differences as a percent of the reference value. Also presented, for quick reference, are the largest diagonal and the largest off diagonal difference percentages.

See Figure (1) for an example of output from the characteristic admittance matrix comparison routine.

2. Eigenvalues - This complex vector is also dependent only on the line configuration. It is of interest since each element represents the propagation constant associated with the respective mode. As such, the real part represents the modal attenuation (per meter) and the imaginary part determines the mode propagation velocity. It is chosen for comparison for obvious and similar reasons as cited previously for the characteristic admittance.

The comparison of eigenvalues was carried out in a manner analogous to that used for the characteristic admittance matrix. Differences in the two routines are simply logical progressions from the fact that no matrices are involved, only complex values. Also, since there were no diagonal and off-diagonal elements, only the single largest difference magnitude was calculated. An example of output

LINE TYPE 103 FREQUENCY CODE 10

INPUT - CHARACTERISTIC ADMITTANCE MATRIX (YO) FOR LINE TYPE 103

2.3827974E-03	-6.6306631E-04	-3.7871159E-04
3.6818999E-05	-3.6365634E-08	7.4458229E-06
-6.6306635E-04	2.4953793E-03	-6.5884310E-04
-3.6367794E-03	3.6858397E-05	-6.5058972E-08
-3.7871159E-04	-6.5884303E-04	2.3926889E-03
7.4458229E-06	-6.5058055E-08	3.6784427E-05

REFERENCE - CHARACTERISTIC ADMITTANCE MATRIX (YO) FOR LINE TYPE 101

2.5745891E-03	-7.5721202E-04	-4.2143699E-04
2.5616943E-05	6.6441100E-06	1.1675823E-05
-7.5721201E-04	2.7149607E-03	-7.5250554E-04
6.6441103E-06	2.3539327E-05	6.5767893E-06
-4.2143704E-04	-7.5250551E-04	2.5860260E-03
1.1675824E-05	6.5767900E-06	2.5481140E-05

DIFFERENCE MATRIX (ALL FIGURES IN PER CENT)

-7.45	12.43	10.13
0.44	-0.88	-1.00
12.43	-3.09	12.45
-0.83	0.49	-0.88
10.13	12.45	-7.47
-1.00	-0.88	0.44

ORIGINAL PAGE IS OF POOR QUALITY

MAXIMUM ON DIAGONAL DIFFERENCE 8.10 %

MAXIMUM OFF DIAGONAL DIFFERENCE 12.48 %

FIGURE (1)

from the eigenvalue comparison routine may be seen in Figure (2).

3. Driving Point Admittance - Another complex square matrix, this was chosen for comparison because it provides a complete electrical representation of a feeder or branch of a feeder as seen from the point of input. As was mentioned before, the driving point admittance includes all loading effects on the network, those inherent to the feeder as well as those due to external devices or conditions. Accordingly, the entire feeder or branch of a feeder may be replaced mathematically by this single matrix.

   The driving point admittance is similar in most respects to the characteristic admittance, the major exception being that it encompasses the total range of loading on the network. As with the characteristic admittance, the elements on the matrix diagonal represent the individual phase to neutral admittances, plus phase to phase cross-coupling admittances, while the off-diagonal elements consist of only cross-coupling admittances. The two matrices are identical in form, so the same comparison routine was used for both. Figure (3) is an example of output from the driving point admittance matrix comparison routine.

4. Voltage Transfer - This aspect of network performance was chosen for comparison for obvious reasons. Because the transfer of voltage from the input point to the output point on the feeder network is the bottom line measure of performance*, this property was used as the major factor in determining the sensitivity of the computer model to parameter variations.

*Because the distribution transformer is most easily viewed in terms of its own voltage transfer ratio.

LINE TYPE 103 FREQUENCY CODE 10

ORIGINAL PAGE IS OF POOR QUALITY

INPUT - EIGENVALUES FOR LINE TYPE 103

6.1310217E-06	1.8990793E-06	2.1986351E-06
1.8964033E-04	1.7897401E-04	1.8026546E-04

REFERENCE - EIGENVALUES FOR LINE TYPE 101

5.7937637E-06	7.9675423E-07	9.3040934E-07
1.8685690E-04	1.7239710E-04	1.7264795E-04

DIFFERENCE VECTOR (ALL FIGURES IN PER CENT)

0.13	0.64	0.73
1.49	3.81	4.41

MAXIMUM DIFFERENCE ELEMENT 4.47 %

FIGURE (2)

LINE TYPE 101 FREQUENCY CODE 10 NETWORK ID # 11.

INPUT - DRIVING POINT ADMITTANCE MATRIX FOR NETWORK # 11

```
 1.6835149E-03 -2.8560106E-04 -2.2957531E-04
-1.5039049E-03  5.3957740E-04  3.4348626E-04

-2.8560125E-04  1.6557826E-03 -2.7410430E-04
 5.3957743E-04 -1.5816209E-03  5.3695645E-04

-2.2957526E-04 -2.7410500E-04  1.6014665E-03
 3.4348619E-04  5.3695733E-04 -1.4857337E-03
```

REFERENCE - DRIVING POINT ADMITTANCE MATRIX FOR NETWORK # 10

```
 1.6887365E-03 -2.7936024E-04 -2.2510780E-04
-1.5169724E-03  5.4013347E-04  3.4541613E-04

-2.7936081E-04  1.6561834E-03 -2.6781226E-04
 5.4013344E-04 -1.5956144E-03  5.3719176E-04

-2.2510722E-04 -2.6781337E-04  1.6037827E-03
 3.4541689E-04  5.3719144E-04 -1.5003339E-03
```

DIFFERENCE MATRIX (ALL FIGURES IN PER CENT)

```
-0.23   -1.03   -1.08
 0.58   -0.09   -0.47

-1.03   -0.02   -1.05
-0.09    0.61   -0.04

-1.08   -1.05   -0.10
-0.47   -0.04    0.66
```

MAXIMUM ON DIAGONAL DIFFERENCE 0.67 %

MAXIMUM OFF DIAGONAL DIFFERENCE 1.18 %

FIGURE (3)

The voltage transfer was established by applying an input of 1.0 + j0.0 volts on each of the three phase conductors at the root section of each network analyzed in the study. Assuming there was no other excitation anywhere along the line, the resulting voltage level was calculated at the terminal section of each network. The output voltages of the three phases were presented as the magnitudes of the output voltage phasors. The comparison routine received these values for the reference network and compared them to corresponding values determined for each altered parameter network. Any differences between the output phase voltages and their respective reference values were computed as a percentage of the reference magnitude. Because the magnitude of the input voltage in every case is known, a simple hand calculation can provide the change in output voltage magnitude as a percent of the input voltage. This property can provide a more stable standard of comparison because the percent change is referred to the same value no matter which reference network was used. It also gives a better feel of how much variation can be expected because of a certain parameter variation. For an example of output from the output voltage magnitude comparison routine, see Figure (4).

Also generated during the analysis of voltage transfer were plots of the phase voltage magnitudes versus distance from the input point. These plots provide a graphic representation of standing wave and line attenuation effects on the voltage level along the line. Production of the plots was more or less a sideline activity performed to enhance the understanding of the effect of parameter variations. In many cases they illustrate damping due to increased attenuation, or other phenomena such as altered standing wave patterns due to changes in line length or speed of propagation on the phase wires. A sample plot can be seen in Figure (5). In this and all other cases, the dotted line is the magnitude of the voltage on phase A, the solid line is phase B, and the dashed line is phase C.

LINE TYPE 101 FREQ. CODE 10 NETWORK ID # 11

INPUT - OUTPUT VOLTAGE AT SECTION 80 OF NETWORK # 11

/V1/	/V2/	/V3/
4.5326012E-01	4.2239881E-01	4.6743567E-01

REFERENCE - OUTPUT VOLTAGE AT SECTION 80 OF NETWORK # 10

/V1/	/V2/	/V3/
4.6315567E-01	4.2709026E-01	4.7204040E-01

DIFFERENCE IN MAGNITUDE (ALL FIGURES IN PER CENT)

-1.06	-1.10	-0.98

FIGURE (4)

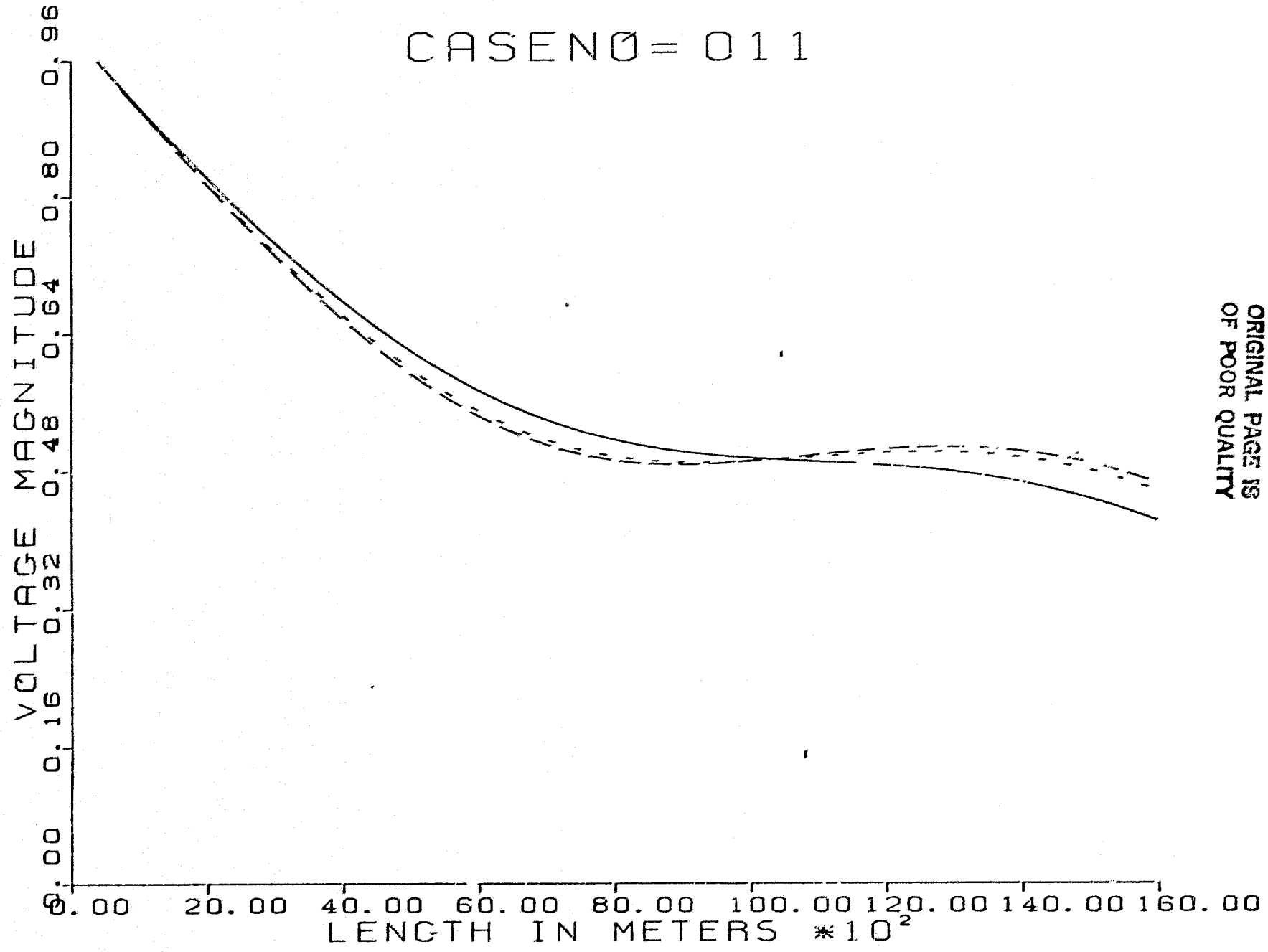

FIGURE (5)

02/03/81 9.874

III. Parameter Variations

The parameters that were varied for the purpose of this study were chosen in accordance with their relevance to the overall goals. Although some limited investigation was made into the compounding of effects when two or more parameters are varied, most comparisons were made with only a single variation. Doing so maintained a "feel" for sensitivity to each parameter that could easily be lost by the compounding of effects. In some cases the parameter being dealt with was binary in nature (i.e., either "yes" or "no"). In these cases, it was not possible to establish a normalized sensitivity. Most variations, however, allowed for simple calculations to determine the relationship between degree of parameter variation and degree of change in the model's computations.

No discussion of parameter variations would be appropriate without first describing the reference used in comparison. In the course of the study it was necessary to establish four separate references. The reasoning here becomes obvious when the scope of the parameter variations is taken into account. First, a reference network was needed for variations on an overhead feeder. A second reference was needed when investigation was made into variations on an overhead feeder approximately one quarter wavelength in total length. The great disparity in length between the original and the one quarter wavelength networks made comparisons to the initial reference somewhat uninformative. Following the same logic, two more references were needed when underground cable networks were investigated. Although confusing, four reference networks were needed to maintain a sense of scale in the sensitivity study.

All four reference networks were essentially the same feeder but each case was altered to fit the specified application. The basic configuration common to all four was a synthetic, cascaded line having no branches, no three-phase to two- or one-phase conversions, and no variations in line configuration anywhere along the feeder. It was broken up into 80 equal length sections, each section loaded by a 25 KVA distribution transformer cyclically connected from phase to neutral. The individual transformer admittances were set at -78.8 db at an angle of -27.3°. The line was terminated by a load having equal matrix-diagonal elements of 4.77×10^{-4} mhos at -68.22° and zero off-diagnoal elements.

The nominal overhead reference network had sections 200 meters long for an overall length of 16,000 meters. Each of the 80 sections was loaded by one of the distribution transformers. When an approximately one-quarter wavelength overhead network was to be investigated, the length of each section was reduced to 110 meters for an overall length of 8,800 meters. This value was established by calculating the wavelength of the 8.13 kHz PLC signal on the nominal reference network using the computed speeds of propagation for each of the three modes. The 8,800 meter length was chosen as a round approximation of the three values calculated for one quarter wavelength. Both the 16,000 meter overhead and the 8,800 meter version were, by unfortunate choice, referred to in the data as Network #10.

The nominal underground cable reference network was identical to the nominal overhead case in most respects. The only differences were the obvious change in line configuration and an increase in the temperature of the conductors. Whereas the overhead case assumed all conductors to be at 25°C, the phase conductors in the underground reference were set at 75°C with the neutral strands at 45°C. All other network parameters were

identical to the overhead version. The length of the one-quarter wavelength underground reference network was computed by the same process used for the overhead line. It resulted in the network being reduced from 16,000 to 3,400 meters. The cable reference networks are referred to in the data as Networks #9 and #8, for the nominal and quarter wavelength versions, respectively. For more information concerning the reference networks, see Figure (6) or refer to Appendix 8.

Now that the reference networks have been established, the parameter variations may be collected into four groups. The groups are divided, in most cases, according to the intent of the parameter variation. The first group consists of variations in overhead configuration intended to establish the relative sensitivity to such changes. The second group included all loading variations intended to determine loading effects. Investigations into "set up" time reduction constituted the third group while cable network variations were separated into the fourth. Obviously the groups are far from mutually exclusive since the results of variations in one group may be of significance to the intentions of variations in another. Divisions are made along logical lines for the clear presentation of results.

A. Overhead Geometry Variations - The following variations were made in the geometry of the overhead feeder:

   1. Phase Conductor Diameter - Three variations were made, both increasing and decreasing the diameter from its reference value. The investigation was carried out because changes in wire diameter are a common occurrence on real-life feeders. If such changes proved to be insignificant to a communication signal, the set up procedure could be simplified without

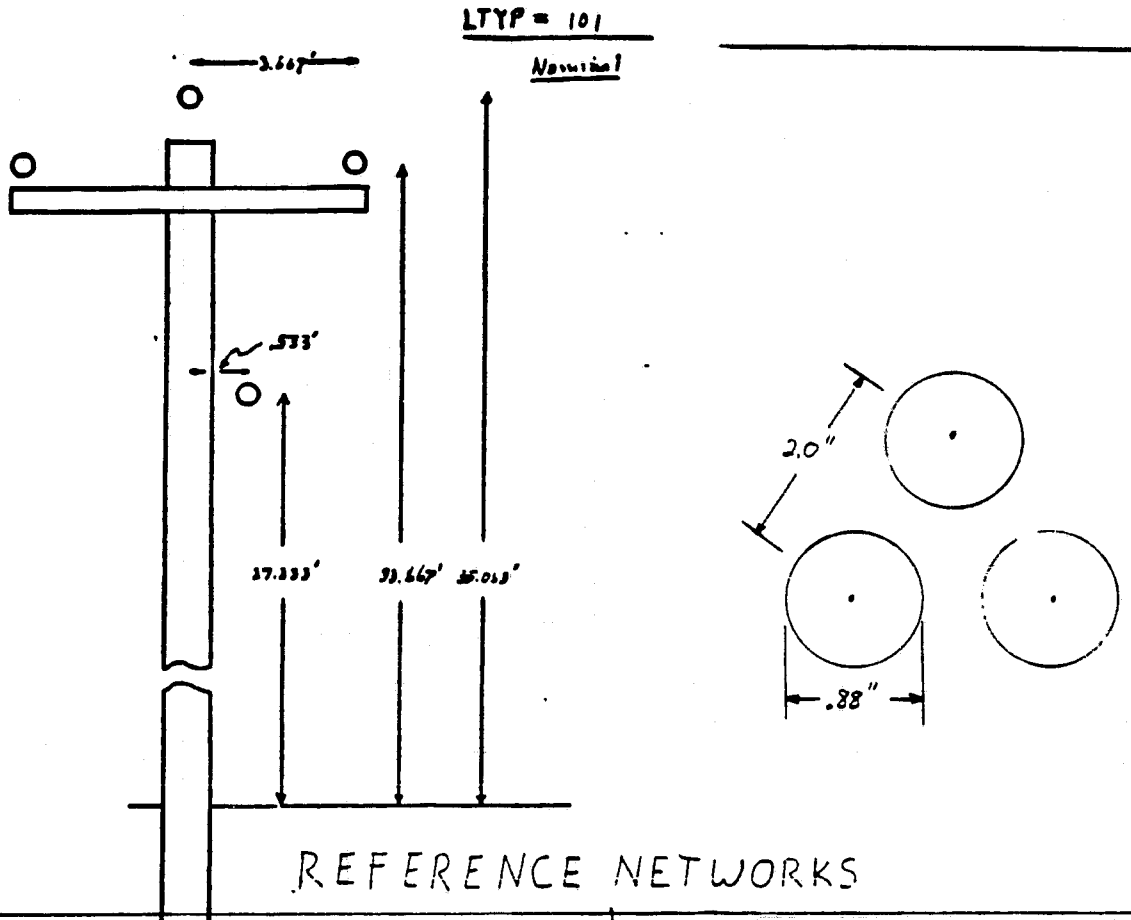

REFERENCE NETWORKS

NOMINAL OVERHEAD		NOMINAL UNDERGROUND	
NETWORK #	10	NETWORK #	9
LINE TYPE	101	LINE TYPE	999
NUMBER OF SECTIONS	80	NUMBER OF SECTIONS	20
LENGTH OF SECTIONS	200 m	LENGTH OF SECTIONS	200 m
TOTAL LENGTH	16,000 m	TOTAL LENGTH	16000 m
TEMPERATURE	25 °C	TEMPERATURE	75 °C
EARTH RESISTIVITY	100 Ω/m^3	EARTH RESISTIVITY	100 Ω/m^3
FREQUENCY	8.13 kHz	FREQUENCY	8.13 kHz
TRANSFORMERS	25 kVA	TRANSFORMERS	25 kVA

1/4 WAVELENGTH OVERHEAD		1/4 WAVELENGTH UNDERGROUND	
NETWORK #	10	NETWORK #	8
LINE TYPE	101	LINE TYPE	999
NUMBER OF SECTIONS	80	NUMBER OF SECTIONS	80
LENGTH OF SECTIONS	110 m	LENGTH OF SECTIONS	42.5 m
TOTAL LENGTH	8800 m	TOTAL LENGTH	3400 m
TEMPERATURE	25 °C	TEMPERATURE	75 °C
EARTH RESISTIVITY	100 Ω/m^3	EARTH RESISTIVITY	100 Ω/m^3
FREQUENCY	8.13 kHz	FREQUENCY	8.13 kHz
TRANSFORMERS	25 kVA	TRANSFORMERS	25 kVA

FIGURE (6)

sacrificing significant model accuracy. If, however, effects were notable, the degree of sensitivity would be of interest.

Analysis was performed on both the nominal system and the quarter wavelength version. Perhaps a comment on the quarter wavelength investigation is appropriate. The investigation was performed to ascertain the sensitivity of quarter wavelength networks with relation to longer networks. It was suspected that the unique standing wave patterns existing on feeders approximately one quarter wavelength long could possibly magnify sensitivity to a given variation. To test this, the same variation was analyzed on the two networks and the resulting sensitivities were compared. In short, the quarter wavelength analysis was performed to see if sensitivity was magnified by standing waves.

2. Neutral Conductor Diameter - One variation of the neutral conductor diameter was made on both the nominal and the one quarter wavelength networks. Sensitivity to the neutral was suspected to be somewhat less than sensitivity to the phase conductors so less attention was afforded this parameter. Reasoning behind this variation was much the same as that behind the phase conductor diameter variations.

3. Phase Conductor to Phase Conductor Spacing - One variation was made in which the spacing was increased. Both the nominal and the quarter wavelength networks were analyzed.

4. Phase Conductor to Earth Spacing - One variation was made on both network lengths. The neutral conductor to earth spacing was held constant so the phase conductor to neutral spacing was increased along with the phase conductor to earth spacing.

5. Neutral Conductor to Earth Spacing - One variation was made in which the phase conductor to earth spacing was held constant as the neutral to earth spacing was increased. As with all overhead geometry variations, analysis was performed on both the nominal and the one quarter wavelength networks.

6. Miscellaneous Conductors - Three variations were made involving miscellaneous conductors being added to the pole below the phase conductors. First one and then two additional neutral conductors were added, all assumed to be at ground potential. Finally, two open circuited secondary conductors were simulated. These were also assumed to be essentially at ground potential.

7. Triplex Neutral Conductor - Analysis was performed to determine the effect of changing the neutral conductor from simple ACSR to Triplex cable.

8. Spacer Cable Configuration - One investigation was made into the sensitivity of the model to a radical change in overhead geometry. The standard cross arm configuration common to all other analysis was altered to a so-called spacer cable or Hendrix cable arrangement. See Figure (8-1) in Appendix 8 for an illustration of this geometry.

B. Loading Variations - Investigation was made into the sensitivity of the model to variations in loading on the network. These variations involved distribution transformer loading, the diagonal load at the end of the network, and a series of combinations to provide information on the compounding effects of multiple variations. It was known from previous work that loading would have a pronounced effect on the output of the model so this group of variations was performed to determine the degree of sensitivity. Very little "set up" time reduction was foreseen.

1. Terminal Load - Analysis was carried out on both the nominal and one quarter wavelength networks with the diagonal load at the end of the line removed. The line was left as an open circuit.

2. Distribution Transformer Loading - Many variations were performed involving the loading due to distribution transformers. These loads were doubled, cut in half, or completely ignored. It should be noted that when these loads were doubled or cut in half, it was the load as seen by the primary that was being altered, not the physical loads on the secondary side of the transformers. Because of the large series leakage reactances that were present, doubling the secondary load would not necessarily double the load seen by the primary. All references to altering loads in this report should be considered in the context of the load on the primary side. Most, but not all of these variations were performed on the one quarter wavelength network as well as the nominal network.

3. Terminal Load and Transformer Loading Combination - One investigation was made into the combined effects of removing the terminal load and doubling the distribution transformer loading. The degree to which one variation would counteract the other was of interest. The variation was made on both network lengths.

4. Transformer Loading and Overhead Geometry Combination - In order to investigate the effects of changes both "internal" and "external" to the feeder, the entire series of overhead geometry variations was repeated with the distribution transformer loading cut in half. It was considered possible that geometry variations might be more significant if the damping effect of the transformer loading was reduced. It was also of interest to note if the variations compounded one another. This series of variations was conducted on the nominal length network only.

C. "Set-up" Time Reduction Variations - The largest number of variations were those concerned mostly with the streamlining of the network description procedure. This time-consuming and exhaustive procedure requires the detailing of every physical aspect suspected to effect

the propagation of a PLC signal. Individual investigation was made into a fair number of these parameters in an attempt to determine if excessive attention was being paid to insignificant parameters. It was hoped that in many instances, prudent engineering assumptions could replace costly precision determinations without a significant loss of model accuracy.

In addition to variations in specific parameters, changes in "set up" procedures were also looked into. Specifically, the procedure of creating a new section at each distribution transformer, even though there is no change in the feeder. Also investigated was the compounding of effects when "set up" variations interacted with loading variations. Many of the "set up" variations were analyzed on the one quarter wavelength network in addition to the nominal length version.

1. Aggregation - Two variations were made involving the reduction of the total number of sections in a network description. Both were demonstrations of aggregation of several shorter sections into a single longer one. Because all sections in the synthetic test network were of the same configuration, it was theoretically possible to create one long section with the corresponding included distribution transformers located at the end of this long section. Variations made in the study, however, were restricted to the more reasonable possibilities of reducing the number of sections to one half and one third of the original 80.

   The aggregation process was accomplished conveniently in the model to calculate the effect by doubling (or tripling) of the length of every other (or third) section and reducing the

in-between sections to zero length.* Because 80 is not evenly divisible by three, it was necessary to merely double the length of the next to last section in the second case. In both cases, the same overall length was maintained, as was the number and loading of the distribution transformers. Although in actuality, the number of sections in the network description was not reduced, the effective number of sections was indeed reduced and the technique of aggregation was demonstrated. The same technique was tested on a real life feeder description. The results of that test are discussed later in this report. Aggregation analysis was performed on both nominal and quarter wavelength networks.

2. Temperature - A series of five temperature variations was made on both length networks. The temperatures investigated covered a wide but possibly low range of conceivable conditions. This study was made to determine if any great concern need be placed on the value of the conductor temperature.

3. Earth Resistivity - Four variations were made covering a range of values likely to be encountered in most areas of the country. Both quarter wavelength and nominal cases were investigated.

4. Ungrounded Neutral - All investigations performed other than this one assumed the neutral wire to be essentially at ground potential. This analysis removed that assumption and was done on both nominal and one quarter wavelength networks.

5. Aggregated Networks with Transformer Admittances Doubled - The aggregation study described earlier was repeated with the loading of the transformers on the feeder doubled. The intent was to see if variations were greatly compounded.

*In actual practice, a simple modification to the model and input file procedure would be made to make this aggregation more convenient.

6. Total Length - The length of each section of the nominal network was reduced to 190 meters for an overall reduction of 5% in the length of the network. To obtain a 5% increase in total length, the length of each section was upped to 210 meters. It was hoped to establish the sensitivity of the model to the accuracy of line length measurements.

In a sense, the same variation can be thought of as a variation in the signal frequency rather than in total line length. If the line loading is held constant, the output voltage for a given input will depend on how many wavelengths are contained on the line at steady state. A given line can be considered to be N wavelengths long, and as long as N remains constant, it doesn't matter whether the line length varies slightly or the wavelength varies slightly. In this case, the speed of propagation was constant so a change in frequency would result in a change in wavelength. Mathematically,

$$\ell = N\lambda$$

$$\lambda = S_{p/f}$$

$$\therefore \ell = \frac{NS_p}{f} \quad \text{or} \quad NS_p = \ell f$$

where ℓ is the length of the line, S_p is the speed of propagation, λ is the wavelength, and f is the signal frequency. Since S_p is a constant and the object is to hold N constant, an increase in ℓ must be accompanied by a decrease in f and vice versa. From this it can be seen that increasing the line length while holding the signal frequency constant is essentially the same as holding the length constant and decreasing the signal frequency, if the same number of wavelengths is to be contained.

D. Cable Network Variations - Many of the variations made on overhead feeders were repeated for underground cables. Although the total number of variations did not approach that of the overhead networks,

those performed were comprehensive enough to indicate cable sensitivity to most parameters of interest. It should be noted that every variation made on the nominal underground network was also analyzed on a one quarter wavelength underground network. As with the overhead case, this was done to determine any possible sensitivity magnification on networks of that length.

The parameter variations performed on the underground feeders were analyzed for much the same reasons as the corresponding overhead variations. The cable variations are considered separately from the overhead feeders because of the large differences in the characteristics of the two configurations. The very low characteristic impedance of the underground cable as compared to overhead lines dramatically alters the sensitivity to variations. Also, the lowered speed of propagation radically changes the standing wave patterns on feeders of the same length. Separate consideration simplifies the presentation of results and conclusions made from those results.

1. Earth Resistivity - Similar to the overhead case, the earth resistivity was varied over a reasonable range of values.

2. Temperature - Cable feeder descriptions allowed for separate specification of phase conductor and neutral strand temperature. In all three variations, the neutral strands were set 30° lower than the phase conductors. The temperatures evaluated were quite high when compared to those analyzed for the overhead case. This reflects the thermal insulation provided by the cable's electrical insulation and by the ground. Analysis at overhead temperatures would not have reflected conditions on existing cable feeders.

3. Aggregation - The analysis of simplified network descriptions was handled as it was for overhead networks.

4. Transformer Loading - Again, this was handled as it was for overhead lines. Admittances were doubled, cut in half, and neglected altogether.

IV. Results

The results of the parameter sensitivity study are most clearly presented when the four major groups of variations are further subdivided according to the parameter varied. Within each of these subdivisions, discussion is made concerning the effects on the various network properties compared for the study. Two of the four properties, the characteristic admittance and the driving point admittance, are matrix quantities and thus present values both on and off the matrix diagonal. When the method of signalling employed involves placing identical signals on all three phases, it is the elements on the matrix diagonal that are of greatest concern. These elements include phase to neutral admittances as well as cross-coupling admittances whereas off-diagonal elements contain only cross-coupling terms. In general, the phase to neutral admittances are an order of magnitude or so greater than the cross-coupling terms and tend to dominate.

This section attempts to make a capsulated presentation of significant results. In order to prevent the inundation of the reader by detailing thousands of percentages and related minutia, every effort has been made to reduce measures of sensitivity to as few numerics as possible. In each case, the percent differences in the magnitudes of the three phase output voltages were averaged to provide a single value

to be used for comparison. For other properties, the largest difference magnitude (on-diagonal for matrices) was used because it represents the limiting case. Whenever possible, a normalized sensitivity is presented. This value is defined as the percent difference in the output voltage magnitude divided by the percent difference in the parameter. Both the numerator and the denominator are expressed as a percent of their reference values. Mathematically, the normalized sensitivity equals

$$\frac{\Delta V_{out}}{V_{out}} \times 100\%$$

$$\frac{\Delta P}{P} \times 100\%$$

where

V_{out} = reference value of output voltage magnitude

ΔV_{out} = change in value of the output voltage magnitude

P = reference value of the parameter

ΔP = change in value of the parameter

Because changes in the output voltage magnitudes are by far the most significant indicators of parameter sensitivity, extra attention was given to this property. In addition to figuring the change in output voltage magnitude as a percent of the reference output voltage magnitude, a calculation was performed to determine the change in output voltage magnitude as a percent of the input voltage magnitude. In each case analyzed, the input voltage was

1.0 $\angle 0°$ volts, so,

$$\frac{/\Delta V_{out}/}{V_{in}} = \frac{/V_{out}/ - /V_{out}'/}{/V_{in}/} \times 100\%$$

$$= \frac{/V_{out}/ - /V_{out}'/}{1} \times 100\%$$

$$= /V_{out}/ - /V_{out}'/ \times 100\%$$

where V_{out} = reference output voltage

V_{out}' = output voltage with a parameter varied.

There was also a normalized sensitivity calculated from this property. In mathematical terms,

$$\frac{/V_{out}/ - /V_{out}'/ \times 100\%}{\frac{\Delta P}{P} \times 100\%}$$

where all values are defined as in earlier equations.

Again, let it be noted that these results were obtained on highly idealized networks. Since the intent is merely to indicate general trends, the results will be presented in as general terms as possible. More specific relationships may be determined via direct analysis of the data.

A. Overhead Geometry Variations

1. Phase Conductor Diameter - The three variations in phase conductor diameter consisted of 21.9% and 38.0% decreases and a 22.5% increase. Results were tabulated for all four of the properties compared by the study - characteristic

admittance, eigenvalues, driving point admittance, and voltage transfer.

Results indicated that sensitivity to phase conductor diameter was not consistent across the range evaluated. The two decreases in diameter produced normalized sensitivities referred to the input voltage of 0.119 and 0.108, values similar enough to be considered constant when computational errors are included. On the other hand, the lone increase in phase conductor diameter indicated a sensitivity of only 0.047, far less than half the values determined in the other variations. The sensitivities of the other three properties pretty much followed the pattern established by the output voltage magnitude. In every case the sensitivity of the property was significantly less for the phase conductor diameter increase than for the decreases. See Figure (7) for the specific numerical values.

One quarter wavelength investigation revealed no increased sensitivity to phase conductor diameter variations. Normalized sensitivities referred to the input voltage assumed nearly the same three values determined in the nominal evaluation 0.117, 0.108, and 0.50, respectively. The characteristic admittance and the eigenvalues were not recomputed for the quarter wavelength study because neither was length dependent. Exact results of the one quarter wavelength study may be seen in Figure (8).

2. Neutral Conductor Diameter - The only variation made was a 37.2% reduction in diameter which resulted in a normalized sensitivity with respect to the input voltage of just 0.018. Changes in every category were slight even though the parameter variation was quite large. Just as with the phase conductor diameter, no change in sensitivity was noted on the quarter wavelength system. Here the final sensitivity measured was just 0.017, virtually the same as on the nominal network. See Figures (7), and (8) for specific results.

3. Phase Conductor to Phase Conductor Spacing - A 10.0% increase in this parameter produced a normalized sensitivity referred to the input voltage of only 0.067. One quarter wavelength evaluation resulted in the similar value of 0.071. As with all overhead geometry variations, the characteristic admittance and the eigenvalues were computed only once even though both nominal and one quarter wavelength networks were analyzed. Numerical results for the two cases may be seen in Figures (7) and (8).

4. Phase Conductor to Earth Spacing - This parameter was increased 10.0% while the neutral conductor to ground spacing was maintained. (In effect, the phase conductor to neutral conductor spacing was increased approximately 52.5%). This resulted in a final sensitivity measure of -0.355. The negative indicates that an increase in spacing results in a decrease in output voltage magnitude. (This value is reduced to approximately -0.067 if the phase to neutral spacing is considered to be the parameter varied). Again, there was no particular increase in sensitivity when the one quarter wavelength network was analyzed. Normalized sensitivity referred to the input voltage for that case was -0.360. Refer to Figures (7) and (8) for other specific ratios and percent changes.

5. Neutral Conductor to Earth Spacing - Effectively the opposite of increasing phase conductor to earth spacing, a 10.0% increase was made while phase to earth spacing was held constant. (In effect, the phase conductor to neutral conductor spacing was decreased approximately 42.5%). The result was a normalized sensitivity referred to the input voltage of 0.427 (or alternately 0.10). As was standard for overhead geometry variations, no increase in sensitivity was noted when the one-quarter wavelength network was analyzed. Results on that network were 0.443 (or (0.104). See Figures (7) and (8).

6. Miscellaneous Conductors - Three variations were made on both nominal and quarter wavelength networks that involved the addition of miscellaneous conductors to the overhead configuration. Because these variations are binary in nature, no normalized sensitivities could be computed. Instead, comparisons will be based on the change in output voltage magnitude, referred to either the reference output value or the input value.

The introduction of a single miscellaneous conductor at ground potential resulted in a 12.7% increase in the output voltage level, as compared to the reference level. Because the reference output voltage magnitude was approximately half of the input magnitude, the increase, as compared to the input voltage, was approximately half of that compared to the output voltage, specifically 5.75%. This condition was a general trend with all overhead geometry variations. The other miscellaneous conductor variations involved two conductors being added to the pole. These resulted in voltage increases of 15.2% and 14.5%, referred to the reference output voltage magnitude. The same increases were 6.87% and 6.56% when referred to the input voltage magnitude.

One quarter wavelength analysis produced much the same results as the longer network. Comparisons here should be made with the change in output voltage magnitude as a percent of the input voltage. This is due to the fact that the reference output voltages are different on the nominal and the one quarter wavelength networks, thus, changes as a percent of these values should not be directly compared across networks. Comparisons within each length network are legitimate. More complete presentation of results may be seen in Figures (7) and (8).

7. Triplex Neutral Conductor - Changing the neutral conductor to a triplex cable was another binary type variation and again, no normalized sensitivity could be obtained. Comparing output

DESCRIPTION OF VARIATION	NETWORK I.D. NUMBER	LINE TYPE	$\Delta\rho$ %	$\Delta\gamma_{o\ MAX}$ %	$\Delta\lambda_{MAX}$ %	$\Delta\gamma_{IN\ MAX}$ %	$\Delta V_{OUT\ AVG.}$ %	$\frac{\Delta V_{OUT\ AVG}}{\Delta\rho}$	$\frac{V_{OUT} - V_{OUT_{REF}}}{V_{IN}}$ %	$\frac{V_{OUT} - V_{OUT_{REF}}}{V_{IN}} \div \frac{\Delta\rho}{\rho}$
PHASE CONDUCTOR DIAMETER	SYSTEM 11	103	-21.9	8.10	4.47	16.4	-5.72	0.261	-2.60	0.119
"	SYSTEM 12	105	-38.0	12.5	5.49	20.9	-9.08	0.239	-4.12	0.108
"	SYSTEM 13	107	22.5	4.19	0.19	3.54	2.37	0.105	1.07	0.047
NEUTRAL CONDUCTOR DIAMETER	SYSTEM 14	109	-37.2	0.16	0.20	0.11	1.47	0.039	0.67	0.018
PHASE TO PHASE SPACING	SYSTEM 15	111	10.0	1.20	0.16	1.02	1.49	0.149	0.67	0.067
PHASE TO EARTH SPACING	SYSTEM 16	113	10.0	1.27	0.32	0.96	-7.85	-0.785	-3.55	-0.355
NEUTRAL TO EARTH SPACING	SYSTEM 17	115	10.0	1.39	0.15	1.31	9.44	0.944	4.27	0.427
MISCELLANEOUS CONDUCTORS	SYSTEM 18	117	—	1.46	2.90	1.88	12.7	—	5.75	
"	SYSTEM 19	119	—	1.70	3.35	2.19	15.2	—	6.87	
"	SYSTEM 20	120	—	1.71	2.53	1.98	14.5	—	6.56	
TRIPLEX NEUTRAL	SYSTEM 21	123	—	0.62	1.26	0.79	5.31	—	2.40	
SPACER CABLE	SYSTEM 22	201	—	65.5	4.26	37.0	47.4	—	21.4	

FIGURE (7)

DESCRIPTION OF VARIATION	NETWORK I.D. NUMBER	LINE TYPE	ΔP %	$\Delta \gamma_{o\ MAX}$ %	$\Delta \lambda_{MAX}$ %	$\Delta Y_{IN\ MAX}$ %	$\Delta V_{OUT\ AVG.}$ %	$\frac{\Delta V_{OUT\ AVG}}{\Delta P}$	$\frac{V_{OUT} - V_{OUT_{REF}}}{V_{IN}}$ %	$\frac{V_{OUT} - V_{OUT_{REF}}}{V_{IN}} \cdot \frac{\Delta P}{P}$
1/4 PHASE CONDUCTER DIAMETER	28	103	-21.9	8.10	4.47	14.1	-5.07	0.231	-2.57	0.117
1/4 "	29	105	-35.0	12.5	5.49	21.5	-8.04	0.211	-4.10	0.108
1/4 "	30	107	22.5	4.19	0.19	8.19	2.20	0.097	1.13	0.050
1/4 NEUTRAL CONDUCTOR DIAMETER	31	109	-37.2	0.16	0.20	0.16	-1.24	0.033	-0.63	0.017
1/4 PHASE TO PHASE SPACING	32	111	10.0	1.20	0.16	2.65	1.42	0.142	0.11	0.071
1/4 PHASE TO EARTH SPACING	33	113	10.0	1.27	0.32	1.38	-7.08	-0.708	-3.60	-0.360
1/4 NEUTRAL TO EARTH SPACING	34	115	10.0	1.39	0.15	1.42	8.80	0.880	4.43	0.443
1/4 MISCELLANEOUS CONDUCTORS	35	117	—	1.46	2.90	1.52	10.7	—	5.49	—
1/4 "	36	119	—	1.70	3.35	1.78	12.8	—	6.52	—
1/4 "	37	120	—	1.71	2.53	1.81	12.4	—	6.33	—
1/4 TRIPLEX NEUTRAL	38	123	—	0.62	1.26	0.64	4.50	—	2.29	—
1/4 SPACER CABLE	39	201	—	65.5	4.26	155	46.8	—	22.7	—

FIGURE (8)

voltage magnitudes showed a 5.31% increase over the reference value, or a 2.40% increase as compared to the input voltage. The same values determined on the one-quarter wavelength network were 4.50% and 2.29%, the latter of which should be used for comparison and is within 5% of the value for the nominal network. As a general note, all neutral variations produced less of a voltage drop as a percent of input on the quarter wavelength network than on the nominal length network. All of the quarter wavelength values were, however, within 5% of the nominal values, so although consistantly less, they were not significantly less. See Figures (7) and (8) for details.

8. Spacer Cable - This change in configuration was so radical it was impossible to establish a degree of change. Accordingly, no normalized sensitivity was determined. As was expected, there was a significant change in the output voltage, up 21.4% on the nominal and 22.7% on the quarter wave network. Both figures are increases as a percent of the input voltage magnitude. Changes in the other properties were comparably great. See Figures (7) and (8) for the specific values.

B. Loading Variations

1. Terminal Load - The equal element diagonal load at the end section of the feeder was removed on both the nomimal length and one quarter wavelength networks. Because this was another binary type of variation, no normalized sensitivity could be obtained. Comparing the change in output voltage as a percent of input voltage, shows a significant difference between the nominal and quarter wave cases. The nominal network showed a 9.98% increase while the quarter wave network jumped 17.1%. No measurements were made of characteristic admittance or eigenvalues because this variation would not effect those properties. See Figure (9) for more detailed results.

2. Distribution Transformer Loading - The results of variations in this parameter established a rather significant link between transformer loading and voltage level on the feeder. The doubling of the transformer loading as seen by the primary side can be thought of as a 100% increase in loading. Similarly, halving the loading can be considered a 50.0% decrease. These variations can thus result in normalized sensitivities. Ignoring the loading altogether is a binary variation and cannot be expressed in normalized terms. Transformer loading was doubled and neglected on both nominal and one quarter wavelength networks. Halving was performed on only the nominal length network.

Doubling of the transformer loading resulted in a normalized sensitivity with respect to the input voltage of -0.297 for the nominal length and -0.282 for the quarter wavelength case. As before, the negative value indicates that loading increases result in voltage decreases. On the other hand, decreasing the loading by 50% resulted in a normalized sensitivity of -0.716, indicating a sensitivity twice as great as the earlier results. This carries through to the other properties to the same general degree. As with analysis of the terminal load variation, characteristic admittance and eigenvalues were not compared because they would not be effected by this variation.

The analysis performed with all transformer loading ignored produced very large differences in the output voltage. More importantly, the voltage increase on the one quarter wavelength network was many times larger than that on the nominal network. The change in output voltage magnitude as a percent of the input voltage was 268% for the quarter wave network and 59.3% for the 16,000 meter version. Because removal of distribution transformer loading eliminates the vast majority of damping effects, the measured output voltage is almost purely dependent on the input voltage and the particular standing wave pattern on the line. As expected, an undamped one quarter wavelength pattern greatly magnified the output voltage level. More complete

results for all distribution transformer loading variations may be found in Figure (9).

3. Terminal Load and Distribution Transformer Loading Combination - Both the quarter wavelength and the nominal length network results indicated that combining these two variations allowed them to cancel each other to some degree. Using $\Delta V_{out}/V_{in} \times 100\%$ as the yardstick for comparison, nominal length analysis resulted in a 25.7% decrease in output voltage. This compares to a 29.7% decrease with the transformer loading doubled and a 9.98% increase with the terminal load removed. Although it is not a linear combination of the components, there is a definite interference between the two. The same pattern was repeated for the quarter wavelength results but the interference had a slighter effect. Results were a 23.3% drop in output voltage as compared to a 17.1% increase and a 28.2% decrease when the terminal load and transformer loading are dealt with separately. A smaller drop would have been expected due to the larger increase from removing the terminal load, assuming the two components counteracted linearly. Obviously, they do not. Figure (9) supplies additional results that may be of interest.

4. Transformer Loading and Overhead Geometry Combination - The results of this series of variations continued along the lines of the previous combination. Because there was more than one variation being made, it was not possible to establish a normalized sensitivity that would have had any worthwhile meaning. Instead, the change in output voltage magnitude as a percent of input voltage magnitude was the standard of measure. In every case, this ratio indicated a significant degree of interference between the effects of the two variations. As an example, consider the case in which the distribution transformer loading was halved and the phase conductor diameter was decreased 21.9%. These variations considered separately produced output voltage changes of +35.8% and -2.60%, respectively. Taken in tandem,

DESCRIPTION OF VARIATION	NETWORK I.D. NUMBER	LINE TYPE	ΔP %	$\Delta Y_{o\,MAX}$ %	$\Delta\lambda_{MAX}$ %	$\Delta Y_{IN\,MAX}$ %	$\Delta V_{OUT\,AVG.}$ %	$\frac{\Delta V_{OUT\,AVG}}{\Delta P}$	$\frac{V_{OUT} - V_{OUT_{REF}}}{V_{IN}}$ %	$\frac{\frac{V_{OUT} - V_{OUT_{REF}}}{V_{IN}}}{\frac{\Delta P}{P}}$
DIAGONAL LOAD REMOVED	13	101	—	—	—	17.6	22.0	—	1.98	—
D.T. ADMITTANCES DOUBLED	14	101	100	—	—	21.7	-65.6	-0.656	-29.7	-0.297
DIAGONAL LOAD REMOVED & D.T. ADMITTANCES DOUBLED	17	101	—	—	—	14.2	-56.7	—	-25.7	—
1/4 DIAGONAL LOAD REMOVED	42	101	—	—	—	24.3	33.6	—	17.1	—
1/4 DIAGONAL LOAD REMOVED & D.T. ADMITTANCES DOUBLED	45	101	—	—	—	52.3	-45.7	—	-23.3	—
1/4 D.T. ADMITTANCES DOUBLED	56	101	100	—	—	51.1	-55.4	-0.554	-28.2	-0.252
1/4 D.T. ADMITTANCES NEGLECTED	57	101	—	—	—	30.4	52.9	—	26.8	—
D.T. ADMITTANCES NEGLECTED	58	101	—	—	—	60.6	131	—	59.3	—
D.T. ADMITTANCES CUT IN HALF	59	101	-50.0	—	—	24.6	79.2	-1.58	35.8	-0.716
"	60	103	—	8.10	4.47	29.9	72.3	—	32.7	—
"	61	105	—	12.5	5.49	32.2	69.0	—	31.2	—
"	62	107	—	4.19	0.19	25.1	50.8	—	36.5	—

ORIGINAL PAGE IS OF POOR QUALITY

FIGURE (9)

result was a 32.7% increase in voltage, clearly indicating some sort of additive effect. Details of the results for this series may be found in Figures (9) and (10). Values for the characteristic admittance and eigenvalues reflect the fact that overhead geometry variations altered these properties. The change in driving point admittance reflects both the altered characteristic admittance and the reduced admittances of the transformer loading.

C. "Set-up" Time Reduction Variations

1. Aggregation - If the number of sections in the network is considered to be the parameter varied in these cases, a normalized sensitivity can be obtained for the aggregation analysis. The two variations were thus a 50.0% reduction and a 66.3% reduction in the effective number of sections. Results indicated that normalized sensitivities with respect to the input voltage magnitude were 0.009 and 0.014 for the two respective cases. Quarter wavelength analysis produced the similarly insensitive values of 0.011 and 0.015. Characteristic admittance and eigenvalues were not compared for these variations because they would not be effected by the number of sections in the network. See Figures (11) and (12) for more complete results.

2. Temperature - The sensitivity of the model to variations in the temperature of the overhead phase conductors was rather firmly established. The results of all five temperature variations indicated a normalized sensitivity with respect to the input voltage of only -.001. Repetition of these same variations on a one quarter wavelength system produced values too small to be meaningfully recorded. Similarly, the driving point admittance was largely unaffected by temperature. The characteristic admittance and the eigenvalues were not recorded even though they would have been altered by temperature variations. Aside from the fact that obtaining comparisons would have been quite difficult for various reasons, the sensitivities computed indicate that differences would have been far too small to have been

DESCRIPTION OF VARIATION	NETWORK I.D. NUMBER	LINE TYPE	ΔP %	$\Delta Y_{o\ MAX}$ %	$\Delta \lambda_{MAX}$ %	$\Delta Y_{IN\ MAX}$ %	$\Delta V_{OUT\ AVG.}$ %	$\frac{\Delta V_{OUT\ AVG}}{\Delta P}$	$\frac{V_{OUT} - V_{OUT_{REF}}}{V_{IN}}$ %	$\frac{\frac{V_{OUT} - V_{OUT_{REF}}}{V_{IN}}}{\frac{\Delta P}{P}}$
D.T. ADMITTANCES CUT IN HALF	63	109	—	0.16	0.20	24.5	77.8	—	35.2	—
"	64	111	—	1.20	0.16	24.5	80.0	—	36.2	—
"	65	113	—	1.27	0.32	24.8	73.4	—	33.2	—
"	66	115	—	1.39	0.15	24.3	86.2	—	39.0	—
"	67	117	—	1.46	2.90	23.8	94.6	—	42.8	—
"	68	119	—	1.70	3.35	28.3	97.7	—	44.2	—
"	69	120	—	1.71	2.53	24.1	95.4	—	43.1	—
"	70	123	—	0.62	1.26	24.3	85.8	—	38.8	—
"	71	201	—	65.5	4.26	39.4	117	—	53.1	—

FIGURE (10)

of great interest anyway. Actual results of these comparisons may be found in Figures (11) and (12).

3. Earth Resistivity - The four earth resistivity variations performed on the quarter wavelength and the nominal length networks resulted in a nearly constant value for the normalized sensitivity referred to the input voltage magnitude. All eight values were within the range of -0.01 to -0.02. All other measures showed similarly low sensitivity. As with the temperature variations, comparisons of characteristic admittance and eigenvalues were not carried out even though they would have been effected by changes in earth resistivity. The same reasons can be cited. See Figures (11), (12), and (13) for the results of comparisons made.

4. Ungrounded Neutral - Analysis performed with it no longer assumed that the neutral was everywhere at ground potential resulted in very slight changes in the output voltage magnitudes. Because this was a binary variation, normalized sensitivities could not be computed. In the absence of this, the change in output voltage magnitude as a percent of input voltage magnitude was used as a yardstick. Results showed a .297% increase on the nominal length network and a .423% increase on the quarter wavelength network. In either case, the increase was small. See Figures (12) and (13).

5. Aggregation Networks With Distribution Transformer Admittances Doubled - Because two variations were made at once, no normalized sensitivity was calculated. Using the change in output voltage as a percent of input voltage as a comparison, the results of these variations could pretty much have been predicted by looking at the results of the component variations when considered separately. Doubling transformer admittances decreased voltage by approximately 29%. Aggregation reduced output voltage approximately 1%. When combined, voltage reductions were 30.0% and 30.2% for networks with total sections reduced 50% and 66.3%, respectively. The figures were 28.5% and 28.8% reductions for one quarter wavelength analysis. These are also in line with

the values found from quarter wavelength analysis of the single parameter variations. Again, a slight interference effect can be noted as the two reductions combine. The doubled loading, of course, is the much more significant of the two variations. Complete results may be found in Figures (11) and (12).

6. Total Length - Increasing and decreasing the overall length of the nominal network resulted, surprisingly enough, in voltage drops for both cases. This is indicative of an alteration in the standing wave pattern rather than a mere change in the point of measurement along that pattern. Study of the voltage vs. distance plots supports this. At any rate, the normalized sensitivities referred to the input voltage were .718 for the 5% decrease and -.988 for the 5% increase. These values show an almost one-to-one ratio of ΔV to ΔP and point out that total length is a parameter of significance. See Figure (13) for additional results.

D. Cable Network Variations

1. Earth Resistivity - The sensitivity of underground cable networks to variations in earth resistivity was even less than that of overhead feeders. Normalized sensitivity with respect to the input voltage was, at most, a mere -0.0015. This figure includes both nominal length and one quarter wavelength results. Typically the results were values too small to meaningfully record the actual digits. The results, as presented in Figures (14) and (15), indicate that for all intents and purposes, underground cables are impervious to variations in earth resistivity.

2. Temperature - The results presented here were calculated considering only the change in temperature of the phase conductors. Because the feeder descriptions of underground cables allow for separate specification of phase conductor and neutral strand temperatures, the percentage differences of the two were not equal even though the number of degrees difference from the reference values were equal. When the percentage difference was needed in a calculation, the value for the phase conductors was used. It should also be noted that percentage differences

DESCRIPTION OF VARIATION	NETWORK I.D. NUMBER	LINE TYPE	ΔP %	$\Delta Y_{o\ MAX}$ %	$\Delta \lambda_{MAX}$ %	$\Delta Y_{IN\ MAX}$ %	$\Delta V_{OUT\ AVG.}$ %	$\frac{\Delta V_{OUT\ AVG}}{\Delta P}$	$\frac{V_{OUT} - V_{OUT_{REF}}}{V_{IN}}$ %	$\frac{\frac{V_{OUT} - V_{OUT_{REF}}}{V_{IN}}}{\frac{\Delta P}{P}}$
AGGREGATION	11	101	-50.0	—	—	0.67	-1.05	0.021	-0.47	0.009
"	12	101	-66.3	—	—	2.63	-2.05	0.031	-0.92	0.014
AGGREGATION & D.T. ADMITTANCES DOUBLED	15	101	—	—	—	21.1	-66.2	—	-30.0	—
"	16	101	—	—	—	20.2	-66.7	—	-30.2	—
TEMPERATURE	18	101	20.0	NOT RECORDED	NOT RECORDED	0.03	-0.03	-0.001	-0.01	-0.001
"	19	101	-20.0			0.03	0.03	-0.001	0.01	-0.001
"	20	101	-60.0			0.08	0.08	-0.001	0.04	-0.001
"	21	101	-100			0.14	0.13	-0.001	0.06	-0.001
"	22	101	-140			0.20	0.19	-0.001	0.09	-0.001
EARTH RESISTIVITY	23	101	-50.0			0.44	2.21	-0.044	1.00	-0.020
"	24	101	-25.0			0.18	0.89	-0.035	0.41	-0.016
"	25	101	25.0			0.14	-0.67	-0.027	-0.30	-0.012

FIGURE (11)

DESCRIPTION OF VARIATION	NETWORK I.D. NUMBER	LINE TYPE	ΔP %	$\Delta \gamma_{o\ MAX}$ %	$\Delta \lambda_{MAX}$ %	$\Delta \gamma_{IN\ MAX}$ %	$\Delta V_{OUT\ AVG.}$ %	$\frac{\Delta V_{OUT\ AVG}}{\Delta P}$	$\frac{V_{OUT} - V_{OUT_{REF}}}{V_{IN}}$ %	$\frac{\frac{V_{OUT} - V_{OUT_{REF}}}{V_{IN}}}{\frac{\Delta P}{P}}$
EARTH RESISTIVITY	26	101	50.0	NOT RECORDED	NOT RECORDED	0.25	-1.20	-0.024	-0.55	-0.011
NEUTRAL NOT ASSUMED AT GROUND POTENTIAL.	27	101	—	—	—	0.02	0.65	—	0.30	—
1/4 AGGREGATION	40	101	-50.0	—	—	1.08	-1.05	0.021	-0.54	0.011
1/4 "	41	101	-66.3	—	—	3.97	-2.03	0.030	-1.02	0.015
1/4 AGGREGATION & D.T. ADMITTANCES DOUBLED	43	101	—	—	—	51.2	-56.0	—	-28.5	—
1/4 "	44	101	—	—	—	51.4	-56.6	—	-28.8	—
1/4 TEMPERATURE	46	101	20.0	NOT RECORDED	NOT RECORDED	0.01	-0.02	-0.001	-0.000	0.000
1/4 "	47	101	-20.0			0.01	0.02	-0.001	0.000	0.000
1/4 "	48	101	-60.0			0.04	0.06	-0.001	0.000	0.000
1/4 "	49	101	-100			0.06	0.10	-0.001	0.000	0.000
1/4 "	50	101	-140			0.09	0.15	-0.001	0.001	0.000
1/4 EARTH RESISTIVITY	51	101	-50.0			0.24	1.83	-0.036	0.93	-0.018

FIGURE (12)

DESCRIPTION OF VARIATION	NETWORK I.D. NUMBER	LINE TYPE	ΔP %	$\Delta \gamma_{o\ MAX}$ %	$\Delta \lambda_{MAX}$ %	$\Delta \gamma_{IN\ MAX}$ %	$\Delta V_{OUT\ AVG.}$ %	$\frac{\Delta V_{OUT\ AVG}}{\Delta P}$	$\frac{V_{OUT} - V_{OUT_{REF}}}{V_{IN}}$ %	$\frac{\frac{V_{OUT} - V_{OUT_{REF}}}{V_{IN}}}{\frac{\Delta P}{P}}$
1/4 EARTH RESISTIVITY	52	101	-25.0	NOT RECORDED	NOT RECORDED	0.10	0.75	-0.03	0.38	-0.015
1/4 "	53	101	25.0	↓	↓	0.08	-0.57	-0.02	-0.29	-0.011
1/4 "	54	101	50.0			0.14	-1.02	-0.02	-0.52	-0.010
1/4 NEUTRAL NOT ASSUMED AT GROUND POTENTIAL	55	101	—	—	—	0.02	0.84	—	0.42	—
TOTAL LENGTH	74	101	-5.00	—	—	15.9	-7.23	1.45	-3.59	0.718
"	75	101	5.00	—	—	14.0	-9.95	-1.99	-4.94	-0.988

FIGURE (13)

were determined in degrees Centigrade. The alternate procedure of determining differences in degrees Kelvin would have resulted in much smaller percentage differences for the same variations and numerical accuracy would have been lost.

Results showed a marked increase in sensitivity as compared to overhead lines. The sensitivity measure was only -0.001 for the overhead case but jumped to an average value of -0.094 for the nominal length cable and -0.036 for the quarter wavelength case. Also notable is that the one quarter wavelength sensitivity is over three times the nominal length sensitivity when both are computed referred to the input voltage. When sensitivity is normalized considering the change in voltage as a percent of the reference output voltage, the values indicate that the nominal network is the more sensitive. This phenomenon is due to the voltage magnification caused by the standing wave pattern on the quarter wavelength network. The output voltage on that network was in the vicinity of three times the value of the input. This greater than unity voltage transfer and the associated magnification of sensitivity are examples of the behavior that was the object of the quarter wave investigation. Complete results of the temperature variations on both length networks may be obtained from Figures (14) and (15).

3. Aggregation - Results of these variations again pointed to quarter wavelength magnification. Normalized sensitivity as referred to the input voltage was infinitesimal on the nominal length network. Exact values were 0.0003 for a 50% reduction in the number of sections and 0.0004 for a 66.3% reduction. The same variations on a one quarter wavelength cable resulted in values of 0.0067 and 0.01, respectively. Although still insignificant to the operation of a PLC network, they nonetheless indicate the magnifying effect of the standing wave pattern. See Figures (14) and (15) for additional details.

4. Distribution Transformer Loading - Unlike the overhead lines, variations in this category had only a small effect on the voltage transfer of the modeled networks. As with the other cable variations, there is evidence of tremendous sensitivity magnification on the one quarter wavelength network. The sensitivities with respect to the input voltage magnitude calculated on the nominal length network were slight but constant. A 100% increase in loading resulted in a value of -0.0134 while a 50% decrease in loading gave a sensitivity of -0.0137. Of course, these values reflect a lot of averaging and round-off and are not really accurate to that many decimal places. Even though, a high degree of consistency is indicated. The corresponding values from the quarter wavelength analysis were -0.254 and -0.288. Most notable is the way the quarter wave magnification has made the loading a parameter of some significance to communications on this network.

Completely ignoring the transformer loading could not be expressed in terms of normalized sensitivities. Looking at $\Delta V_{out}/V_{in}$ x 100% again points up the magnification of sensitivity due to a total length of essentially one quarter wavelength. A relatively small increase of only 1.37% was experienced on the nominal length network when all transformer loading was removed. This was multiplied to 29.3% on the quarter wavelength feeder. Again, the parameter variation has become of some significance to communication. More complete details may be obtained from Figures (14) and (15).

5. Total Length - The sensitivity determined by these variations indicated that length was relatively important to the model predictions. The sensitivity calculations produced values of -0.228 for a 5% decrease in line length and 0.358 for a 5% increase. These values establish total length as the most significant parameter on the nominal length underground cable. See Figure (16) for complete results.

DESCRIPTION OF VARIATION	NETWORK I.D. NUMBER	LINE TYPE	ΔP %	$\Delta Y_{o\ MAX}$ %	$\Delta \lambda_{MAX}$ %	$\Delta Y_{IN\ MAX}$ %	$\Delta V_{OUT\ AVG.}$ %	$\frac{\Delta V_{OUT\ AVG}}{\Delta P}$	$\frac{V_{OUT} - V_{OUT_{REF}}}{V_{IN}}$ %	$\frac{\frac{V_{OUT} - V_{OUT_{REF}}}{V_{IN}}}{\frac{\Delta P}{P}}$
EARTH RESISTIVITY	76	UG CABLE	-50.0	0.00	0.01	0.00	0.03	-0.000	0.016	-0.000
"	77		50.0	0.00	0.01	0.00	-0.02	-0.000	-0.001	-0.000
"	78		100	0.00	0.01	0.00	-0.03	-0.003	-0.015	-0.001
TEMPERATURE OF PHASE CONDUCTOR	79		-13.3	0.35	4.91	0.63	2.91	-0.219	1.44	-0.108
"	80		13.3	0.29	0.34	0.50	-2.35	-0.177	-1.16	-0.087
"	81		26.6	0.57	5.15	0.98	-4.61	-0.173	-2.29	-0.086
AGGREGATION	82		-50.0	--	—	0.05	-0.04	0.001	-0.017	0.000
"	83		-66.3	—	—	0.17	-0.06	0.001	-0.031	0.000
D.T. ADMITTANCES DOUBLED	84		100	—	—	1.28	-2.70	-0.027	-1.34	-0.013
D.T. ADMITTANCES CUT IN HALF	85		-50.0	—	—	0.66	1.38	-0.027	0.687	-0.014
D.T. ADMITTANCES NEGLECTED	86		—	—	—	1.34	2.80	—	1.37	—

ORIGINAL PAGE IS OF POOR QUALITY

FIGURE (14)

DESCRIPTION OF VARIATION	NETWORK I.D. NUMBER	LINE TYPE	ΔP %	$\Delta \gamma_{o\ MAX}$ %	$\Delta \lambda_{MAX}$ %	$\Delta Y_{IN\ MAX}$ %	$\Delta V_{OUT\ AVG.}$ %	$\frac{\Delta V_{OUT\ AVG}}{\Delta P}$	$\frac{V_{OUT} - V_{OUT_{REF}}}{V_{IN}}$ %	$\frac{\frac{V_{OUT} - V_{OUT_{REF}}}{V_{IN}}}{\frac{\Delta P}{P}}$
1/4 EARTH RESISTIVITY	87	U.G. CABLE	-50.0	0.00	0.01	0.01	0.02	-0.000	0.072	-0.001
1/4 "	88		50.0	0.00	0.01	0.01	-0.01	-0.000	-0.034	-0.001
1/4 "	89		100	0.00	0.01	0.01	-0.02	-0.000	-0.065	-0.001
1/4 TEMPERATURE OF PHASE CONDUCTOR	90		-13.3	0.35	4.91	1.89	1.84	-0.138	5.53	-0.416
1/4 "	91		13.3	0.29	0.34	1.52	-1.48	-0.111	-4.46	-0.335
1/4 "	92		26.6	0.57	5.18	2.97	-2.90	-0.109	-5.72	-0.328
1/4 AGGREGATION	93		-50.0	—	—	0.14	-0.11	0.002	-0.33	0.007
1/4 "	94		-66.3	—	—	0.55	-0.22	0.003	-0.663	0.010
1/4 D.T. ADMITTANCES DOUBLED	95		100	—	—	9.52	-8.43	-0.084	-25.4	-0.254
1/4 D.T. ADMITTANCES CUT IN HALF	96		-50.0	—	—	5.45	4.69	-0.094	14.1	-0.255
1/4 D.T. ADMITTANCES NEGLECTED	97		—	—	—	11.4	9.75	—	29.3	—

FIGURE (15)

DESCRIPTION OF VARIATION	NETWORK I.D. NUMBER	LINE TYPE	ΔP %	$\Delta \gamma_{o\ MAX}$ %	$\Delta \lambda_{MAX}$ %	$\Delta \gamma_{IN\ MAX}$ %	$\Delta V_{OUT\ AVG.}$ %	$\frac{\Delta V_{OUT\ AVG}}{\Delta P}$	$\frac{V_{OUT} - V_{OUT_{REF}}}{V_{IN}}$ %	$\frac{\frac{V_{OUT} - V_{OUT_{REF}}}{V_{IN}}}{\frac{\Delta P}{P}}$
TOTAL LENGTH	98	UG CABLE	-5.00	—	—	11.0	2.29	-0.458	1.14	-0.228
TOTAL LENGTH	99	UG CABLE	5.00	—	—	10.3	-3.61	-0.722	-1.79	-0.358

ORIGINAL PAGE IS OF POOR QUALITY

FIGURE (16)

V. Conclusions

Conclusions drawn from the results of the parameter sensitivity study are presented in two groups. These groups correspond to the two overall goals of the study - to determine the sensitivity of the model to various parameters and to evaluate possibilities of reducing "set up" time. Accordingly, the conclusions will be based on two slightly different criteria. The first goal was more or less a pure knowledge endeavor while the second was specifically practice-oriented for a PLC communications network. It would, therefore, be possible for the model to be highly sensitive to a parameter, making that parameter of great interest for the first goal, yet because the parameter varies only over a narrow range, it is insignificant to a PLC communications network. Actual instances such as described here occurred during the course of the study.

Due to the fact that performance of a PLC communications network would not suffer serious adverse effects unless the signal level dropped by several dB, the voltage transfer ratio of the network would necessarily have to be altered by 40 or 50 percent before any great significance could be assigned to a parameter variation. On the other hand, the sensitivity of the model was better judged by the ratio of change in output to change in parameter. By this determination, the voltage transfer did not necessarily have to change by a great amount to establish a high degree of sensitivity. These two criteria formed the basis for the conclusions of this report.

A. Sensitivity of the Model to Various Parameters

1. Overhead Geometry - The model showed greatest sensitivity to radical changes in the overhead configuration. The change to spacer cable from the reference cross-arm caused the voltage transfer ratio to jump to nearly 150% of its reference value. Approximately the same change was recorded on the quarter wavelength system so it can be concluded that there is no increase in sensitivity to a change of this nature. From the results of this variation, it should be determined that any change in the basic overhead format (i.e., cross-arm to armless, armless to spacer cable, etc.) will result in a significant change in the model predictions if the lengths of such configurations are significant.

Also causing a notable increase in the voltage transfer ratio is the addition of miscellaneous conductors. Simply adding a wire or two bumped the voltage to 110% or 112% of its initial value, slightly more for quarter wavelength analysis. Even changing to a triplex neutral wire improved the ratio, but only by 5% or so.

Of the variations for which normalized sensitivities could be computed, it turned out that changes in the phase to earth and neutral to earth spacing resulted in the greatest changes in the voltage transfer. If, however, these variations are considered to be phase conductor to neutral conductor spacing variations, the normalized sensitivity value is greatly reduced. The modelled network proved to be relatively insensitive to phase to phase spacing and neutral conductor diameter. Only phase conductor diameter showed signs of slight significance to the model. Sensitivity to this parameter was such that small variations (less than 30% or so) could easily be ignored but larger ones begin to have noticeable effects on the model computations. In virtually every case, the model showed little or no increase in sensitivity when the network length was reduced to

approximately one quarter wavelength of the communication signal. This is largely the result of the transformer loading, which remained constant through all of these variations and was responsible for most of the damping of the standing waves via signal attenuation.

Generally speaking, unless there is a change in the basic geometric pattern of the overhead configuration, the model will be only slightly sensitive to variations. Changes in the neutral wire are mostly insignificant. Miscellaneous conductors will improve the voltage transfer ratio by a few percent. Phase conductor to neutral conductor spacing and phase conductor diameter should be watched because sizable variations will have effects on the model calculations.

2. Loading - In contrast to overhead geometry, the model proved to be quite sensitive to changes in the loading along the line. In every single variation made involving loading, the voltage transfer ratio computed by the model was significantly altered. In the many combined variations involving loading, the effects of the loading variation tended to swamp out those of the other variation made in the combination. Because the leakage reactances of the distribution transformers constitute a significant portion of their total loading effect, loading variations on the secondary side will not necessarily produce a variation of the same magnitude when seen from the primary side. This tends to dampen variations but nonetheless, loading can vary widely. The variations analyzed attempted to cover a broad range by taking a reference load and ranging it from half that value to twice that value. It would be fair to say that at the limits of this range, one could expect the voltage transfer ratio to have changed by approximately 30% (at least on the synthetic test network). Logically, as the loading increases the voltage transfer ratio decreases and vice versa.

The quarter wavelength analysis performed for loading variations provided a wealth of information. Most importantly, it pointed out the tremendous damping of the standing wave pattern caused by the loading. When the loading, as seen on the primary side of each distribution transformer was doubled, virtually the same change in the voltage transfer ratio was noted on both network lengths. When the loading was reduced or eliminated, the quarter wavelength network showed signs of greatly increased sensitivity. As the damping of the standing wave pattern lessened, the voltage magnification became more and more pronounced. The extreme case occurred when the distribution transformer loading was ignored altogether. In this case, the voltage transfer ratio increased on the quarter wavelength network by over four times the amount that it increased on the nominal length system. The quarter wavelength analysis demonstrated how much of the standing wave suppression is due to transformer loading. To a lesser degree, the terminal load on the line also damped the standing waves. This was also demonstrated by this study.

The conclusions drawn from study of loading variations ar' that loading is the most significant parameter to overhead lines. This sensitivity is caused by the damping effect the loading has on standing waves. Also, there appears to be a saturation point, beyond which model sensitivity to loading increases drops off dramatically. This was indicated by the fact that there was no significant magnification in sensitivity on the quarter wavelength network when the reference loading was doubled. The standing wave pattern had reached a point where it was so damped that it was no longer responsive to quarter wavelength magnification.

3. "Set-up" Time Reduction - This group of variations can be broken up so the parameters varied can be dealt with separately. These parameters were the number of sections in the network, the temperature of the conductors, the earth resistivity, and the total length of the line. It can safely be said that the model is

completely insensitive to all of these parameters except total length. Twenty-six variations were conducted with the first three parameters and not one indicated any signficant sensitivity in the model. Also, analysis with the neutral no longer assumed to be at ground potential pointed up no sensitivity to that parameter. The one quarter wavelength analysis simply pointed out that any effects due to these parameter variations were insufficient to overcome the suppression of standing waves caused by transformer loading.

Total length variations were of some consequence, however. The sensitivity of the model to length variations was due to the alteration of the standing wave pattern caused by changing the length. The variations were not great enough for a change in the sum total of the characteristic impedance to be of any importance. The only logical conclusion is that model sensitivity was a direct consequence of standing wave pattern sensitivity. As was discussed earlier, this variation can also be seen as a variation in signal frequency. Thus, the propagation will be sensitive to some degree to variations in either parameter. Since the standing wave pattern will be different for each specific length of line, signal frequency, and loading level, it would be impossible to state beforehand how much of an effect a certain error in line length estimation or signal frequency will have. The sensitivity of the propagation will vary with each individual case.

4. Cable Networks - Because of the very low characteristic impedance of underground cables, in most cases they proved to be far less sensitive to parameter variations, particularly in the case of the nominal length network. On that network, even the neglecting of all transformer loading increased the voltage transfer ratio by little more than 1%. This near total insensitivity reflects the fact that the impedances of the distribution transformers and other loads are so high when compared to that of the cable, that they are seen almost as open circuits. Variations in these

external loads are of little consequence when the model is dealing with cables. The greatest sensitivity noted was to variations in the temperature of the phase conductors. Even this sensitivity was slight. Sensitivity to earth resistivity and aggregation was too small to accurately determine.

One quarter wavelength analysis pointed out that even though sensitivity was reduced, it still could become significant if standing waves are such that voltages are magnified. Under these conditions, the loading on the line produced sizable damping effects, as did increases in the temperature. It would be safe to conclude that under quarter wavelength magnification effects the propagation becomes sensitive to loading and temperature variations.

Variations in the total length of the nominal underground cable showed a small but possibly significant degree of sensitivity. Results showed this sensitivity to be about one-third of that on the overhead line version of the simple test network. It can be argued along the same line used in the overhead case that this sensitivity can vary greatly depending on each specific case. Therefore, it is difficult to make conclusions on its importance based on the data available.

B. Possibilities of Reducing "Set-up" Time

Almost every variation made had some implication with regard to "set-up" time reduction. The most direct of these were, of course, the aggregation demonstrations. Many other variations indicated that the model did not necessarily require a highly accurate value for certain parameters - a single, rough estimate for the entire network would provide accurate enough results. Obviously, reducing the amount of accurate information needed will reduce the complexity of the "set up" procedure and thus the time and cost. For this reason, conclusions will

be drawn from results of many variations not directly intended to reduce "set-up" time.

Here we encounter the question - How accurate is accurate enough? As was discussed earlier, a change in voltage transfer of perhaps 40% is the minimum variation significant to a PLC communications network. Only a handful of variations made during the study had such an impact. The combination variations indicated that there was an additive effect when two variations occured together. It is this effect that must be accounted for when the standards of accuracy are established.

1. Overhead Geometry - These variations indicate that changes in the neutral conductor can largely be ignored. Sensitivity of the model to these variations was so small that a single, standard neutral may be assumed with little loss of accuracy. Only two aspects of the neutral need be considered. If the phase to neutral spacing varies by a large amount, or if additional neutral wires are present, then these variations should be accounted for. This is true only if the variation is present on a significant portion of the network. If it exists on only 100 meters of a 10,000 meter line, it could easily be ignored. However, 3,000 meters out of 10,000 might be significant enough for consideration.

   Along similar lines, only significant lengths of line containing miscellaneous conductors or phase conductor diameter changes need be bothered with. Actually, small changes in conductor diameter can be ignored completely no matter how much of the line they effect. Even very short lengths of radical geometry changes can safely be passed over. Any change that exists for more than 5% of the total length should be considered significant, however. Variations in phase to phase spacing can safely be ignored.

2. Loading - A sizable variation in loading on the line may be enough to significantly effect the voltage transfer all by itself. Because of the sensitivity here, it may be well to conduct a systematic loading variation study over a plausible range of relative loading to determine a worst case for each modeled feeder.

This is particularly true on quarter wavelength networks because of the greatly enhanced sensitivity to loading, especially light loading. It would be safe to say that no variation in loading greater than 10% or 15% should be ignored.

3. "Set-Up" Time Reduction - The most promising results of these variations indicated that aggregation of several shorter sections into one long one was an effective way of simplifying network descriptions without introducing any significant loss of accuracy. As was alluded to earlier, the demonstration of this technique was taken one step further. Analysis was performed on an actual computer description of a real life network. Every possible aggregation was made and the new description was reanalized with results compared to the original. The original network may be found in the data as network #72. The aggregated version is network #73. Results of this real life test case showed that the number of sections in the network was reduced over 36.8%, yet the voltage magnitudes at the terminal section were changed by an average of only 0.187% of the input value. Clearly a significant simplification can be achieved with no great loss of model accuracy. It is important to note that total length and transformer loading were held exactly constant during these demonstrations.

The other results of this group of variations also indicate that descriptions can be further simplified. Overhead networks are for all intents and purposes completely insensitive to variations in conductor temperature and earth resistivity. This allows basically one default value to be used for almost every network. Results will be sufficiently accurate and there need be no undue concern over the exact values for temperature or

earth resistivity. Also, results point out that model calculations are not very dependent on the assumption that the neutral is at ground potential everywhere. It can be inferred that the model description will be accurate even if this assumption is totally untrue.

The only variation that showed a necessity for accuracy in description was the total length of the network. Because the standing wave pattern is so easily upset, it is somewhat important that overall length be judged within $\pm$ 5% of its actual value.

4. Cable Networks - Conclusions regarding cable networks are not so concrete. As was pointed out before, variations that indicated no sensitivity at all on the nominal length network resulted in sizable sensitivity values when analyzed on a quarter wavelength line. Consequently, a knowledge of how long the network is in terms of signal wavelengths might be helpful in the process of deciding which variations can be safely ignored. No matter how long the feeder is, the total length is a parameter that should be documented within $\pm$5% or thereabouts. As with overhead lines, the length of the entire network is somewhat important and must be accurately determined if the model is to produce valid results.

The loading on the line and the temperature of the phase conductors are parameters that varied in significance depending on whether or not analysis was performed on a quarter wavelength line. At that length, they were significant enough to warrant attention. Any variation of 20% or more that could be determined should be considered significant. At longer lengths, these parameters fade in significance and no tremendous attention need be paid to them. Specification of a default temperature value would perhaps be accurate enough, and any realistic loading value would suffice.

Finally, aggregation and earth resistivity had almost no effect on the model. This leads to the conclusions that aggregation can be carried out successfully on underground cables, and that a default value for earth resistivity is accurate enough for any computations. In the general case, "set up" procedures for underground cable networks can be streamlined even more than for overhead lines because model sensitivity is generally lower.

By far the most important conclusion reached by this study is that aggregation is a valid method for reducing network description complexity without adversely effecting results. In conjunction with other simplifications, this will significantly reduce the time and effort now being expended for accurately detailed descriptions. By determining variations in certain parameters to be of little significance, the number of different line types and configurations can now be greatly reduced. Earth resistivity and conductor temperatures need not be accurately measured. These and other simplifications will go a long way toward making model descriptions easier to deal with and yet just as accurate.

Establishment of sensitivities for the model also aids in actual operation of the programs by enhancing the user's feel for the tool he is utilizing. Although these results were obtained on a highly idealized network, they shed light on other networks. Basic trends can be identified and applied elsewhere. Unusual phenomena may be understood when knowledge of the model's sensitivities is available. All in all, application of the model may provide results that can now be interpreted in a more meaningful way.

VI. Comments on Numerical Round-off Error

As with any process involving a great deal of computation, some error is introduced by rounding-off or truncating numbers. This was initially thought to be significant in some instances, so an evaluation was made. This evaluation involved the analysis of a 10,000 meter, 3-phase line, having a single 25 kva transformer load. Analysis was performed both as a line with 100 sections and as a line aggregated into one section. The following results indicate the overall voltage transfer matrix computation was subject to, in most cases, $\leq$ 1% error due to round-off. This indicates that only a very small part of all error is due to numerical round-off error. For all practical purposes, the error is of no great significance. See Figures (17) and (18) for the results of this experiment.

Attachment to DIFNAP Memo #26 (Cont'd)

Voltage Transfer Matrix Obtained by Matrix-Matrix Multiplication
100 Section Line

2.2205505E-00	1.2949408E-01	1.9955678E-01
-1.0050040E-01	-6.1201580E-02	-1.5897823E-01
1.5582932E-01	2.1916808E-01	2.0303388E-01
-7.4422400E-02	-8.8912366E-02	-1.6863907E-01
1.6295392E-01	1.3002984E-01	2.3463748E-00
-8.6615614E-02	-6.8101263E-02	-3.0640301E-01

Voltage Transfer Matrix Single Section Line

2.2207349E-00	1.2963878E-01	1.9850288E-01
-1.0166037E-01	-6.2126620E-02	-1.5408064E-01
1.5608706E-01	2.1918909E-00	2.0209737E-01
-7.5870808E-02	-9.0067551E-02	-1.6419739E-01
1.6379893E-01	1.3070214E-01	2.3349881E-00
-8.9224265E-02	-7.1059561E-02	-3.0308890E-01

Output Voltage for a Dirac-Delta Voltage Drive on Phase 1
100 Section Using Matrix-Vector Multiplication

2.22073E-00	1.56087E-01	1.63794E-01
-1.01660E-01	-7.58708E-02	-8.92234E-02

100 Section Using Matrix-Matrix Multiplication

2.2205505E-00	1.5582932E-01	1.6295392E-01
-1.005004E-01	-7.4422400E-02	-8.5515614E-02

Single Section Line

2.220735E-00	1.560870E-01	1.637989E-01
-1.016604E-01	-7.587081E-02	-8.922426E-02

FIGURE (17)

Attachment to DIFNAP Memo #26

Input Admittance 100 Section Line

Input Admittance 100 Section Line
DB-Angle

-46.23	-58.62	-65.86
88.58	-87.66	-77.21
-58.62	-45.90	-58.72
-87.66	88.83	-86.04
-65.86	-58.72	-45.59
-77.21	-86.04	83.52

Rectangular

1.2128379E-04	4.7941084E-05	1.1276417E-04
4.8796294E-03	-1.1714650E-03	-4.9680188E-04
4.7941134E-05	1.0354070E-04	8.0014984E-05
-1.1714569E-03	5.0669665E-03	-1.1565391E-03
1.1276163E-04	8.0014310E-05	5.9263794E-04
-4.9681725E-04	-1.1565352E-03	5.2191951E-03

Input Admittance 1 Section Line

Input Admittance Single Section Line
DB-angle

-46.23	-58.62	-65.86
88.58	87.66	77.21
-58.62	-45.90	-58.72
-87.66	88.83	-86.04
-66.86	-58.72	-45.59
-77.21	-86.04	83.52

Rectangular

1.2128418E-04	4.7941197E-05	1.1276341E-04
4.8796358E-03	-1.1714630E-03	-4.9680814E-04
4.7941195E-05	1.0354079E-04	8-0014670E-05
-1.1714629E-03	5.0669705E-03	-1.1565380E-03
1.1276339E-04	8.0014676E-05	5.9263896E-04
-4.9680826E-04	-1.1565380E-03	5.2191989E-03

FIGURE (18)

TASK 4

TRANSFORMER MODELING

TABLE OF CONTENTS FOR TASK 4

	Page
Foreword	4-1
Purpose	4-1
Synopsis of Phase I Transformer Modeling Activities	4-2
Synopsis of Inter Phase Transformer Modeling Activities	4-3
Synopsis of Phase II Transformer Modeling Activities	4-4
Measurement Technique for Phase II	4-5
Transformer Construction	4-13
Transformer Symmetry	4-14
Response Measurements	4-20
Algebraic Model	4-31
Lumped Parameter Model	4-32
Verification	4-48
Measured and Computed Performance as a Function of Load Changes	4-58
Extended Frequency Measurements	4-66
Three Phase Transformer Measurements	4-68
Data Bank	4-76

TASK 4
TRANSFORMER MODELING

R. C. Rustay
J. T. Gajjar
R. W. Rankin
A. M. Dunham

FOREWORD

This chapter reports on the activities associated with modeling of two winding transformers in the context of use at PLC frequencies. Distribution transformers are included in this category by assuming them electrically symmetric and having balanced secondary loads with the net result they become effectively two winding transformers.

PURPOSE

The purpose behind the effort to obtain a suitable computational model was to obtain an automated software procedure (not requiring manual intervention) for predicting two-way propagation through the transformers, i.e., from primary to secondary and secondary to primary. Also, with such a model, the effect of different levels of secondary loading (deterministic and random, i.e., MONTE CARLO) could be easily accomplished. From a system engineering point of view, PLC propagation through transformers represents a critical item in system performance and having a physical model is very useful for understanding these limitations and the effects of possible fixes such as tuning and bypass procedures.

Transformers of interest are:

Distribution Transformers (assuming electrical symmetry and balanced secondary loading)

Single Phase Ratio Bank Transformers

Three Phase Transformer Banks (Three Single Phase Transformers) including open delta banks.

Single Core Three Phase Transformers were not considered.

Synopsis of Phase I Transformer Modeling Activities

Transformer modeling was initiated in Phase I of this project. At that time, little previous apriori knowledge existed regarding the behavior of distribution transformers at PLC frequencies and, in particular, when the various higher order levels of distributed/stray capacity became important. Also, it was originally intended that models be developed for frequencies to 500 kHz. Therefore, it did not appear that an analog type lumped parameter model could be developed and an associated parameter data base established within the time, available manpower and funding constraints associated with the Phase I effort. Therefore, it was decided to base modeling on measured "Y" parameters which would be frequency dependent (and of course KVA and other constructional features) but otherwise completely general. This approach was encouraged by several references on the subject*.

Therefore, concurrent activities of measurement, and model development and software implementation were initated. An extensive set of "Y" parameter measurements** were made on 5, 10, 15, 25, 50 KVA distribution transformers for frequencies to 500 kHz. Subsequently, when attempting to use these measured "Y" parameters, significant inconsistencies were discovered. After much deliberation, it was

---

*See pgs. 635-641 "Magnetic Circuits and Transformers", MIT EE Staff John Wiley & Sons.

**Six "Y" parameters plus an open circuit impedance.

hypothesized that the "Y" parameters must be measured/determined with an accuracy and precision that was not realized and would probably not be practical even with more sophisticated procedures.

By the time this conclusion was reached, only limited resources and time remained. In order to temporarily overcome this problem, a procedure was implemented using a file containing measured primary driving point admittances (for specified level of secondary loading). This allowed predictions to be made on the feeder for the specified loading implied in the transformer file being used. Prediction "down to" the secondary would be a second manual step using again measured voltage transfer characteristics. This "two step" procedure was not in any way deficient as an approximation but did require manual interaction, and did not admit random "MONTE CARLO" procedures.

Synopsis of "Inter Phase" Transformer Modeling Activities

During the approximately one year interval between the conclusion of PHASE I contract effort and the commencement of this PHASE II contract, the General Electric Co. sponsored extensive response type measurements on distribution transformers, single phase power transformers, and various single core three phase transformers. These measurements were made at Corporate Research and Development with the cooperation of the Niagara Mohawk Power Company [NMPC] who provided access to the various transformers, and Mobile Radio Department, both General Electric operations. The measurements included bi-directional driving point admittance and voltage transfer ratios as a function of frequency (limited range) and various loadings (primary and secondary). It was from these measurements that adequacy of a single RLC lumped

parameter model for frequencies up to, say, 50-100 kHz, was suggested.

Synopsis of PHASE II Transformer Modeling Activities

Still faced with need and solution for an adequate transformer model, this activity was continued as Task 4 in the PHASE II contract. Four modeling approaches were considered:

1) All "Y" parameter model (as in PHASE I) with greater measurement precision.

2) "Y" parameter derived algebraic model

3) Table look-up of measured responses

4) Simplified lumped parameter model

Approach 1) was rejected because of the reasons cited previously and the uncertainty whether sufficient measurement precision could be obtained. Approach 3) was rejected (after 2 and 4 appeared feasible) because of the large number of interpolating dimensions (frequency, magnitude of loading, primary and secondary, phase of loading) and the prohibitively large amount of measurements required.

During the above deliberations, an algebraic basis was developed, corresponding preliminary measurements were made, and a computer program written to establish the feasibility of approach 2). Appendix 3 contains analyses relevant to this approach. The key difference between this approach and the "Y" parameter approach 1) was to assume that:

a) at frequencies of interest, distribution transformers are electrically symmetric (two secondary windings),

b) a balanced secondary load (no basis exists for assuming otherwise for purposes of PLC propagation modeling),

and to replace some of the "Y" parameters with other more readily and algebraically less sensitive measurements such as open circuit voltage

transfer ratios. As a result of laboratory measurements on several transformers, a set of derived parameters was selected which were relatively insensitive to transformer construction. The resulting algebraic model was implemented in a temporary test (computer) program which very successfully predicted responses corresponding to measurements. The feasibility of this approach appears to be proven. Like "Y" parameters, these derived parameters would be frequency and KVA dependent, but independent of loading, and would predict bi-directional driving point admittances and voltage transfer ratios. It does not appear that this model has any frequency limitations (other than measuring them at such frequencies). It does not, of course, represent a physical model.

Measurements (see last page of Appendix 3) made during the inter phase interval strongly suggested that a simple RLC lumped parameter model might be adequate for frequencies limited to, say, less than 50-100 kHz. A test computer program was written to evaluate the model and quite successfully duplicated the measurements cited above. On this basis, subject to the limitations on upper frequency, the simplified lumped parameter model also became a viable contender. It should be noted that it is realized a more complicated lumped parameter model could be derived to extend this frequency limitation, but doing so at this time, is not considered necessary.

Measurement Technique for Phase II

In determining the performance of a transformer at PLC frequencies, four characteristics are significant for the purpose of this program and these include; voltage transfer ratio from primary to secondary [V_s/V_p],

and from secondary to primary [V_p/V_s], along with the admittance looking into the primary [Y_{pri}] and the admittance looking into the secondary [Y_{sec}] from line to line. All of these quantities must be known as a function of primary and secondary loading and the frequencies of interest.

Several distribution transformers were brought into the laboratory from the NMPC facility at Seneca St. in Schenectady, NY. A test set-up was developed that provided the desired data with sufficient accuracy and in an expeditious manner. Figure 1 is a block diagram of the test set-up showing the equipment configuration used in all of the measurements. Terminals 1 and 2 always provide the transformer excitation and terminals 3 and 4 are used to monitor either voltage or current.

The Quantech Wave Analyzer is used solely to provide a ramp function, and this ramp function linearly varies the frequency of the Lin/Log Sweep Generator from 3 to 100 kHz and, in addition, is used to drive the x-input of the x-y plotter. The period of the ramp is a front panel adjustment on the Quantech and is set for 500 sec. so as to assure adequate response time for the measurement equipment. The attenuator shown on the VCG input of the Lin/Log Sweep Generator adjusts the frequency range of the sweep generator.

The output of the sweep generator drives the Bogen power amplifier which has an impedance matching transformer on its output. Thus, the output can be either floating as when driving the secondary line-to-line, or have one side tied to ground as when driving the primary.

The Hewlett-Packard Gain Phase Meter is used to measure the magnitude and phase of a voltage-to-voltage or a current-to-voltage ratio where the A input is always the reference and is always a

Figure 1

Test Set-Up for Transformer Measurements

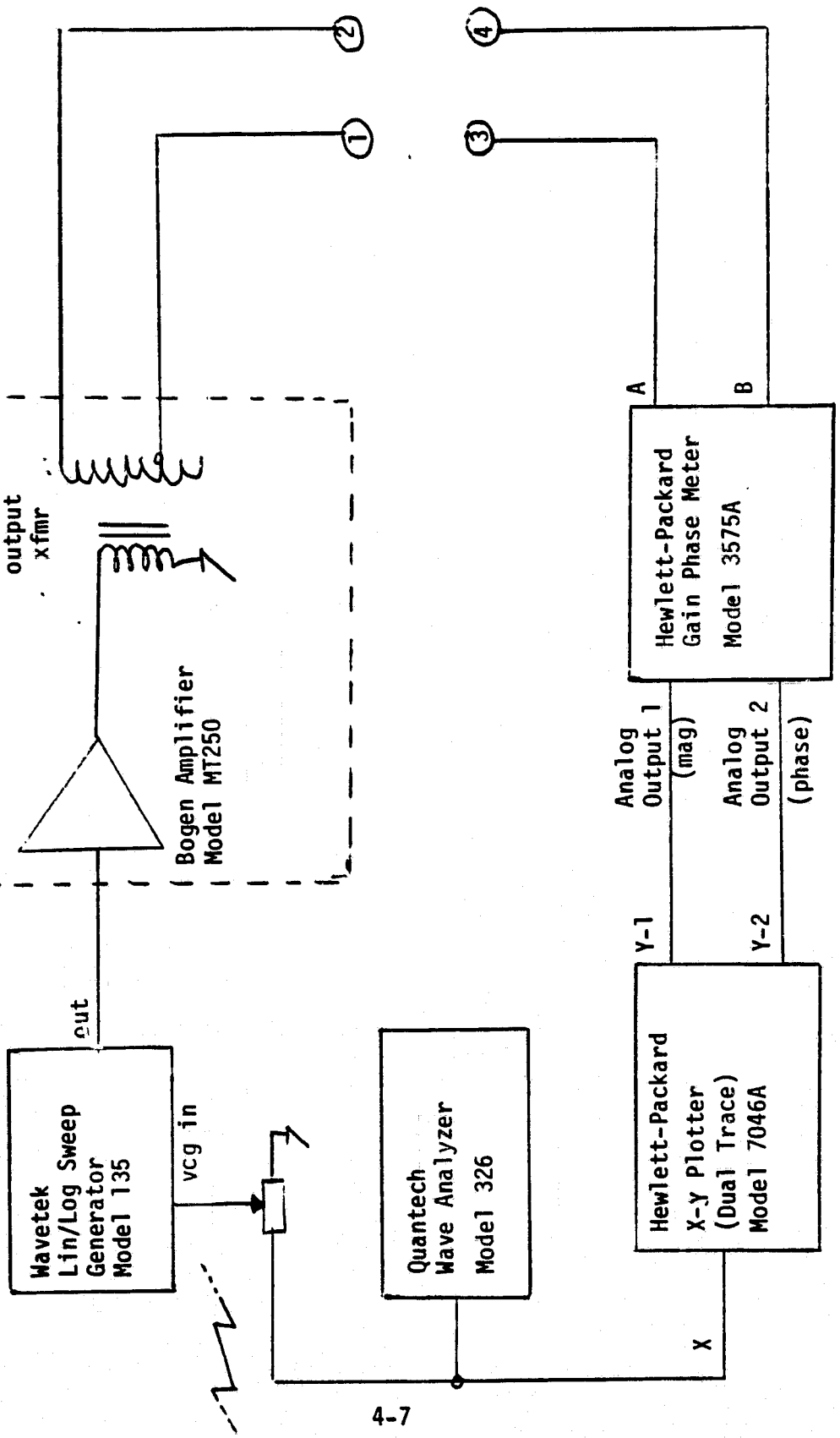

voltage. The response time of the analog outputs of the gain phase meter is set to 0.02 sec. by putting the frequency range switch in the 100 Hz-1mHz position. There is no digitizing involved in generating the analog outputs.

The 2 analog outputs of the gain phase meter, magnitude and phase, are used as inputs to the two y-drives of the x-y plotter. Because of the skew on the two pens of the plotter, there is a frequency error between the magnitude and phase of about 500 Hz [1 small division on the graph paper with the 100 kHz range]. That is, when a magnitude value is read at a certain frequency, the corresponding phase value should be read at a frequency which is 500 Hz less.

Figure 2 shows the connections to terminals 1-4 of Fig. 1 which are used to measure the magnitude and phase of the voltage transfer ratio from primary to secondary, V_s/V_p, of the subject transformer.

Figure 3 shows the connections used in obtaining V_p/V_s.

Figure 4 shows the connections used in determining the admittance looking into the primary, Y_{pri}, as a function of secondary load, R_s.

Figure 5 shows the connections for measuring the admittance looking into the secondary, Y_{sec}, as a function of the primary load, R_p.

The magnitude tolerance of the ratio (B/A) configuration is given as $\pm$ 1.5 db for the gain phase meter with input amplitudes of greater than -64 dbv [$\approx$ 0.6 mv] and $\pm$ 2.5 dbv with input amplitudes of less than -64 dbv. Similarly, the phase angle error is not more than 10° in our frequency range with input amplitudes of greater than -44 dbv [$\approx$ 6 mv]. It was judged that these tolerances were in keeping with the scope of this program.

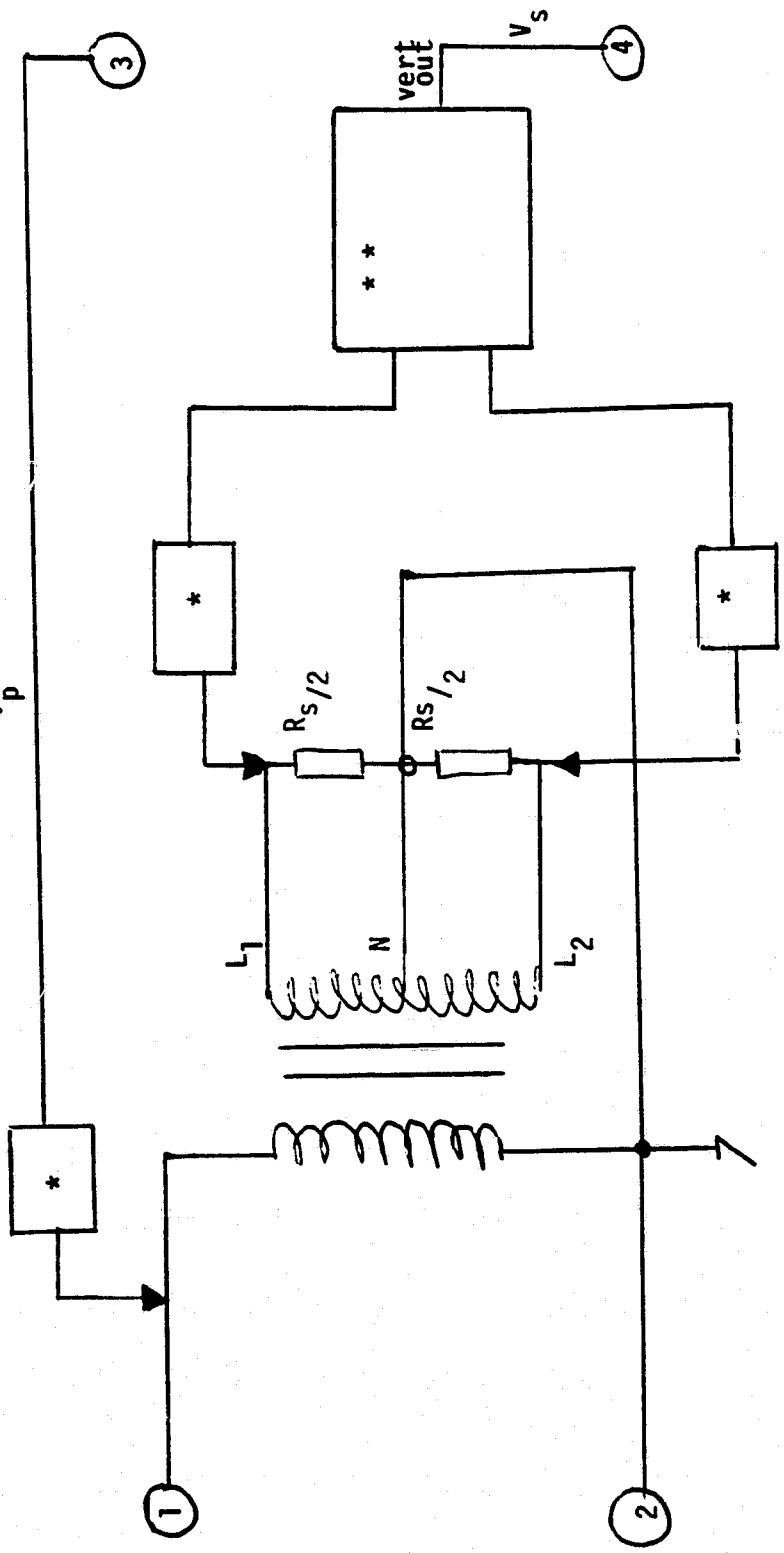

Figure 2

Measurement of V_s/V_p

*Tektronix Probe
Model 6054A 10X

** Tektronix 7603 Oscilloscope with
7A12 Dual Trace Amplifier
[Used as a Differential Amplifier]

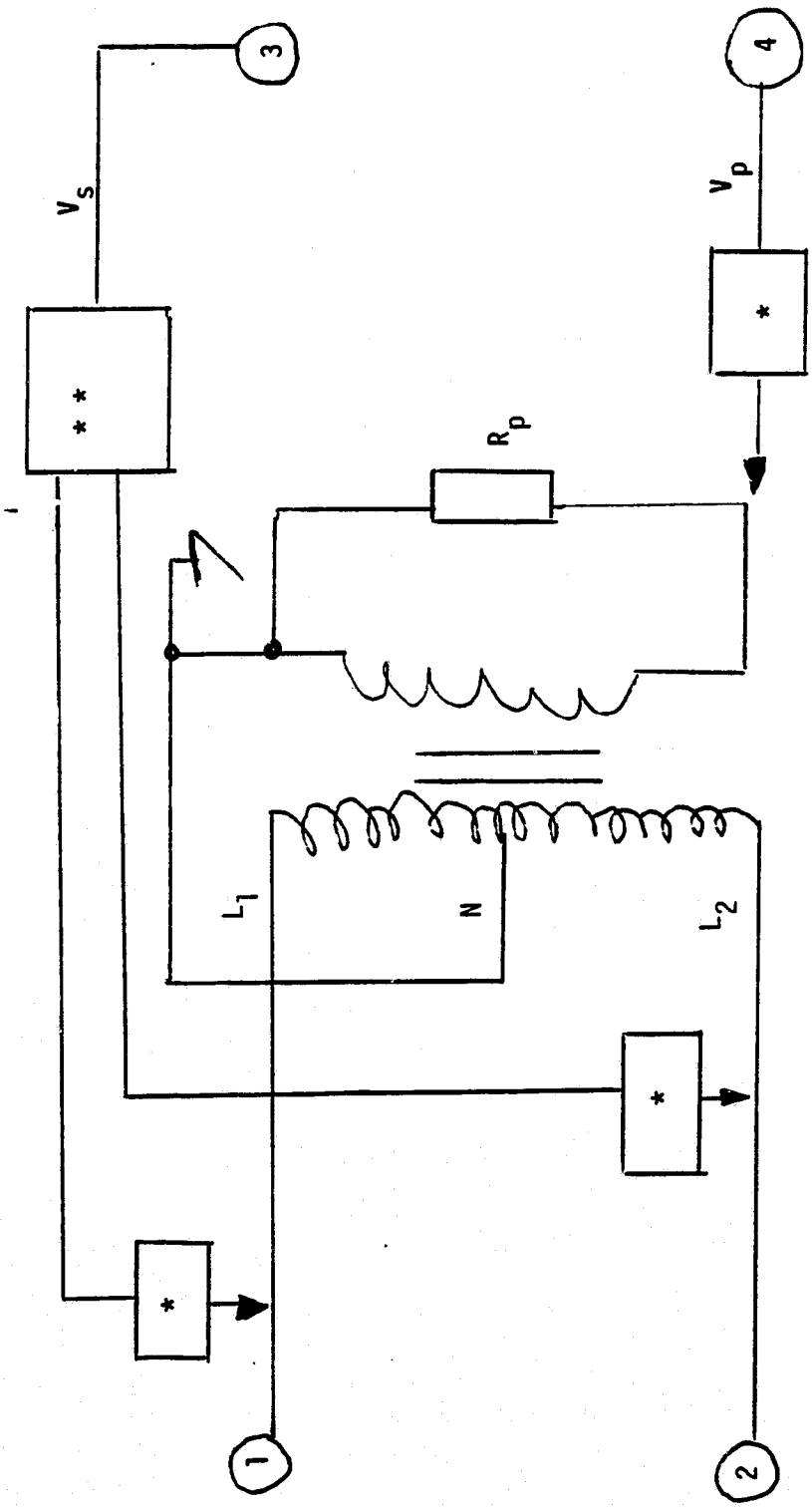

Figure 3
Measurement of V_p/V_s

*)See Fig. 2
**)

Figure 4
Measurement of Y_{pri}

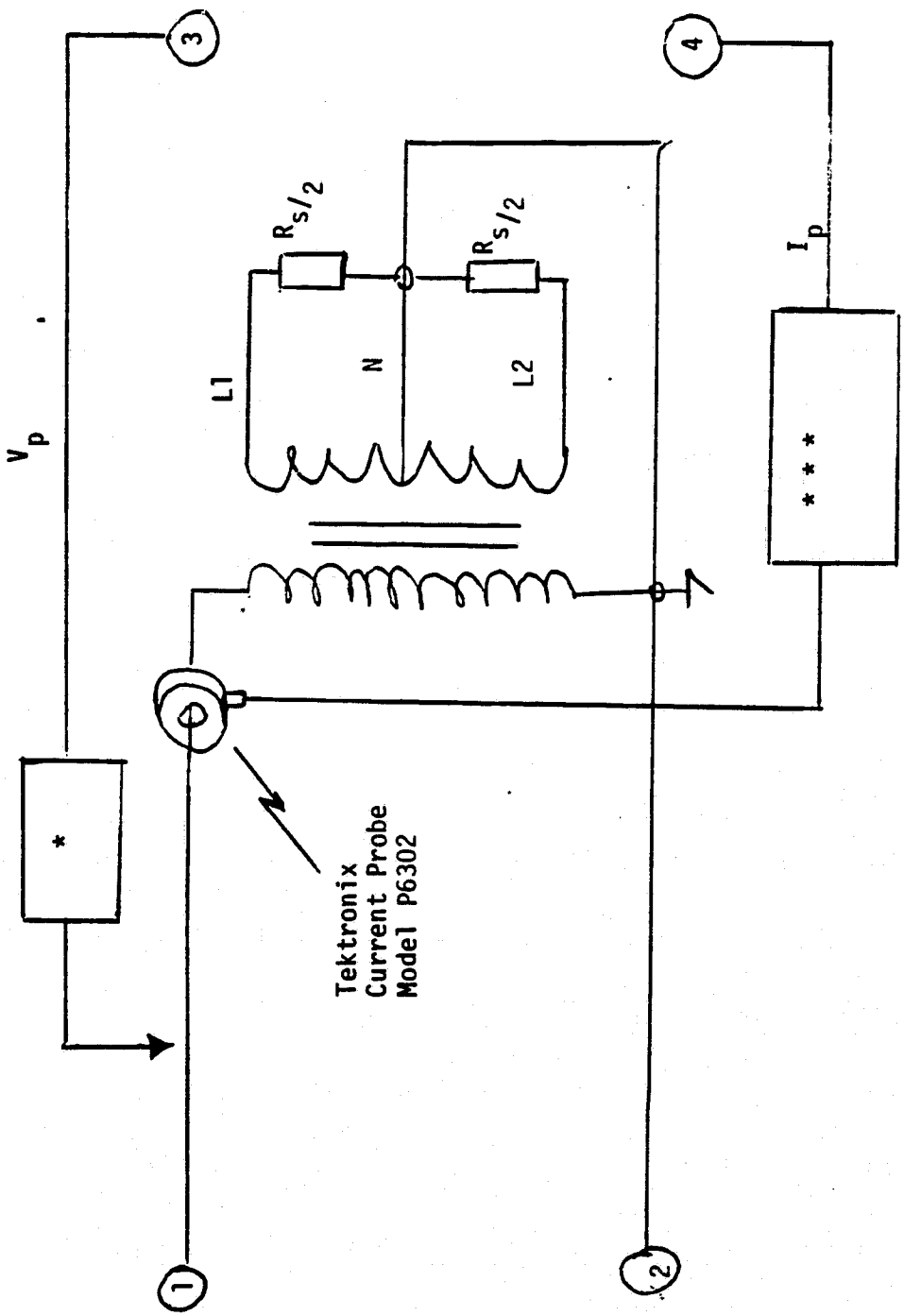

* See Fig. 1

***Tektronix Current Probe
Amplifier, Model AM503

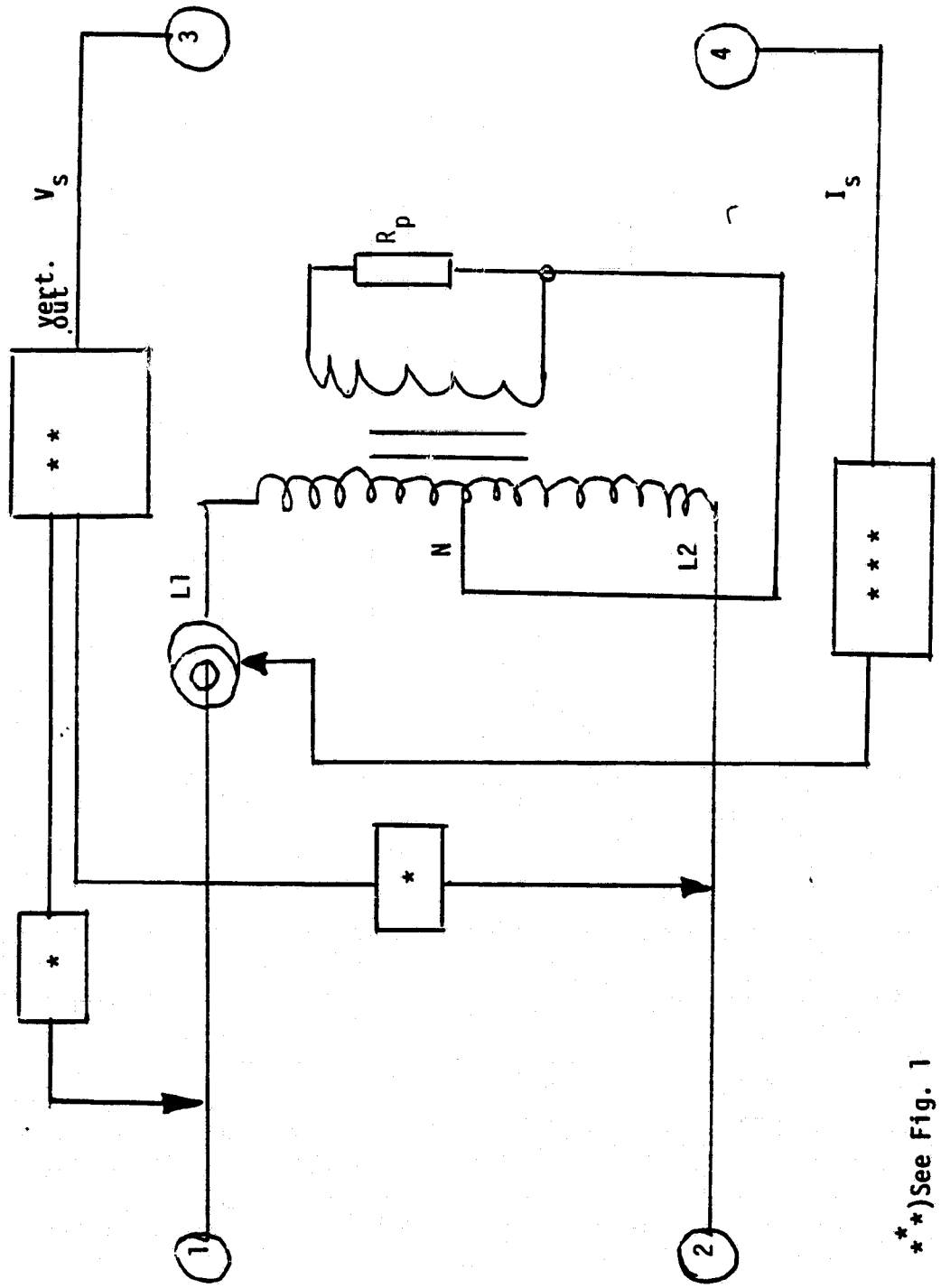

Figure 5
Measurement of Y_{sec}

* *)See Fig. 1
*** See Fig. 4

Transformer Construction

Two types of transformer construction are in common use, and these are classified as core type and shell type. When the magnetic circuit takes the form of a single ring encircled by two or more groups of primary and secondary windings distributed around the periphery of the ring, we have a core type transformer. A simple core-type transformer is shown below.

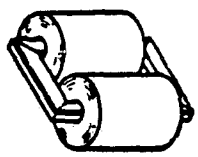

The term "core type" implies that the coils are cylindrical and concentric with an outer winding over an inner winding.

When the primary and secondary windings take the form of a common ring which is encircled by two or more rings of magnetic material distributed around its periphery, we have a shell type transformer. A simple shell-type transformer is shown below.

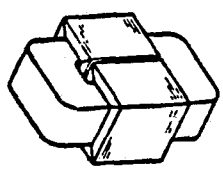

The term "shell-type" denotes large pancake coils which are stacked or inter-leaved to make primary-secondary groups.

The characteristic features of the core-type transformer are a long mean length of magnetic circuit and a short mean length of windings and vice versa for the shell-type. Apparently the choice of which

construction to choose is largely a matter of manufacturing facilities and individual preference.

According to the distribution transformer people at General Electric, in the 10-100 kva distribution transformer range, General Electric Company and RTE make core types and all other domestic manufacturers make shell types.

Both types were measured during the course of this program because it was initially felt that there might be some significant difference in their performance at PLC frequencies. No such difference was observed.

Transformer Symmetry

The assumption has been made in the transformer modeling program that the two halves of the secondary are symmetrical [and have balanced loads] so that we can, in effect, deal with a two winding transformer.

Measurements were made to justify that assumption. The results of these measurements are shown in Figs. 6-9. Figure 6 shows the voltage transfer ratio, V_p/V_s, of a 25 kva General Electric transformer (core-type], when the secondary is driven L1-N in one case and L2-N in the other case. This measurement is made essentially as shown in Fig. 3, with R_p = 11Ω, except that the differential amplifier of Fig. 3 is not needed here. Figure 6 shows that the magnitude of V_p/V_s at a frequency of 5 kHz differs by about 4.5 db. Beyond 50 kHz, the two magnitudes tend to converge. Because of the way the measurement was made, the phase angle associated with V_p/V_s is 180° different in each case. The phase angle difference at 5 kHz (neglecting the 180°) is about 3°, and at 50 kHz is about 6°. The maximum angular difference occurs at about 65 kHz and is on the order of 24°.

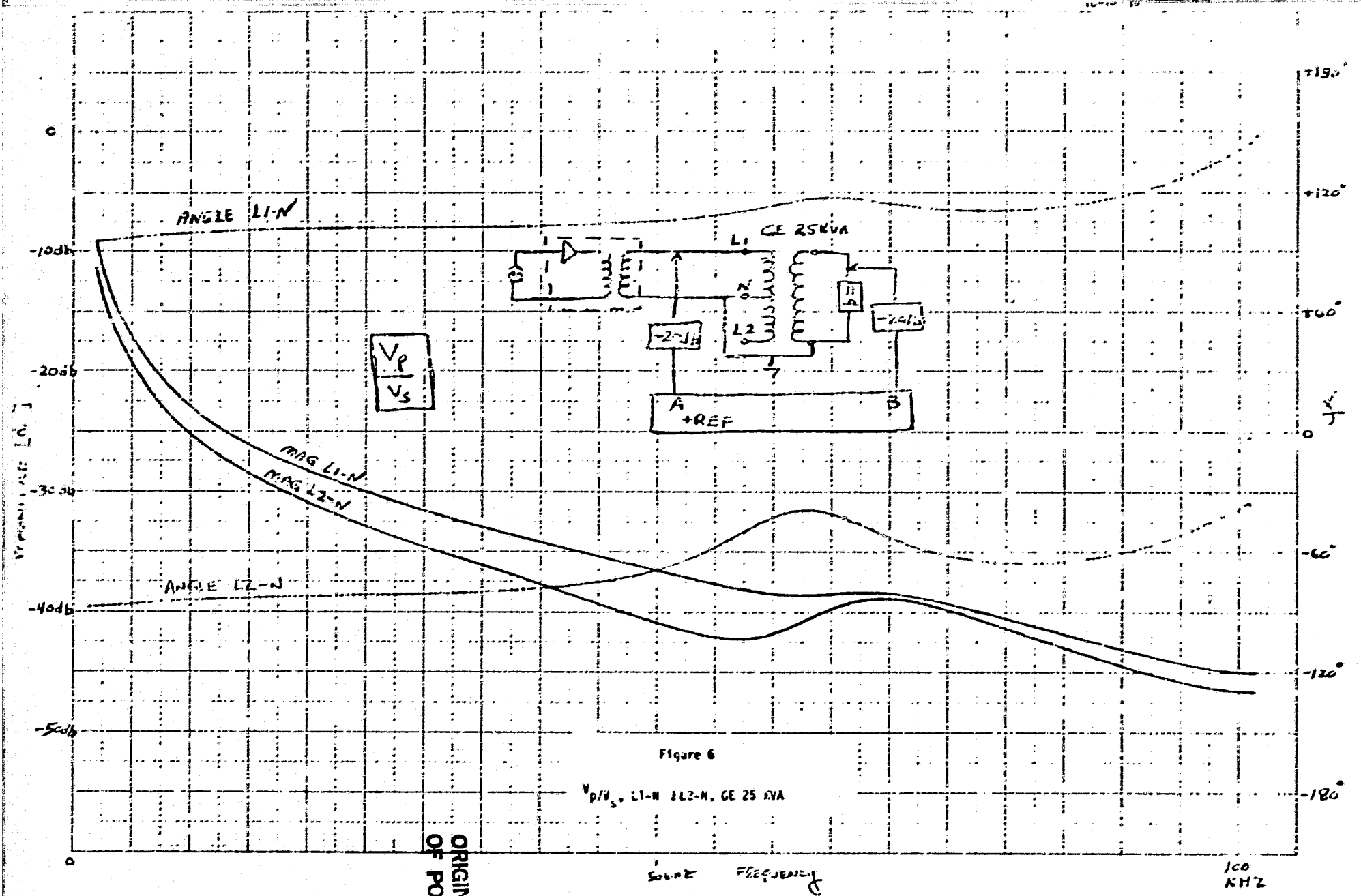

Figure 6

V_p/V_s, L1-N & L2-N, GE 25 KVA

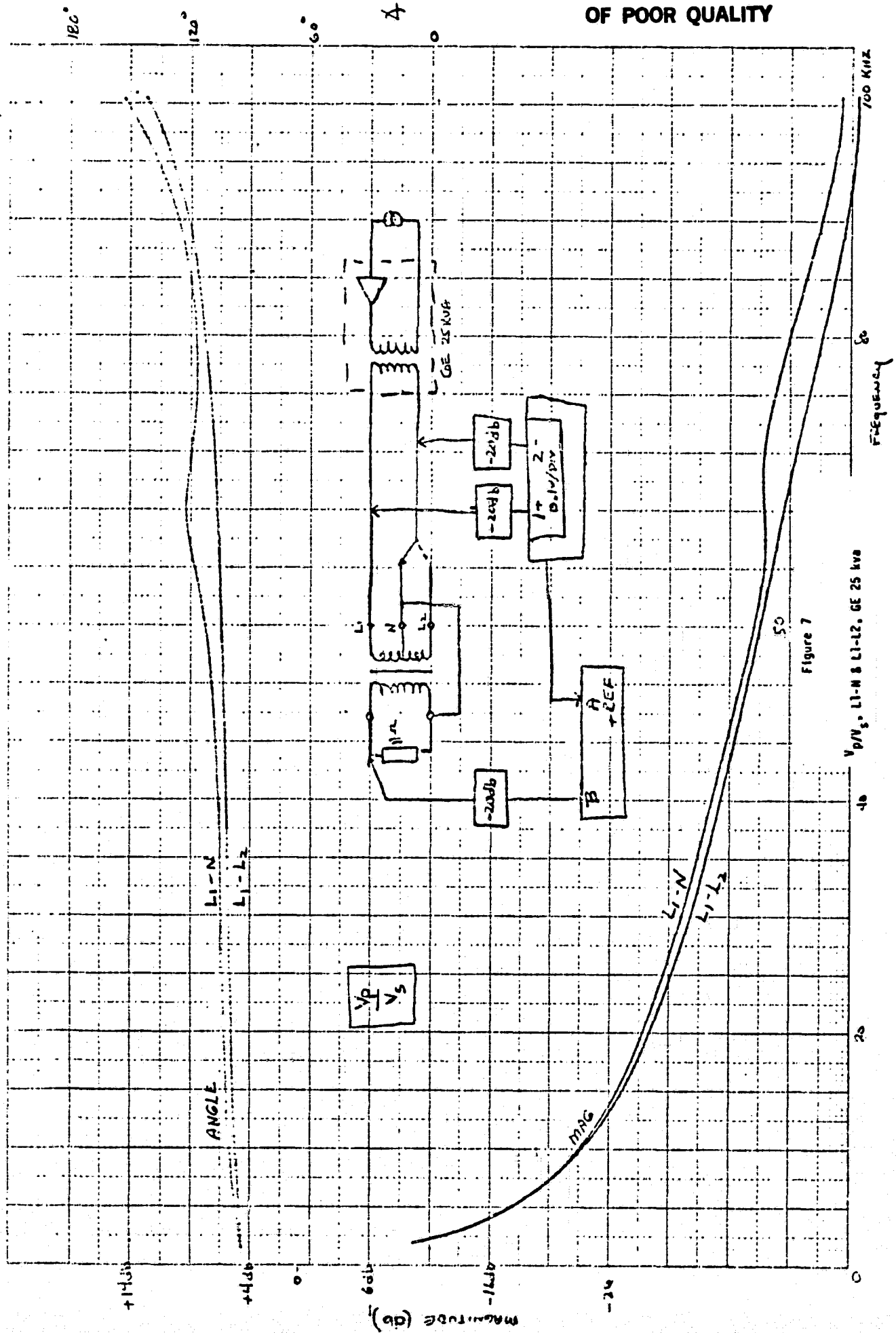

Figure 7

V_p/V_s, L1-N & L1-L2, GE 25 kva

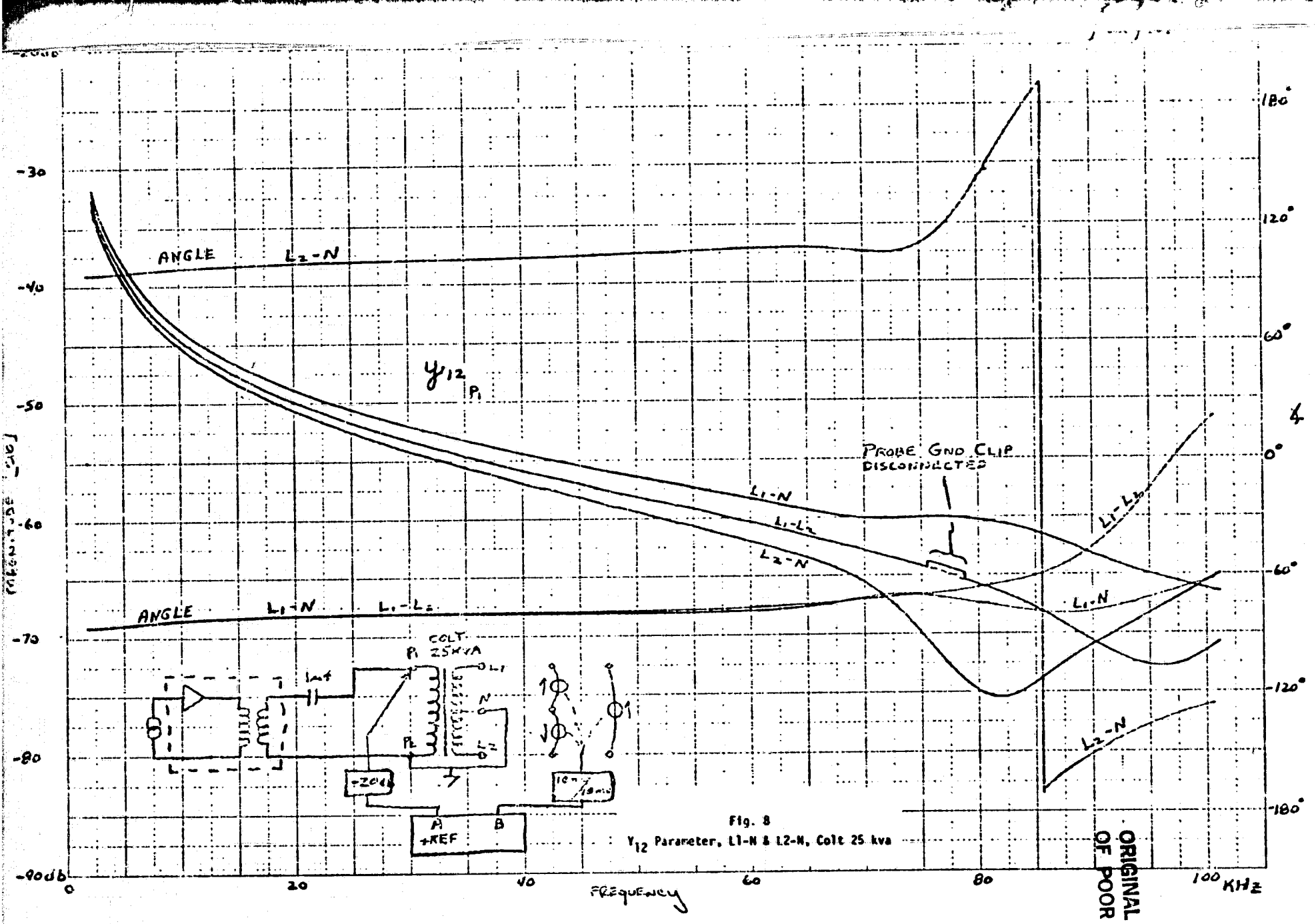

Fig. 8
Y_{12} Parameter, L1-N & L2-N, Colt 25 kva

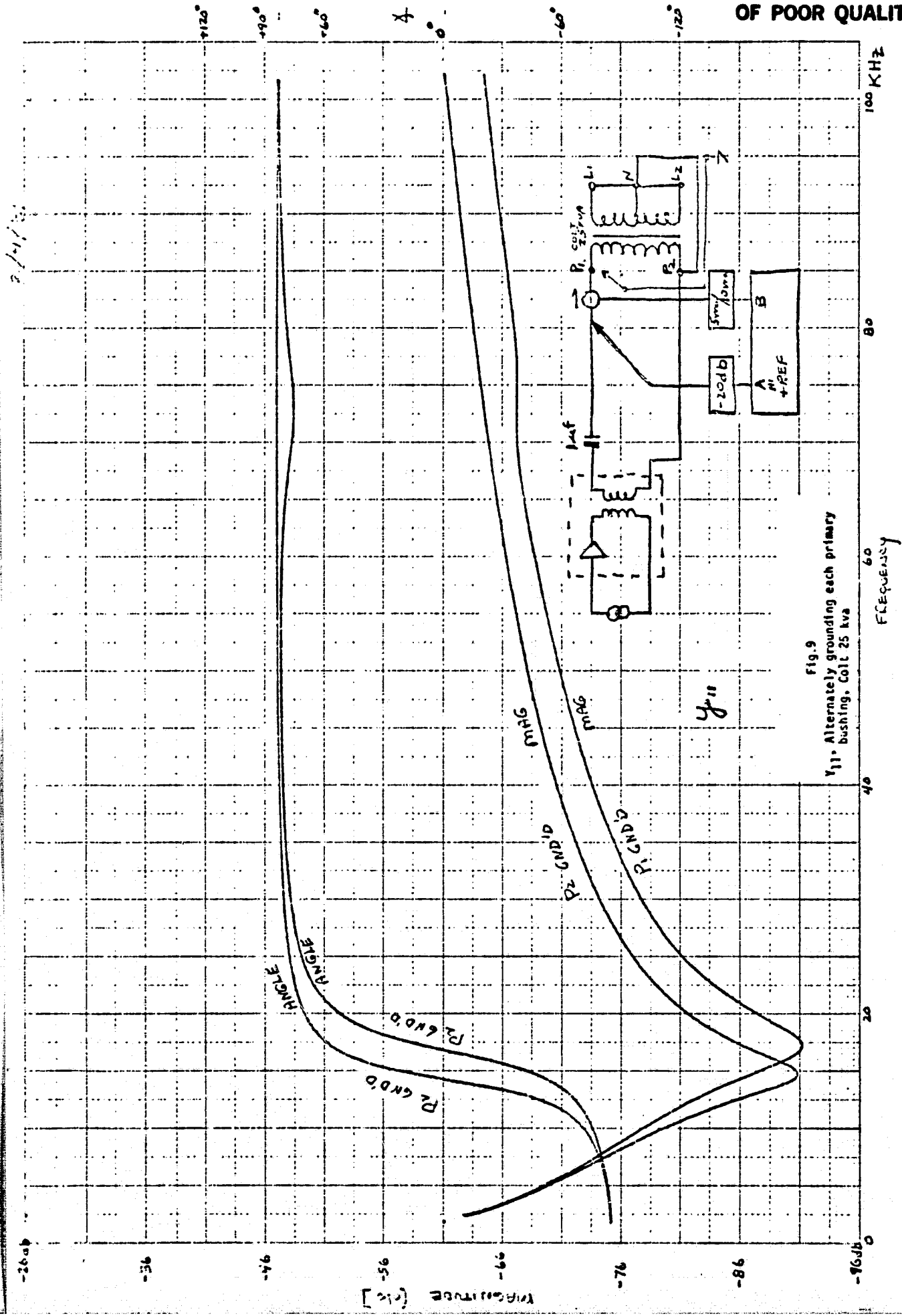

Fig.9
Y_{11}, Alternately grounding each primary bushing, Coil 25 kva

Figure 7 shows V_p/V_s for the 25 kva General Electric transformer again, but this time comparing the case of driving 1/2 of the secondary as opposed to driving the full secondary. It can be seen that, up to about 60 kHz, the difference both in magnitude and phase is trivial.

Figure 8 shows the y_{12} parameter of a 25 kva Colt transformer (shell type) with the secondary current measured in the L1-N leg and the L2-N leg. The y_{12} parameter is defined as the transfer admittance looking into the primary with the secondary shorted and given by the formula:

$$y_{12} = \frac{I_{sec}}{V_{pri}} \quad \text{[sec shorted]}$$

In Figure 8, I_{sec} was measured in the L1-N leg, in the L2-N leg, and in the L1-L2 leg. Again, in the frequency range up to 50 kHz, the maximum difference in magnitude of y_{12} did not exceed about 3 db and the angular difference did not exceed about 3°. No attempt will be made to explain the performance of y_{12} at frequencies above 60 kHz.

Figure 9 shows the behavior of y_{11} of a 25 kva Colt transformer when each of the primary bushings [2 bushing transformer] are connected to the secondary center tap in turn. The term y_{11} is defined as the input admittance looking into the primary with the secondary short circuited and is given by the equation

$$y_{11} = \frac{I_{pri}}{V_{pri}} \quad \text{[sec shorted]}$$

It can be seen that the point of minimum magnitude of y_{11} has changed frequency by about 2500 Hz with a corresponding change in the point where the phase angle goes through zero degrees.

Finally, the errors incurred as a result of assuming symmetry in the two halves of the secondary of a distribution transformer are of the same order as those of the instrumentation previously discussed, and again, were judged to be in keeping with the scope of this program.

Response Measurements

Response measurements were made on the 25 kva Colt transformer and the 25 kva GE transformer, referred to as the laboratory transformers, and the results of these are shown in Figs. 10-17. These curves represent the kind of information the computer model must be capable of generating for each of the transformers associated with the feeder section to be modeled. These measurements were made of unenergized, as regards 60 Hz power, transformers and with simulated resistive primary and secondary loading.

In regard to secondary loading, most of the response measurements were made with the distribution transformers at about 1/2 load. The value of load resistor (R_L) for full load is determined by the formula

$$R_L = \frac{V^2_{sec(L-L)}}{kva}$$

which, for a 25 kva transformer, becomes $R_L = \frac{(240v)^2}{25{,}000va} = 2.3$ ohms.

Primary loading of a distribution transformer in the PLC frequency range is a function of many things, including type of construction, i.e., overhead or underground, number of other transformers on the primary, the secondary loads of other transformers on the primary, power factor convection capacitor banks, etc. Our experience has shown that the magnitude of the primary impedance varies from about 10 ohms [for some underground distribution] to several hundred ohms

ORIGINAL PAGE IS
OF POOR QUALITY

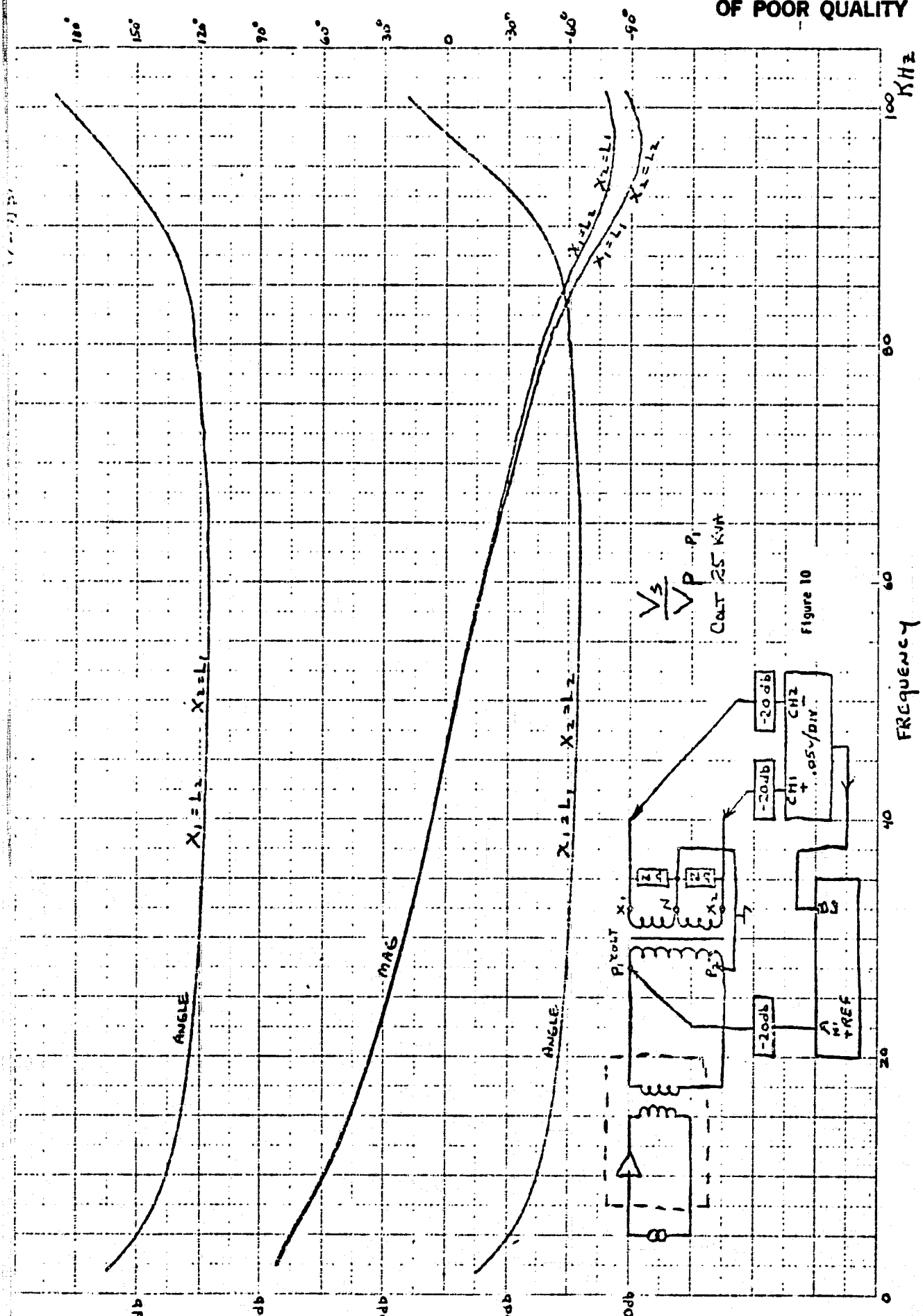

Figure 10

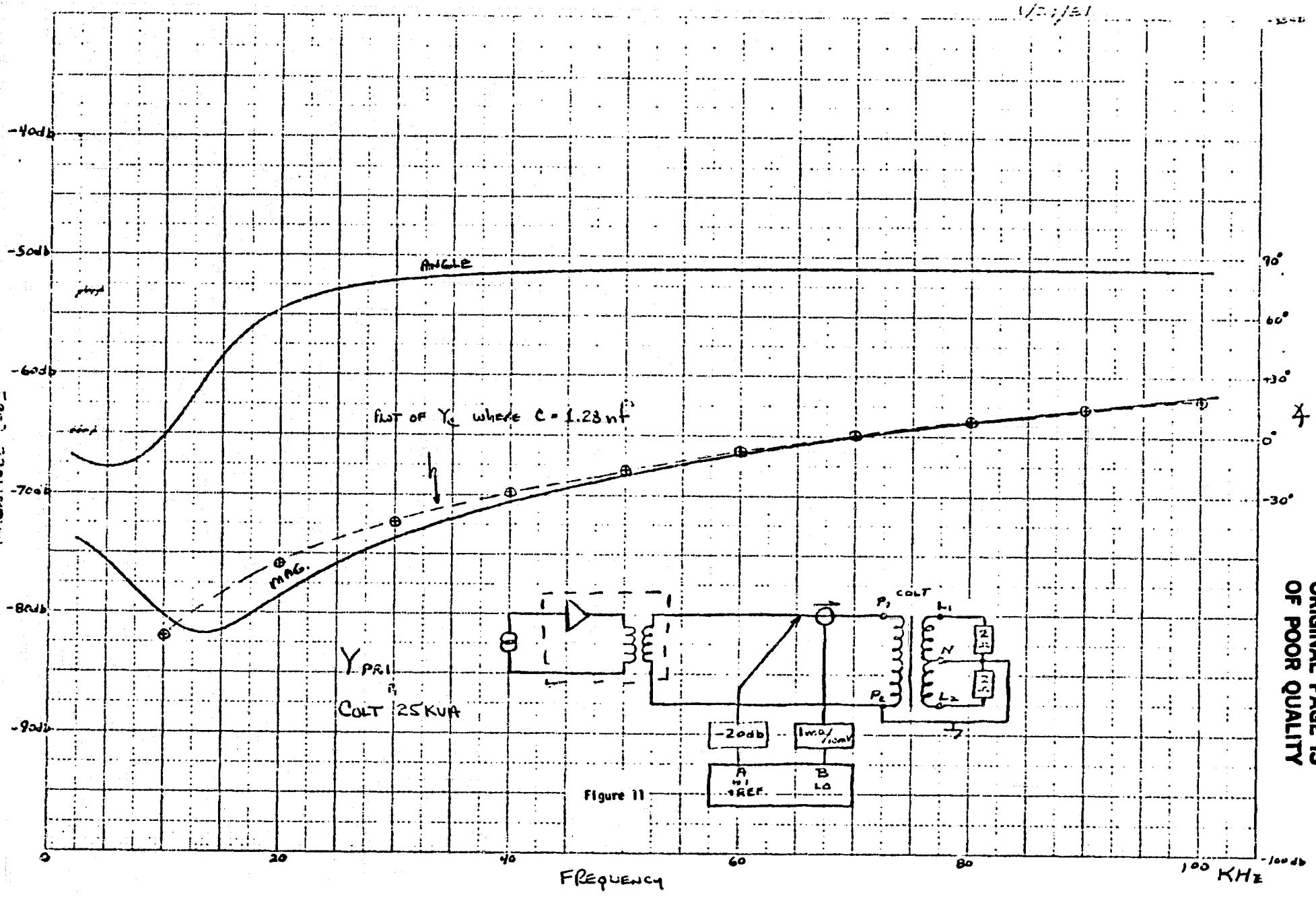

Figure 11

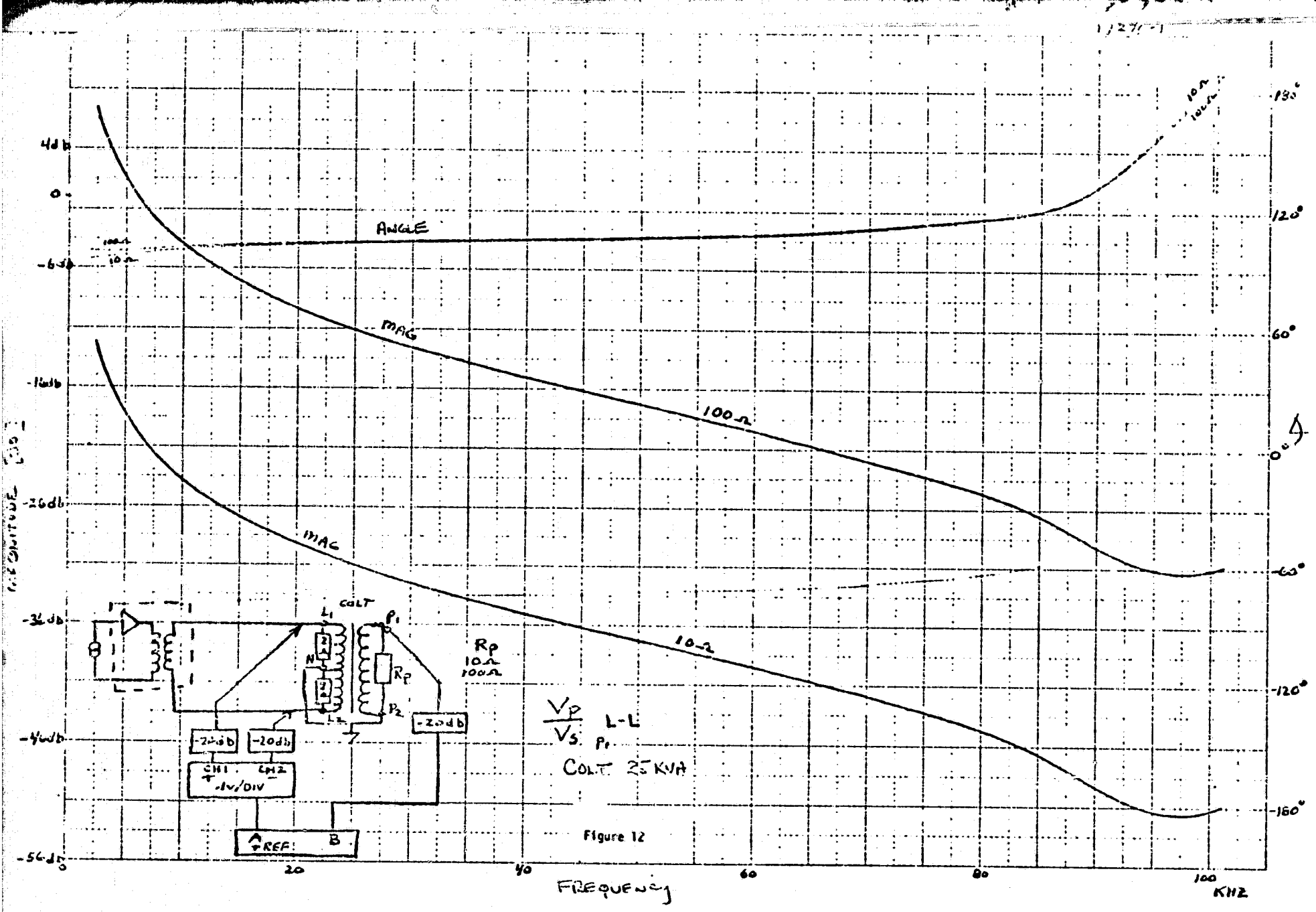

Figure 12

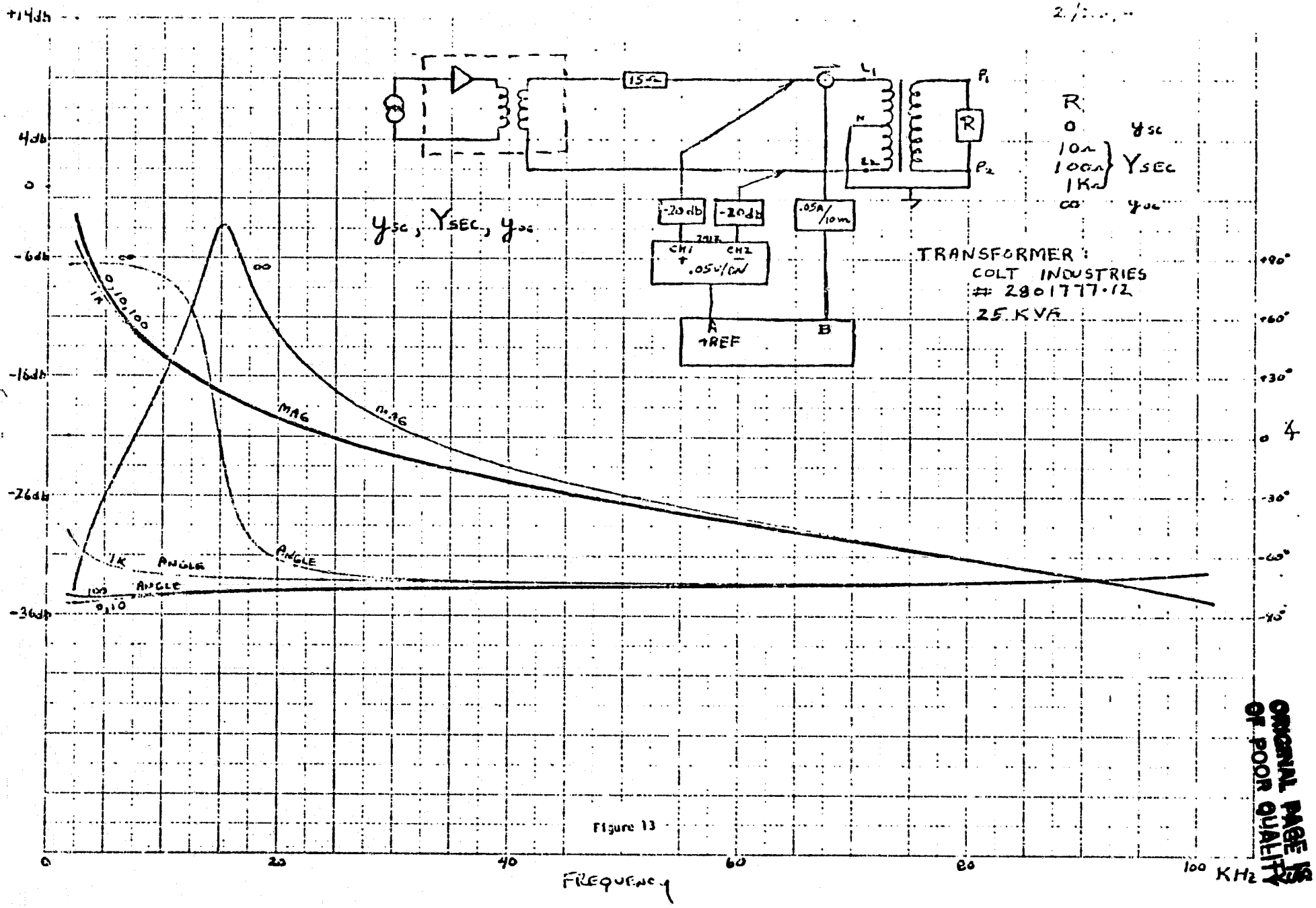

Figure 13

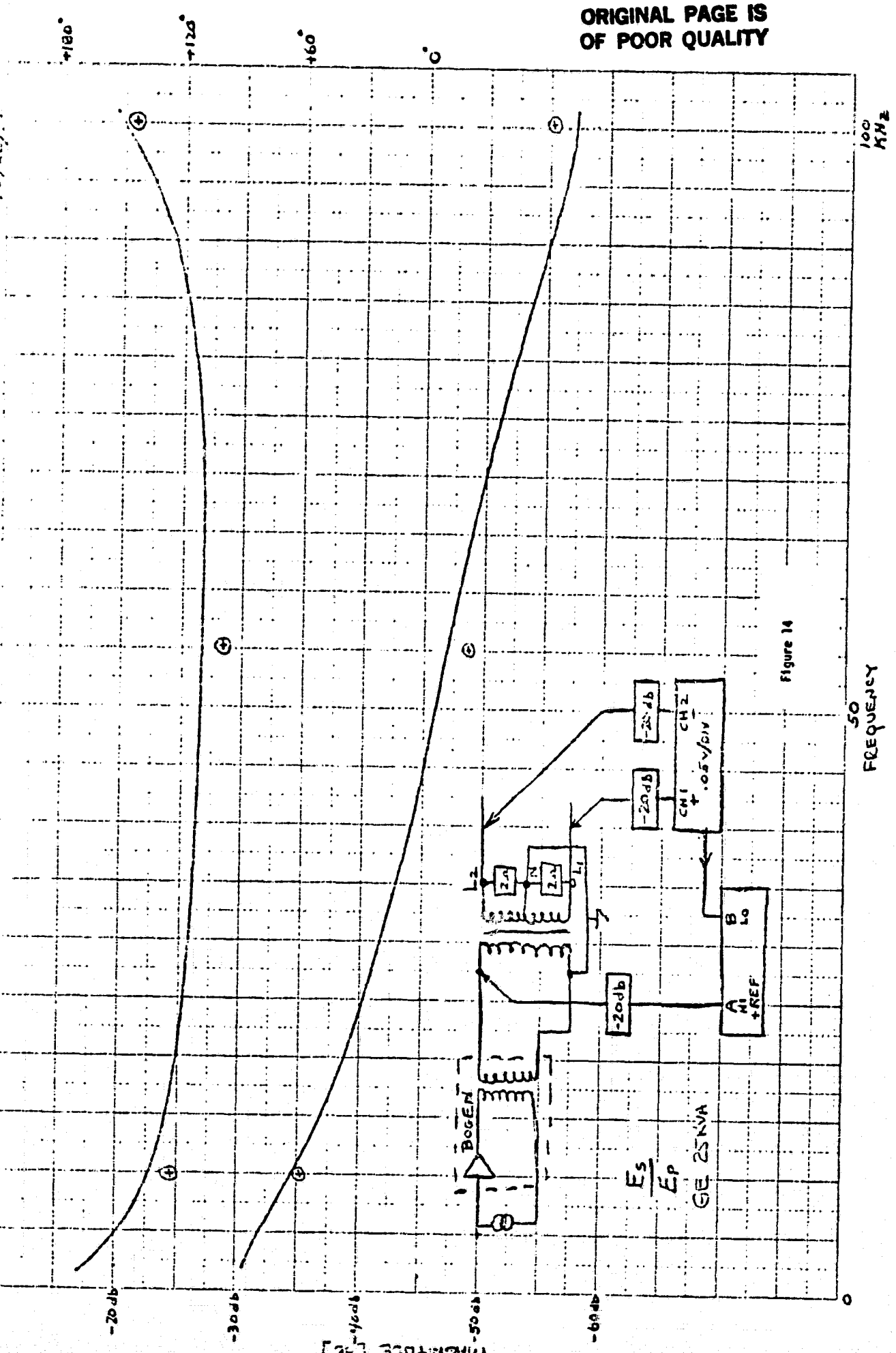

Figure 14

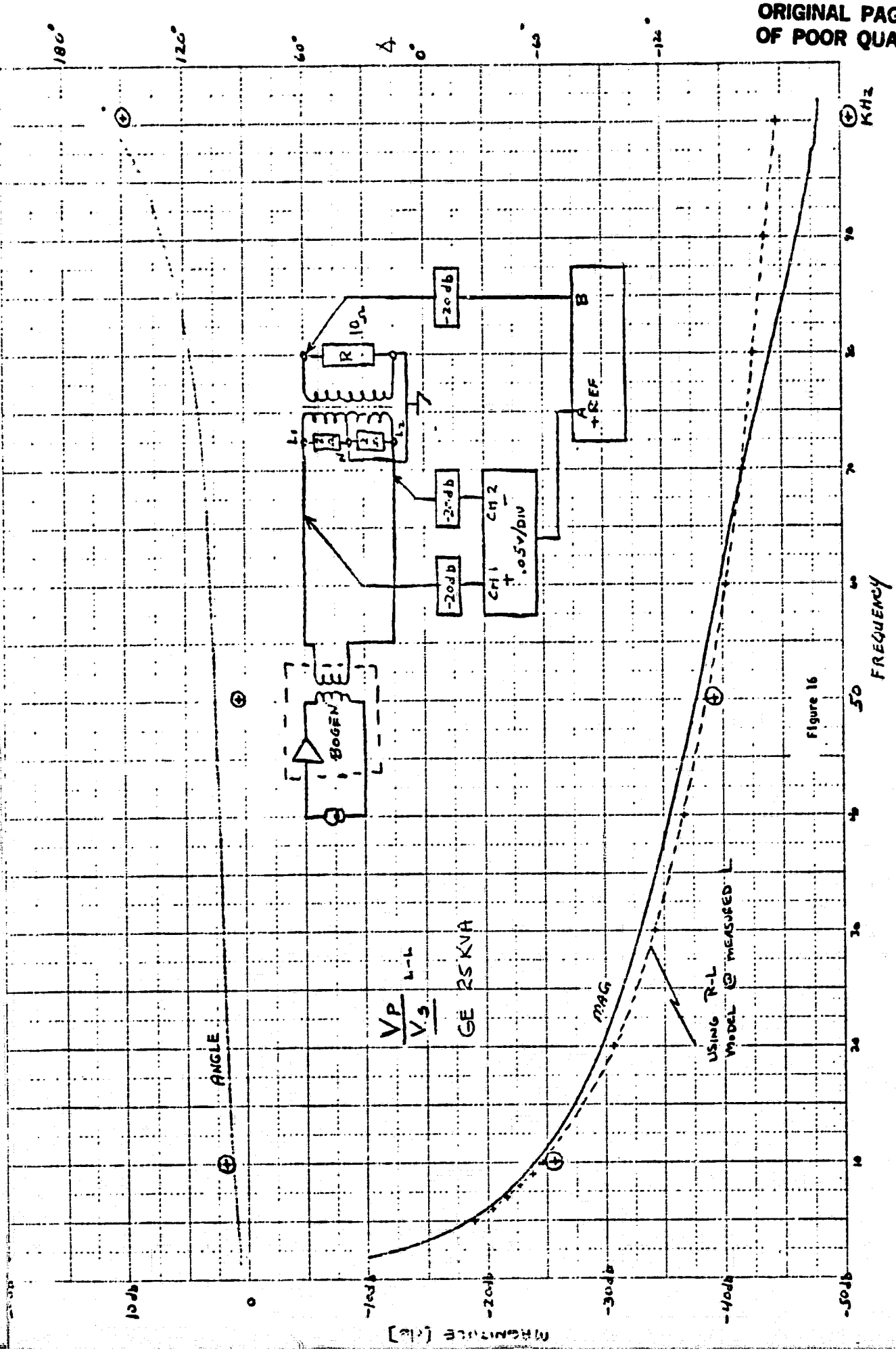
180°
120°
60°
0°
-60°
-120°
KHz
FREQUENCY
MAG
ANGLE
USING R-L MODEL @ MEASURED
$\frac{V_P}{V_S}$ L-L
GE 25 KVA
BOGEN
R
10Ω
-20db
-20db
-20db
CH 1
CH 2
.05V/DIV
A
+REF
B
-10db
0
-10db
-20db
-30db
-40db
-50db

Figure 16

ORIGINAL PAGE IS
OF POOR QUALITY

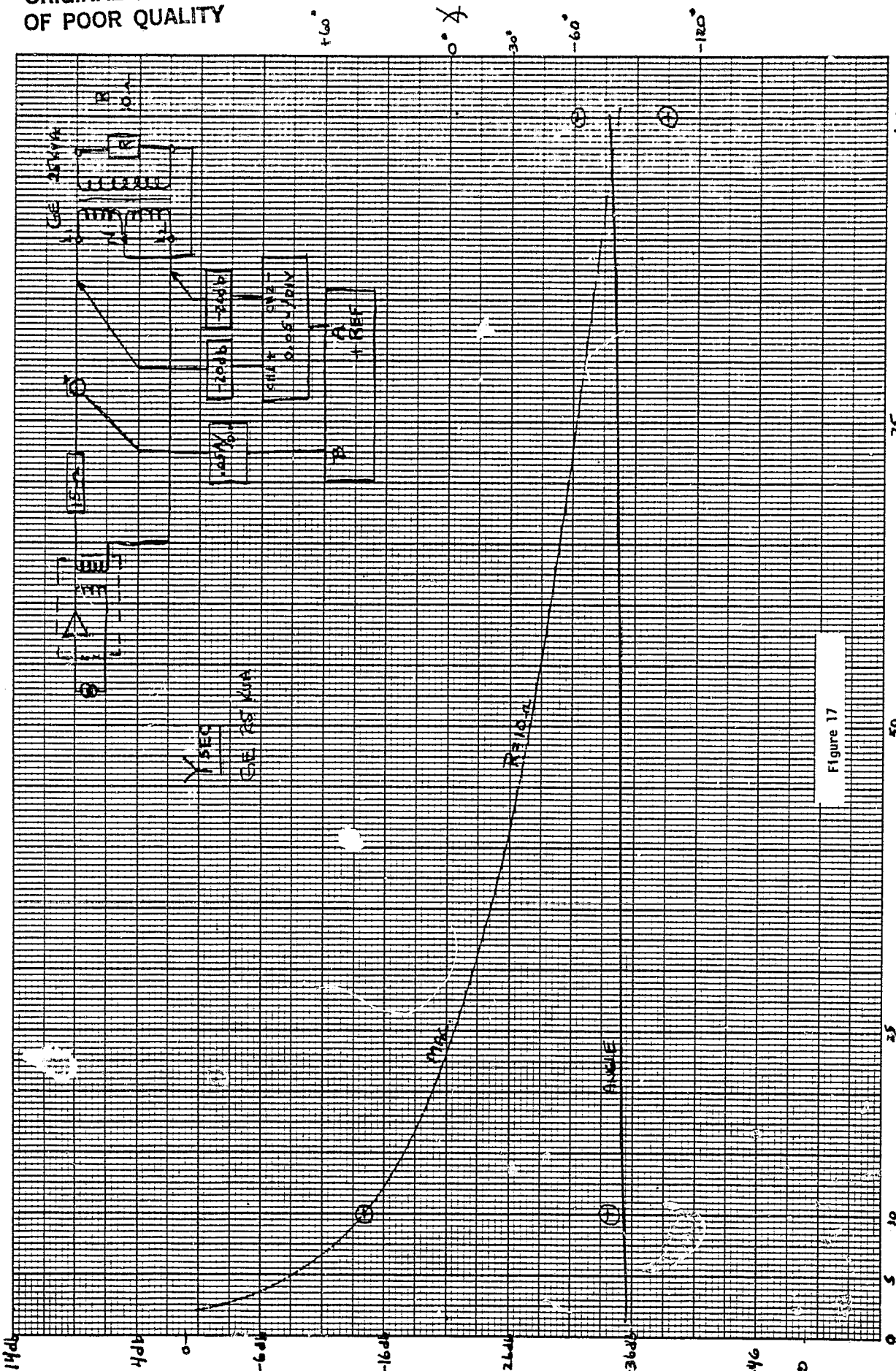

Figure 17

[for some overhead distribution].

Referring to Fig. 10, this shows the magnitude and phase of the voltage transfer ratio from primary to secondary, $\frac{V_s}{V_p}$. It can be seen that at about 5 kHz, $|\frac{V_s}{V_p}|$ is approximately -33 db which is an attenuation nearly equal to the transformer turns ratio of 31.75 [20 log $\frac{1}{31.75}$ = -33.04 db]. With increasing frequency $|\frac{V_s}{V_p}|$ decreases and in the frequency range from about 20 kHz to 60 kHz, this decrease is around 6 db/octave. The phase relation for $\frac{V_s}{V_p}$ is nearly 0° [or 180° depending on the measurement probe placement] at the lowest frequency and then becomes about -66° at 50 kHz, indicating significant reactive components.

The $\frac{V_s}{V_p}$ curves for the 25 kva GE transformer, Fig. 14, are almost identical to those for the Colt just described.

The Y_{pri} curves of Fig. 11 for the 25 kva Colt transformer exhibit a parallel resonance phenomenon at about 13.5 kHz. The minimum admittance [maximum impedance] that this 1/2 loaded transformer presents to the line is -82 db or 79μmhos. This corresponds to 12.6 kohms of impedance. The minimum impedance of this transformer is 1.26 kohms and occurs at the maximum frequency (100 kHz). At 100 kHz, Y_{pri} is almost completely capacitive and has been since about 50 kHz, as shown by the phase angle curve. A curve of capacitive susceptance has been superimposed on Fig. 11 to show that Y_{pri} becomes increasingly capacitive above 50 kHz and to show the general shape of capacitive susceptance curves when plotted on a linear frequency scale. The value of capacitance used to plot this curve was C = 1.28 nf. This capacitance susceptance curve can be used as an overlay template as

an alternative procedure to estimate the equivalent lumped capacitor.

Again, the Y_{pri} curves of Fig. 15 for the 25 kva GE transformer are very similar to those for the Colt.

Figure 12 shows the $\frac{V_p}{V_s}$ characteristic of the Colt transformer for a primary load resistance of 10 and 100 ohms. It can be seen that the magnitude curves of the $\frac{V_p}{V_s}$ ratio decrease at 6 db/octave up to about 50 kHz and further, that the differences between the magnitude curves for the 10 ohm and 100 ohm values of primary resistance is exactly 20 db over the entire frequency range. It will be shown later that the leakage reactance of the transformer essentially forms a constant current source when compared to the value of R_p transformed to the secondary and that therefore $\frac{V_p}{V_s}$ is proportional to R_p over a wide range of R_p.

The phase curves of $\frac{V_p}{V_s}$ indicate that V_p and V_s are about 90° out of phase up to 50 kHz and in phase [or 180° out of phase] at about 100 kHz.

Again, the $\frac{V_p}{V_s}$ curves of the 25 kva GE transformer, Fig. 16, are very similar to those for the Colt.

Figure 13 shows the Y_{sec} curves for the 25 kva Colt transformer for a variety of primary resistance [R_p] values ranging from 0 to infinity. There is minimal difference in the magnitude and phase curves when R_p varies from 0 ohms to 1000 ohms. When R_p = 0, there is a series resonance at 15 kHz. For values of R_p of 10,000 and 1000 ohms, the magnitude of Y_{sec} decreases at a 6 db/octave rate over the entire frequency range and the phase angle curve shows Y_{sec} to be mainly inductive over the frequency range. Inductive susceptance plotted on a linear frequency scale has the same form as an inverted

capacitive susceptance.

Figure 17 shows that, for R_p = 10 ohms, the Y_{sec} curves of the GE transformer and the Colt transformer are again similar.

Algebraic Model

From Appendix 3, the four equations of interest, assuming symmetrical secondary windings, line to line secondary measurements and drive, and balanced secondary loads are:

$$\frac{V_s}{V_p} = 2\left[\frac{2}{g_{12}} - \frac{Y_2}{y_{12}}\right]^{-1}$$

where Y_2 = admittance of load on each half of secondary

$g_{12} = \frac{V_s}{V_p}$ with secondary open-circuited

$y_{12} = \frac{I_s}{V_p}$ with secondary short circuited

$$Y_{pri} = \frac{I_p}{V_p} = \frac{1}{Z_{11}} + \left[y_{11} - \frac{1}{Z_{11}}\right]\left[\frac{Y_2}{Y_2 - \frac{2y_{12}}{g_{12}}}\right]$$

where $\frac{1}{Z_{11}} = \frac{I_p}{V_p}$ with secondary open-circuited

$y_{11} = \frac{I_p}{V_p}$ with secondary short-circuited

$$\frac{V_p}{V_s} = \frac{g_{21}}{1 + \frac{Y_1}{y_{11}}}$$

where Y_1 = admittance of primary load

$g_{21} = \frac{V_p}{V_s}$ with primary open-circuited

$$Y_{sec} = \frac{I_s}{V_s} = \frac{y_{12}}{g_{12}} + \frac{y_{12}g_{21}}{1 + \frac{Y_1}{y_{11}}}$$

The quantities g_{12}, y_{12}, $\frac{1}{Z_{11}}$, y_{11} and g_{21} were measured, as a function of frequency, for both the 25 kva Colt and GE transformers. Figures 18-27 show these characteristics.

For the 25 kva GE transformer, the value of $\frac{V_s}{V_p}$, Y_{pri}, $\frac{V_p}{V_s}$, and Y_{sec} were computed at several frequencies using the above four equations with data from Figs. 23-27. The results of these computations have been plotted on the measured characteristics of Figs. 14-17.

It can be seen that using the algebraic model with measured values of open and short circuited parameters provides reasonable correlation with actual measured performance. To use the algebraic model in feeder modeling work would require the measurements and storage of g_{12}, y_{12}, $\frac{1}{Z_{11}}$, y_{11} and g_{21} for all transformers of interest (at least some representative types) and at all frequencies of interest. This is a large amount of data to obtain and to store.

The advantage of this type of model is that it does not depend on a valid lumped parameter RLC model and therefore could be used at any frequency providing the necessary measurements were available.

Lumped Parameter Model

As mentioned in Appendix 3, earlier work by several parties had indicated that a simple "RLC plus ideal transformer" model could adequately represent distribution transformers in the frequency range of 5-50 kHz, again assuming electrically symmetrical secondaries and balanced secondary loads.

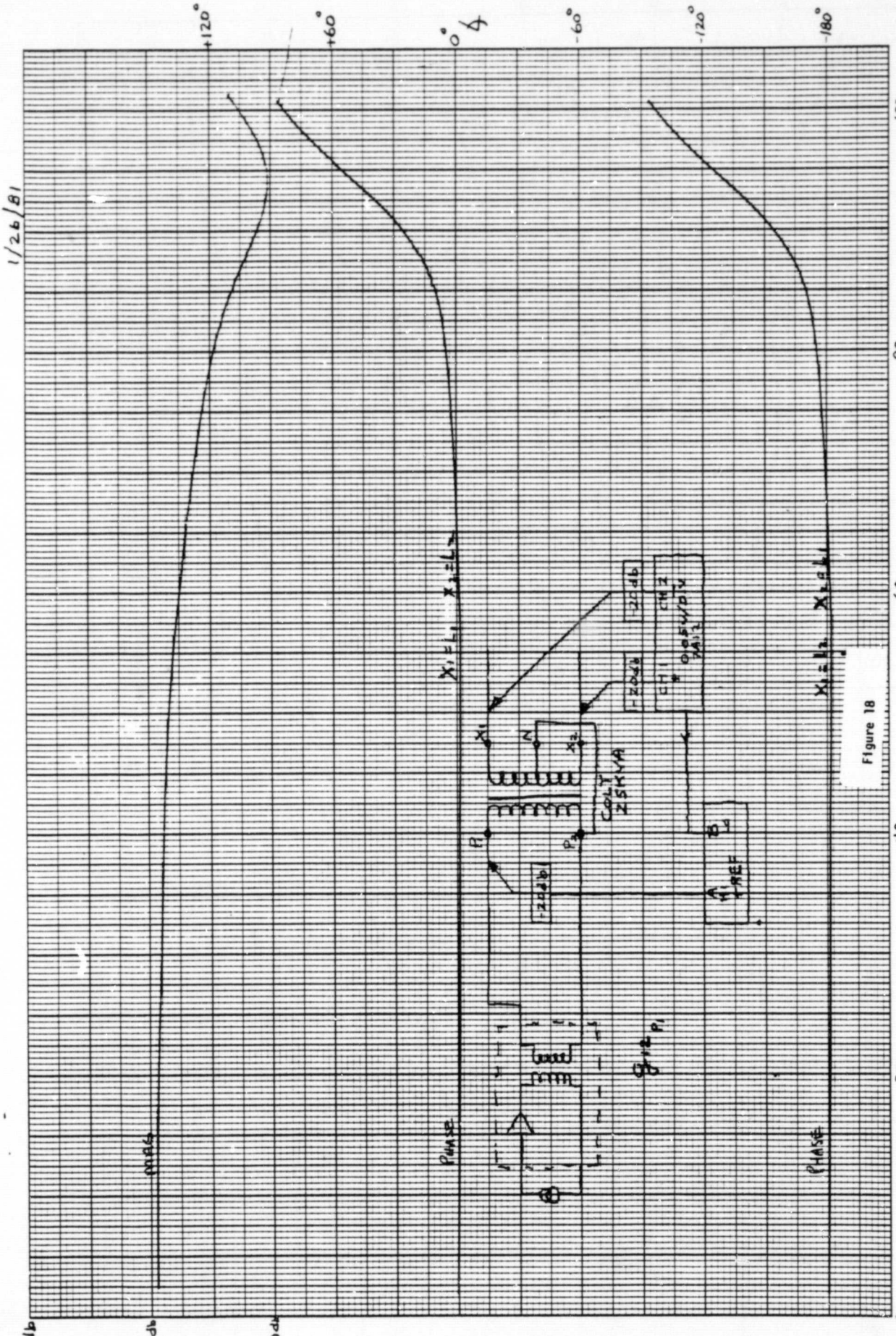

Figure 18

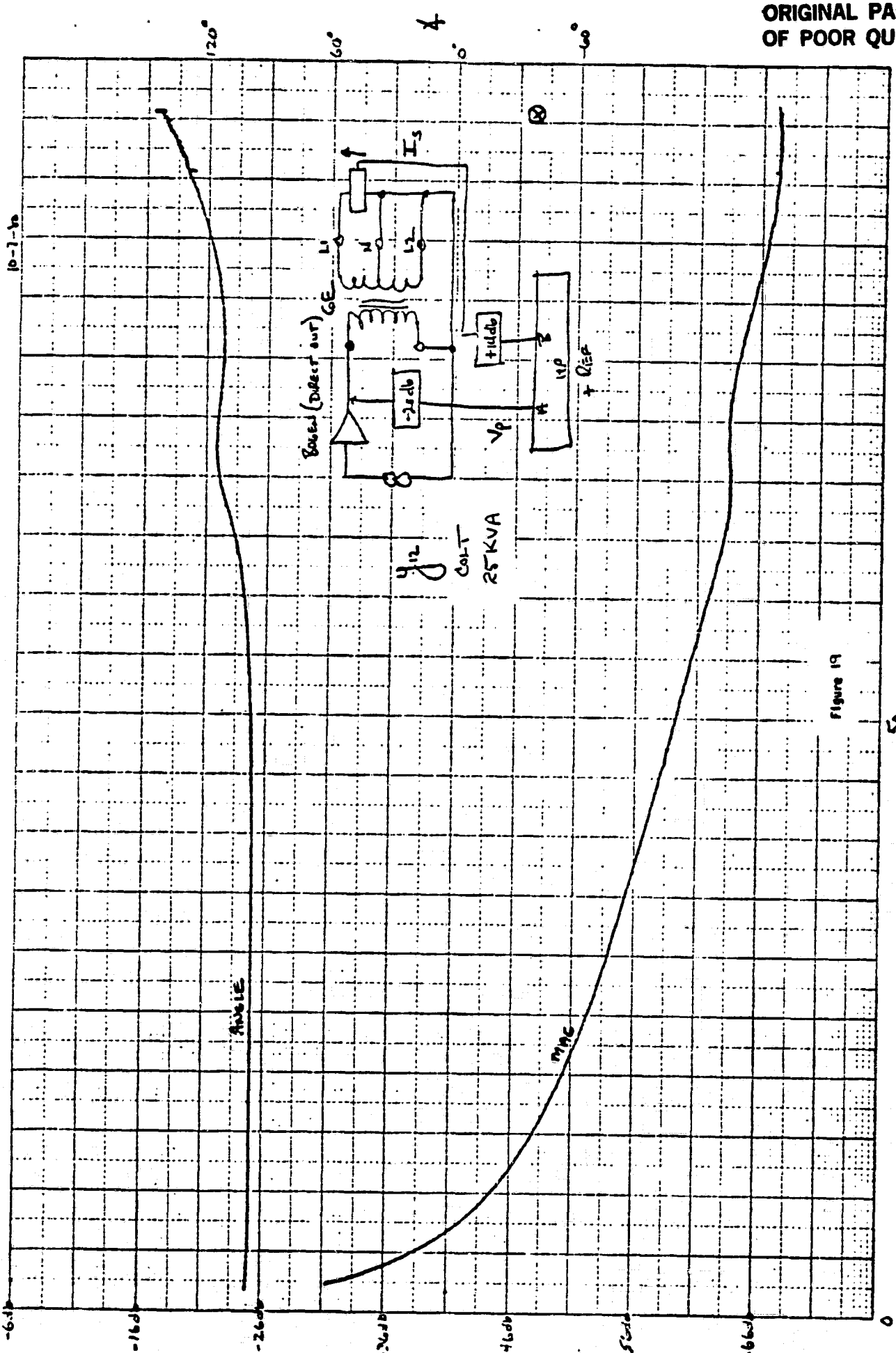

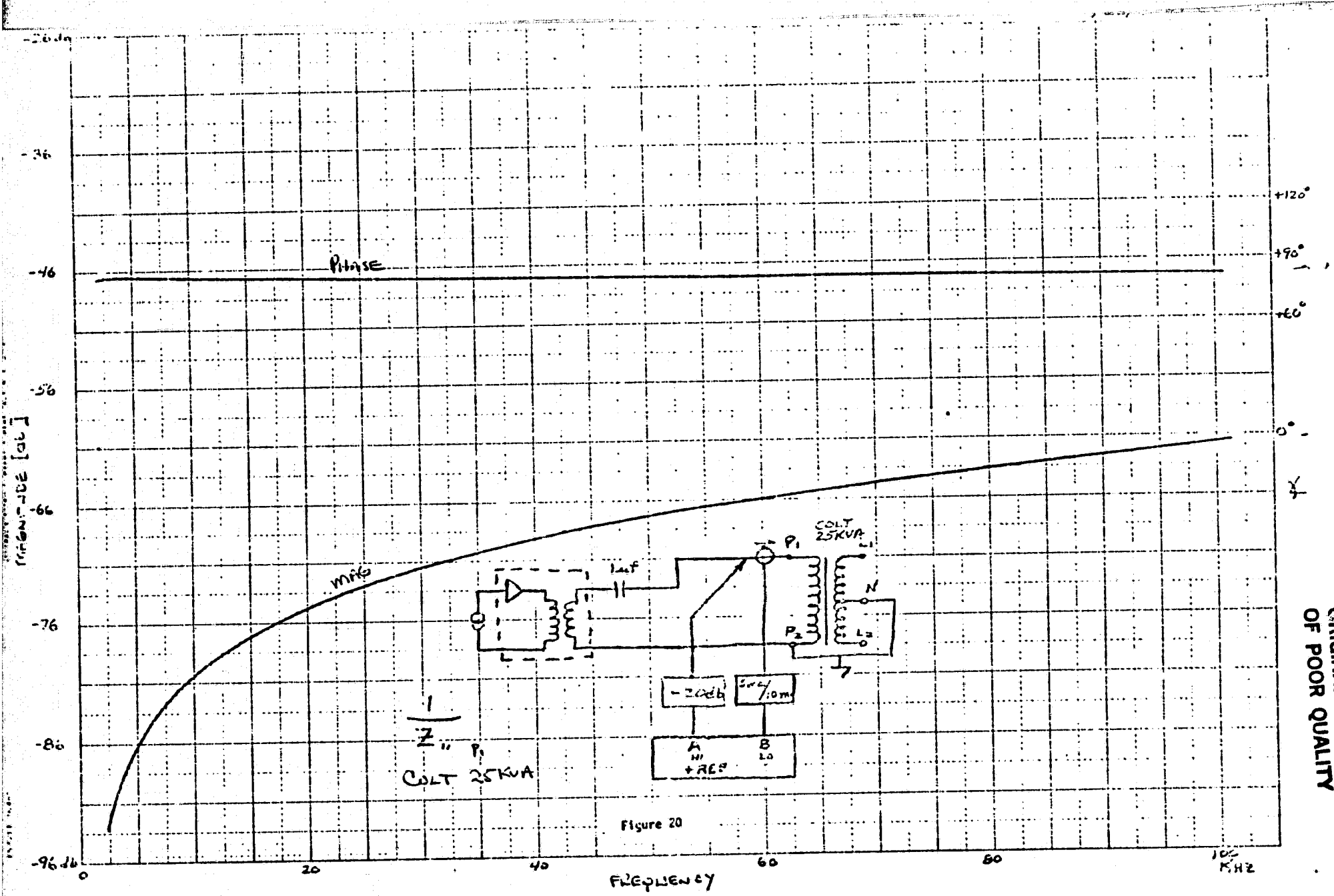

ORIGINAL PAGE IS OF POOR QUALITY

Figure 21

1/26/81

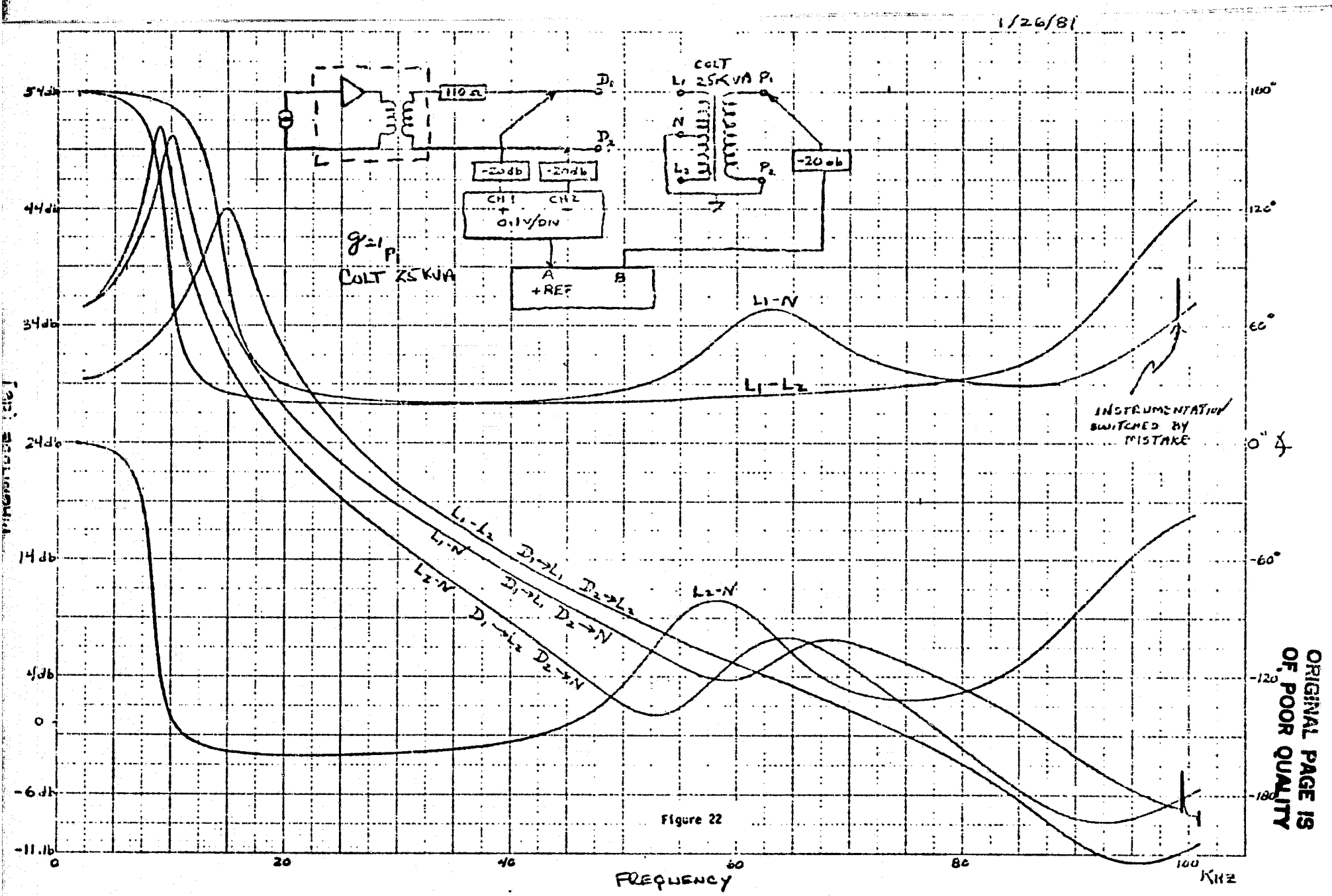

Figure 22

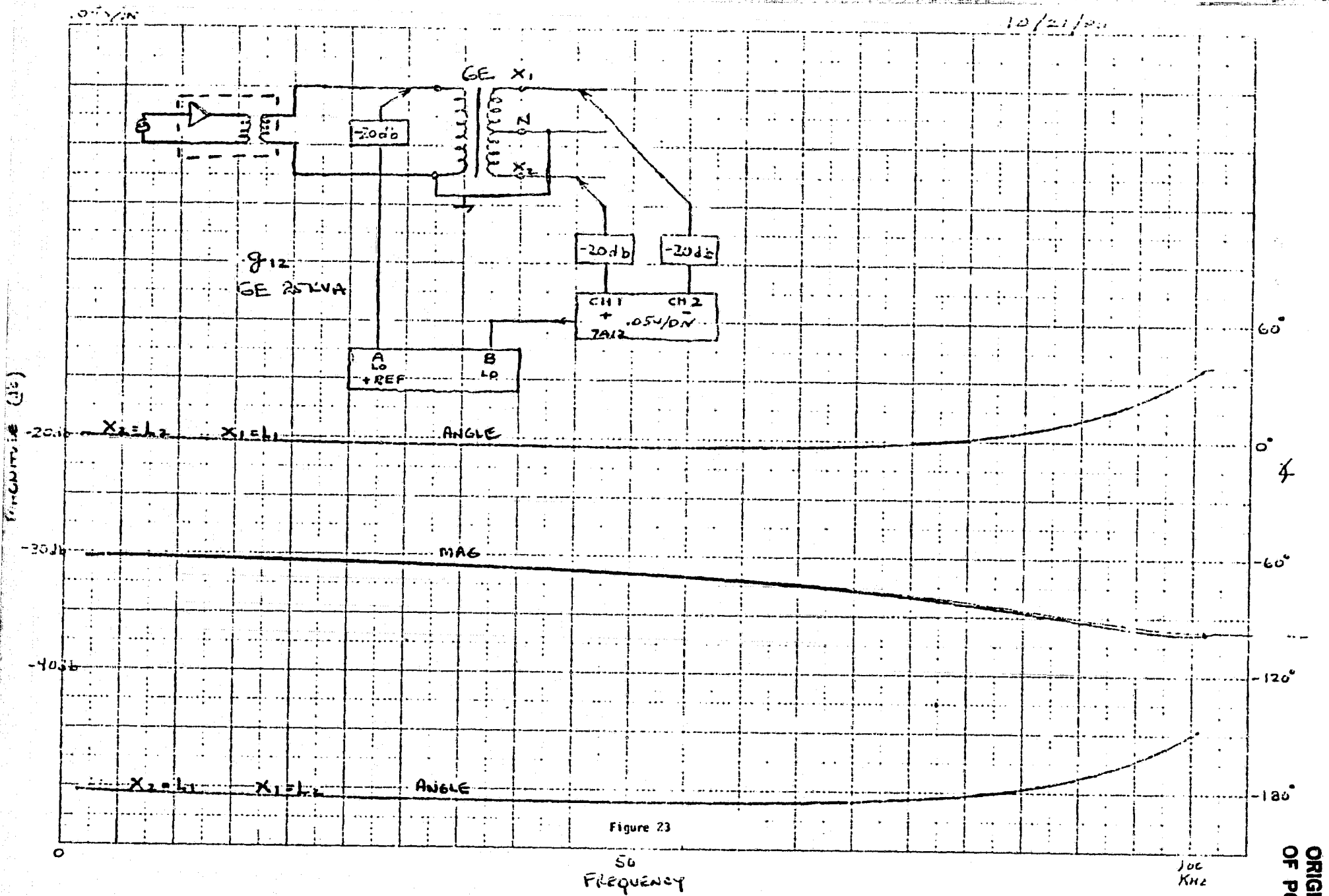

Figure 23

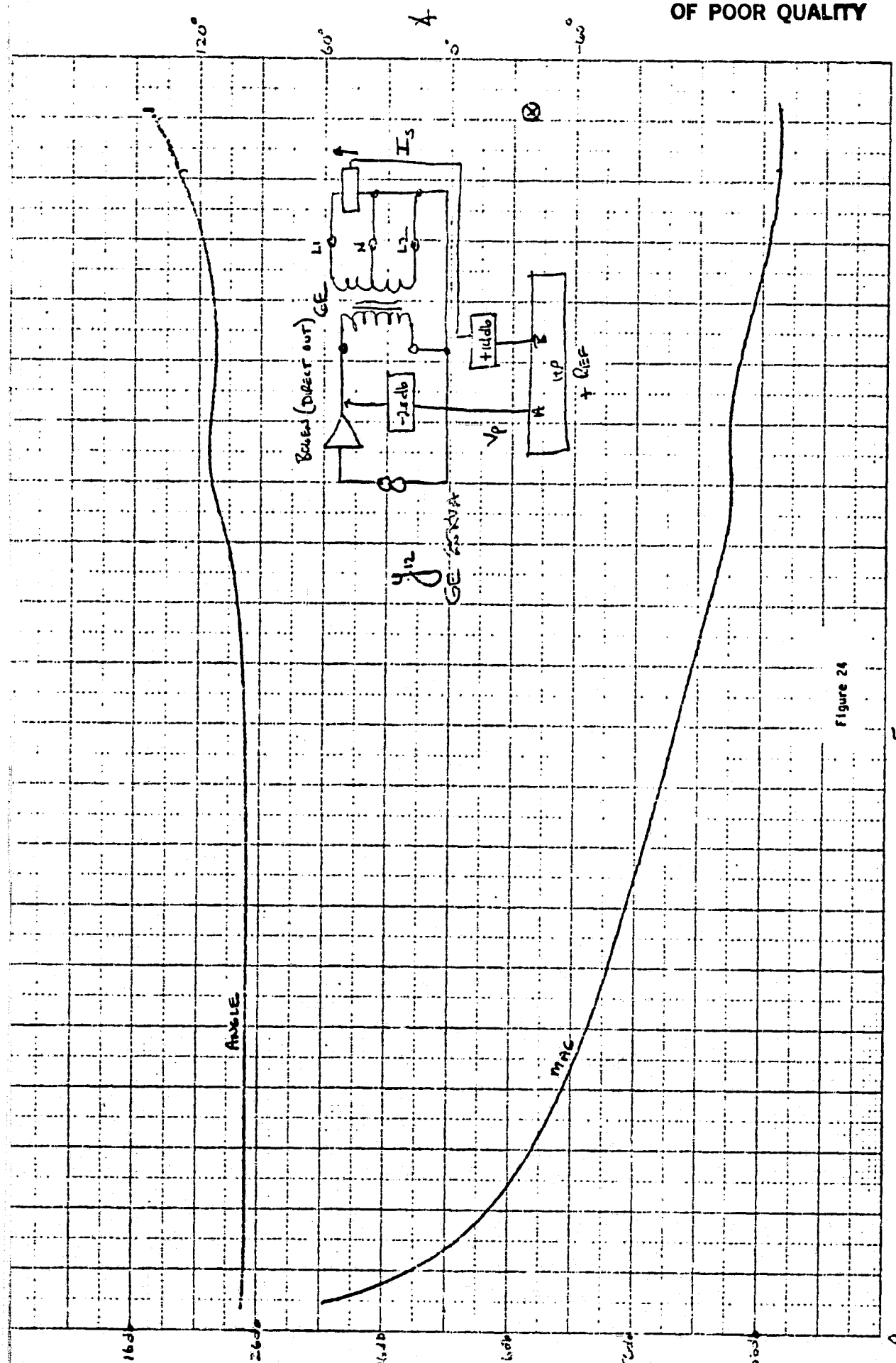

Figure 24

10/2:/90

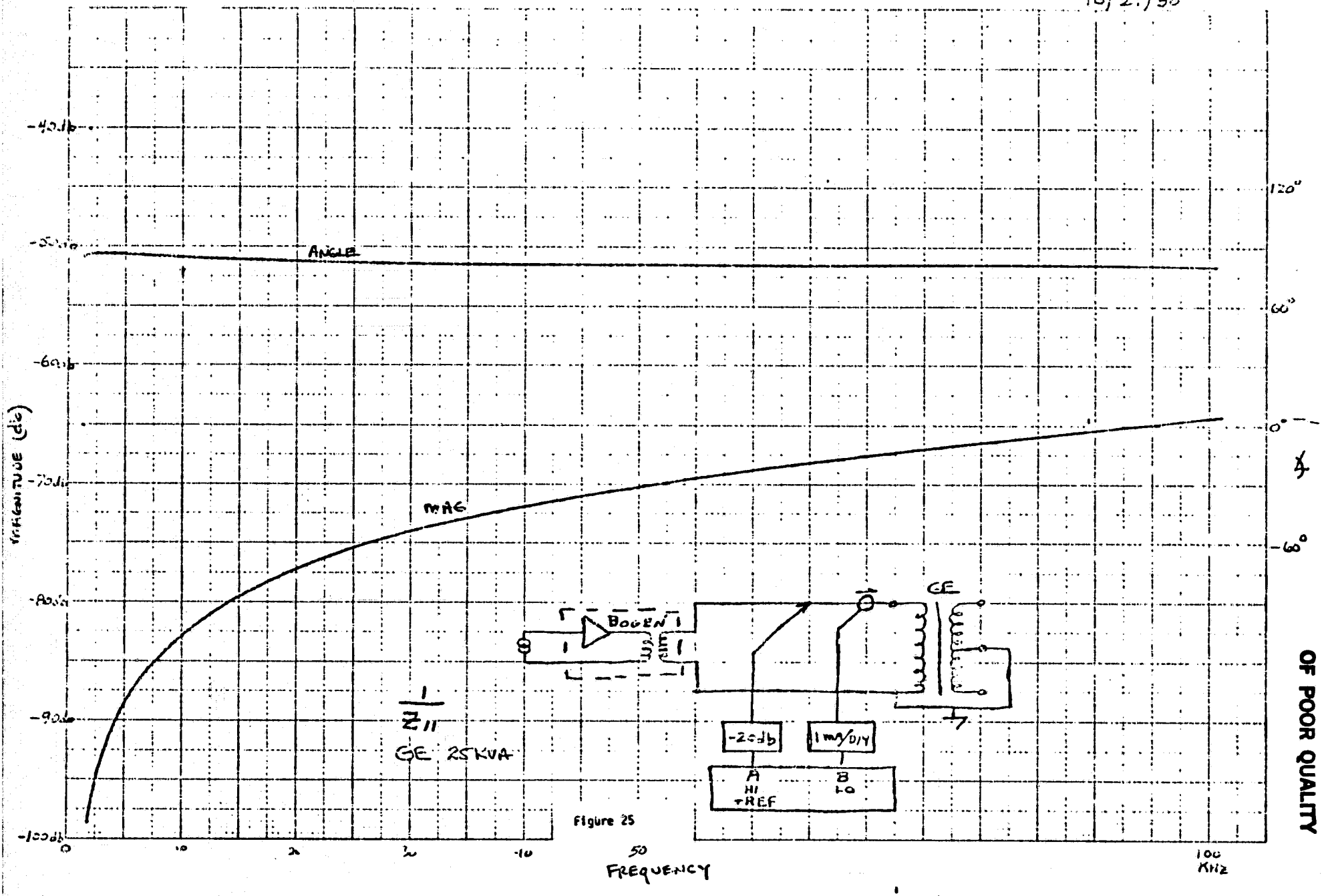

Figure 25

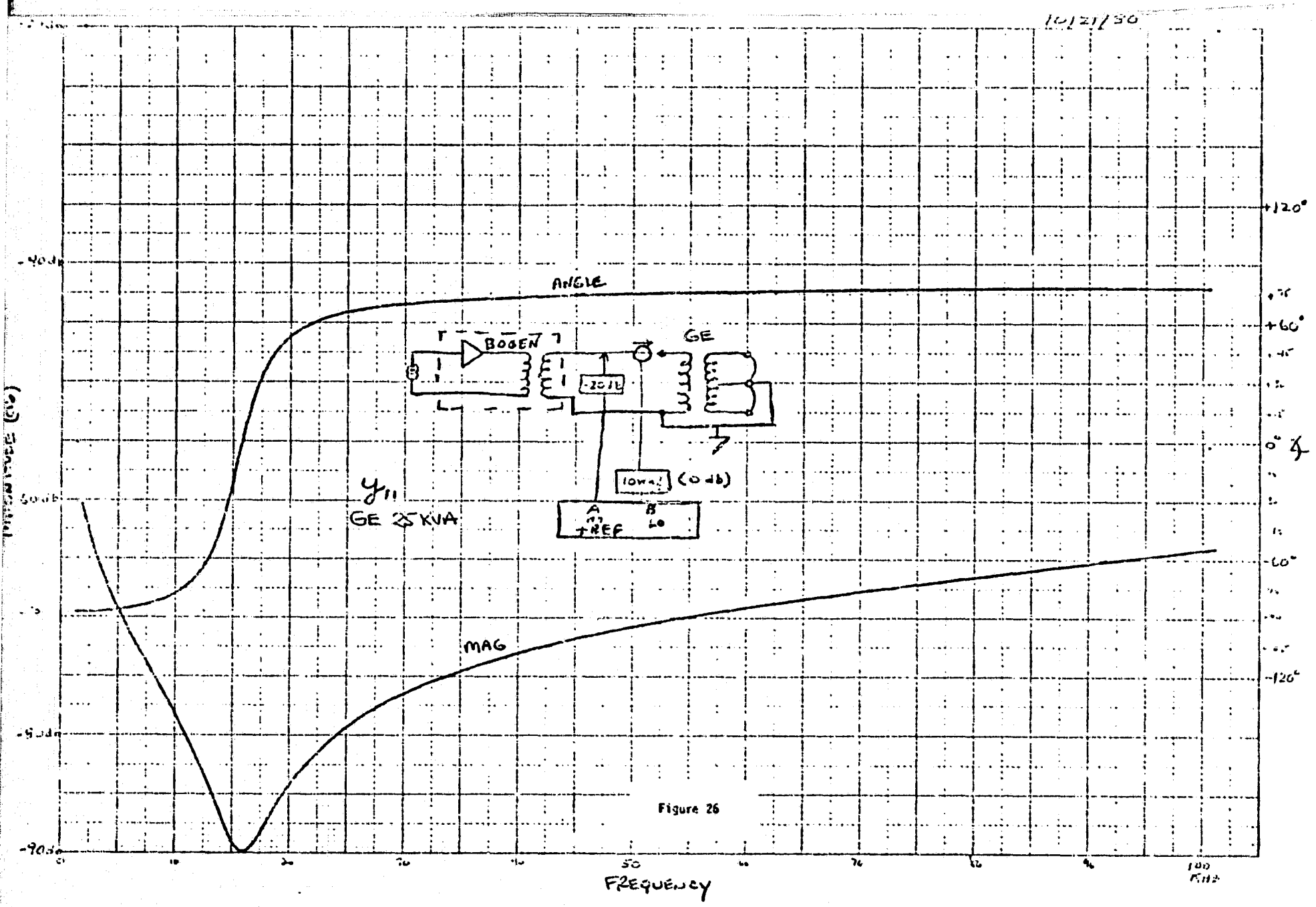

Figure 26

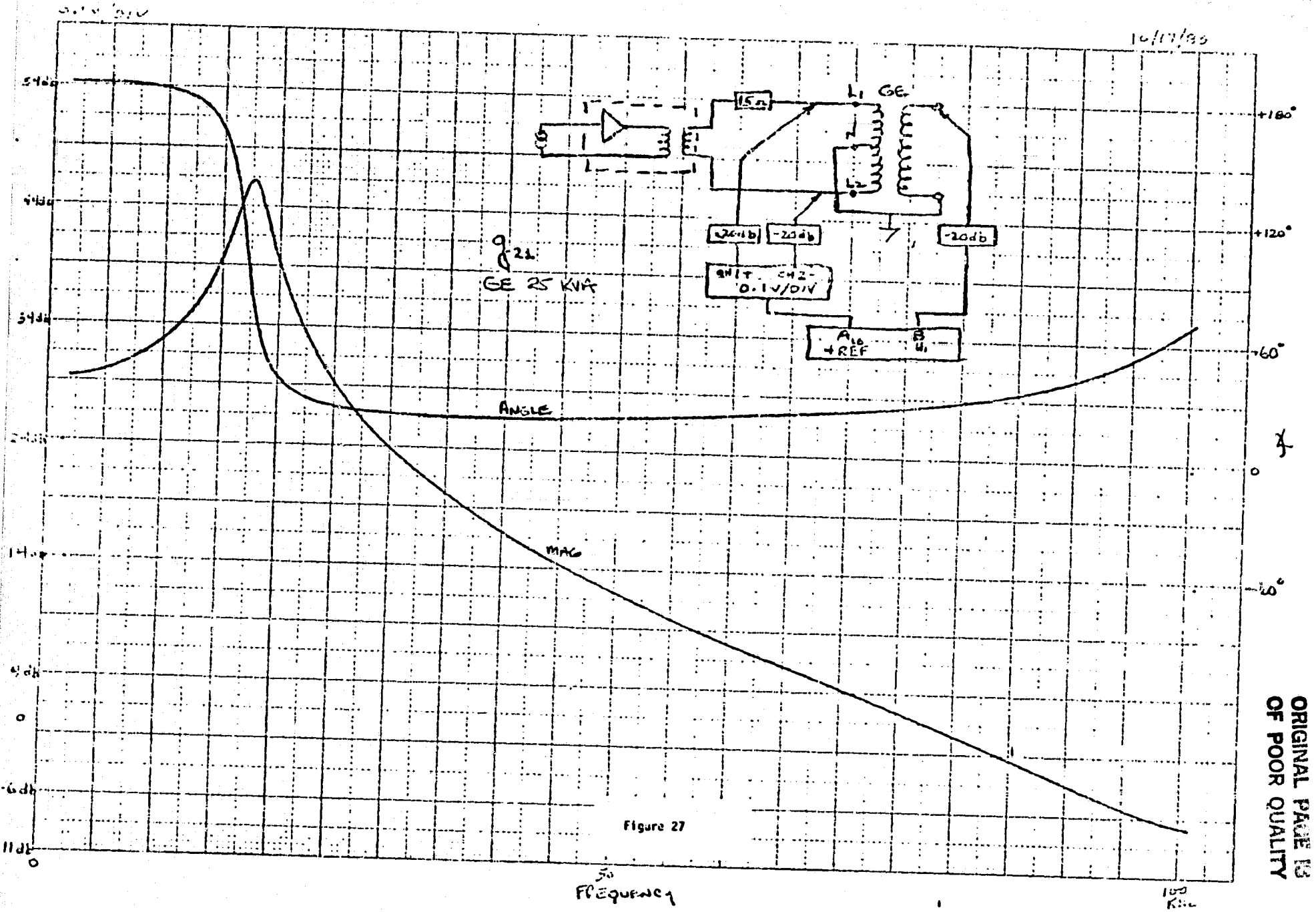
10/17/85
L1 GE
15Ω
L2
-20db
-20db
-20db
CH1. CH2-
0.1V/DIV
A
+REF
B
GE 25 KVA
ANGLE
MAG
+180°
+120°
+60°
0
-60°
50
FREQUENCY
100
KHz
ORIGINAL PAGE IS
OF POOR QUALITY

Figure 27

From this earlier work, the analysis presented in Appendix 3 and a study of the response measurements of Figs. 10-17, the model shown below was developed.

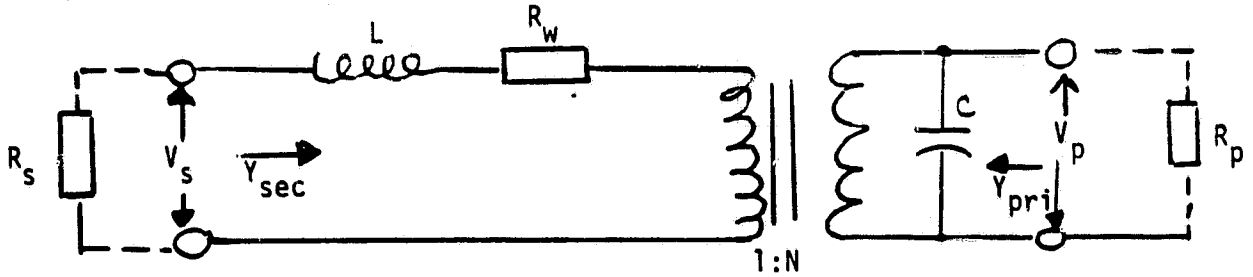

where N = turns ratio [31.75]

V_s = L-L secondary voltage

V_p = primary voltage

Y_{pri} = admittance looking into the primary

Y_{sec} = admittance looking into the secondary

R_p = primary load

R_s = L-L secondary load

L = leakage reactance (referred to secondary)

R_w = winding resistance (referred to secondary)

C - stray capacity (primarily bushing)

Using this model, the equations for the quantities of interest become:

$$\frac{V_s}{V_p} = \frac{R_s}{N\,[R_s + R_w + jwL]}$$

$$Y_{pri} = jwC + \frac{1}{N^2\,[R_s + R_w + jwL]}$$

$$\frac{V_p}{V_s} = \frac{\frac{1}{jwC + \frac{1}{R_p}}}{N\left[R_w + jwL + \frac{1}{N^2(jwC + \frac{1}{R_p})}\right]}$$

If $jwC << \frac{1}{R_p}$ and $\frac{R_p}{N^2} << \sqrt{R_w^2 + (jwL)^2}$ then

$$\frac{V_p}{V_s} = \frac{R_p}{N\,[R_w + jwL]}$$

$$Y_{sec} = \left[R_w + jwL + \frac{1}{N^2(1/R_p + jwC)}\right]^{-1}$$

If $jwC << \frac{1}{R_p}$ and $\frac{R_p}{N^2} << \sqrt{R_w^2 + (jwL)^2}$ then

$$Y_{sec} = (R_w + jwL)^{-1}$$

The unknowns in these equations are R_w, L and C. To check the validity of the model, it was necessary to determine values for these unknowns and thus was done as follows.

To find C for the 25 kva GE transformer, we take the curve of Fig. 25 ($\frac{1}{z_{11}}$), which is the admittance looking into the primary with the secondary open-circuited, determine jwC for any frequency and then determine C at that frequency. If we believe the model, then this value of C will represent the C of the model and for this transformer the value of C, measured at 5 kHz, is determined as follows:

$$\frac{1}{Z_{11}} = y_{in} = -88.5\text{db} \angle -85° \text{ @ 5 kHz}$$

$$Z_{in} = 88.5\text{db} \angle 85°$$

$$Z_{in} = 2319 - j26506$$

$$C = 1.2 \text{ nf}$$

The small resistive component has not been identified, but may be attributed to measurement error. The value of C for the 25 kva Colt transformer can be similarly determined from Fig. 20 and is found to be 1.5 nf.

We would expect the value of C measured at any other frequency from Fig. 25 to remain the same as that for 25 kHz and this is the case within reasonable limits. Figure 25 can be seen to be pretty much a curve of jwC versus frequency as shown in the jwC plot of Fig. 11.

To determine the values for R_w and L for the 25 kva GE transformer, we take the curve of Fig. 17, which is the admittance looking into the secondary (L-L) with a 10 ohm primary resistance, and determine Y_{sec} at a given frequency. From this value of Y_{sec} we can determine R_w and L as follows:

$$Y_{sec} = -21.7\text{db} \angle -84° \text{ @ 25 kHz}$$

$$Z_{sec} = 21.7\text{db} \angle 84°$$

$$= 12.16 \angle 84° = 1.27 + j\,12.10$$

and then

$$\left.\begin{array}{l} R_w = 1.27\Omega \\ L = 77\ \mu h \end{array}\right) \quad \text{measured at 25 kHz}$$

Ideally, this measurement should be made with the primary short-circuited, however, the 10 ohm primary resistor becomes insignificant because 10 ohms $<< \frac{1}{jwC}$ and, when transferred to the secondary, 10 ohms divided by N^2 ($N^2 \tilde{=} 1000$) is much less than jwL.

Determining R_w and L at other frequencies from the curves of Fig. 17 yield the following results:

Frequency (kHz)	R_w(ohms)	jwL (ohms)	L (μh)
5	0.14	2.72	86
10	0.3	5.29	83
25	1.27	12.10	77
50	2.76	23.8	76
100	11.90	58.0	82

Similar determinations can be made for the Colt 25 kva transformer from the curves of Fig. 12, where $R_p = 0$, as shown below:

Frequency (kHz)	R_w(ohms)	jwL (ohms)	L (μh)
5	0.23	2.59	82
10	0.68	4.85	77
25	2.21	10.87	69
50	4.75	20.59	66
100	21.52	51.95	83

With regard to the GE transformer, several observations can be made about both R_w and L. R_w is significantly less than jwL up to about 50 kHz and behaves, to a first approximation, according to the equation

$$R_w = \frac{R_w'}{.14}\left(\frac{f}{20{,}000}\right)^{1.4}$$

where f = frequency in Hz

R_w' = R_w(ohms) measured at 5 kHz

up to about 50 kHz. Computing R_w versus frequency using the above equation yields the following result:

Frequency (kHz)	R_w(ohms)
5	0.14
10	0.38
25	1.37
50	3.61
100	9.52

It can be seen that the maximum apparent change in L with frequency is less than 19% or less than 2 db, for either transformer.

The Colt transformer behaves similarly to the GE except that its R_w values are about twice that for the GE which makes them more significant when compared to jwL. Computing R_w versus frequency using the above equation yields the following results:

Frequency (kHz)	R_w(ohms)
5	0.23
10	0.62
25	2.25
50	5.93
100	15.64

Verification

A model of a distribution transformer has been developed and equations derived for the characteristics of interest as a function of frequency. The unknown quantities in the equations have been measured [for 2 transformers] and now it is appropriate to determine how well the model can predict measured performance. A computer plotting program was developed to accept R_w, L and C as inputs and plot the equations previous given of $\frac{V_s}{V_p}$, Y_{pri}, $\frac{V_p}{V_s}$ and Y_{sec}, as a function of frequency, and to match the abscissa and ordinate dimensions as generated by the x-y plotter.

Figures 28 through 31 show these curves for the GE 25 kva transformer and are to be compared with the measured performance of Figs. 14-17. The value used to generate the curves of Figs. 28-31 are as follows:

$R_w = 0.14\Omega$ @ 5000 Hz

L = 86 μh

C = 1.2 uf

The equation used here to determine R_w as a function of frequency was implemented in the plot routine as

$$R_w = \frac{f}{20{,}000}^{1.4}$$

instead of

$$R_w = \frac{R_{ws}}{.14} \frac{f}{20{,}000}^{1.3}$$

For the 25 kva GE transformer, this makes a trivial difference since R_w is nearly ten times less than jwL at any frequency up to 50 kHz.

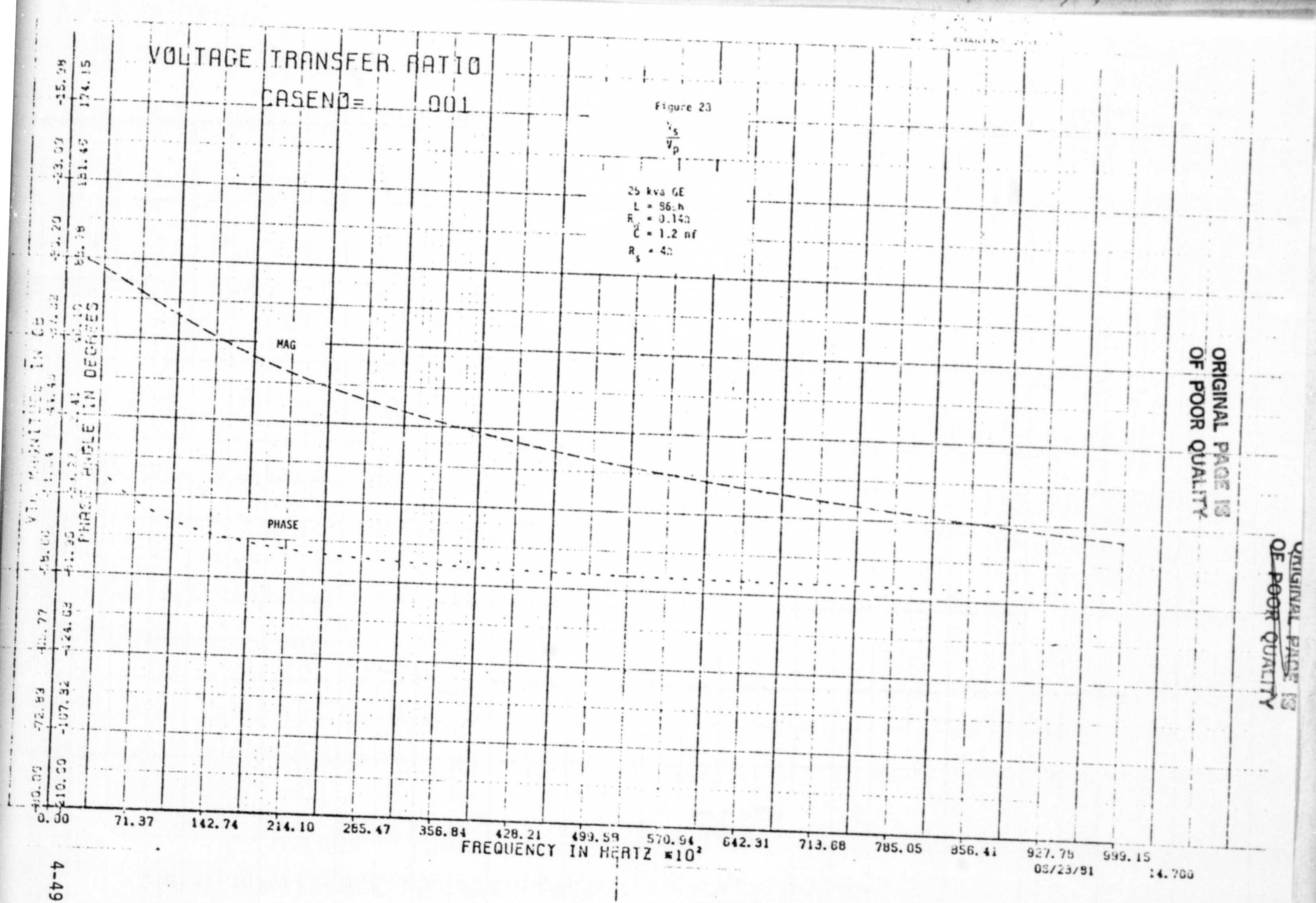

ORIGINAL PAGE IS
OF POOR QUALITY

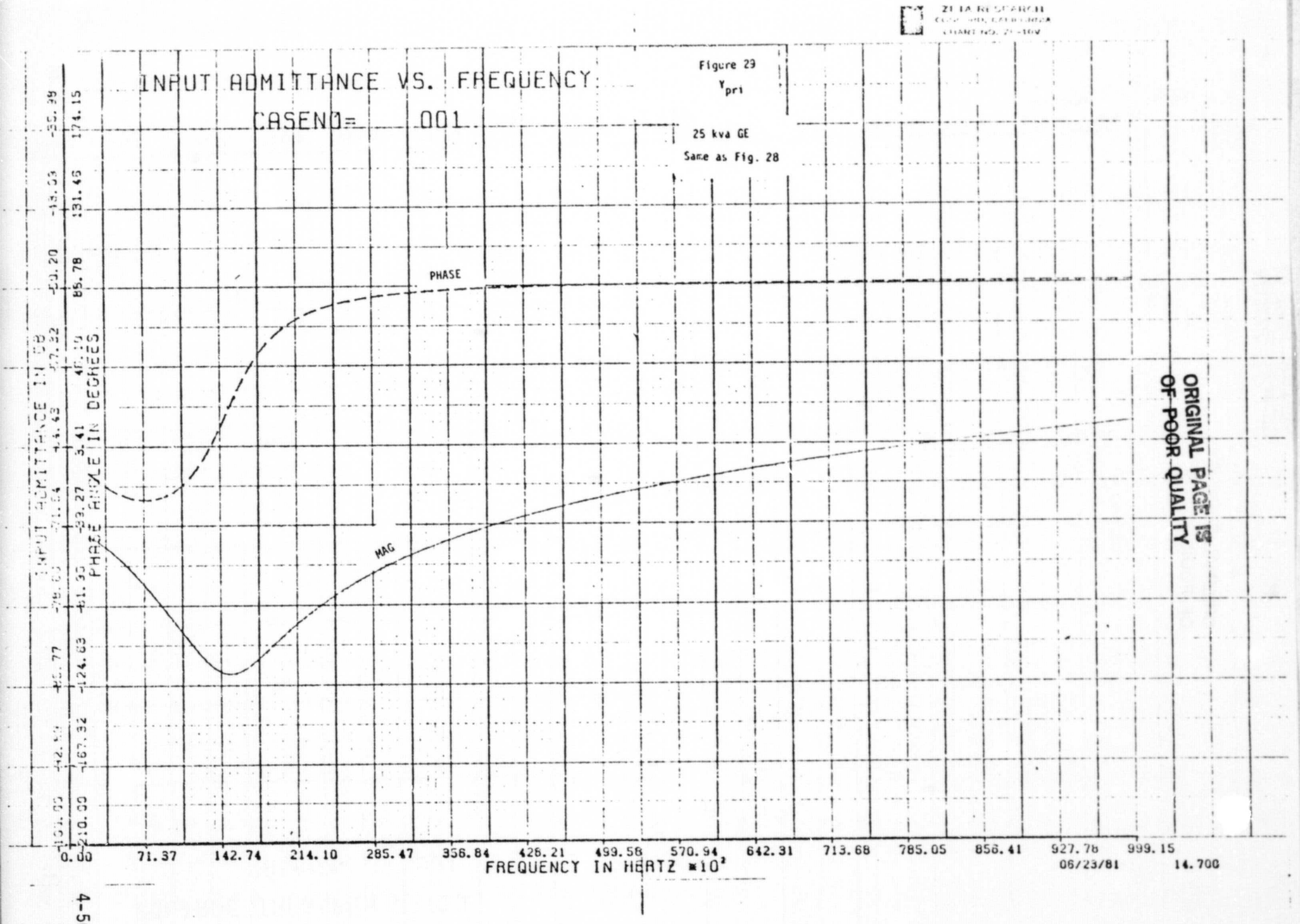

ORIGINAL PAGE IS
OF POOR QUALITY

Figure 30

$\frac{V_p}{V_s}$

25 k.a GE
L, R_w, C same as Fig. 28
R_p = 10Ω

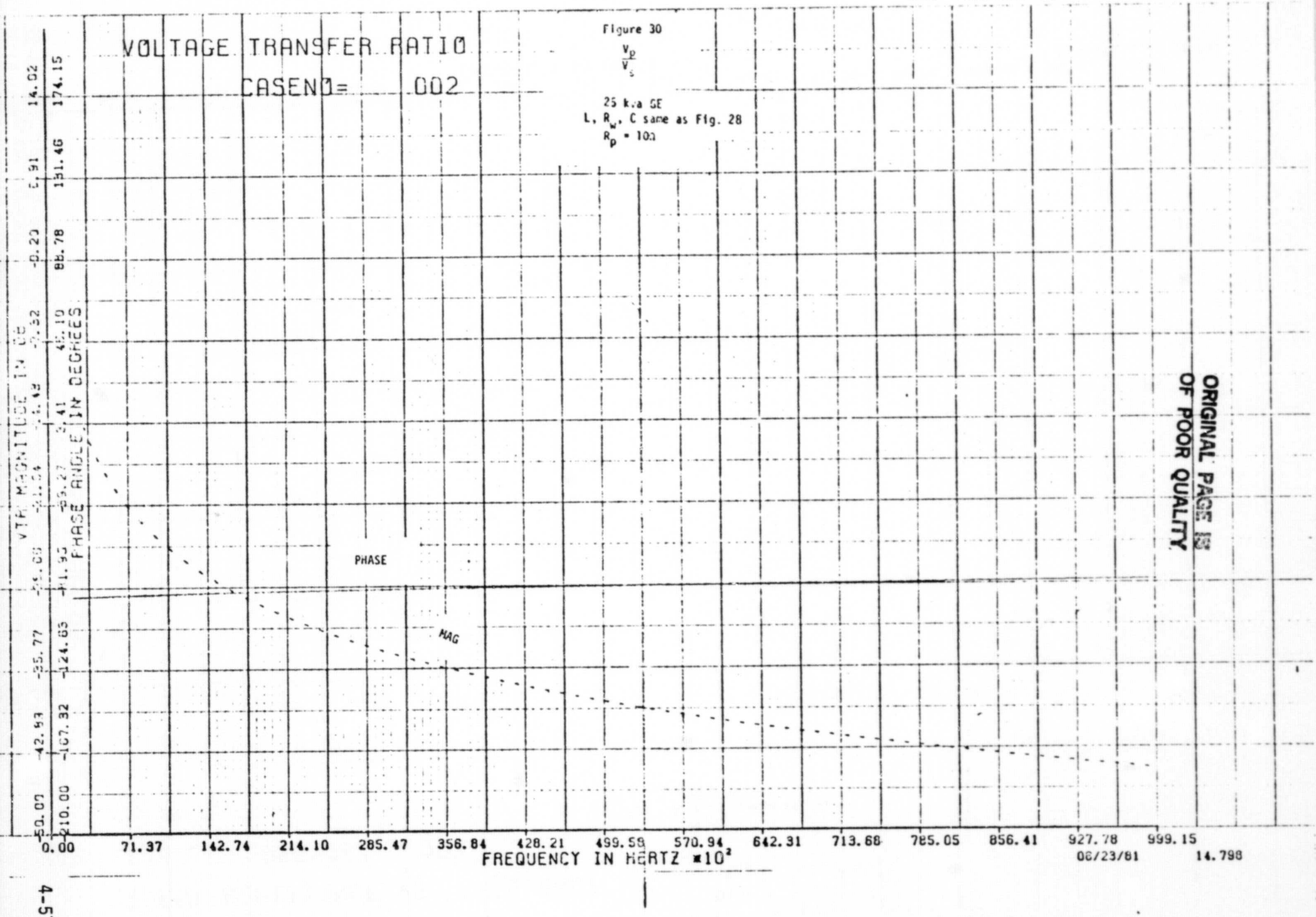

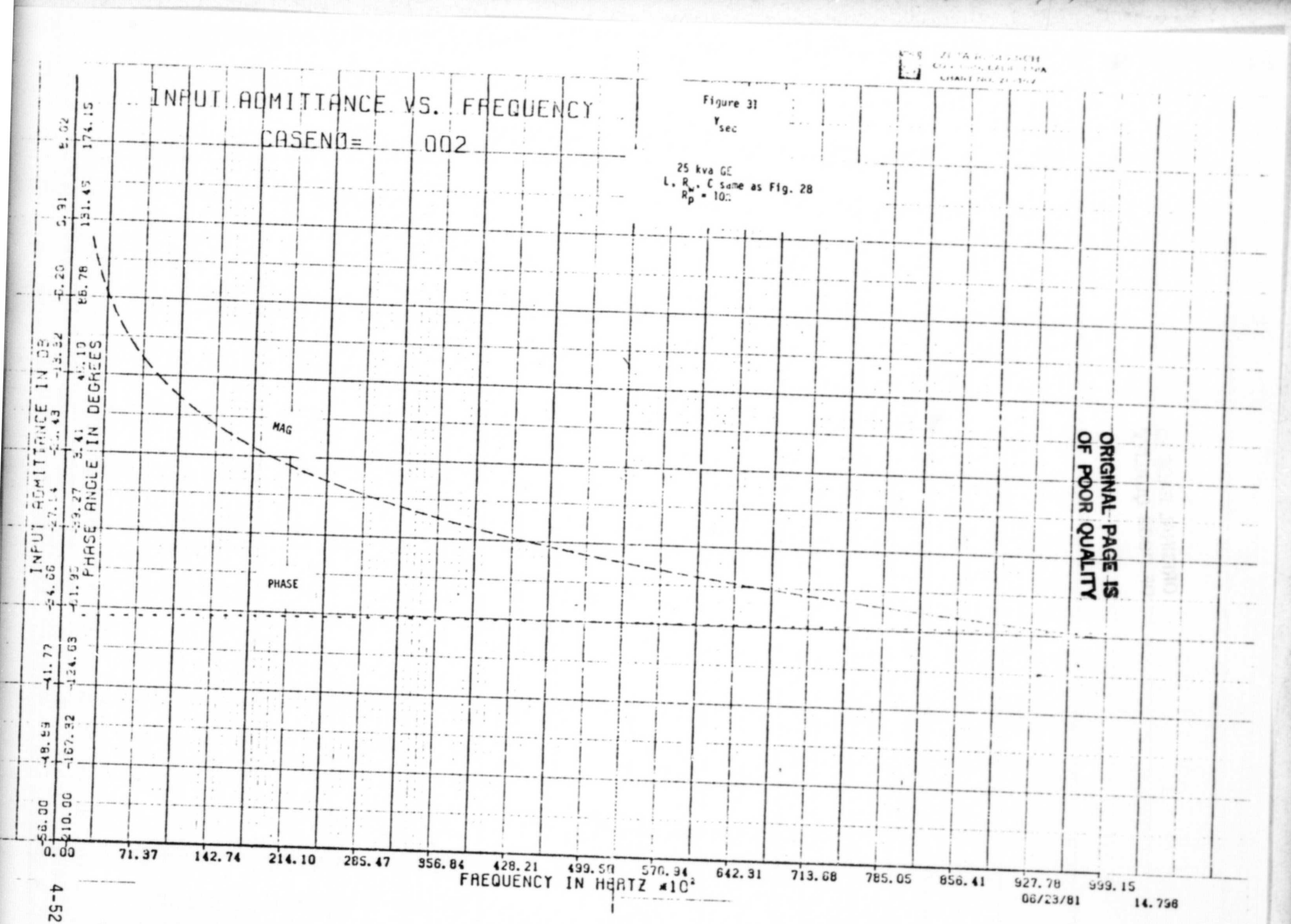

ORIGINAL PAGE IS
OF POOR QUALITY

A comparison of the computed curves with the measured curves shows the following:

1. Both curves of $\frac{V_s}{V_p}$ show agreement within 1 db up to 50 kHz. Incidently, the computed curve falls exactly on the 3 points computed from the algebraic model.

2. For Y_{pri}, the resonance occurs at essentially the same frequency; however, the "Q" of the computed curve appears to be somewhat higher and the maximum variation in magnitude, up to 50 kHz, is about 5 db. In this case, the algebraic model seems to more closely follow the measured curve than the computed curve.

3. The curves for $\frac{V_p}{V_s}$ track within 1 db up to 50 kHz.

4. Y_{sec} also shows good agreement between the computed and measured curves.

A similar comparison can be made between the measured [Figs.10-13] and computed curves [Figs. 32-35] for the 25 kva Colt transformer and the above statements, in general, appear to be applicable here.

In conclusion, we believe that the simple "RLC" plus ideal transformer" model that we have developed, describes the required performance characteristics of distribution transformers, up to 50 kHz, with sufficient accuracy for the intent of this program.

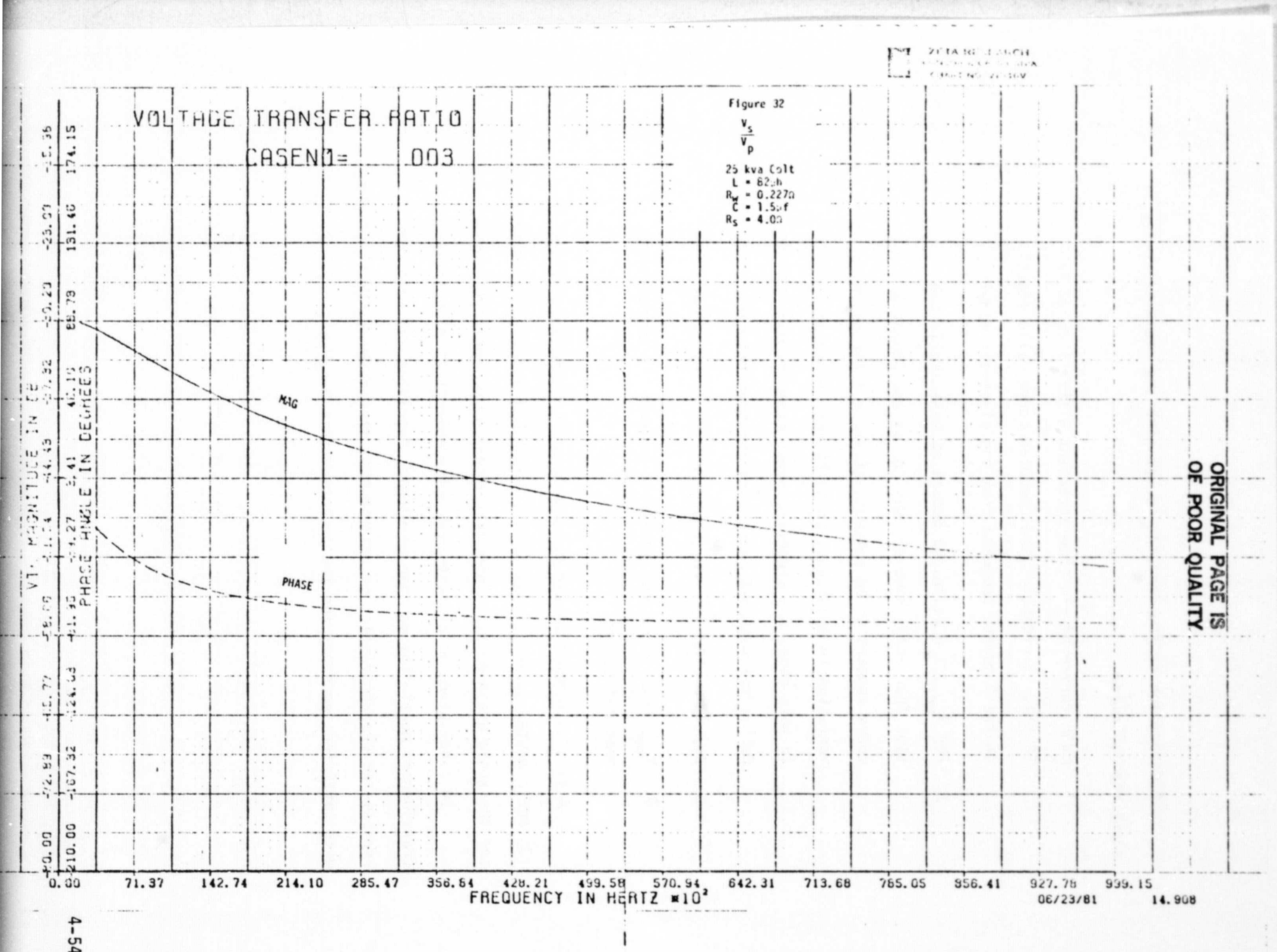

ORIGINAL PAGE IS
OF POOR QUALITY

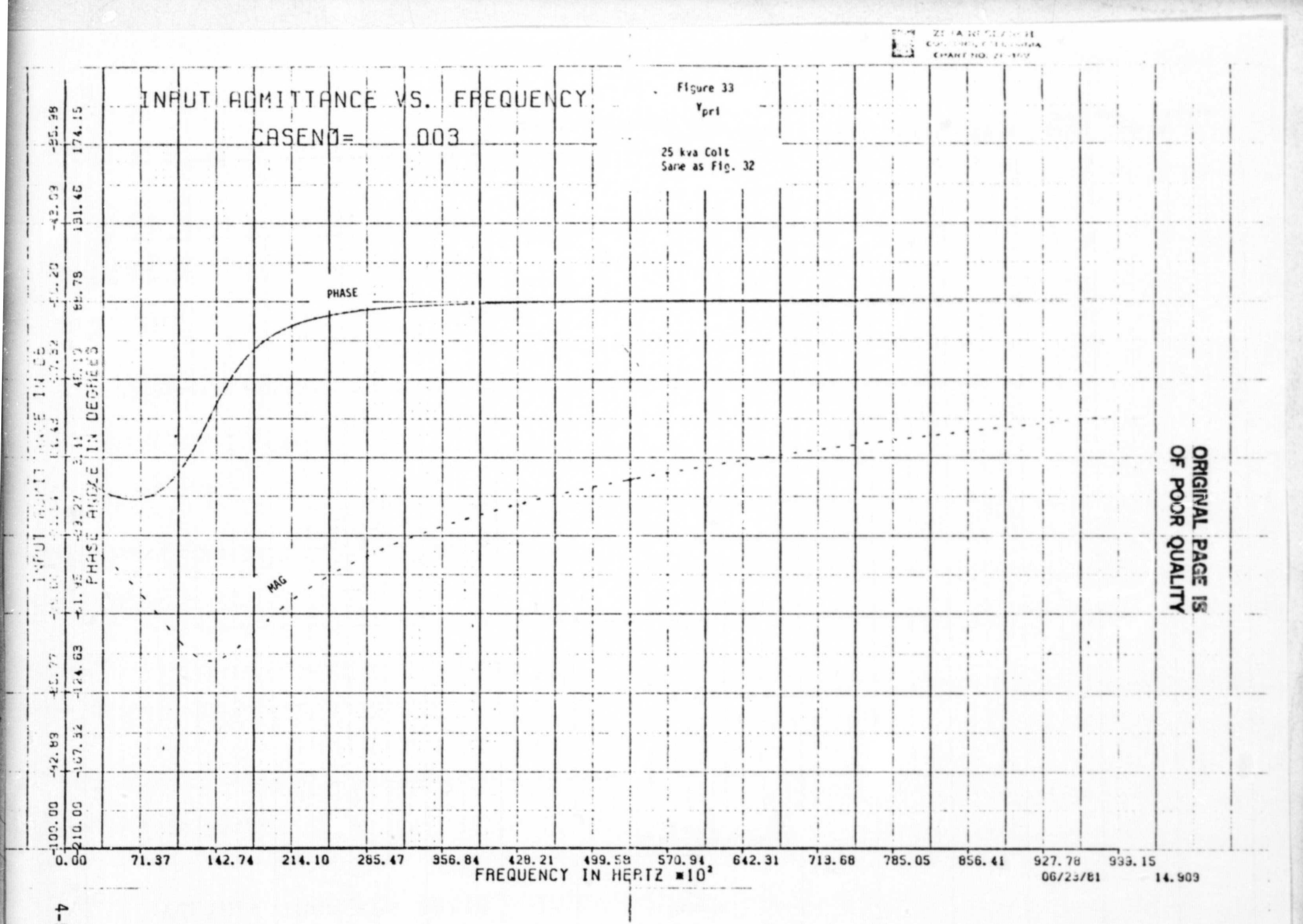

ORIGINAL PAGE IS
OF POOR QUALITY

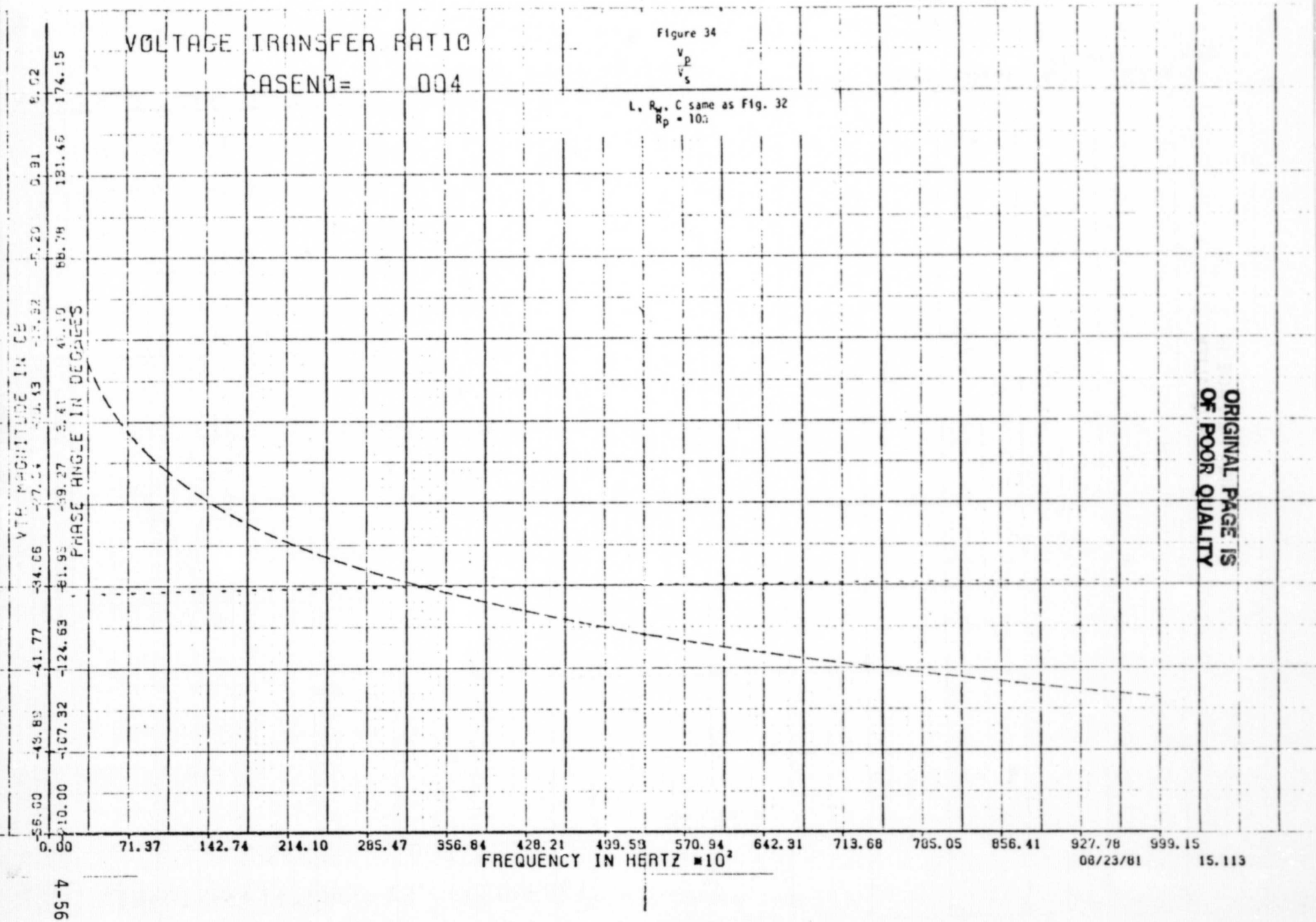

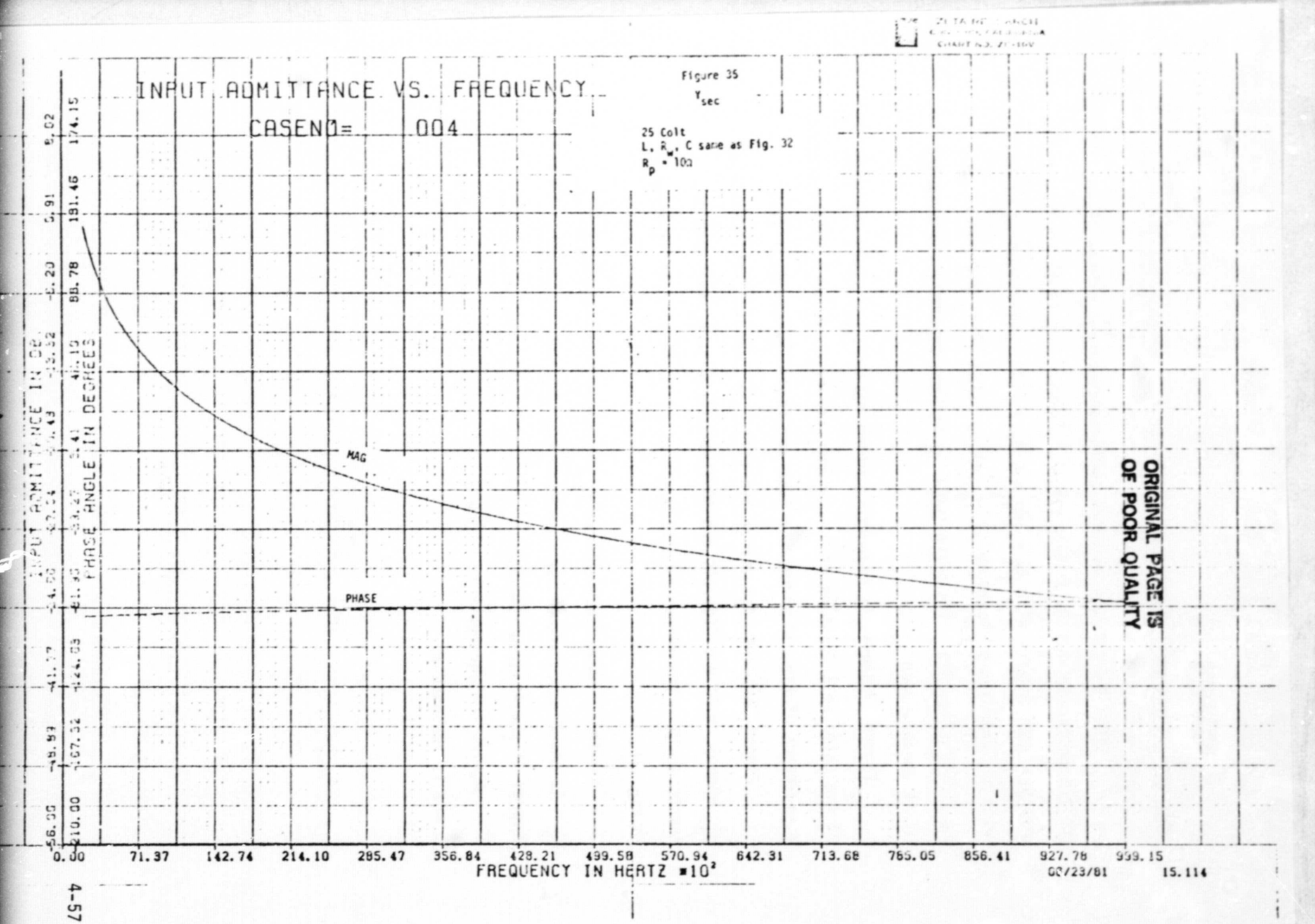

ORIGINAL PAGE IS
OF POOR QUALITY

Measured and Computed Performance as a Function of Load Changes

Figure 36 shows the measured performance of $\frac{V_P}{V_S}$ of the 25 kva Colt transformer when $R_P = 100\Omega$ and $R_P = 1000\Omega$. Figure 12 shows the measured performance when $R_P = 10\Omega$ and $R_P = 100\Omega$. These can be compared with the computed performance of $\frac{V_P}{V_S}$ at $R_P = 10\Omega$ [Fig. 34] and at $R_P = 100\Omega$ [Fig. 37]. The correspondence between measured and computed is reasonably good.

Figure 13 shows the measured performance of Y_{sec}, again for the 25 kva Colt, as a function of R_P and thus can be compared to the computed performance of Fig. 38 where $R_P = 100\Omega$ and Fig. 35 where $R_P = 10\Omega$.

Figure 32 shows, for the 25 kva Colt, the computed performance of $\frac{V_S}{V_P}$ when $R_S = 4\Omega$ and Figs. 39 and 40 show this when $R_S = 2\Omega$ and 8Ω, respectively. The measured performance of $\frac{V_S}{V_P}$ when $R_S = 4\Omega$ is shown in Fig. 10.

Figure 11 shows the measured Y_{pri} for the Colt transformer when $R_S = 4\Omega$ and Fig. 33 shows the computed curve for this condition. Figures 41 and 42 show computed Y_{pri} for $R_S = 2\Omega$ and 8Ω, respectively.

Again, the agreement in measured and computed performance up to 50 kHz is reasonable.

Figure 36

$\frac{V_p}{V_s}$

25 kva Colt

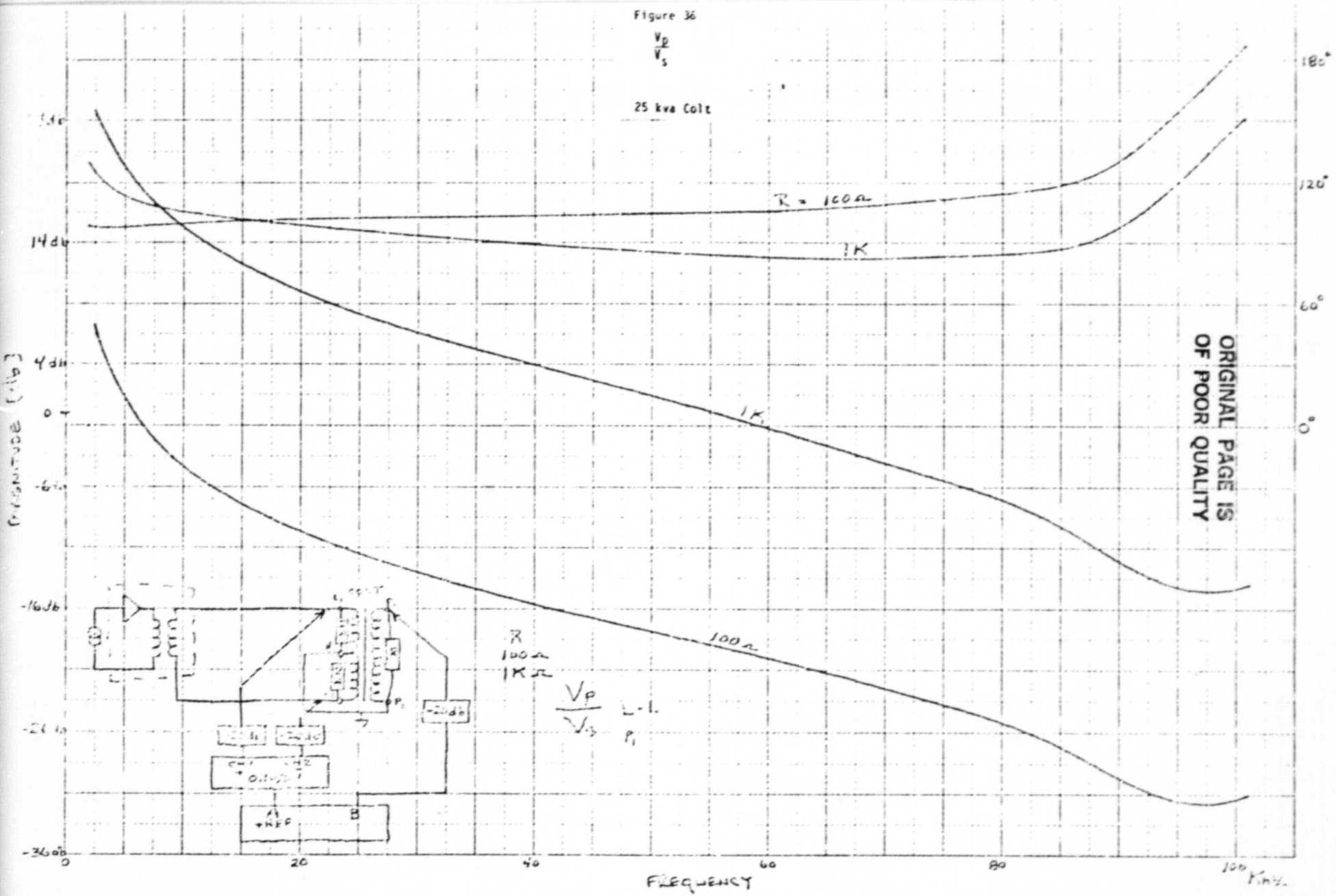

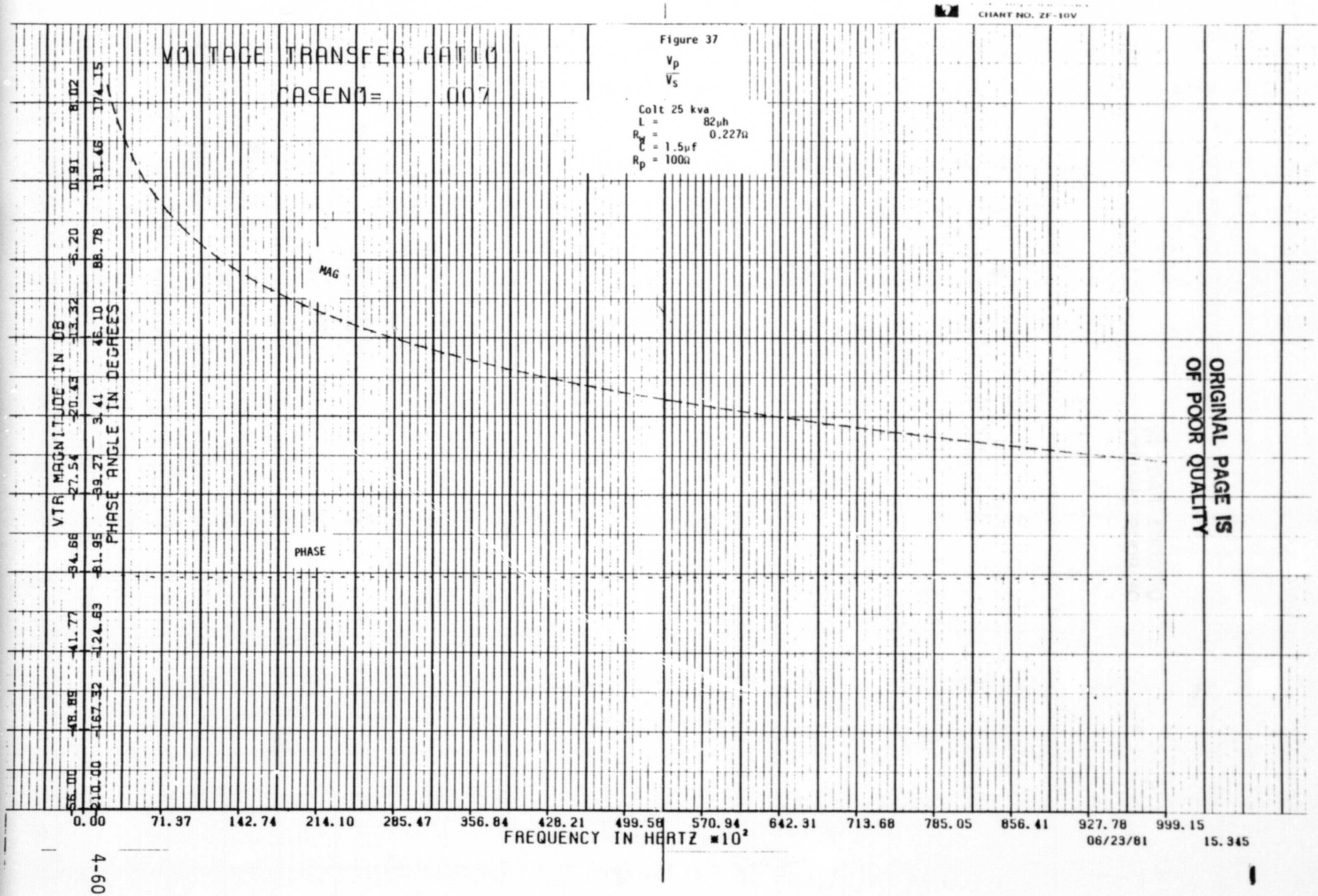

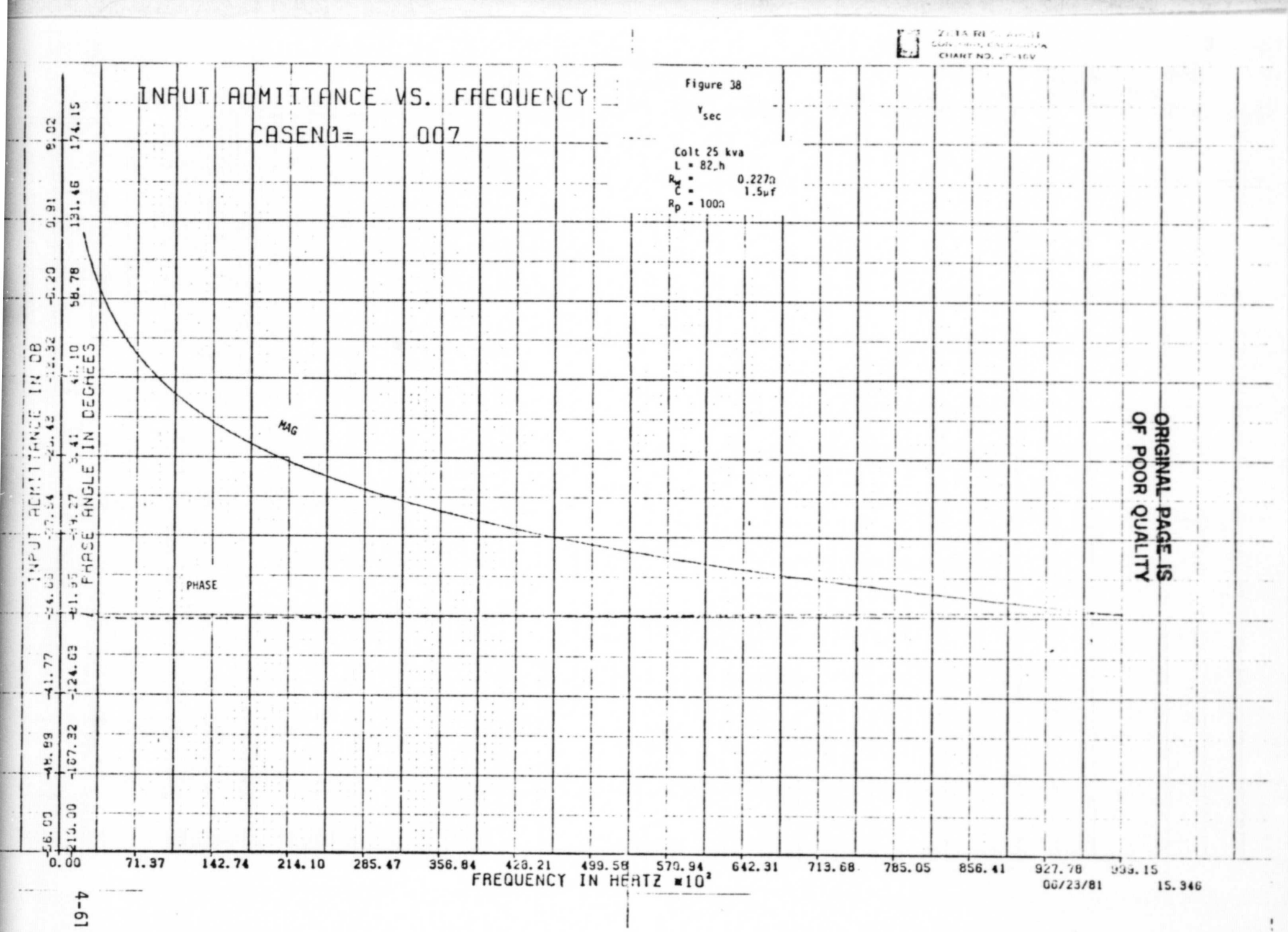

ORIGINAL PAGE IS
OF POOR QUALITY

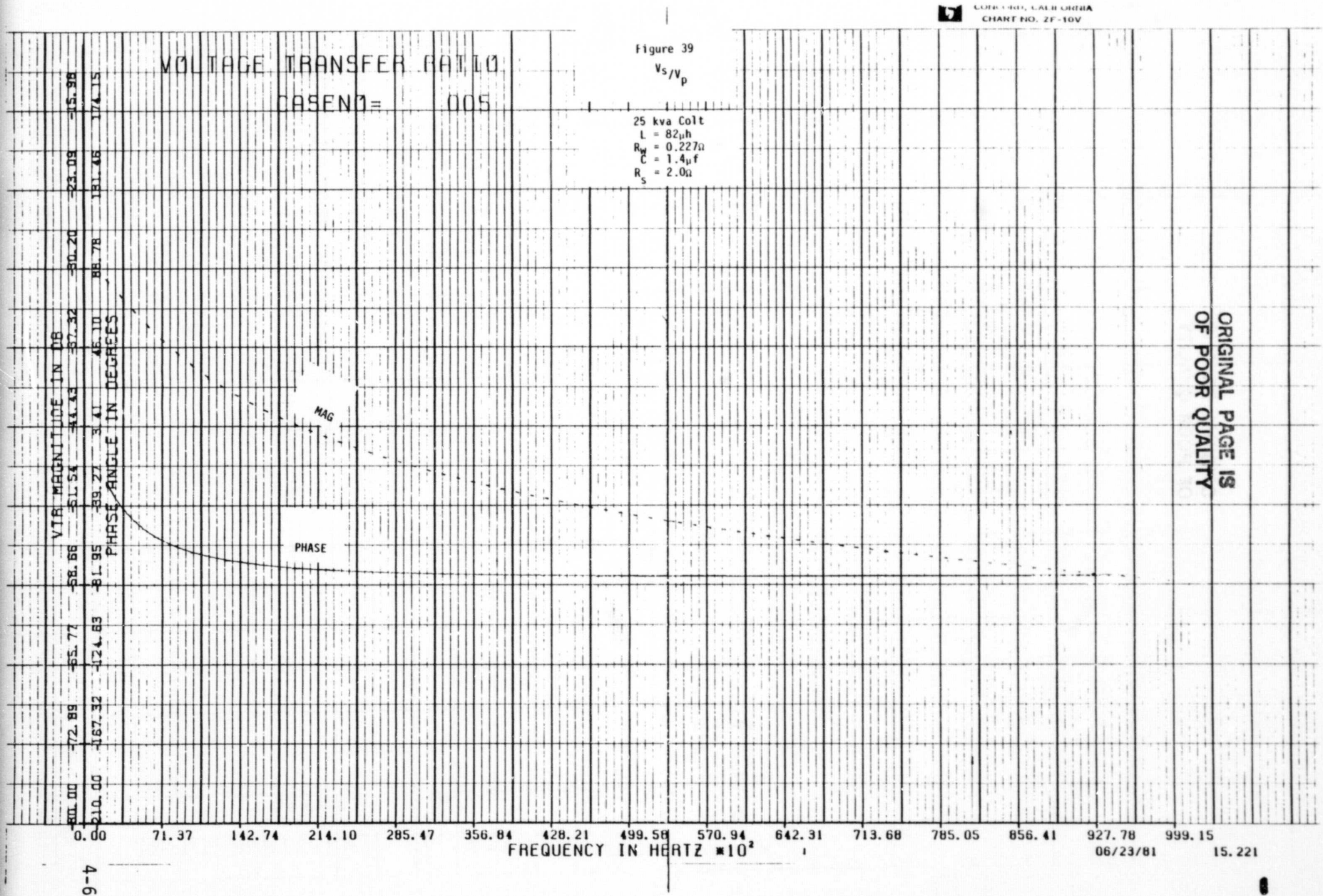

ORIGINAL PAGE IS
OF POOR QUALITY

ZETA RESEARCH
CONCORD, CALIFORNIA
CHART NO. ZF-10V

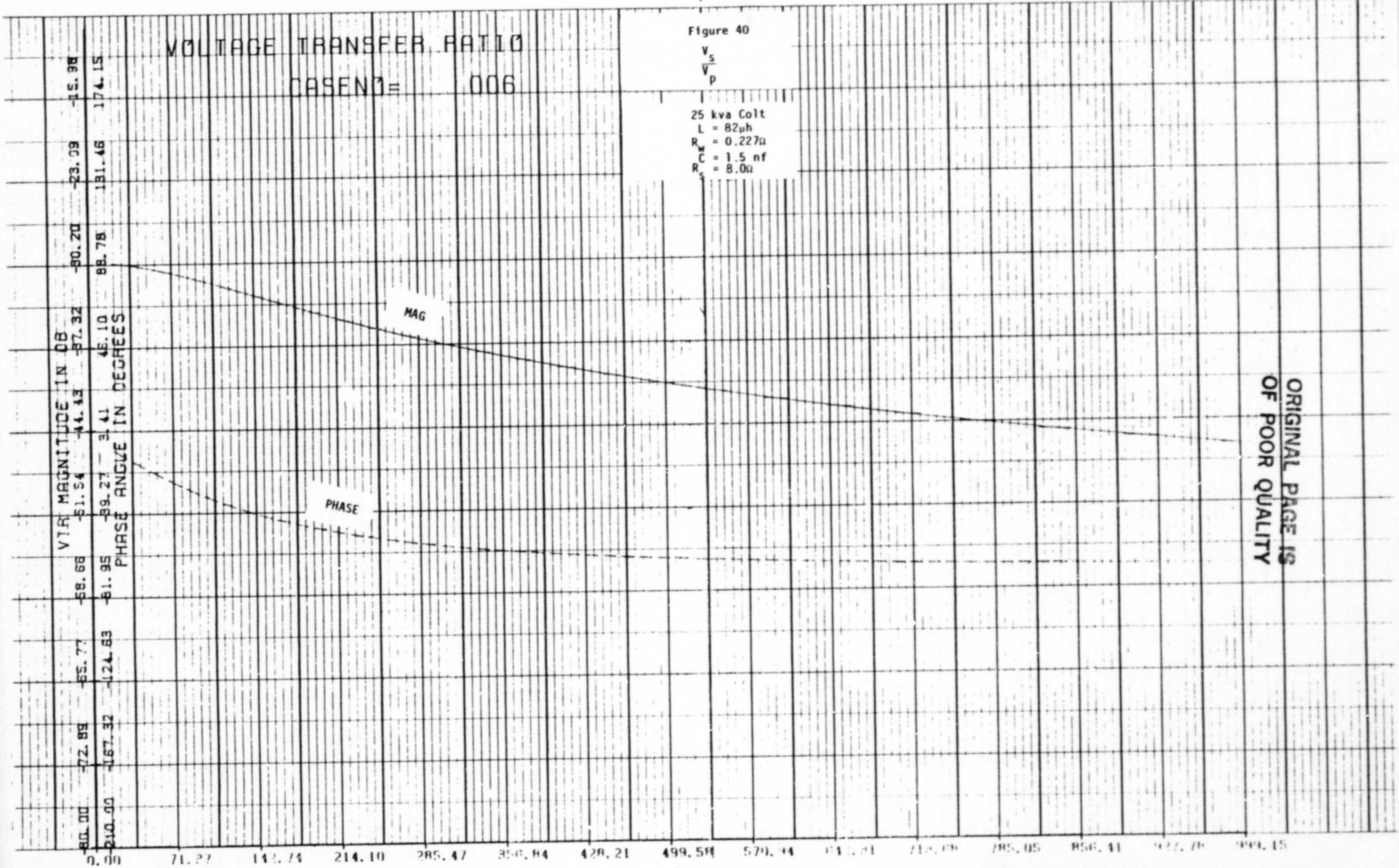

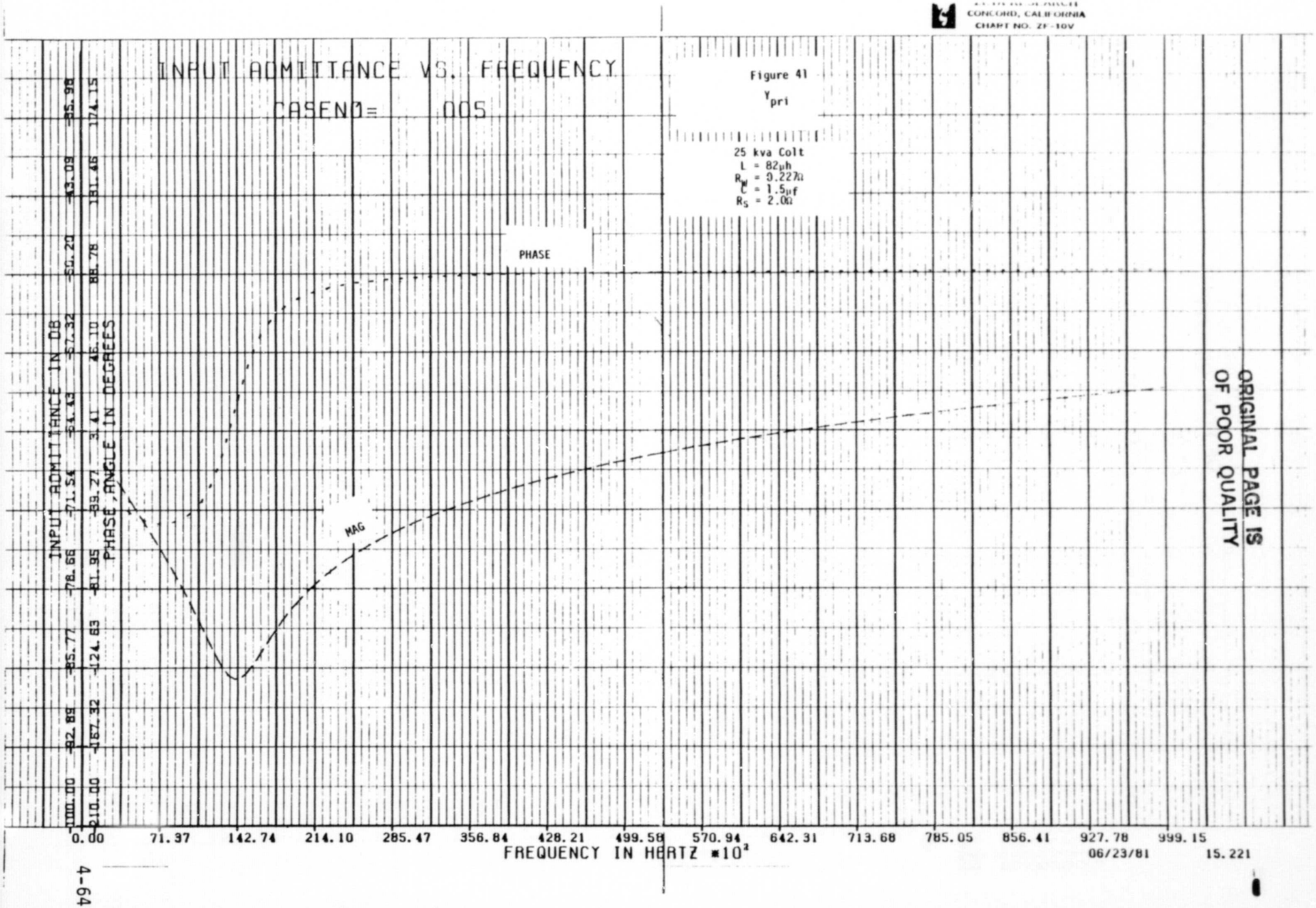

ORIGINAL PAGE IS
OF POOR QUALITY

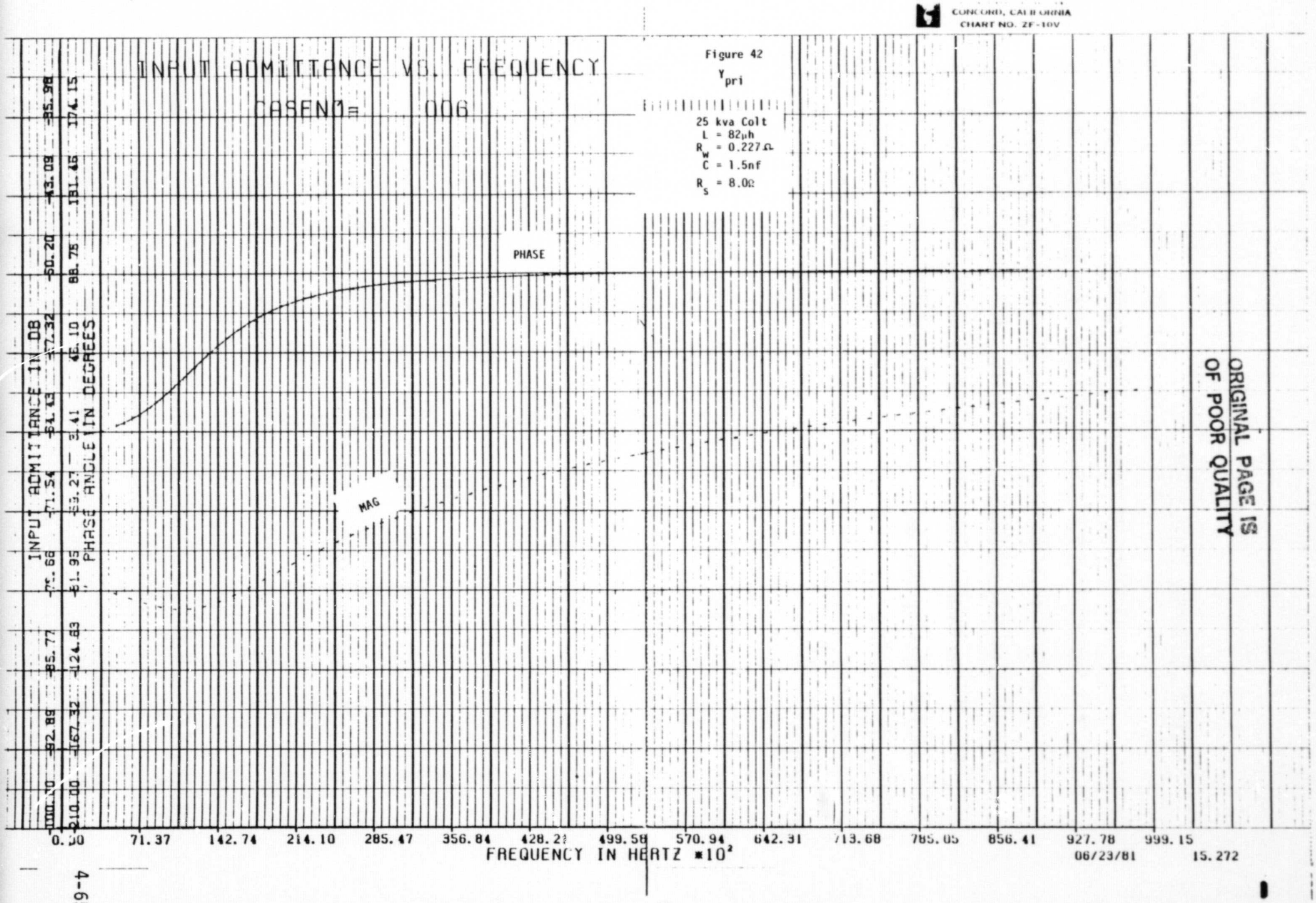

ORIGINAL PAGE IS
OF POOR QUALITY

Extended Frequency Measurement

Figure 43 shows the measured $\frac{V_p}{V_s}$ performance of the 25 kva GE transformer, from 5 kHz to 500 kHz for different values of R_p. It can be seen that, up to 50 kHz, these curves agree closely with the corresponding measured curves of Fig. 16. It can also be seen that the performance above 100 kHz indicates significantly more complex behavior than described by our simple model.

Figure 43

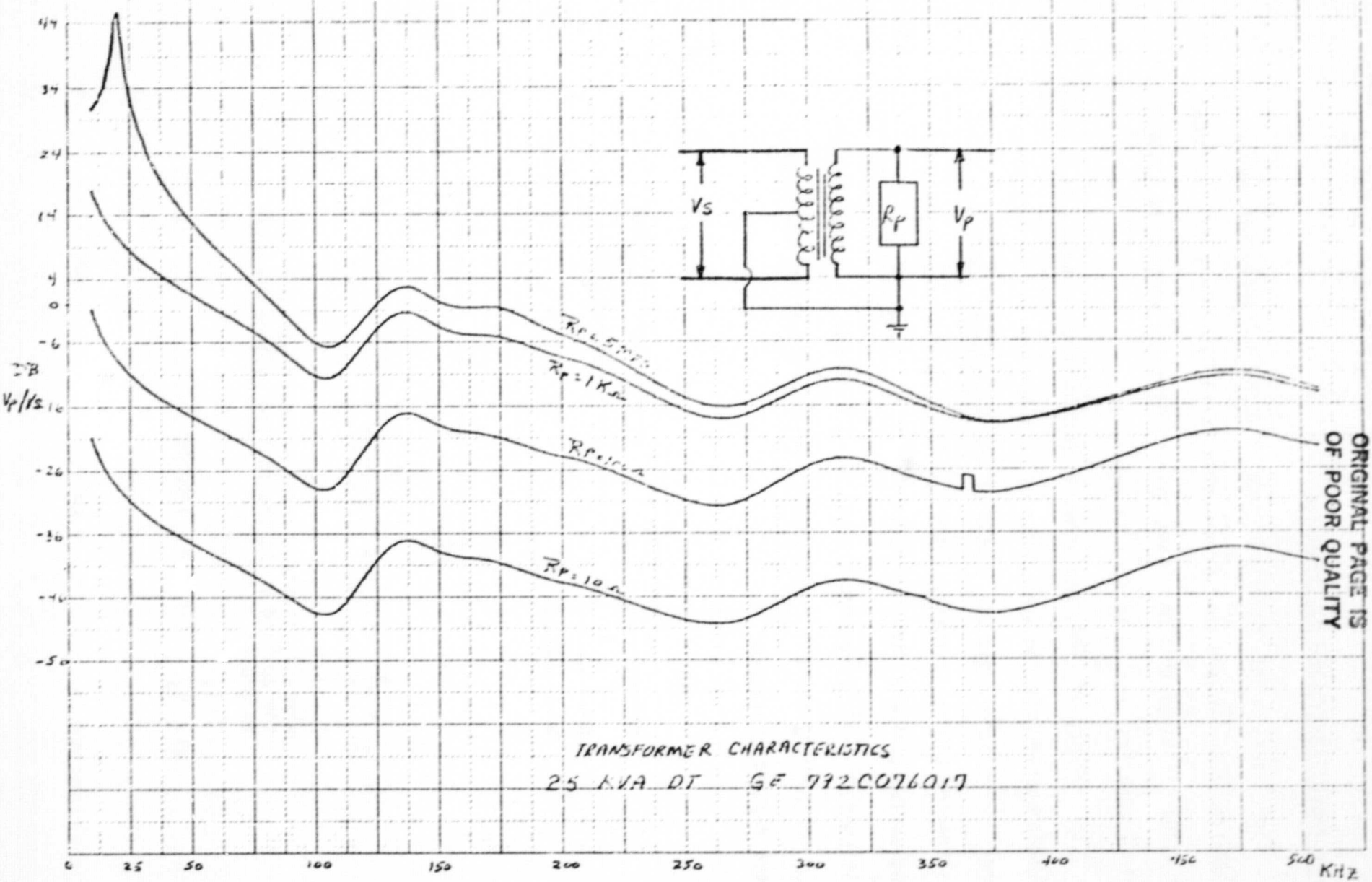

TRANSFORMER CHARACTERISTICS

25 K.V.A. DT GE 912C076017

Three Phase Transformer Measurements

Some measurements have been made of 3 phase transformer banks on earlier programs and that information is included here only to show the kinds of things that have been done to date and perhaps to suggest further work that should be done in this area.

In February of 1980, measurements were made on a number of 3 phase grounded wye to grounded wye pad mount transformers in the following manner. A resistor load was placed on the transformer secondary which consisted of 20% delta load and 80% wye load and with the total load being variable from no load to full load for each kva rating. Measurements were made at 4 frequencies from about 5-10 kHz and consisted of a Y_{11} measurement and a Y_{21} measurement which are defined according to the following diagram.

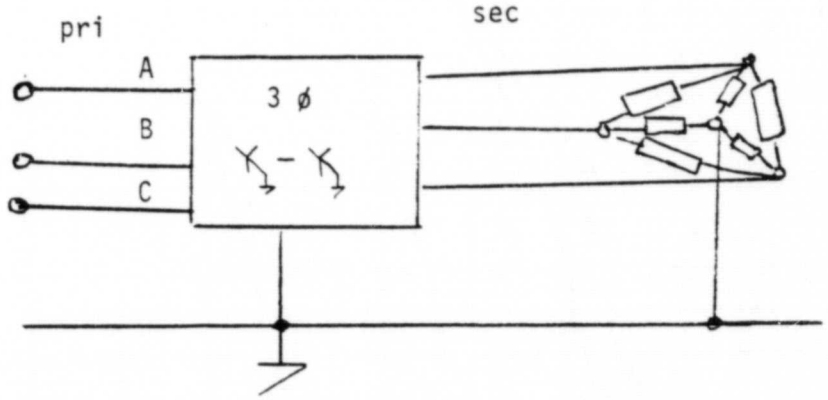

$$Y_{11} = \frac{I_A}{V_A}$$ with B & C grounded

where I_A is the current measured going into the box and V_A is the applied voltage measured to ground.

$$Y_{21} = \frac{I_A}{V_B}$$ with A & C grounded

The results of these measurements are shown in Fig. 44 for a 500 kva GE pad mount.

Similar measurements were made on a 3 phase bank connected also grounded wye to grounded wye and consisting of three 75 kva distribution transformers as shown in Fig. 45. Figure 46 shows the results of those measurements.

The same kind of measurements were made on a 3 phase bank consisting of two 25 kva transformers in an open delta configuration as shown in Fig. 47. Figure 48 shows the results of those measurements.

Figure 49 shows Y_{pri} for the 25 kva GE transformer previously mentioned when its secondary is connected in parallel for 3 phase wye-wye bank configuration. This is shown for various secondary loads.

Figure 44

500 KVA 277/480V
GENERAL ELECTRIC

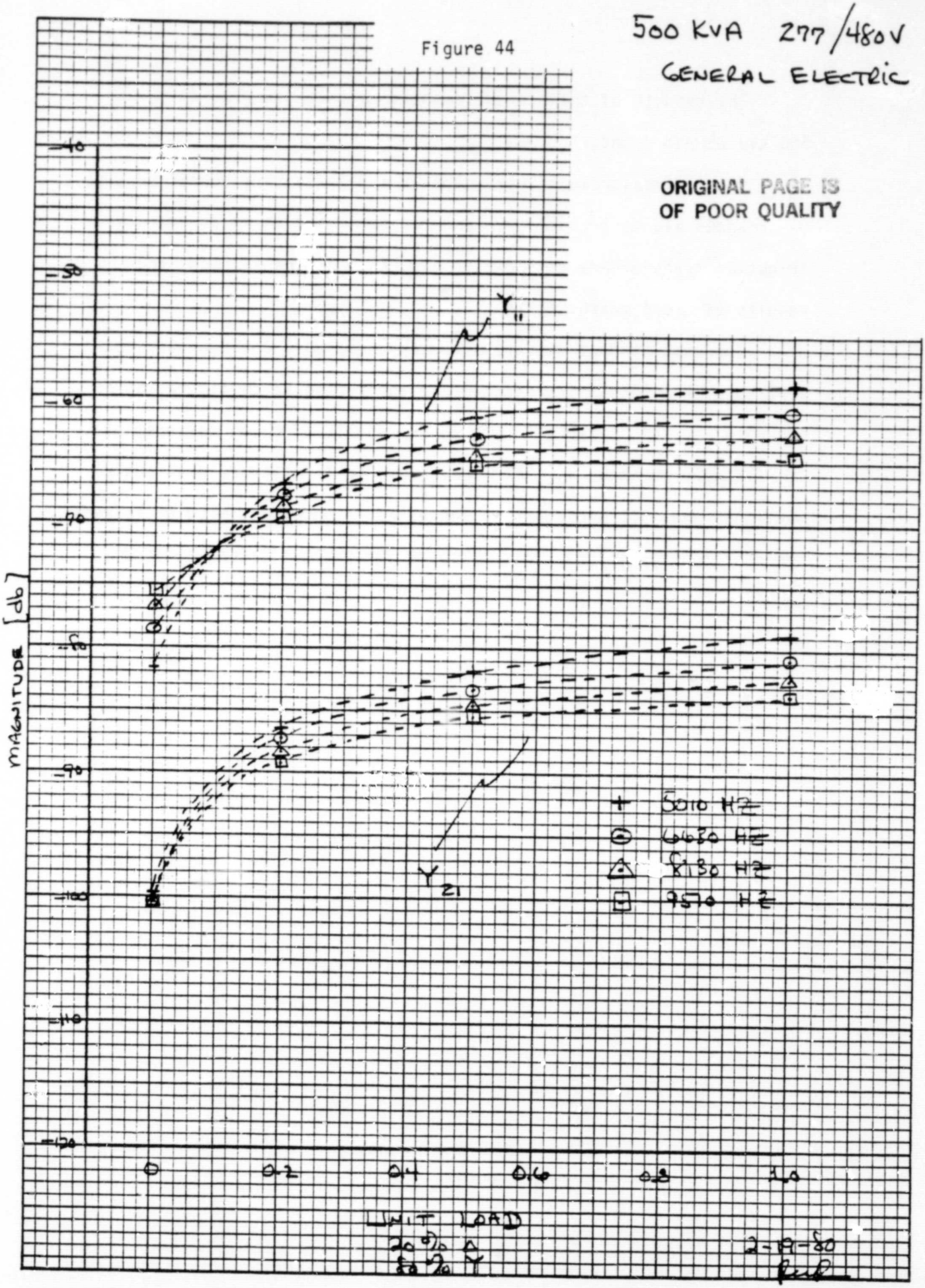

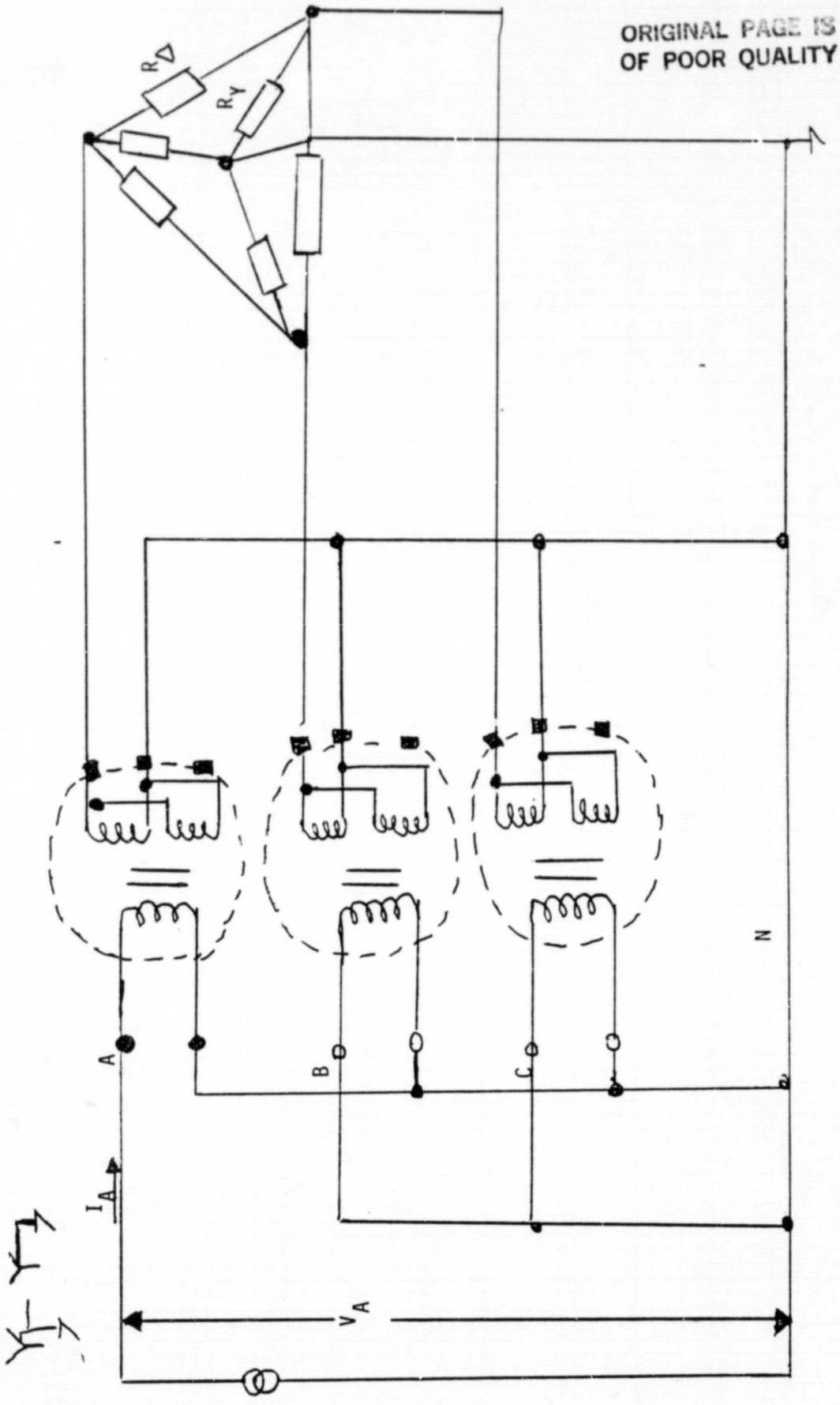

Figure 45
3-PHASE BANK

Figure 46

75 KVA
3 PHASE BANK

Primary → Secondary

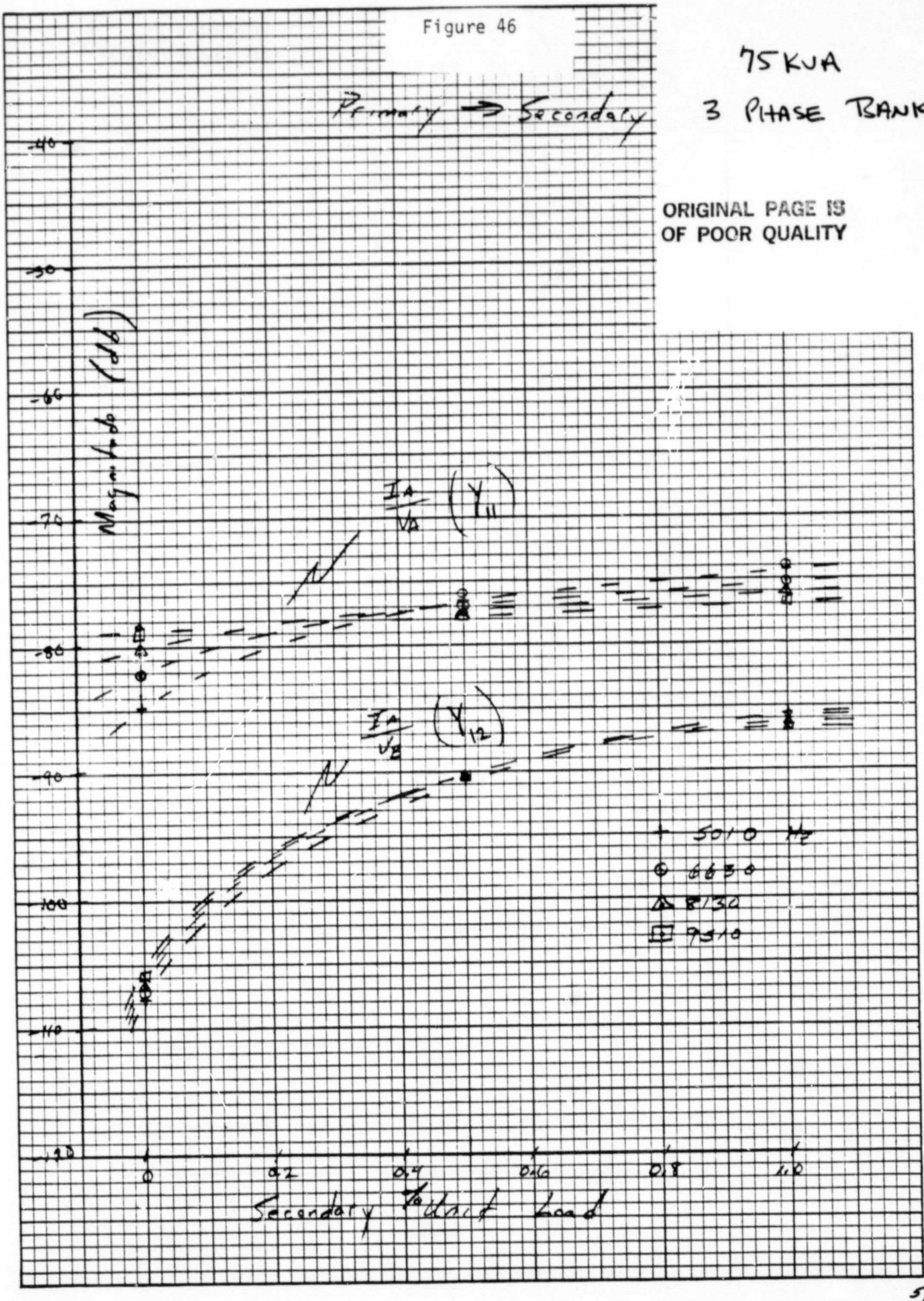

5/6/80
WPS

3-PHASE BANK

Using 2 2-Bushing 25 kva xfmrs [open delta]

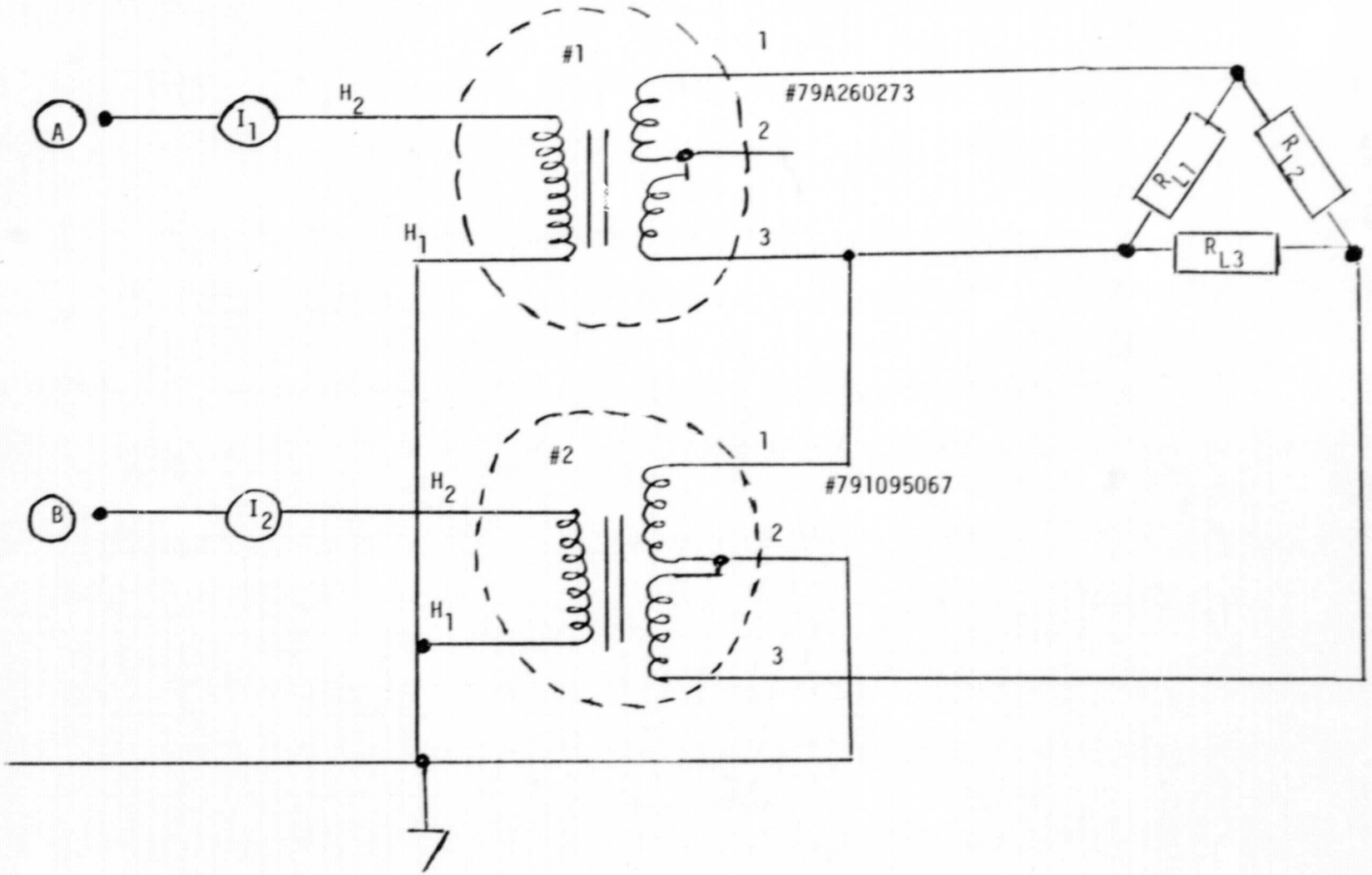

Figure 47

Figure 48

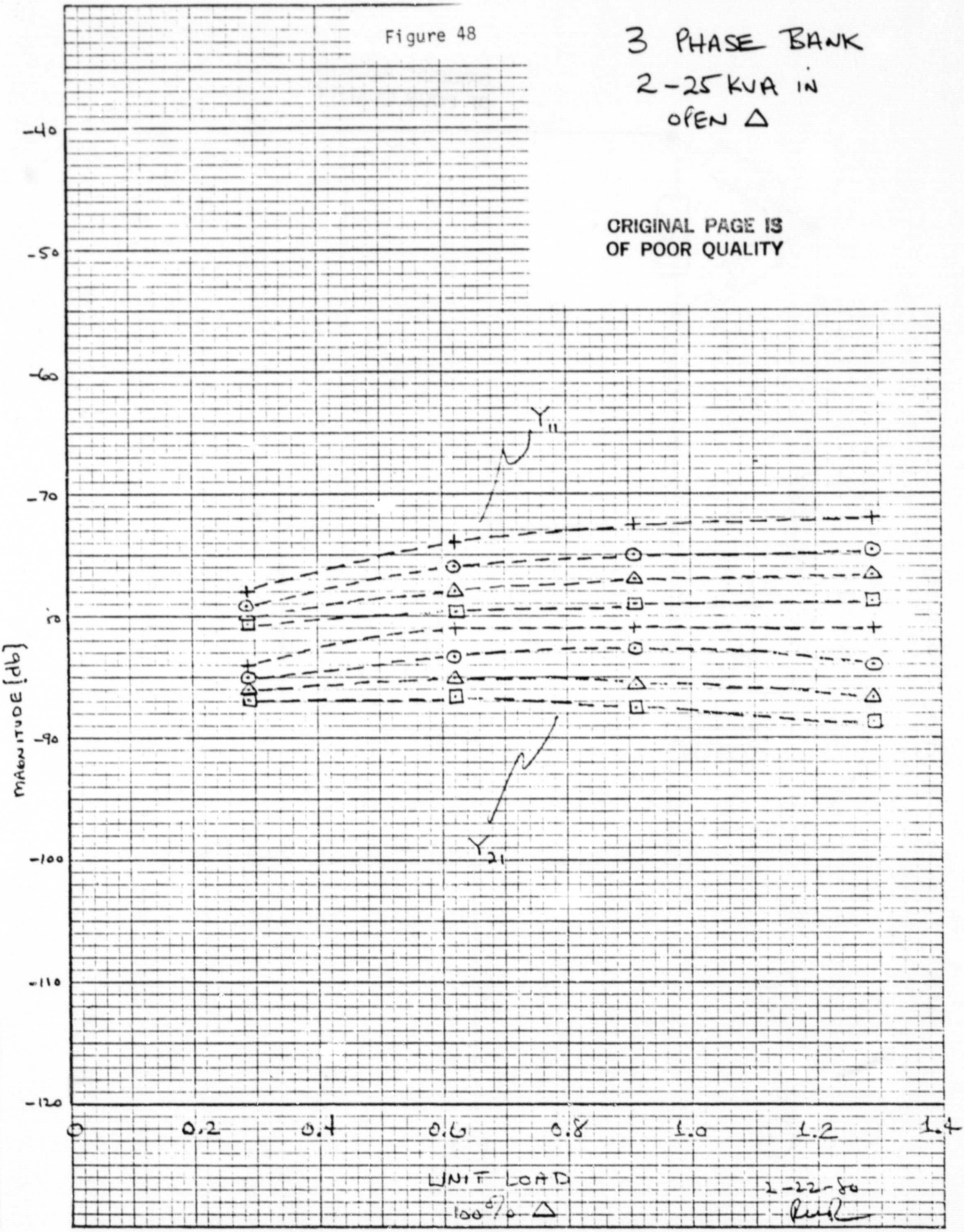
3 PHASE BANK
2-25 KVA IN
OPEN Δ
ORIGINAL PAGE IS
OF POOR QUALITY
-40
-50
-60
-70
-80
-90
-100
-110
-120
MAGNITUDE [db]
Y_{11}
Y_{21}
0
0.2
0.4
0.6
0.8
1.0
1.2
1.4
UNIT LOAD
100% Δ
2-22-80

Figure 49

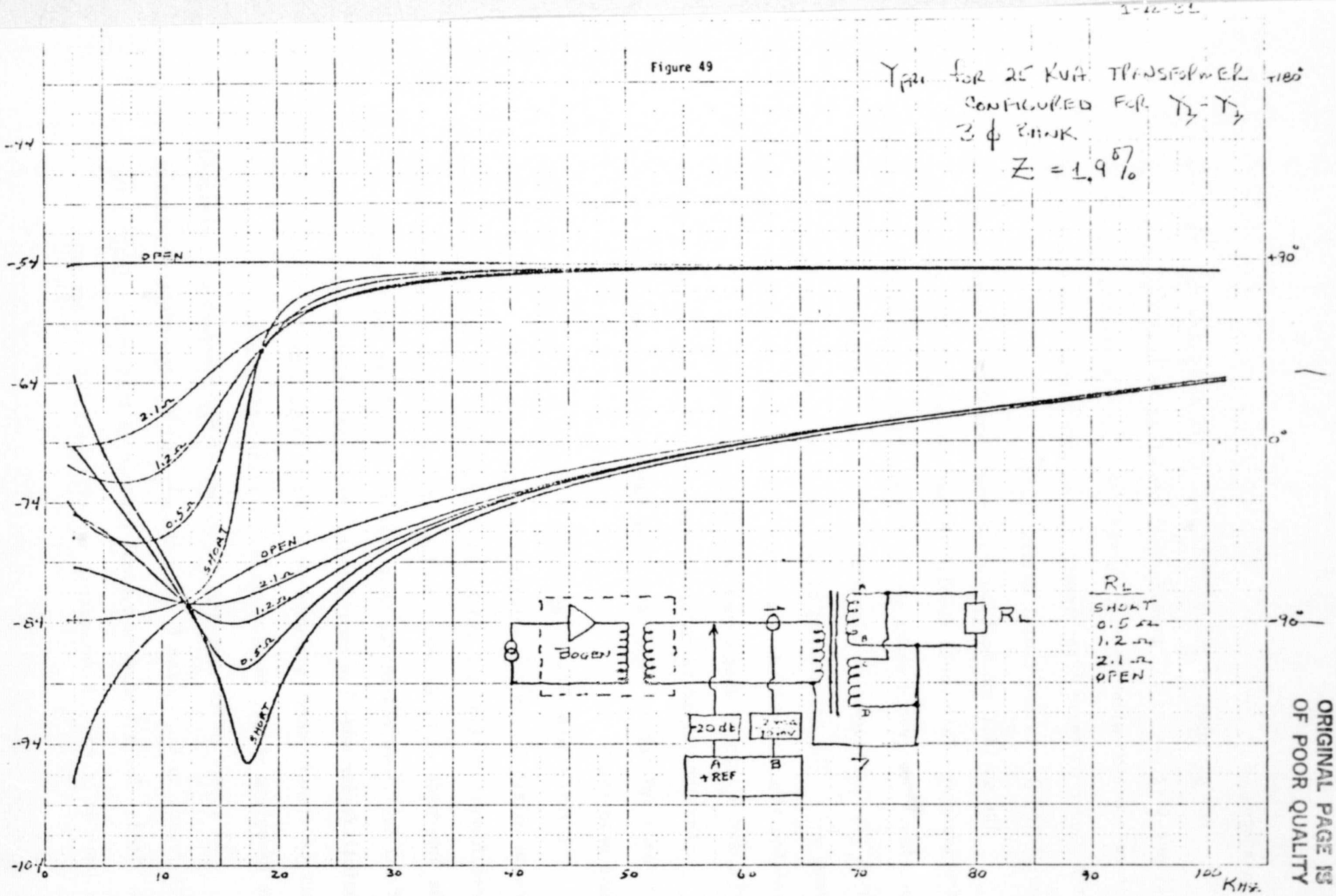

Data Bank

For purposes of feeder modeling, it is necessary to obtain the R_w, L, and C values of all transformers connected to that feeder so that, in conjunction with the transformer model just developed, the effect on the feeder of these transformers can be determined. Several ways of obtaining R_w, L, and C will be discussed.

The obvious and most accurate means would be to measure each transformer. This would involve the measurement of $\frac{1}{Z_{11}}$ and Y_{sc} as previously described where $\frac{1}{Z_{11}}$ is the admittance looking into the primary with the secondary open circuited. The value of C can be determined from $\frac{1}{Z_{11}}$. The measurement of Y_{sc} consists of measuring the admittance looking into the secondary with the primary short circuited. The values of L and R_w can be determined from this measurement.

Another method is to take a statistical average of R_w, L and C for each KVA rating based on a large number of measurements of the type just described.

A third method is to determine R_w and L from the nameplate data and to obtain C from a statistical average. The nameplate of each transformer contains a Z value, for example Z = 1.9%, which represents the impedance at 60 Hz when looking into the primary, as a percentage of the full load rating for that transformer. It is not clear, in typical feeder modeling applications, that the nameplate data of in-service transformers is always available without actually looking at the nameplate which, in most cases, is rather difficult.

As a part of this program, a number of transformers were measured with regard to R_w, L, and C using the $\frac{1}{Z_{11}}$ and Y_{sc} technique previously described. Table 1 shows a typical portion of that data. Table 2 is a summation of the L measurements for different KVA ratings and

DATA TAKEN AT 5.010 KHZ.

KVA	*** IDENTIFIER *** MANUFACTURER & SERIAL NUMBER			ZPC %	YS/SCP MAGNIT.	YS/SCP PHASE	YP/OCS MAGNIT.	YP/OCS PHASE	R OHMS	XL OHMS	L MH	C UF
10.0	GEN. ELEC.	M753081YCRA	S	2.03	-14.7 DB	-82.9	-92.8 DB	82.0	.671	5.391	.1713E+00	.7207E-03
10.0	MCGRAW EDISON	79NJ168-002	D	2.40	-18.3 DB	-87.5	-98.9 DB	81.7	.359	8.215	.2610E+00	.3508E-03
10.0	GEN. ELEC.	K312191Y1A	D	1.70	-10.8 DB	-82.1	-94.3 DB	85.1	.477	3.434	.1091E+00	.6101E-03
15.0	GEN. ELEC.	G974258-07Y	D	1.60	-8.4 DB	-81.7	-92.1 DB	85.6	.380	2.603	.8268E-01	.7865E-03
37.5	GEN. ELEC.	L264213Y74AA	D	2.15	-6.3 DB	-83.0	-90.0 DB	71.3	.252	2.050	.6512E-01	.9515E-03
37.5	WESTINGHOUSE	81A053308	D	3.10	-7.4 DB	-84.9	-90.7 DB	85.1	.208	2.335	.7418E-01	.9234E-03
37.5	WESTINGHOUSE	81A053801	D	3.10	-7.7 DB	-85.3	-92.0 DB	85.1	.199	2.418	.7683E-01	.7950E-03
50.0	MCGRAW EDISON	80NL121-020	D	2.60	-2.7 DB	-82.6	-95.0 DB	79.0	.176	1.353	.4299E-01	.9545E-03
50.0	MCGRAW EDISON	80NL121-015	D	2.00	-4.0 DB	-83.6	-94.9 DB	79.2	.177	1.575	.5003E-01	.8613E-03
50.0	MCGRAW EDISON	80NL121-011	D	2.00	-3.8 DB	-83.2	-97.1 DB	80.1	.183	1.538	.4886E-01	.4370E-03
75.0	MCGRAW EDISON	81ZA172-002	D	1.60	2.2 DB	-81.9	-97.8 DB	79.2	.109	.769	.2441E-01	.4020E-03
75.0	MCGRAW EDISON	81ZA172-003	D	1.60	2.1 DB	-82.1	-96.8 DB	79.1	.108	.778	.2471E-01	.4509E-03
100.0	WESTINGHOUSE	71AD9549	D	1.60	2.6 DB	-84.0	-87.3 DB	84.7	.077	.737	.2342E-01	.1365E-02

DATA TAKEN AT NIMPC — SENECA ST

TABLE 1

TABLE 2

L(mh) Measured at 5010 Hz

	10 KVA	15 KVA	25 KVA	37.5 KVA	50 KVA	75 KVA	100 KVA
Allis-Chalmers	.133		.049	.032			
GE	.171 .109	.109 .083	.086 .090 .041	.065			
McGraw-Edison	.261		.116 .114 .076	.059	.042 .050 .049	.024 .025	
Colt			.082 .076 .060 .109 .046 .113	.041	.064		
Westinghouse	.152		.086	.074 .076	.056		.023 .020
Kuhlman			.043	.025	.042 .040		
Porter	.209 .202 .154	.177	.088	.037	.050		
Howard	.075						
RTE			.046 .052		.028		
Line Material			.045	.025 .023			
Mean	0.16	0.123	0.075	0.046	0.045	0.024	0.022
Standard Deviation	.06	.05	.03	.02	.01	—	—

manufacturers. Table 3 is a summation of the C measurements, again as a function of KVA and manufacturer and Table 4 is the same for R_w.

In Table 3, the values under the "measured" column were obtained from a measurement of $\frac{1}{Z_{11}}$ and the values under the "Bridge" column were obtained using an ECD Model 100 capacitance bridge from one primary terminal to the neutral connection.

A comparison of C values obtained from both actual measurement and bridge measurement on the same 25 KVA transformers is shown below:

Manufacturer	$\frac{1}{Z_{11}}$	ECD Bridge
Colt	1.47 nf	2.1 nf
McGraw-Edison	1.25 nf	1.24 nf
" "	1.25 nf	1.25 nf

The agreement between the 2 measurement techniques is good for the two McGraw-Edison's, however, the bridge reading for the Colt is about 43% higher.

Figures 50-52 show statistical values for L, R_w, and C as a function of KVA as obtained from Tables 2, 3 and 4.

As previously mentioned, another method for obtaining R_w and L is to use the Z percentage value stamped on the nameplate of all distribution transformers.

Table 5 shows R_w and X_L (at 5010 Hz) obtained from nameplate data of all the transformers measured and compares the accuracy of this method with that for the statistical determination.

Looking at Table 5, the Z column, in percent, is nameplate data and represents that part of the impedance, at 60 Hz, seen when looking

Figure 50

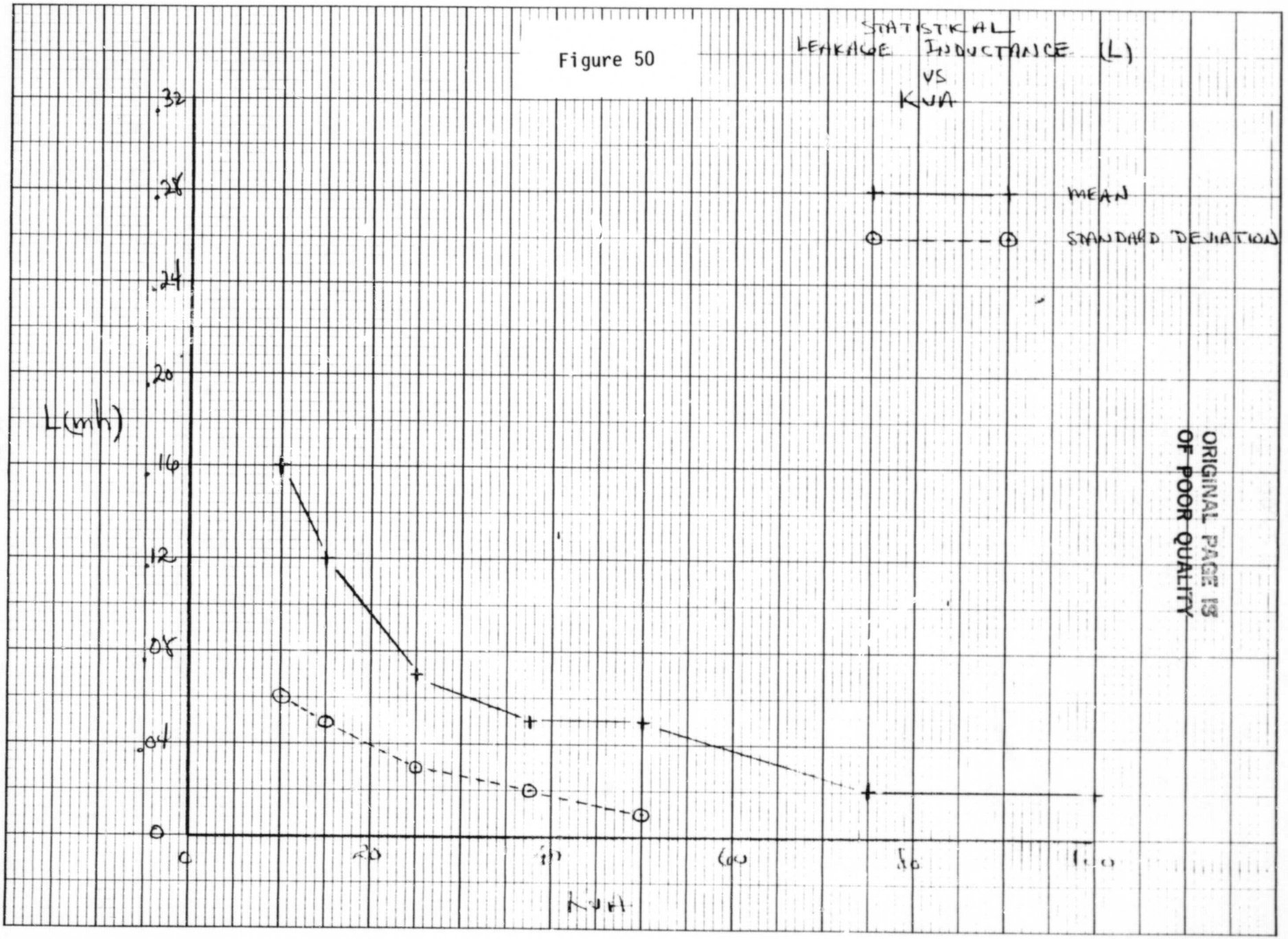

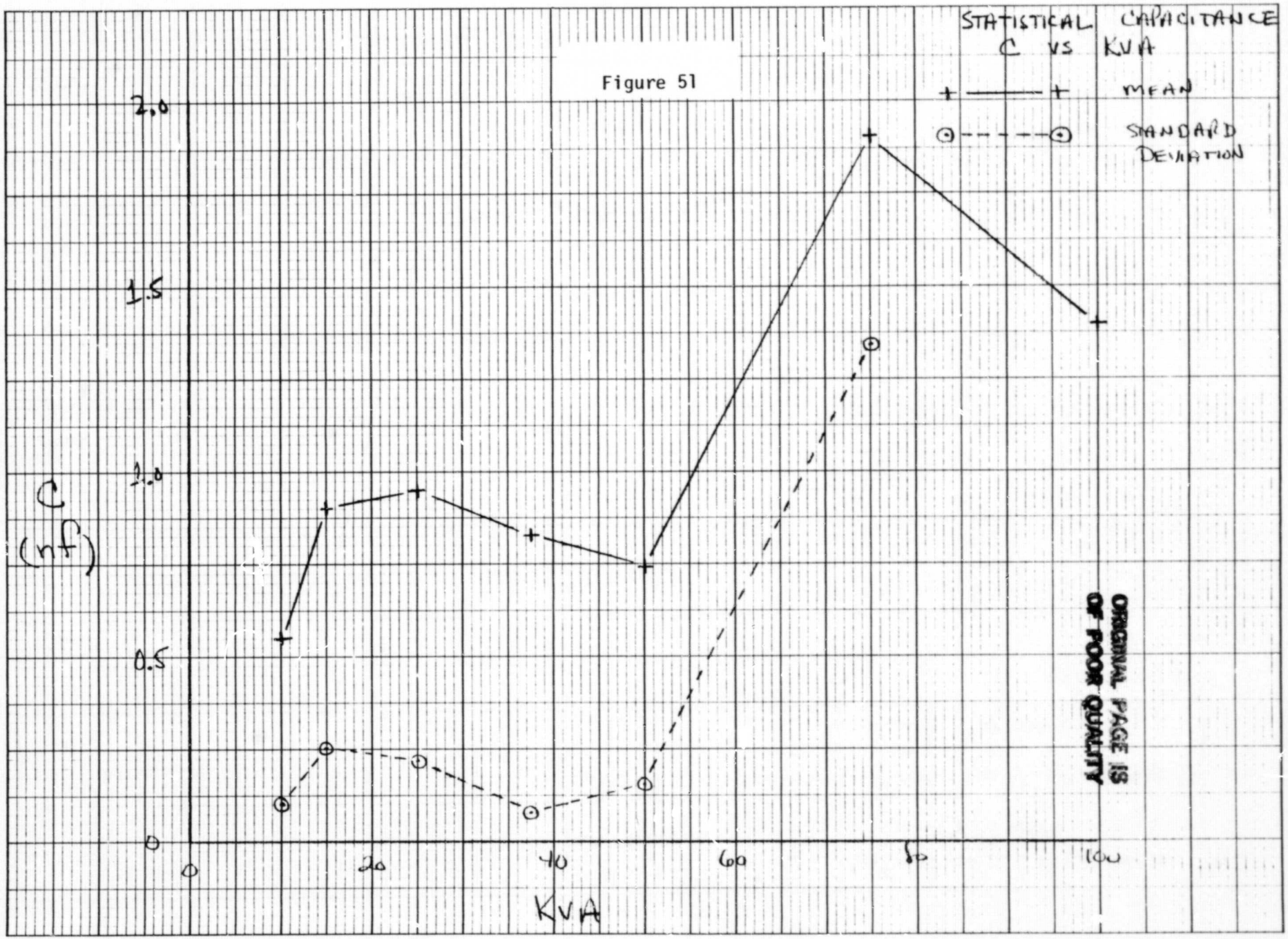

Figure 51

Figure 52

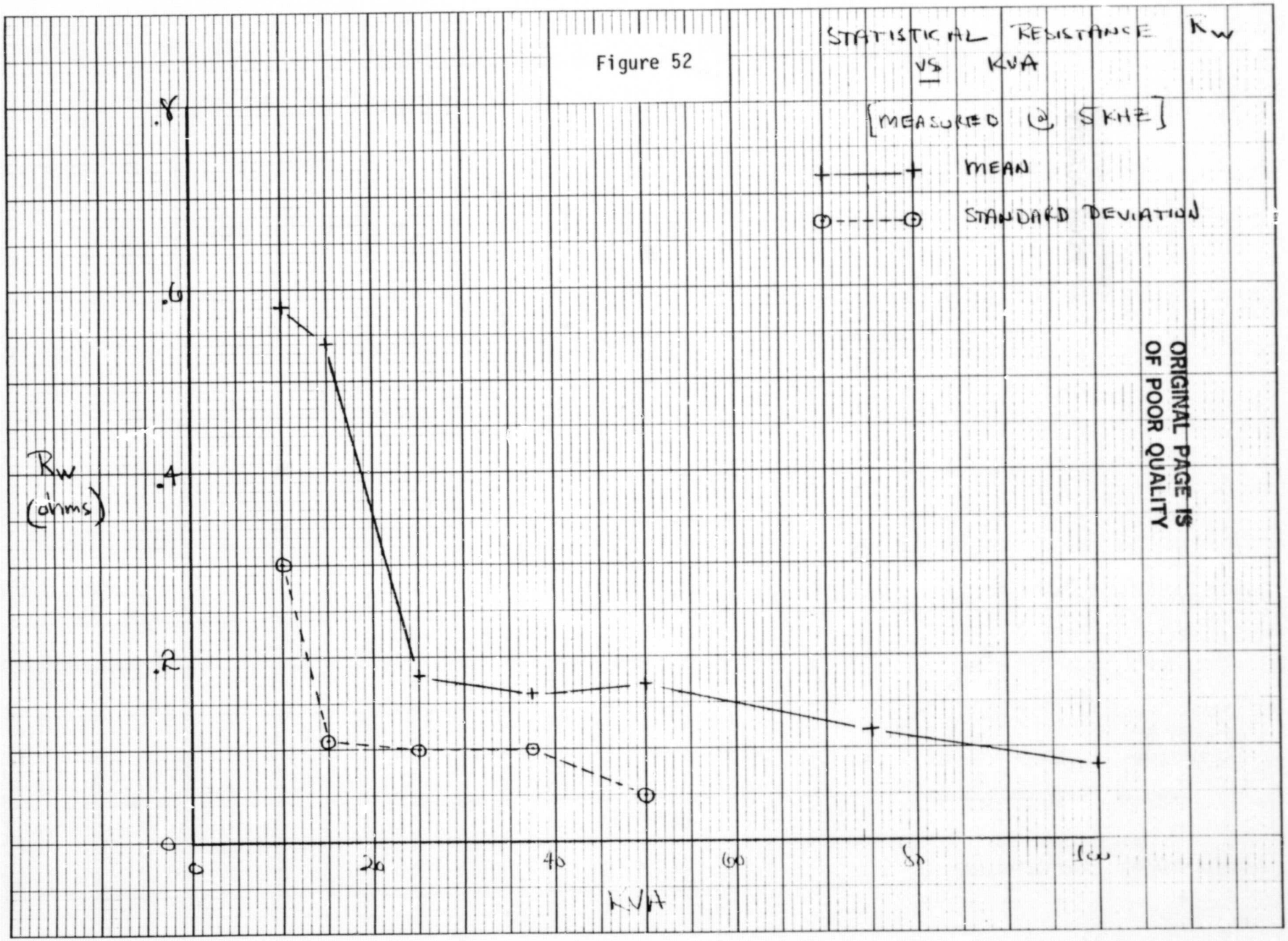

TABLE 3

C (nf) Measured at 5010 Hz

Allis-Chalmers	10 KVA		15 KVA		25 KVA		37.5 KVA		50 KVA		75 KVA		100 KVA	
	Meas.	Bridge	Meas.	Bridge	Meas.	Bridge	Meas.	Bridge	Meas.	Bridge	Meas.	Bridge	Meas.	Bridge
GE	.72 .61	.59 .56	.79	.6 1.5 .9 .8 .9 .8 .8	1.2	.6 .63	.95					2.7 2.9 3.1		
McGraw-Edison	.36				1.2 1.2	.73 .61 .99 1.05			.55 .56 .44	.84 .84 .89 .79 .78 .85 .83	.40 .45			
Colt					1.4									
Westinghouse				.93 .7 1.2		.85 .88 .73	.92 .80	.75 .77 .79					1.4	
Kuhlman						1.0 .9 1.0 1.0								
Porter														
Howard		.55 .54 .55												
RTE						1.0 1.0								
Line Material														
Mean	0.56		0.90		0.95		0.83		0.74		1.91		1.4	
Standard Deviation	0.10		0.25		0.22		0.88		0.16		1.36		---	

TABLE 4

R_w (ohms) Measured at 5010 Hz

	10 KVA	15 KVA	25 KVA	37.5 KVA	50 KVA	75 KVA	100 KVA
Allis-Chalmers	1.25		0.08	.04			
GE	.73 .53	.42 .62	0.30 .14 .08	.28			
McGraw-Edison	.40		.23 .19 .17	.16	.19 .19 .20	.12 .12	
Colt			.1 .23 .19 .24 .23 .48	.04	.17		
Westinghouse	.53		.19	.23 .22	.19		.09 .07
Kuhlman			.09	.04	.18 .19		
Porter	.40 .43 .33	.58	.23	.08	.19		
Howard							
RTE			.09 .09		.04		
Line Material			.14		.04 .04		
Mean	0.58	0.54	0.18	0.16	0.17	0.12	0.08
Standard Deviation	0.30	0.11	0.10	0.10	0.05	---	---

into the primary of the transformer, at rated load, which is contributed by the transformer itself.

As an example, take the 1st transformer of Table 5, a 10 KVA Allis-Chalmers transformer with a nameplate Z value of 1.5%. To get this Z value in terms of 5000 Hz, which are the values listed in column 1, use the formula:

$$Z_{NP\text{-}5000} = .015 \left(\frac{240^2}{10{,}000}\right) \left(\frac{5000}{60}\right)$$

Columns 3, 4, and 5 show the actual measured values of R_W, X_1 and Z for each transformer at 5000 Hz. A comparison of columns 1 and 5 shows that the Z value obtained from the nameplate is larger than the measured value. No attempt is made here to explain this difference. Column 6 is a ratio of measured Z to the nameplate Z and averaging this ratio for all the 10 KVA transformers led to the .55 value shown in column 6. The nameplate Z's were then multiplied by this .55 factor and column 2 was generated and called Z'_{NP}.

Obviously Z_{NP} consists of both R_W and X_1 but it is not obvious in what proportion. Again, the measured ratio of X to R_W was computed and this is shown in column 7. An average of the ratio, for 10 KVA transformers, was found to be 14.46 and this means that, at 5000 Hz, the R_W is an insignificant part of Z and therefore the following is assumed to be true:

$$X'_L = Z'_{NP} \text{ at 5000 Hz.}$$

Column 8 represents the difference between the value of X_1 determined from the nameplate and the measured value for each transformer. Column 9 shows the difference between the value of X_L obtained by averaging all the measured values of X_L and the measured value itself.

A comparison of columns 8 and 9 shows that the average difference is less for the nameplate method but perhaps not significantly.

While R_W is not significant at 5000 Hz, it does become significant at higher frequencies and therefore, if nameplate data is to be used, a determination of R_W must be made at 5000 Hz so that it can be used in the previously mentioned formula

$$R_W = \frac{R'_W}{.14} \left(\frac{f}{20,000}\right)^{1.4}$$

where $R'_W = R_W$ (in ohms) measured at 5000 Hz

To obtain R'_W, the Z obtained from the nameplate was divided by the averaged ratio of $\frac{X_L}{R_W}$ of column 7 and these values of R'_W are shown in column 10.

Column 11 shows the difference between the R_W values of column 10 and the measured R_W values of column 4. Column 12 shows the difference between the measured values of column 4 and the averaged values of column 4. A comparison of columns 11 and 12 show minimal difference between the 2 methods.

It appears that taking a statistical average for the values of R_W and L does not appreciably degrade the results as compared to the nameplate method and it is probably significantly easier to achieve.

It is recommended that more statistical data be taken on transformers, especially with regard to L and C.

TABLE 5

A Comparison of Measured, Statistical and Nameplate Values for X_L and R_W at 5000 Hz

		1	2	3	4	5	6	7	8	9	10	11	12
		Z_{NP} (ohms)	Z'_{NP} (ohms)	X_L (ohms)	R_W (ohms)	Z_m (ohms)	$\frac{Z_m}{Z_{NP}}$	$\frac{X_L}{R_W}$	X'_L Deviation (ohms)	X''_L Deviation (ohms)	R'_W (ohms)	R'_W Deviation (ohms)	R'' Deviation (ohms)
10 KVA	**Z**												
Allis-Chalmers	1.5	7.21	3.97	4.18	1.25	4.36	.61	3.34	.21	.97	.27	.98	.75
GE	2.03	9.96	5.37	5.39	0.67	5.43	.56	8.04	.02	.24	.37	.30	.17
McGraw-Edison	2.4	11.54	6.35	8.22	0.36	8.23	.71	22.83	1.87	3.07	.44	.08	.14
GE	1.7	8.18	4.50	3.43	0.48	3.46	.42	7.15	1.07	1.72	.31	.17	.02
Porter	1.9	9.12	5.26	6.59	0.41	6.60	.69	16.07	1.33	1.44	.36	.05	.04
Porter	2.8	13.44	7.39	6.42	0.43	6.43	.48	14.93	.97	1.27	.51	.08	.07
Porter	1.8	8.64	4.75	4.89	0.34	4.90	.57	14.38	.14	.26	.33	.01	.16
Westinghouse	1.7	8.18	4.50	4.43	0.53	4.92	.60	9.11	.33	.32	.31	.22	.03
Howard	1.8	8.64	4.75	2.40	0.07	2.40	.28	34.29	2.35	2.75	.33	.26	.43
	Avg ⇒			5.15	0.50		.55	14.46	.92	1.34		.24	.21
15 KVA													
GE	1.8	5.77	3.02	3.43	0.62	3.49	.6	5.53	.49	.45	.54	.08	.12
GE	1.6	5.13	3.49	2.60	0.38	2.63	.51	6.84	.89	1.28	.36	.02	.12
Porter	1.9	6.08	4.13	5.62	0.59	5.65	.93	9.53	1.49	1.74	.77	.15	.09
	Avg ⇒			3.88	0.53		.68	7.3	.96	1.16		.09	.11
25 KVA													
GE	1.9	3.66	2.34	2.71	.14	2.71	.74	19.36	.37	.55	.17	.03	.05
Colt	1.9	3.66	2.34	2.58	.23	2.59	.71	11.22	.24	.22	.17	.06	.04
McGraw-Edison	2.3	4.42	2.83	3.65	.21	3.66	.83	17.38	.82	1.29	.20	.01	.02
McGraw-Edison	2.3	4.42	2.83	3.59	.19	3.60	.81	18.89	.76	1.23	.20	.01	0
Colt	1.7	3.27	2.09	1.89	.48	1.95	.60	3.94	.20	.47	.15	.33	.28
Kuhlman	1.7	3.26	2.09	1.41	.09	1.41	.43	15.67	.68	.95	.15	.06	.10
RTE	1.7	3.26	2.09	1.46	.09	1.46	.45	16.22	.63	.90	.15	.06	.10
Westinghouse	1.9	3.65	2.34	2.69	.19	2.70	.74	14.16	.35	.33	.17	.02	0
GE	1.7	3.26	2.09	2.78	.32	2.80	.86	8.69	.69	.42	.15	.17	.13
GE	2.0	3.84	2.46	1.30	.08	1.30	.34	16.25	1.16	1.06	.18	.10	.11
Colt	2.0	3.84	2.46	1.45	.11	1.45	.38	13.18	1.01	.91	.18	.07	.08
Colt	1.7	3.26	2.09	2.44	.20	2.45	.75	12.20	.35	.08	.15	.05	.01
Line Material	2.1	4.03	2.58	1.42	.15	1.43	.35	9.47	1.16	.94	.18	.03	.04
Allis-Chalmers	2.1	4.03	2.58	1.54	.08	1.54	.38	19.25	1.04	.82	.18	.10	.11
McGraw-Edison	1.8	3.46	2.21	2.39	.23	2.40	.69	10.39	.15	.03	.16	.07	.04
Porter	1.8	3.46	2.21	2.76	.23	2.71	.60	12.00	.55	.40	.16	.07	.04
Colt	1.9	3.66	2.34	3.49	.24	3.50	.96	14.54	1.15	1.13	.17	.07	.05
Colt	2.0	3.84	2.46	3.63	.24	3.64	.95	15.13	1.17	1.27	.18	.06	.05
RTE	2.3	4.42	2.83	1.66	.09	1.66	.38	16.44	1.17	.70	.20	.11	.13
	Avg ⇒			2.36	0.19		.64	14.02	.42	.71		.08	.07

Table 5 (cont'd)

A Comparison of Measured, Statistical and Nameplate Values for X_L and R_W at 5000 Hz

		1	2	3	4	5	6	7	8	9	10	11	12	
		Z_{NP} (ohms)	Z'_{NP} (ohms)	X_L (ohms)	R_W (ohms)	Z_m (ohms)	$\frac{Z_m}{Z_{NP}}$	$\frac{X_L}{R_W}$	X'_L Deviation (ohms)	X''_L Deviation (ohms)	R'_W (ohms)	R'_W Deviation (ohms)	R'' Deviation (ohms)	
37.5 KVA	**Z**													
Colt	1.5	1.92	1.04	1.29	.036	1.29	.67	35.83	.25	.16	.060	.024	.024	
GE	2.15	2.76	1.49	2.05	.252	2.07	.75	8.13	.50	.60	.087	.165	.142	
Westinghouse	3.1	3.97	2.14	2.31	.208	2.36	.59	11.25	.20	.89	.124	.084	.084	
Westinghouse	3.1	3.97	2.14	2.42	.199	2.43	.61	12.16	.28	.97	.124	.075	.089	
Kuhlman	1.5	1.92	1.04	0.80	.041	.80	.42	19.51	.24	.65	.060	.019	.069	
Porter	2.3	2.94	1.59	1.17	.088	1.17	.40	13.30	.42	.28	.092	.004	.022	
McGraw-Edison	1.8	2.30	1.24	1.88	.166	1.89	.82	11.33	.64	.43	.072	.094	.056	
Line Material	1.6	2.05	1.11	0.80	.048	.80	.39	16.67	.31	.65	.065	.017	.015	
Line Material	1.65	2.11	1.14	0.73	.037	.73	.35	18.72	.41	.72	.060	.027	.071	
Allis Chalmers	1.9	2.43	1.31	1.03	.041	1.03	.42	25.12	.28	.42	.076	.035	.069	
	AVG ⇒			1.45	0.11		.54	12.20	.36	.58		.054	.075	
50 KVA														
Kuhlman	1.5	1.44	1.17	1.29	.18	1.30	.90	7.17	.12	.19	.123	.031	.01	
McGraw-Edison	2.0	1.92	1.56	1.35	.176	1.36	.71	7.67	.21	.13	.164	.012	.01	
McGraw-Edison	2.0	1.92	1.56	1.58	.177	1.59	.83	8.93	.02	.10	.164	.013	.01	
McGraw-Edison	2.0	1.92	1.56	1.54	.183	1.55	.81	8.42	.02	.06	.164	.019	.01	
Kuhlman	1.6	1.54	1.25	1.27	.185	1.28	.83	6.86	.02	.21	.131	.031	.02	
Westinghouse	2.1	2.02	1.64	1.81	.203	1.82	.90	8.92	.17	.33	.172	.031	.03	
Porter	2.0	1.92	1.56	1.61	.200	1.62	.84	8.05	.05	.13	.164	.036	.03	
Colt	2.0	1.92	1.56	2.01	.174	2.02	1.05	11.55	.45	.53	.164	.010	0	
RTE	2.2	2.11	1.71	0.89	.049	.89	.42	18.16	.82	.59	.179	.130	.12	
	AVG ⇒			1.48	.17		.81	9.53	.21	.25		.04	.03	
75 KVA														
McGraw-Edison	1.6	1.03	.78	0.77	.109	.78	.76	7.06	.01	0	.109	0	0	
McGraw-Edison	1.6	1.03	.78	0.78	.108	.79	.77	7.22	0	.01	.109	0	0	
	AVG ⇒			0.77	.108		.76	7.14	.01	.01		0	0	
100 KVA														
Westinghouse	1.6	0.77	.77	0.74	.077	.74	1.0	9.601	0	—	.08	0	—	

TASK 5

COMPENSATION OF POWER DISTRIBUTION SYSTEMS FOR ENHANCEMENT OF POWER LINE CARRIER COMMUNICATION RELIABILITY

TASK 5

TABLE OF CONTENTS

	Page
Introduction	5-1
Simple, Lossless Two-Wire Line with Transformer	5-2
Reverse Path Considerations in a Two-Wire System	5-5
Signal-To-Noise Ratio Considerations on a Simple Line	5-6
Compensation of Simple Lines	5-11
Generalization of Compensation Procedure to Lossless Tree Networks	5-13
Extension to Two Wire, Loaded, Lossy Lines	5-15
Generalization of Compensation Procedure to Lossy Tree Networks	5-19
Compensation Over a Band of Frequencies	5-20
Extension to Polyphase Lines	5-22
Conclusions	5-22

CONTRIBUTORS

J. T. Gajjar

Introduction

Power distribution systems are increasingly being used for communications and control using power line carrier technology. For applications like meter reading, it is important to have a two-way communication path.

Often, due to the length of sections of line involved, and due to branching, some points on a distribution feeder are difficult to access. This may occur due to standing wave nulls in the voltage profile. In such cases, it may be desirable to compensate sections of distribution feeders so as to improve reliability of communications to and from such points. In the present report we investigate the mechanisms of signal propagation on distribution systems and develop procedures useful in determining locations and types of compensations which can be used to enhance communication reliability on such systems.

Inasmuch as the compensation approach we use is procedure oriented, it is useful to obtain an understanding of the factors which determine propagation transfer functions on networks having structures similar to those of distribution systems; distributed tree networks. To that end, we first consider propagation on a lossless section of two-wire line having a transformer on it and look at the factors which determine propagation to and from the transformer secondary, taking into consideration

typical properties of the distribution transformers. Following this, we develop compensation procedures on such a line. The results of this analysis are then extended to distributed tree networks of two-wire lines and subsequently to multi-conductor systems. In order to simplify analysis, we introduce appropriate approximations. These are motivated and justified from practical considerations and from experience gained in working with distribution system computer models and field experimental measurements.

A. Simple, Lossless Two-wire Line with Transformer

Figure 1 shows a lossless two-wire transmission line of length ℓ, with a distribution transformer connected at a distance d from the input end. The transformer primary input impedance is assumed to be large in comparison with the characteristic impedance of the line Zo (= 1/Yo). Typical values of line characteristic impedances range from 100 ohms to 400 ohms, while primary side input impedances of distribution transformers range from 10 Kilo-ohms to 100 Kilo-ohms.

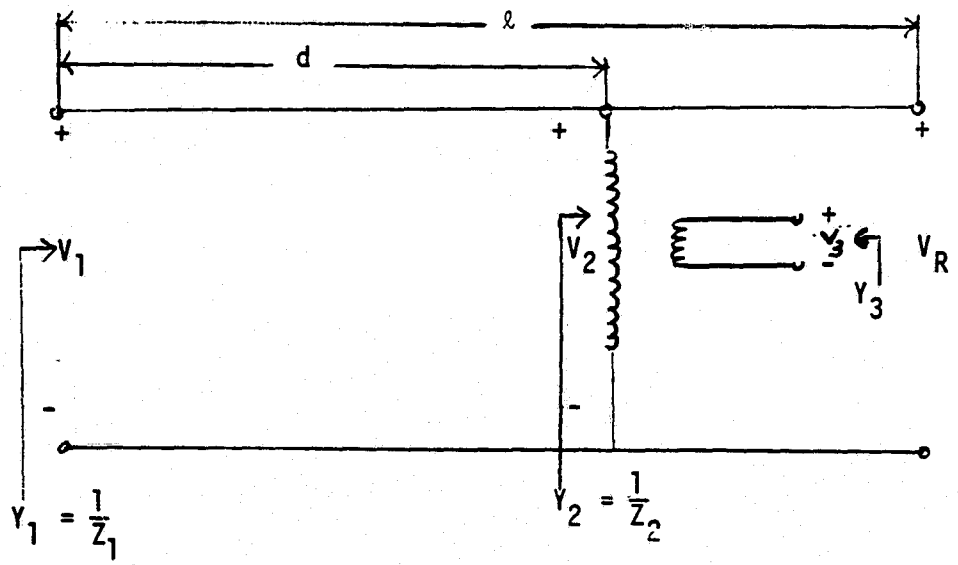

Figure 1

In order to obtain the voltage transfer, one may proceed as follows. Let the secondary terminals of the distribution transformer be open circuited. Let a voltage vector of value V_1 be impressed at the input.

The voltage V_3, developed at the secondary terminal of the transformer, will be equal to the product of the voltage V_2 developed at the primary terminals of the distribution transformer and the voltage ratio of the transformer. The current , at the input end, will be the product of the input admittance Y_1 and the impressed voltage V_1. Inasmuch as the individual transformer primary input impedances are large and do not significantly affect the propagation on the line, the voltage V_2 at the transformer primary terminals will be determined principally, by the position of the transformer on the section. The voltage transfer across the transformer will be independent of the position of the transformer.

With the receiving end open circuited, if we define V_R as the receiving end voltage, we can express

$$V_2 = V_R \text{ Cos } \beta (\ell - d)$$

$$V_1 = V_R \text{ Cos } \beta\ell$$

where d = distance from source to DT

Similarly, if we express the impedances looking towards the receiving end, we can write

$$Z_2 = jZo \text{ Cot } \beta (\ell - d)$$

$$Z_1 = jZo \text{ Cot } \beta\ell$$

Then, $$\frac{V_2}{V_1} = \frac{\text{Cos } \beta (\ell - d)}{\text{Cos } \beta\ell}$$

$$\text{Now, } \cos^2 x = \frac{\cot^2 x}{\operatorname{cosec}^2 x} = \frac{\cot^2 x}{1 + \cot^2 x}$$

$$\therefore \left(\frac{V_2}{V_1}\right)^2 \quad \frac{\cos^2 \beta (\ell - d)}{\cos^2 \beta \ell} = \left(\frac{Z_2}{Z_1}\right)^2 \quad \frac{Z_0^2 + Z_1^2}{Z_0^2 + Z_2^2}$$

Figure 1 shows a plot of impedance Z_2 magnitude normalized to Z_0 vs. voltage V_2 normalized to V_R.

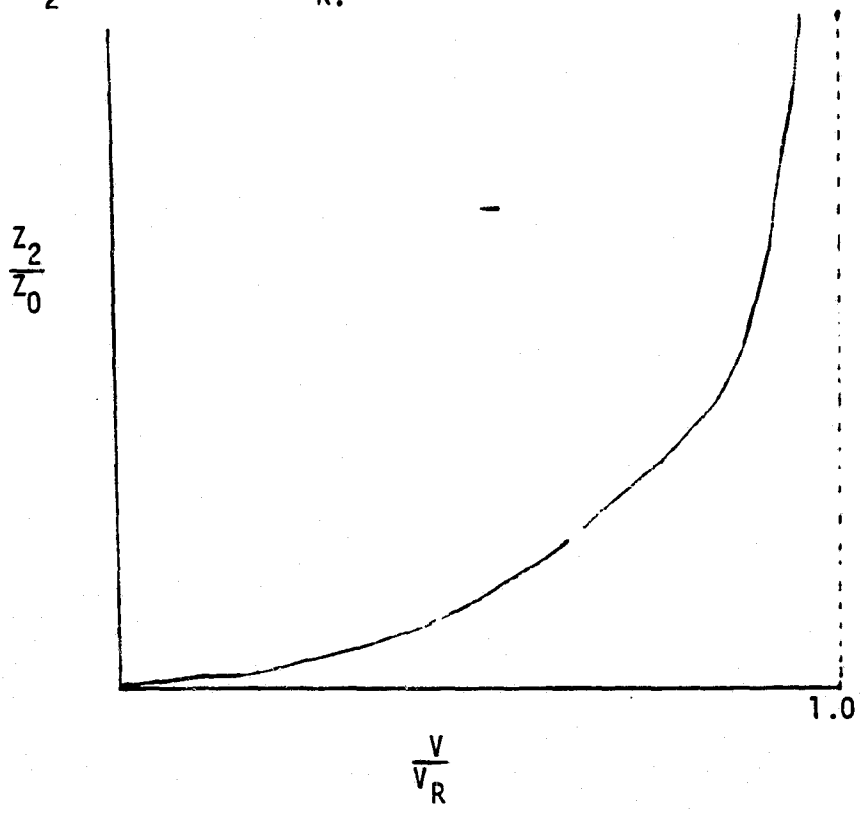

Figure 2

The relationship is monotonic, indicating that high voltage transfer corresponds to a high impedance at load point and voltage nulls correspond to impedance nulls. The essence of any compensation scheme will be to eliminate voltage nulls. The above analysis indicates that, at least in the case of a single line section, this can be accomplished by the elimination of impedance nulls.

Reverse Path Considerations in a Two-Wire System

In order to understand the factors which influence the reverse path propagation, we make use of reciprocity theorems which state that the trans-impedances and trans-admittances of a passive, bi-linear networks are equal. For a two-port, specifically, the theorem states that $Z_{12} = Z_{21}$ and $Y_{12} = Y_{21}$.

The voltage ratio of the outbound path (β_F) can be expressed as

$$\beta_F = \frac{V_3}{V_1} = \frac{V_3}{I_1} \cdot \frac{I_1}{V_1}$$

where I_1 is the current flowing into the network at the input. The second term is the input admittance of the network. If we define Z_{31} as the trans-impedance, then the above can be expressed as

$$\beta_F = \frac{V_3}{V_1} = Z_{31} \cdot Y_1$$

where Y_1 is the input admittance at point V_1.

The reverse path voltage ratio β_R can be expressed as

$$\beta_R = \frac{V_1}{V_3} = Z_{13} \cdot Y_3$$

where Z_{13} is the trans-impedance from the secondary side and Y_3 is the secondary circuit input admittance. Using the reciprocity relationship, we can express the reverse path voltage ratio as

$$\beta_R = \beta_F \cdot Y_3/Y_1$$

Before proceeding further, we wish to remark that the above relationship is valid regardless of the complexity of the network

intravening between the source point and the transformer secondary encountered. The above relation is also valid for lines with losses, and is not restricted to lossless lines, and can be extended to n and m terminal two ports.

The above equation indicates that the reverse path voltage gain will be highest when V_F and Y_3 are high, and Y_1 is a minimum. The value of Y_1 to be used is the value of the input admittance in parallel with the source admittance.

Due to the presence of a relatively high leakage reactance at power line carrier frequencies, the secondary input admittance Y_3 is relatively independent of the primary side admittance loading of the transformer.

Of the two remaining factors, Y_1 depends upon the admittance of the outbound source (or the inbound receiver admittance) and upon the line admittance at its location. V_F, as shown earlier, is related to the outbound line impedance at the point where the transformer is located.

Thus, in order to obtain a high reverse path voltage gain from all points of the simple line section, it is necessary to have a high outbound line impedance at the different transformer location and to locate the receiver at a point of standing wave maxima and also have a high receiver impedance.

Signal-to-Noise Ratio Considerations on a Simple Line

Consider a simple line section with several transformers on it. The transformers are assumed to be randomly placed on the line section. Furthermore, it is assumed that noise originates on each transformer secondary with a mean value of v_m and a standard deviation of v_σ.

The noise amplitude distribution is assumed Gaussian. We wish to investigate the effects of line VSWR on worst case signal-to-noise ratio, of inbound signals.

In the following, we will assume that the secondary input admittance Y_3 is independent of transformer location. As before, we assume that the transformer does not significantly load the line. For a detector located at the point Y_1 on the primary, the reverse path voltage transfer ratio, for the simple section, will be expressed by

$$\beta_R = \beta_F \ Y_3/Y_1$$

β_F, the forward path voltage transfer, will be a product of the transformer primary to secondary voltage ratio and of the voltage transfer ratio to the primary of the transformer. For a simple line segment, if K is the VSWR on the line, for any given primary receiver for inbound communications, the signal to noise ratio can be estimated as follows.

Let N be the number of transformers, let the maximum reverse path gain be G_{max}, and let $|\rho|$ be the magnitude of the reflection coefficient. The range of reverse path gains, G, will vary between

$$G_{max}\frac{(1-|\rho|)}{1+|\rho|} \leq G \leq G_{max}.$$

Since $|\rho|$ is related to the VSWR K by

$$|\rho| = \frac{K-1}{K+1}$$

we can express the above relation as

$$\frac{G_{max}}{K} \leq G \leq G_{max}.$$

If V_s is the amplitude of the secondary signal (assume constant on every secondary), the worst case signal amplitude in the receiver V_{min} will be $G_{min} \cdot V_s$

i.e.,

$$V_{min} = \frac{V_s \, G_{max}}{K}$$

If Y_{or} is the real part of the receiver admittance, the minimum signal power $P_{s\,min}$ will be $Y_{min}^{\ 2} \, Y_{or}$, i.e.,

$$P_{s\,min} = \frac{V_s^{\ 2} \, G^2_{max}}{K^2} \; Y_{or}$$

In order to obtain the mean noise level, we consider the relationships represented by the phaser diagram shown below.

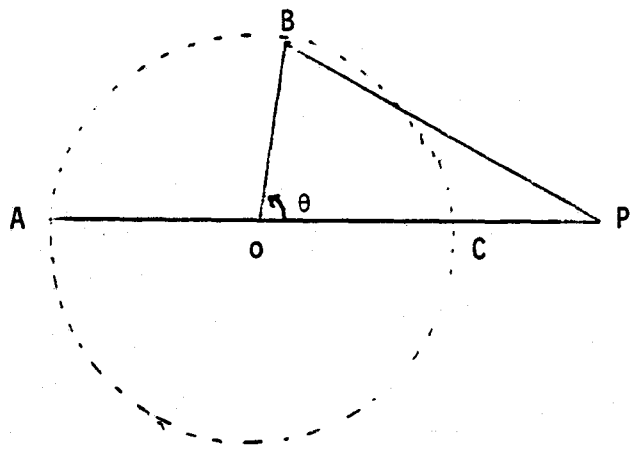

Figure 3

PA represents the maximum gain $G_{max.}$, the ratio $\frac{OA}{OP}$ is the magnitude of the reflection coefficient $|\rho|$. PC represents the minimum gain. PB is the gain to a general point.

C-4

$$(PB)^2 = (OP)^2 + (OB)^2 - 2\,(OP)(OB)\cos\theta.$$

The average value of $(PB)^2$ will be

$$\frac{1}{2\pi}\int_0^{2\pi} (PB)^2\, d\theta = \frac{1}{2\pi}\int_0^{2\pi} (OP)^2\, d\theta + \frac{1}{2\pi}\int_0^{2\pi} (OB)^2\, d\theta$$

$$- \frac{1}{\pi}\int_0^{2\pi} (OP)\,(OB)\,\cos\theta\, d\theta.$$

i.e.,

$$\langle (PB)^2 \rangle = \langle (OP)^2 \rangle + \langle (OB)^2 \rangle = \frac{(PA)^2}{(1+|\rho|)^2} + \frac{|\rho|^2\,(PA)^2}{(1+|\rho|)^2}$$

$$= \frac{1+|\rho|^2}{(1+|\rho|)^2}\,(PA)^2$$

where < > denote the expected value.

The mean noise power will be:

$$P_N = \frac{1+|\rho|^2}{(1+|\rho|)^2}\, G_{max}^2\, N\,(\nu_m^2 + \nu_\sigma^2)\, Y_{or}$$

$$= \frac{K^2+1}{2K^2}\, G_{max}^2\, N\,(\nu_m^2 + \nu_\sigma^2)\, Y_{or}$$

Thus, the ratio of minimum signal power to mean noise power will be

$$\frac{P_{s\,min}}{P_N} = \frac{2}{N\,(K^2+1)}\left(\frac{V_s^2}{\nu_m^2 + \nu_\sigma^2}\right)$$

The ratio $\frac{V_s^2}{\nu_m^2 \quad \nu_\sigma^2}$ is the ratio of the signal to mean noise powers on each secondary.

Thus

$$\left(\frac{P_{S_{min}}}{P_N}\right)\Bigg|_{\text{receiver}} = \frac{2}{N\,(K^2+1)} \left(\frac{P_S}{P_N}\right)\Bigg|_{\text{secondary}}$$

We should make the following observations. The above result indicates that the worst case signal-to-noise ratio will depend upon the VSWR and will be poor for high VSWR. The dependence on VSWR is, in reality, only a dependence on the ratio of maximum to minimum gains. For an uncompensated line, this ratio is the voltage standing wave ratio. Thus, in order to operate the line so as to maximize the worst case signal to noise ratio, it is necessary to reduce the ratio of maximum to minimum gain on the line.

The analysis suggests that the signal to noise ratio, as far as noise generated from the secondaries, is independent of the location of the receiver and its impedance level. On the other hand, location of the receiver and its impedance level will affect the received level of noise generated on the primary.

The analysis of this section is not limited to simple lines, and can be extended to branched lines. In the latter case, the concepts of minimum gain of signal to average gain of secondary noise will yield worst case signal to noise ratios.

Compensation of Simple Lines

We first investigate the compensation of simple lines so as to provide guidelines for approaches to be used in branched situations. The purpose of compensation is to provide maximum reverse path signal to noise ratios. Ideally, the elements used to compensate the line should draw minimal amounts of power from the signal, and from the power line.

As noted earlier, the worst case signal to noise ratio depends upon the ratio of maximum to minimum gains and for maximizing S/N ratios it is desirable to reduce this ratio. In a simple line, this can be achieved, in theory at least, by terminating the section with its characteristic impedance. There are two problems with this approach. On one hand, the characteristic impedance of most line sections is resistive (dissipative) and of a relatively low value, ranging from 15Ω (for underground cables) to approximately 400Ω for overhead lines. In order to overcome primary generated noise, this entails the use of large secondary signal transmitter power. On the other hand, impedance mismatches between overhead and underground sections will create standing waves with large VSWR.

Experimental evidence obtained during field verification of the DIFNAP model indicate that as far as signal propagation on the primary is concerned, the distribution line behaves like a lightly loaded transmission line. The line parameters we have computed indicate a propagation constant tangent angle ($\tan^{-1}$ of α/β) of less than 2° for overhead lines increasing to about 6° for underground cables. Even with loading, the

effective propagation constant tangent angle usually is less than 10°. A line terminated by its characteristic impedance will require from 10 to 20 times the signal power to establish the same voltage level as an unterminated line. Some standing waves will also be created at branch points.

Another approach is to employ reactive shunt compensations. In order to understand this method of compensation, let us consider a short length of 2 wire lossless line open circuited at its end. The length ℓ is less than a quarter wave-length.

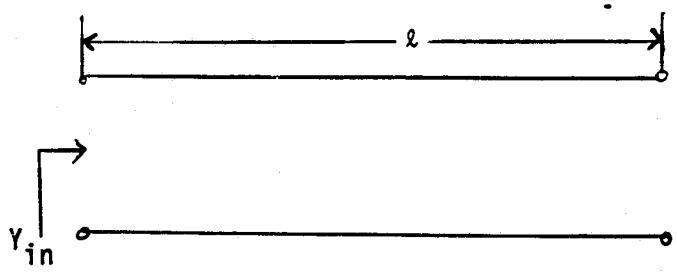

Figure 4

The input admittance will be

$$Y_{in} = jY_o \tan \beta \ell$$

where Y_o is the characteristic admittance of the line section and β is the propagation constant, at the frequency of operation. Let a lossless compensation of admittance jY_c be placed at the midpoint of the line section. The admittance of the line to the right of the compensation will be

$$Y_R = jY_o \tan \frac{\beta \ell}{2}$$

The sum of this admittance, together with that of the compensation, will serve as the load on the left hand section of length $\ell 2/_2$ and the overall input admittance can be calculated using transmission line

formulae to be

$$Y_{in}^{c} \text{ (with compensation)} = Y_o \frac{Y_2 \cos \frac{\beta\ell}{2} + j\, Y_o \sin \frac{\beta\ell}{2}}{Y_o \cos \frac{\beta\ell}{2} + j\, Y_L \sin \frac{\beta\ell}{2}}$$

Substituting for $Y_L = j[Y_c + Y_o \tan \frac{\beta\ell}{2}]$

we obtain

$$Y_{in}^{c} = Y_o \frac{jY_c \cos \frac{\beta\ell}{2} + j\, 2\, Y_o \sin \frac{\beta\ell}{2}}{Y_o \cos \frac{\beta\ell}{2} - Y_c \sin \frac{\beta\ell}{2} - Y_o \sin \frac{\beta\ell}{2} \tan \frac{\beta\ell}{2}}$$

Dividing numerator and denumerator by $\cos \frac{\beta\ell}{2} \neq o$

we have

$$Y_{in}^{c} = jY_o \cdot \frac{Y_c + 2Y_o \tan \frac{\beta\ell}{2}}{Y_o [1-\tan^2 \frac{\beta\ell}{2}] - Y_c \tan \frac{\beta\ell}{2}}$$

If $Y_c = -2\, Y_o \tan \frac{\beta\ell}{2}$ then

$$Y_{in}^{c} = jY_o \frac{-2Y_o \tan \frac{\beta\ell}{2} + 2Y_o \tan \frac{\beta\ell}{2}}{Y_o[1 + \tan^2 \frac{\beta\ell}{2}]} = 0$$

The magnitude of the maximum admittance along the line section will be $Y_o \tan \frac{\beta\ell}{2}$. What has been achieved is that the admittance on the line looking toward the receiving end will vary from zero to a (+) maximum magnitude of Y_c just at $\frac{\ell}{2} + t$ and back to zero at the sending end.

By dividing a given length of line L into n equal line sections, each shorter than $\frac{\lambda}{8}$ and placing a compensation at the center of each section, it is possible to make the maximum admittance to be

$$Y_o \tan \frac{\beta L}{2n} < 0.41\, Y_o.$$

The ratio $\frac{V_{max}}{V_{min}}$, which is equal to the ratio of maximum to minimum gains will be $\text{Sec}\ \frac{\beta L}{2n} < 1.083$.

If each section was approximately a quarter wave long, the ratio of maximum to minimum gains would be 1.414, with this approach. The plot of Fig. 4A shows the relation between the electrical length section and the ratio of maximum to minimum gains.

It should be remarked that at one frequency, the ratio K of the maximum to minimum reverse path gains will hold regardless of the overall length of line as long as the individual compensated sections have the corresponding maximum electrical length. As shown below, this procedure can be generalized to tree configured networks.

Generalization of Compensation Procedure to Lossless Tree Networks

Consider a lossless 2 wire tree network as shown in Fig. 5. Without loss of generality, we assume that the receiver is located in the root section of the tree. Transformers are distributed in a random fashion throughout the network. As before, we assume the generation of noise with a Gaussian Amplitude distribution with an R.M.S. mean value ν_m and an R.M.S. standard deviation ν_σ. Let T_i be the i^{th} number of the total N transformers on the system.

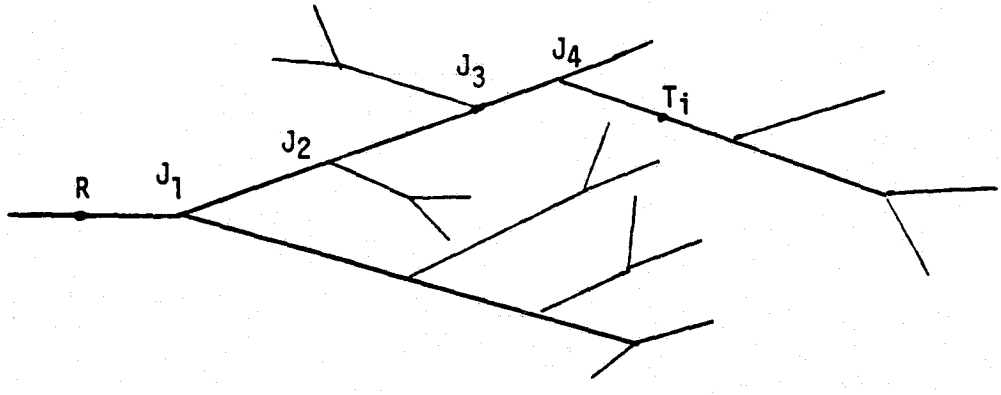

Figure 5

ORIGINAL PAGE IS
OF POOR QUALITY

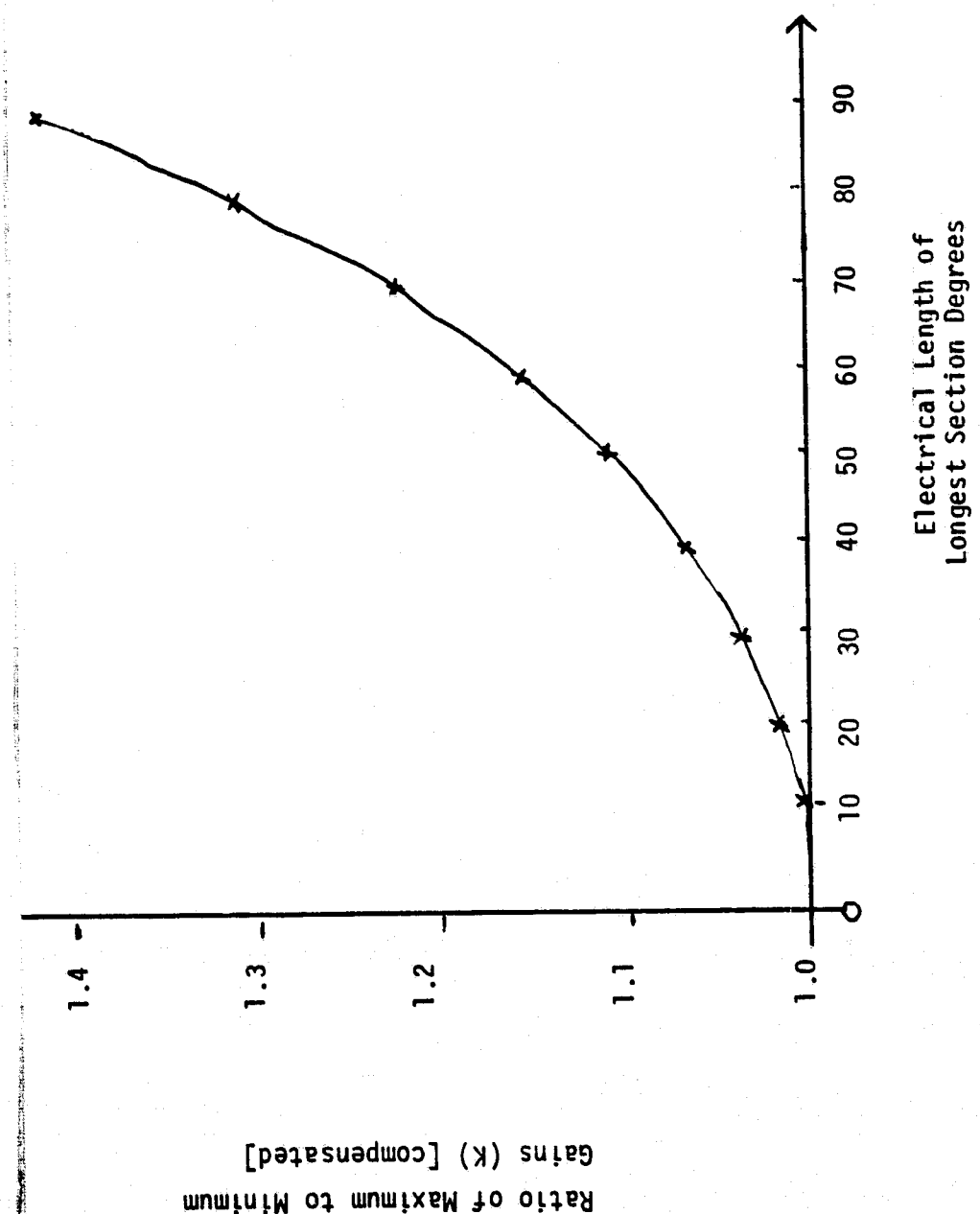

Figure 4A

Let Gi denote the reverse path gain from the i^{th} transformer to the receiver. As noted earlier, this gain will be directly related to the forward path gain, between R and Ti, along the primary circuit. If J1, J2, --- JP denote the junction points on the path from the receiver to Ti, then the forward path voltage gain V_{Fi} from the receiver to Ti can be expressed as

$$V_{Fi} = \frac{V_{Ti}}{V_R} = \frac{V_{Ti}}{V_{JP}} \text{ ---- } \frac{V_{J3}}{V_{J2}} \cdot \frac{V_{J2}}{V_{J1}} \cdot \frac{V_{J1}}{V_R}$$

In general, because of branching, many terms in the above product will have a magnitude less than 1. A few of the terms, especially on sections at the end of the tree, may have magnitudes greater than 1.

The worst case gain, $V_{F_{min}}$ will result from V_{Ti} being at a voltage minimum of a VSWR and a low combination of transfers to the branch point at the source end of the branch on which the corresponding transformer is located. The worst case reverse path gain G_{min} will correspond to such a transformer.

The worst case signal to noise power will be

$$\frac{P_{smin}}{P_{noise}} = \frac{G_{min}^2}{\sum_{i=1}^{N} G_i^2} \cdot \frac{V_s^2}{(V_m^2 + \nu_\sigma^2)}$$

In order to obtain an optimum worst case signal to noise ratio, we have to maximize G_{min} in magnitude. This implies maximizing the forward primary level path gain. This can be accomplished by minimizing the maximum to minimum gain ratio on each branch, treated as an isolated

branch and also maximizing the voltage transfer across each branch. The former can be accomplished using the procedure outlined in the previous section, while the latter can be achieved by minimizing the magnitude of the input admittance to each branch.

Extension to Two-Wire, Loaded, Lossy Lines

In order to extend the above analysis to real life situations, it is important to realize that power distribution feeders, at the carrier frequencies, are low-loss transmission lines and the loading on them corresponds to a lightly loaded situation. As a result, they exhibit moderately high VSWR. The analytic treatment of the problem is relatively complex, even for a two-wire line using low loss approximations.

Before we begin to extend the analysis to the lossy situation, it is instructive to observe the effect of compensation of lossless lines, analyzed earlier, on a Smith Chart. Figure 6 on the Smith Chart shows the impedance paths along the uncompensated and compensated paths for a line of electrical length 0.18 wavelengths. The maximum to minimum voltage ratios for the uncompensated and compensated cases can be determined by using the cosines of the appropriate electrical angles. For the case illustrated, the angles for the uncompensated case are 0° at the beginning of the section and 65° at the end of the section. The V_{max} to V_{min} ratio for the uncompensated would be 1: 0.422. For the corresponding compensated case, the angles would be 0° and $\pm$ 32.5° and the V_{max} to V_{min} ratio would be 1:0.843. A 6 db improvement in worst case signal to noise ratios will result, according to the previous analysis.

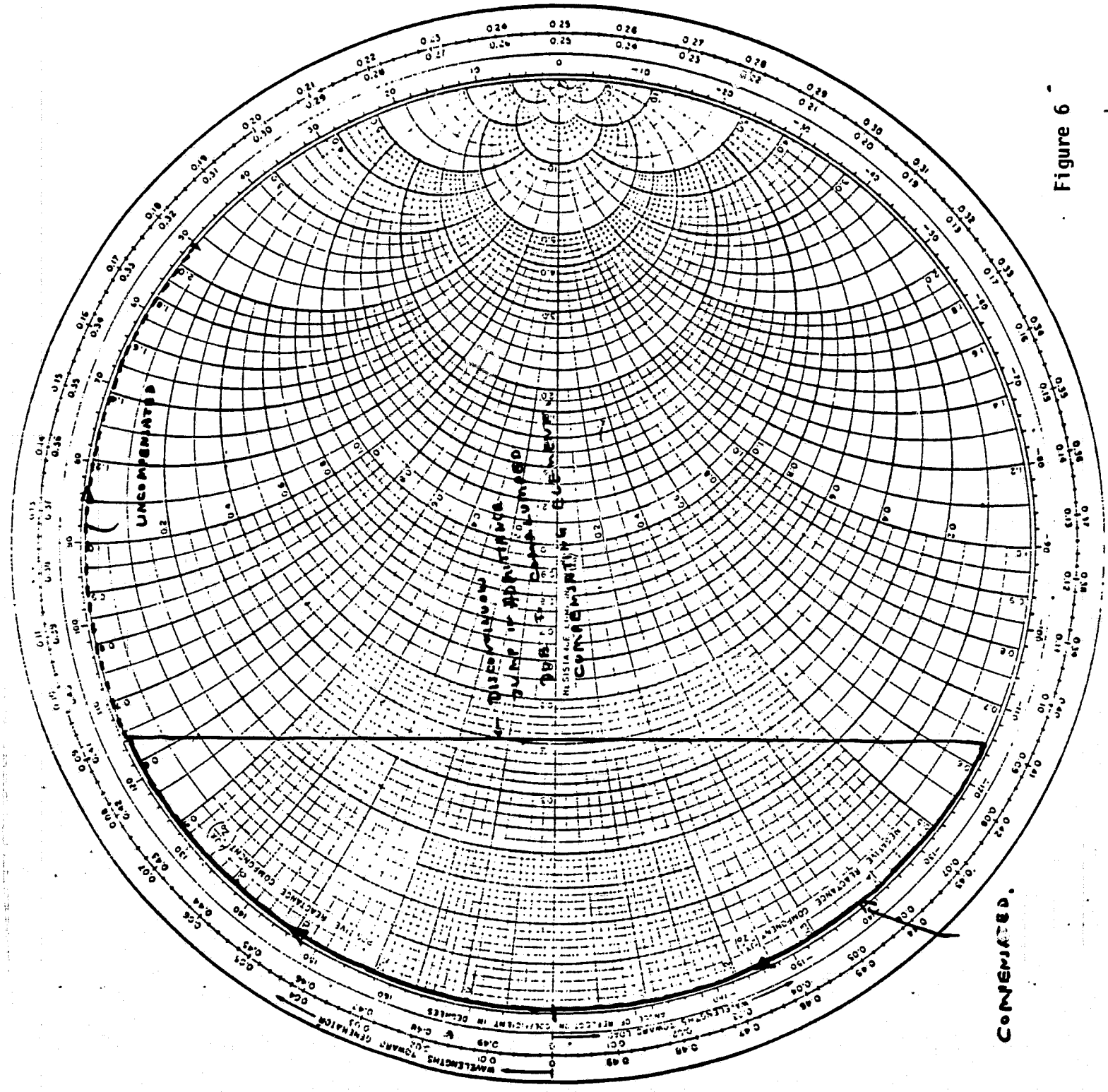

Figure 6

In extending the analysis to the lossy, loaded situation, we make the following observations:

a) The path along the lossy line will represent a spiraling circular path along the Smith Chart.

b) The lumped transformer load admittances will create small discontinuities in the path. The aggregate effect of these discontinuities will be to change the nature of the spiral in a small way.

c) Because the spiraling (which occurs as a result of the lossy medium), the input admittance of the compensated section cannot be made zero by the use of a lossless compensation. In order to make the input admittance zero, the compensation would have to add the energy consumed by the loss of the network.

d) The implication of the previous observation is that in subsequent sections the section load admittance will be non-zero. At a single frequency, it may be assumed that this load admittance will be real and will have a magnitude much smaller than that of the characteristic admittance of the line.

In order to demonstrate the effect of loading with the Smith Chart, consider the loaded section shown in Figure 7.

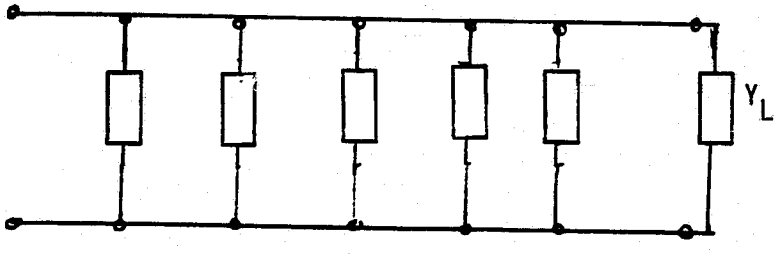

Figure 7

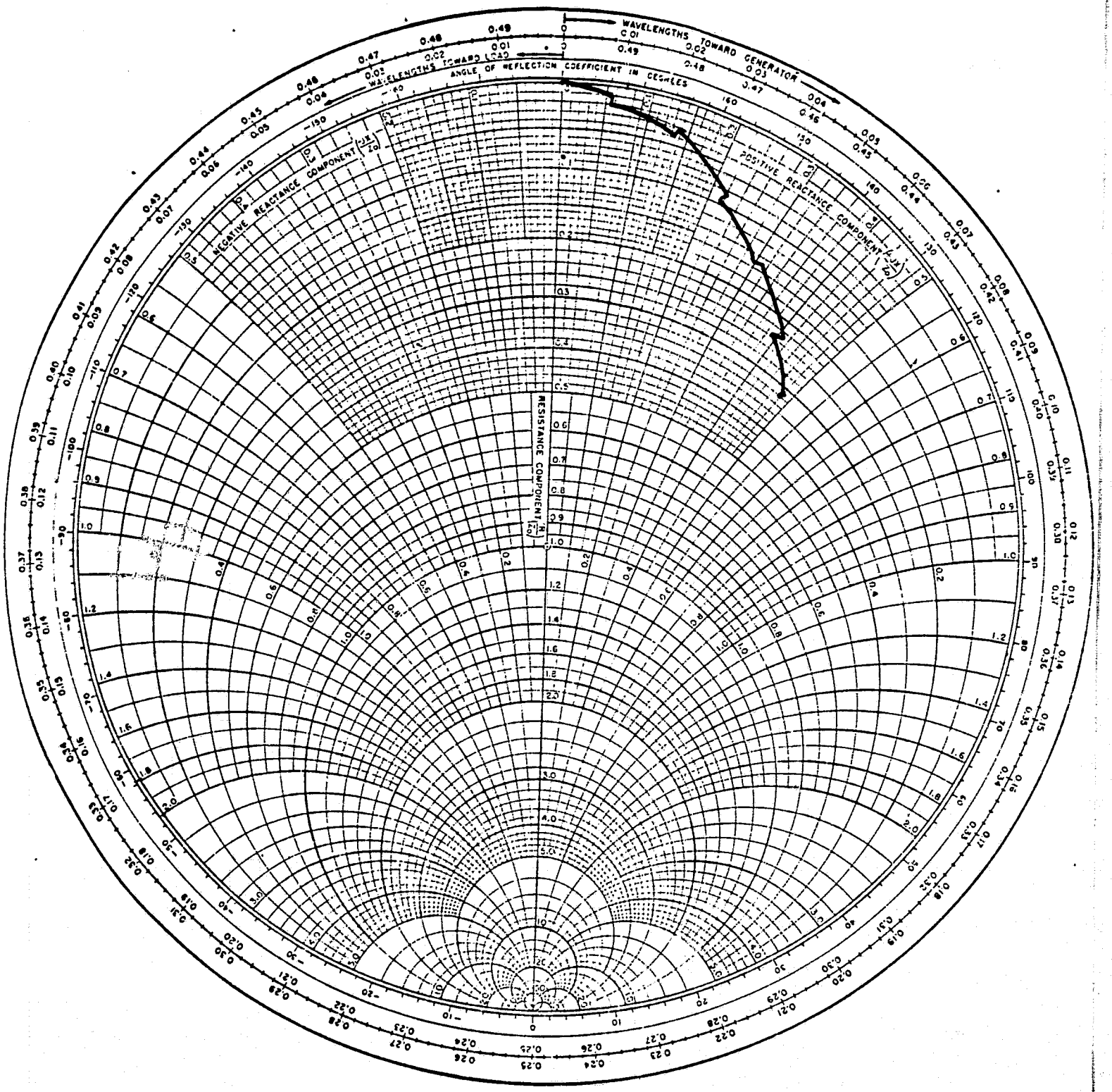

Fig. 1.20*b*

Figure 8

Profile of Admittance Along a Loaded, Lossy Section

In Figure 7, Y_L represents the terminal load admittance which we assume is non-zero and almost resistive with a magnitude substantially less than that of Y_o. The admittances of the loads connected (representing distribution transformers) have magnitudes much smaller than that of Y_o. The plot on the Smith Chart of Figure 8 represents the impedance profile along the line section. The discontinuities represent the effect of lumped admittances of the load. The diagram, since it is used to demonstrate the effects, has been deliberately exaggerated.

Two observations need to be made regarding this diagram. The discontinuities, since they represent passive elements, will always shift the curve towards the right, i.e., in the direction of increasing Re(Y). In the top half of the chart they represent a decrease in the magnitude of the reflection coefficient, i.e., they tend to push the spiral inwards. From the considerations of the previous section, it is clear that we will prefer to operate in this region of the Chart.

The second observation which should be made is that the process of computing voltage transfer ratio in the case of the loaded line is somewhat complicated. As can be seen from the previous sections, control of voltage transfer ratios will be the principal objective of any compensation procedure. In order to explain this computation, we will demonstrate it using one discontinuity and exaggerate the effect of the discontinuity on the Smith Chart of Figure 9. The corresponding circuit is shown in Fig. 10.

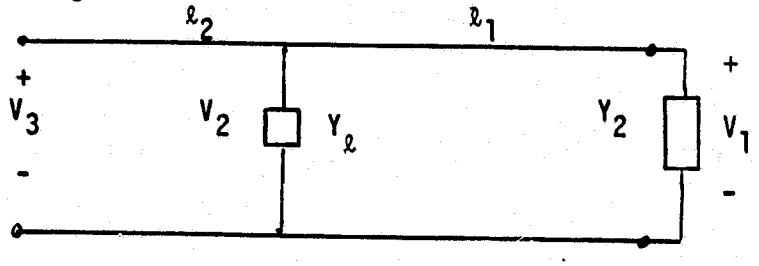

Figure 10

In the circuit of Fig. 10, Y_L represents the terminal admittance and Y_i represents the loading admittance. The voltage ratio $\frac{V_1}{V_2}$ is the same as the ratio of the vectors $\frac{V_A}{V_B}$. Similarly, the voltage ratio $\frac{V_2}{V_3}$ is the same as the ratio $\frac{V_C}{V_D}$. Thus, the voltage ratio $\frac{V_1}{V_3}$ will be the product of the voltage ratios $\frac{V_A}{V_B}$. $\frac{V_C}{V_D}$. In the case of multiple load discontinuities, the products of the voltage transfer ratios across each section must be taken.

This procedure can become complex, even on a Smith Chart, and the problem can quickly become intractable. In order to obtain a better handle on the situation, we use the following approach. Consider a section of lossy loaded line, with a compensation to be placed somewhere near the middle of the line. The two sections of line, on either side of the compensation, can be looked upon as lumped sections having a set of circuit parameters, as shown below.

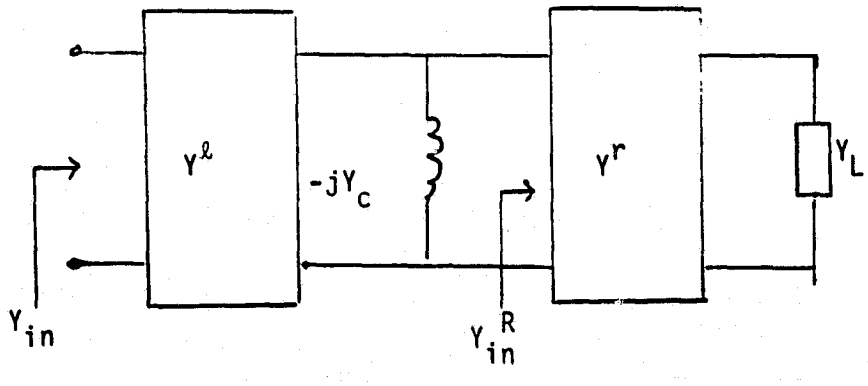

Figure 11

For a given load Y_L, one can always determine the input admittance Y_{in}^R of the right hand section. With a lightly loaded short line and a terminal load Y_L which is real and has an admittance magnitude much less than the characteristic admittance of the

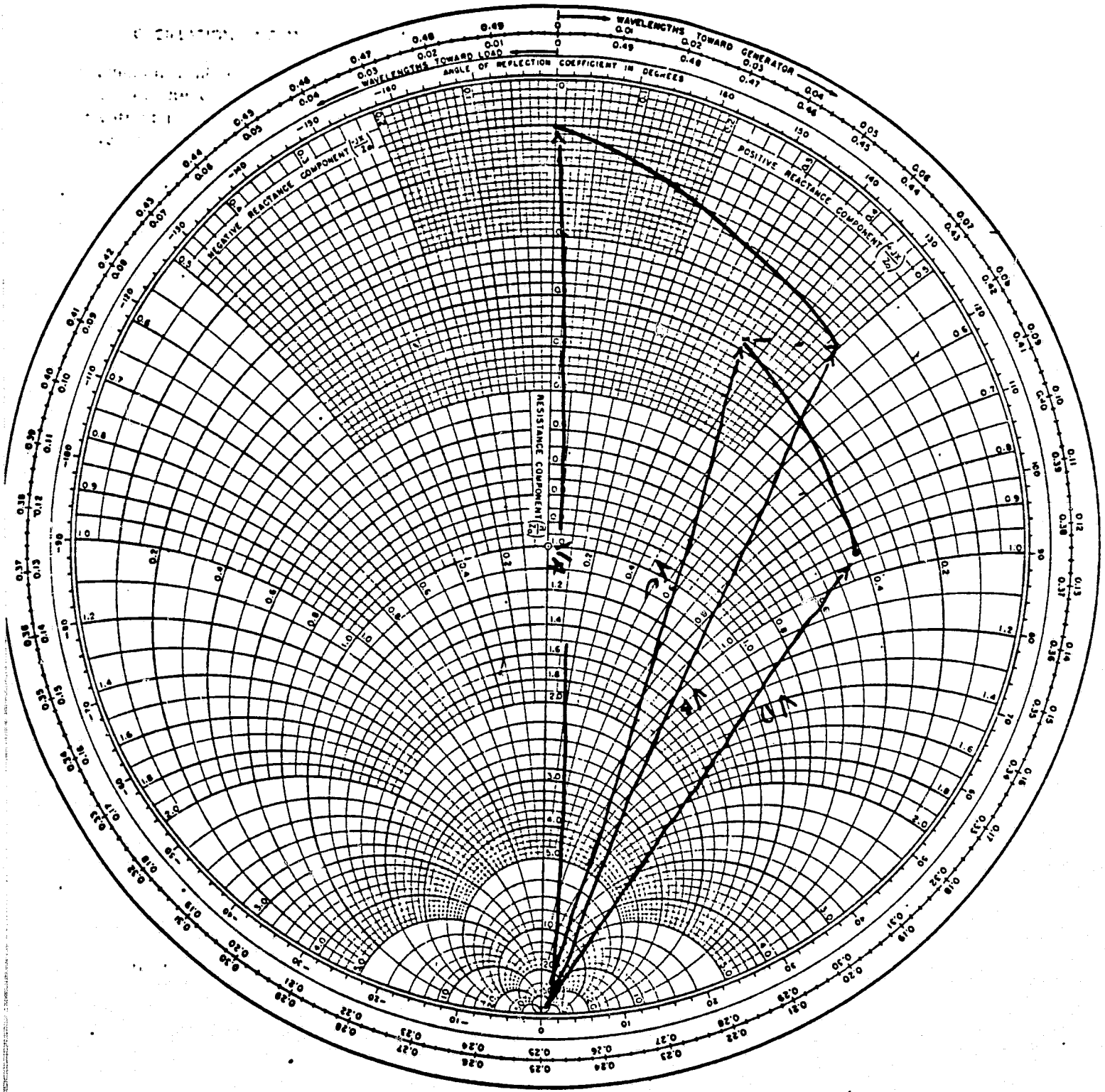

Fig. 1.20*b*

Figure 9

Demonstration of Computation of Voltage Transfer Ratio

transmission line, Y_{in}^{R} will be largely capacitive admittance with a small real part.

We can express Y_{in}^{R} as $G_1 + jS_1$ where G_1 and S_1 are both real and $G_1 << S_1$. The load on the left hand section can be expressed as $G_1 + j\ S_1 - jY_c$ where Y_c is the admittance of the inductive, non-dissipative, compensating element.

The input admittance Y_{in} to the entire section can be expressed as

$$Y_{in} = y_{11}^{\ell} - \frac{(y_{12}^{\ell})^2}{(y_{22}^{\ell} + G_1 + jS_1 - jY_c)}$$

where y_{ij}^{ℓ} are the short-circuit admittance parameters of the left hand section. It should be clear that in the above expression, Y_c, S_1 and G_1 are real while in general, the short-circuit admittance parameters are complex. It should also be clear that with a suitable choice of Y_c, the imaginary part of Y_{in} can be made zero. From the discussions of the previous sections and comparison with the lossless case, it should be clear that with a choice of Y_c that makes Im Y_{in} equal to zero, the magnitude of the admittance will be a minimal.

Generalization of Compensation Procedure to Lossy Tree Networks

The compensation procedure of lossy, loaded sections can be extended to lossy and lightly loaded tree sections. The extension is analogous to the extension of the compensation procedure for lossless section to lossless tree networks. The compensation of each major

branch at the tree permits control of the ratio of maximum to minimum voltages on the branch. The input admittance to each major branch is minimized in magnitude and is made nearly real at and near the operating frequency. In addition, the voltage transfer ratio across each major branch is controlled to have a magnitude close to unity. As a consequence, the ratio of maximum to minimum voltages on the entire network is controlled by the procedure to approximately equal the ratio of maximum to minimum voltage on any one branch, and a corresponding control of signal to noise ratios is obtained.

Compensation Over a Band of Frequencies

The preceeding discussion has been expressly directed to single frequency or narrow-band operation. The passive compensation schemes proposed will provide control only for a narrow range of frequencies. The use of passive compensation can become ineffective at certain frequencies, as can be seen from the following example.

Consider a two-wire lossless line operating over a frequency range f_1 to $2f_1$. Let us assume that we wish to compensate this line and choose a procedure so that the compensators are placed so that the first one is placed at a distance of $\frac{\lambda}{8}$ from the open end at the highest frequency. Furthermore, we choose to make the admittance at midband frequency minimal at every quarter wave section at the highest frequency from the end. The admittance values normalized to Y_0 at various points on the compensated section are tabulated below at each of the frequencies.

Distance from open end in Wavelength at highest freq.	Admittance normalized to Y_0			Condition
	f_1	$1.5f_1$	$2f_1$	
0	0	0	0	
$\lambda/8$	j 0.4142	j 0.6681	j1	before compensation
$\lambda/8$	-j 1.595	-j 0.6681	-j 0.004	after compensation
$\lambda/4$	-j 0.71	j 0	+j 1.05	
$3\lambda/8$	-j 0.218	j 0.6681	j 50	before compensation
$3\lambda/8$	-j 2.226	-j 0.6681	j 49	after compensation

Clearly, at the higher frequency, an impedance null will be observed close to the second compensation.

Thus, using simple inductive compensations at the mid-band frequency is not an adequate compensating mechanism to control VSWR for broadband operation. Some improvement in the above situation may be realized by the use of compensators whose admittance vs. frequency characteristics are different from those of simple inductors.

Alternatively, we may ask: what type of compensator can be used so that the input admittance to a section, having a length ℓ is nearly zero at all frequencies in the band? In the lossless case, assuming that the compensator is placed in the middle of the section, the compensator should have an admittance vs. frequency characteristic of $Y = -j2Y_0 \tan \frac{\beta\ell}{2}$ over the band. If ℓ is small such that $\tan \frac{\beta\ell}{2}$ can be approximated by $\frac{\beta\ell}{2}$ over the band of frequencies involved, an element having the characteristics of a negative capacitor may be used. Such elements can be generated using active circuits and may be used if proper coupling practices are followed and appropriate drain inductors are used to ensure system stability at the power frequency and at

harmonic frequencies. Sections having lengths approximately equal to $\frac{\lambda}{4}$ at the highest frequency may be compensated in this manner.

Extension to Polyphase Lines

The compensation procedures outlined above can be extended to polyphase lines. The compensator used will be six-element devices and computations will be based on complex matrix arithmetic. The procedures, which need further investigation are clearly beyond the scope of the present report. They will involve the definition of appropriate optimation criteria and the development of computer algorithms to determine optimum selection and siting of compensators. In addition, sensitivity to load line parameter variation and network reconfigurations will have to be investigated.

Conclusions

In this report, we have investigated the problem of compensating distribution lines, with transformer loading, so as to improve their performance and communication media in two-way communication systems. After investigating the principal phenomena which are responsible for the degradation of the medium as a communication channel we have developed criteria which can be used to determine the performance of the channel. Using these criteria as a basis, we have evolved methods of compensating the lines. The methods, first developed for compensating lossless, simple lines, are extended to the compensation of lossless tree networks. The procedures are then extended to lines with low losses and loads and to lossly, loaded tree networks operating at a

single frequency. Finally, the compensation procedure is extended to broadband operation and to polyphase networks. It is shown that by appropriate compensation schemes, lines can be conditioned to serve as reliable two-way communication media.